

**ASSESSMENT OF SUSPENDED DUST FROM PIPE RATTLING  
OPERATIONS**

A Dissertation

by

JU-MYON PARK

Submitted to the Office of Graduate Studies of  
Texas A&M University  
in partial fulfillment of the requirements for the degree of

DOCTOR OF PHILOSOPHY

August 2005

Major Subject: Interdisciplinary Engineering

**ASSESSMENT OF SUSPENDED DUST FROM PIPE RATTLING  
OPERATIONS**

A Dissertation

by

JU-MYON PARK

Submitted to the Office of Graduate Studies of  
Texas A&M University  
in partial fulfillment of the requirements for the degree of

DOCTOR OF PHILOSOPHY

Approved by:

Chair of Committee James C. Rock  
Committee Members, Ian S. Hamilton  
Charles S. Lessard  
James A. Calvin  
Head of Department, N.K. Anand

August 2005

Major Subject: Interdisciplinary Engineering

## ABSTRACT

Assessment of Suspended Dust from Pipe Rattling Operations. (August 2005)

Ju-Myon Park, B.E, Hoseo University, Korea;

M.S., Texas A&M University

Chair of Advisory Committee: Dr. James C. Rock

Six types of aerosol samplers were evaluated experimentally in a test chamber with polydisperse fly ash. The Andersen sampler overestimates the mass of small particles due to particle bounce between stages and therefore provides a conservative estimate of respirable particulate mass and thoracic particulate mass. The TSP sampler provides an unbiased estimate of total particulate mass. TSP/CCM provides no information below ESD 2  $\mu\text{m}$  and therefore underestimates respirable particulate mass. The  $\text{PM}_{10}$  sampler provides a reasonable estimate of the thoracic particulate fraction. The RespiCon sampler provides an unbiased estimate of respirable, thoracic, and inhalable fractions. DustTrak and SidePak monitors provide relative particle concentrations instead of absolute concentrations because it could not be calibrated for absolute particle concentrations with varying particle shape, composition, and density.

Six sampler technologies were used to evaluate airborne dust concentrations released from oilfield pipe rattling operations. The task sampled was the removal of scale deposited on the inner wall of the pipe before it was removed from service in a producing well.

The measured mass concentrations of the aerosol samplers show that a Gaussian plume model is applicable to the data of pipe rattling operations for finding an attainment area. It is estimated that workers who remain within 1 m of the machine centerline and directly downwind have an 8-hour TWA exposure opportunity of  $(13.3 \pm 9.7) \text{ mg/m}^3$  for the Mud Lake pipe scale and  $(11.4 \pm 9.7) \text{ mg/m}^3$  for the Lake Sand pipe scale at 95 % confidence. At distances more than 4 m downwind from the machine centerline, dust concentrations are below the TWA-TLV of  $10 \text{ mg/m}^3$  for the worker in both scales. At positions crosswind or upwind from the machine centerline there is no measurable exposure. Available data suggest that the attainment area for the public starts at about 9 m downwind from the machine centerline in both scales, as 24 hour average concentrations at these distances are smaller than the  $0.15 \text{ mg/m}^3$ , the NAAQS for unrestricted public access. The PSD of the suspended plume is dominated by particles smaller than ESD  $50 \mu\text{m}$ .

## DEDICATION

“If any of you lacks wisdom, he should ask God,  
who gives generously to all without finding fault,  
and it will be given to him.” (James 1:4)

I would like to dedicate this work first to God,  
who always guides me the correct ways.

Secondly, with my all love to my lovely wife,  
Sang-Hee, for her devotional prayers and belief in me,  
to my daughter Mary, the sparkle in my life,  
and to my mother and to my parents in law,  
who have encouraged me with their endless love and prayers  
during my time at Texas A&M University.

## ACKNOWLEDGMENTS

I would like to express my sincere appreciation to all those who gave me the opportunity to complete this dissertation. In particular, very special thanks go to my graduate advisor, Dr. James C. Rock, who is a real scholar and guided me with constant encouragement. I will never forget Dr. Rock's belief which allows me to have the courage and wisdom to study Ph.D. curriculums. I also thank the committee members, Dr. Ian S. Hamilton, Dr. Charles S. Lessard, and Dr. James A. Calvin, for taking time from their busy schedules and giving valuable advice.

Sincere thanks are extended to Dr. Calvin Parnell and Dr. Lingjuan Wang in the Department of Agricultural Engineering for allowing me to use their chamber and instruments for this study. This work and the related pipe rattling operations were financially supported by the Exxon Mobil Corporation.

## TABLE OF CONTENTS

	Page
ABSTRACT.....	iii
DEDICATION .....	v
ACKNOWLEDGMENTS.....	vi
TABLE OF CONTENTS .....	vii
LIST OF FIGURES.....	x
LIST OF TABLES....	xiii
NOMENCLATURE.....	xvi
 CHAPTER	
I    INTRODUCTION.....	1
II   PERFORMANCE EVALUATION OF SIZE SELECTIVE AEROSOL SAMPLERS .....	2
A. Introduction.....	2
1. Introduction: Operating Principles of Six Aerosol Samplers.....	7
a) Andersen Sampler.....	8
b) RespiCon Sampler .....	12
c) Total Suspended Particulate Sampler and a Coulter Counter Multisizer.....	14
d) PM <sub>10</sub> Sampler.....	15
e) DustTrak and SidePak Monitors.....	16
2. Particle Sizing Methods Introduction.....	18
3. Statistical Analyses Introduction.....	23
B. Methods.....	23
C. Results.....	26
1. Total Concentration .....	26
2. Particle Size Distribution .....	30
3. Mass Fraction for the Convention....	38

CHAPTER	Page
D. Discussion.....	40
1. Mass Fraction by Aerosol Samplers .....	40
2. Microscopic Analysis .....	43
E. Conclusions.....	45
 III RISK ASSESSMENT OF PETROLEUM PIPE SCALE FROM A PIPE RATTLING PROCESS .....	47
A. Introduction.....	47
B. Methods .....	49
C. Results .....	56
1. Mass Concentration .....	56
2. Particle Shape and Density Influence Estimated AED.....	61
3. Particle Size Distribution .....	68
4. PM <sub>10</sub> and PM <sub>4</sub> mass concentration .....	74
5. Risk Assessment .....	76
D. Discussion.....	84
E. Conclusions.....	85
 IV CONCLUSIONS .....	87
 REFERENCES .....	88
 APPENDIX A CHAMBER STUDY RESULTS USING FLY ASH .....	92
 APPENDIX B PIPE RATTLING STUDY RESULTS.....	106
 APPENDIX C RANDOMIZED BLOCK DESIGN.....	114
 APPENDIX D PERFORMANCE CHARACTERISTICS OF A PM <sub>10</sub> SAMPLER .....	118
 APPENDIX E CUTOFF SIZE CALCULATION (ANDERSEN SAMPLER) ..	136
 APPENDIX F PARTICLE SIZE DISTRIBUTION MODELS.....	144
 APPENDIX G SHAPE FACTOR REVIEW .....	157
 APPENDIX H GAUSSIAN DISPERSION MODEL.....	161
 APPENDIX I LINEAR AND NONLINEAR FIT .....	166



VITA ..... 197

## LIST OF FIGURES

FIGURE	Page
2-1 ACGIH sampling criteria .....	3
2-2 EPA regulated PM pollutants .....	4
2-3 ACGIH Thoracic vs. EPA PM <sub>10</sub> .....	5
2-4 Andersen sampler .....	9
2-5 Andersen sampler collection efficiency at 1 ACFM .....	11
2-6 Inside schematic diagram of a RespiCon sampler .....	13
2-7 Schematic diagram of a TSP sampler .....	14
2-8 Schematic diagram of a PM <sub>10</sub> sampler showing its circularly symmetric inlet as a plate impactor with side walls to minimize particle bounce and subsequent carry through of large particles .....	16
2-9 Impactors used as size selective pre-filters in real-time monitors .....	17
2-10 Aerosol samplers used in a chamber study .....	18
2-11 The general shape of fly ash .....	22
2-12 Experimental setup in a chamber .....	26
2-13 Average concentration measured with Andersen and TSP samplers ...	28
2-14 PSD of fly ash's bulk sample .....	32
2-15 PSD of Andersen sampler .....	33
2-16 PSD of TSP/CCM .....	34
2-17 PSDs by samplers vs. PSD of fly ash's bulk sample .....	36

FIGURE	Page
2-18 Measured concentration by real-time monitor .....	43
2-19 Particle images from a RespiCon sampler and a TSP sampler .....	44
3-1 Pipe rattling process .....	51
3-2 Aerosol samplers setup for field tests 1 and 2 with wind rose .....	55
3-3 Total mass concentration by distance.....	58
3-4 Minimum mean square error fit showing unsuitability of the Inverse Square Law as a model for $PM_{Total}$ data .....	59
3-5 Minimum mean square error fit showing Gaussian Point Source Model fit to $PM_{Total}$ data.....	60
3-6 The front and back images of Teflon filter .....	61
3-7 The images of Mud Lake scale .....	62
3-8 The images of Lake Sand scale .....	63
3-9 Electrostatic and cluster (Lake Sand).....	65
3-10 Deposition mapping .....	66
3-11 The images of black and gray particle .....	68
3-12 PSD of Andersen Sampler (Field test) .....	70
3-13 PSD of TSP/CCM (Field test).....	71
3-14 PSD comparison, showing that the fitted PSD for the Andersen and the TSP/CCM analyses are consistent with one another .....	72
3-15 Minimum mean square error fit showing unsuitability of the Inverse Square Law as a model for $PM_{10}$ data .....	78
3-16 Plume centerline concentrations of $PM_{10}$ showing maximum concentration between 1 m and 2 m distance from the source .....	79

FIGURE	Page
3-17 Plume centerline concentrations of $PM_{Total}$ showing maximum concentration between 1 m and 2 m distance from the source .....	80
3-18 Nonlinear fit of Gaussian plume model to task average exposures compared with the NAAQS used for the public exposure standard ....	82
3-19 Nonlinear fit of Gaussian plume model to task average exposures compared with the TLV used for the occupational exposure guideline	83
3-20 Plume dispersion by distance .....	84
A-1 Estimated $GM_{AED}$ and $GSD_{AED}$ of the Andersen sampler (Chamber) ..	104
B-1 Estimated $GM_{AED}$ and $GSD_{AED}$ of the Andersen sampler (Field).....	112
D-1 Penetration efficiency usable region for a $PM_{10}$ sampler with parameters falling in the acceptable range as defined by FRM .....	121
D-2 Penetration efficiency usable region for a $PM_{2.5}$ sampler with parameters falling in the acceptable range .....	121
H-1 Coordinate system showing Gaussian distribution in the horizontal and vertical .....	163
H-2 The images of particle dispersion.....	165

## LIST OF TABLES

TABLE		Page
2-1	Dimension of the Andersen Impactor Orifices .....	10
2-2	Total Mass Concentration Measured with Andersen and TSP Samplers .....	27
2-3	Average Mass Concentration Measured with Andersen and TSP Samplers .....	28
2-4	Parameters for Estimated PSD from Andersen Sampler Data .....	31
2-5	Parameters for Estimated PSD from TSP/CCM Data .....	31
2-6	Average Mass Fractions of Respirable PM and Thoracic PM from Andersen, TSP/CCM, and RespiCon Samplers.....	39
2-7	Comparison of the Concentration of Real-time Monitors to the Unbiased Concentrations of Size Selective Samplers.....	41
3-1	Accepted Limits for PM.....	48
3-2	Measured Concentrations from Each Aerosol Sampler by Distance ...	57
3-3	Measured Mass Fraction of Settled Dust within 3m Distance from the Centerline of Source .....	66
3-4	Parameters for Estimated PSD from Andersen Sampler Data .....	73
3-5	Parameters for Estimated PSD from TSP/CCM Data .....	74
3-6	Mass Concentrations for Respirable and Thoracic PM.....	75
3-7	Mass Fractions for Respirable and Thoracic PM.....	76
A-1	Estimated Mass Concentrations from Andersen Sampler Measurements (Chamber) .....	93

TABLE	Page
A-2 Estimated Mass Concentrations for a Respirable, Thoracic, and Inhalable Convention from Andersen Sampler Data in TABLE A-1 above (Chamber) .....	94
A-3 Mass Concentrations for a Respirable, Thoracic, and Inhalable Convention Estimated from RespiCon Measurements (Chamber) .....	95
A-4 Relative Mass Concentrations from DustTrak Measurements (Chamber).....	96
A-5 Relative Mass Concentrations from SidePak Measurements (Chamber).....	97
A-6 Estimated TSP/CCM Volume Percentile (Chamber).....	98
A-7 Estimated Mass Concentrations for a Respirable, Thoracic, and Inhalable Convention from TSP/CCMs (Chamber) .....	99
A-8 Estimated Bulk Sample Volume Percentile (Chamber) .....	100
A-9 Mass Fractions Estimated from Andersen Samplers (Chamber) .....	101
A-10 Mass Fractions Calculated from RespiCon Samplers (Chamber).....	101
A-11 Mass Fractions Estimated from TSP/CCMs (Chamber) .....	101
A-12 Mass Fraction Estimated from Each Stage of Andersen Sampler (Chamber).....	103
A-13 Standard Normal Random Variables from the Mass Fraction Estimated in TABLE A-12 above (Chamber).....	103
B-1 Measured Mass Concentration of Each Stage of Andersen Samplers (Field) .....	106
B-2 Estimated Mass Concentrations for a Respirable, Thoracic, and Inhalable Convention from Andersen Sampler Data in TABLE B-1 above (Field) .....	107
B-3 Mass Concentrations for a Respirable, Thoracic, and Inhalable Convention Estimated from RespiCon Measurements (Field) .....	108

TABLE	Page
B-4 Relative Mass Concentrations from DustTrak Measurements (Field).	109
B-5 Relative Mass Concentrations from SidePak Measurements (Field)...	109
B-6 Estimated TSP/CCM Volume Percentile (Field) .....	110
B-7 Estimated Mass Fractions for a Respirable, Thoracic, and Inhalable Convention from TSP/CCMs (Field) .....	111
B-8 Mass Fraction Measured from Each Stage of Andersen Samplers (Field) .....	111
B-9 Standard Normal Random Variables from the Mass Fraction Measured in TABLE B-8 above (Field).....	112
D-1 Penetration Efficiency of PM <sub>10</sub> Sampler .....	122
D-2 Penetration Efficiency of PM <sub>2.5</sub> Sampler .....	123
E-1 Cunningham Correction Factor Comparison in Air at 298K and 1 atm	140
E-2 Stage Cutoff Size as a Function of Density and Flow Rate .....	142
E-3 Dimension of the Andersen Sampler Orifices.....	143
G-1 Dynamic Shape Factor for a Cube and Orthorhombic Crystals.....	159

## NOMENCLATURE

### Abbreviations

$(x, y, z)$	Line coordinate system
$AED$	Aerodynamic Equivalent Diameter
$ANOVA$	Analysis of variance
$C$	Steady state concentration at a point $(x, y, z)$
$C1, C2$	Andersen samplers (Cascade impactors)
$C_A$	Overall average concentration
$CCM$	Coulter counter multisizer
$CDF$	Cumulative density function
$C_P$	Cunningham correction factor of particle $d_P$
$C_{P50}$	Cunningham correction factor corresponding to $d_{P50}$
$d_{15.9}$	Diameter corresponding to the 15.9 % of the PSD or 15.9 % of the stage collection efficiency curve
$d_{84.1}$	Diameter corresponding to the 84.1 % of the PSD or 84.1 % of the stage collection efficiency curve
$d_c$	Diameter of the round nozzle or jet
$d_{ec}$	Effective cutoff size
$D_o$	Orifice meter
$d_P$	Particle physical diameter
$d_{P50}$	Impactor stage cutoff size in particle diameter
$ER$	Emission rate [mg/s]



$ESD$	Equivalent Spherical Diameter
$ESEM$	Environmental Scanning Electron Microscope
$GDM$	Gaussian dispersion model
$GM$	Sample geometric mean of data
$GM_{AED}$	Median AED of $PM_{10}$ or $PM_{2.5}$ sample
$GM_{BS}$	Median AED of bulk sample
$GM_{ESE}$	Estimated median AED of sampling efficiency for $PM_{10}$ or $PM_{2.5}$ sample from Andersen samplers and TSP/CCMs
$GM_{PE}$	Median AED of the penetration curve
$GM_{SE}$	Median AED of sampling efficiency in Andersen sampler, TSP/CCM, $PM_{10}$ or $PM_{2.5}$ sample
$GOF$	Goodness of fit
$GSD$	Sample geometric standard deviation of data
$GSD_{AED}$	Slope of the $PM_{10}$ or $PM_{2.5}$ sample
$GSD_{BS}$	Slope of CDF for the bulk sample
$GSD_{ESE}$	Estimated slope of sampling efficiency for $PM_{10}$ or $PM_{2.5}$ sample from Andersen samplers and TSP/CCMs
$GSD_{PE}$	Slope of penetration curve
$GSD_{SE}$	Slope of sampling efficiency in Andersen sampler, TSP/CCM, $PM_{10}$ or $PM_{2.5}$ sample
$H$	Effective height
$h$	Pipe location height
$H_A$	Alternative hypothesis

$H_o$	Null hypothesis
$K$	Flow coefficient
$LCL$	Lower confidence limit
$n$	The number of cases
$P1 \sim P4$	PM <sub>10</sub> samplers
$PDF$	Probability density function
$PM$	Particulate matter
$PM_{10}$	Particulate matter with an AED of 10 $\mu\text{m}$ collected with 50 % efficiency by a PM <sub>10</sub> sampling collection device
$PM_{2.5}$	Particulate matter with an AED of 2.5 $\mu\text{m}$ collected with 50 % efficiency by a PM <sub>2.5</sub> sampling collection device
$PSD$	Particle size distribution
$Q$	Airflow rate through the orifice meter
$R1 \ \& \ R2$	RespiCon sampler
$SD$	Standard deviation of sample
$SE$	Standard Error of sample mean = $(SD/\sqrt{n})$
$SU$	<p>Sampling uncertainty = <math>\frac{SD_C}{\bar{C}_T} = \sqrt{\left(\frac{SE}{\bar{C}_T}\right)^2 + \left(\frac{SD_1}{\bar{C}_1}\right)^2 + \dots + \left(\frac{SD_n}{\bar{C}_n}\right)^2}</math>, half of the 95 % confidence intervals around an estimated mean (<math>1.96 \cdot SE</math>), where <math>\bar{C}_T</math> = Average concentration of n samplers; <math>SE</math> = standard error of sample mean; <math>SD_n</math> = Standard deviation of <math>n^{\text{th}}</math> sampler; <math>\bar{C}_n</math> = Concentration of <math>n^{\text{th}}</math> sample.</p>
$T1 \sim T4$	TSP samplers
$t_s$	Sampling time

$TSP$	Total suspended particulate
$TSP/CCM$	TSP sampler by a coulter counter multisizer
$TWA$	Time-weighted average
$u$	Average wind speed on the ground
$UCL$	Upper confidence limit
$V_o$	Aerosol (Stage) Velocity
$W_a$	Weight of particle in the air
$W_w$	Weight of particle in the water
$y$	Horizontal distance from the plume centerline
$Z$	Height of the receptor above the ground
$\Delta h$	Average plume height from the pipe location
$\Delta P$	Pressure drop cross the orifice
$\theta$	Angle made by the centerline of source with the wind vector
$\mu$	Dynamic air viscosity
$\rho_0$	Unit density [1 g/cm <sup>3</sup> ]
$\rho_{air}$	Air density
$\rho_p$	Particle density
$\rho_s$	Density of scale
$\sigma_y$	Horizontal dispersion coefficient as a function of downwind distance from the source
$\sigma_z$	Vertical dispersion coefficient as a function of downwind distance from the source

$\chi$	Dynamic shape factor
$\psi$	Dimensionless inertial parameter
$\psi_{50}$	Dimensionless parameter corresponding to the 50th percentile of the stage the collection efficiency ( $\psi_{50} = 0.1444$ by Ranz and Wong)

## Definitions

$AED_{50}$	An aerodynamic equivalent diameter which has 50 % collection efficiency for size selective aerosol sampler.
AED	The diameter of the unit density ( $\rho_p = 1 \text{ g/cm}^3$ ) sphere that has the same settling velocity as the particle.
Aerosol	A suspension of solid particles in a gas.
Air sampling	The collection of samples of air to measure the radioactivity or to detect the presence of radioactive material, particulate matter, or chemical pollutants in the air.
Area sample	An air sample taken at a fixed location in a workplace.
Area source	Any source of air pollution that is released over a relatively small area but which cannot be classified as a point source.
Attainment Area	A geographic area in which levels of a criteria air pollutant meet the health-based primary standard (national ambient air quality standard, or NAAQS) for the pollutant.
Breathing zone	A hemisphere of 300 mm radius extending in front of their face and measured from the midpoint of an imaginary line joining the ears.
Collection Efficiency	The efficiency of various filters can be established on the basis of entrapped particles.
Cutoff size	The performance of particle size selective devices. The 50 % cut point is the size of the dust that the device collects with 50 % efficiency.

ESD	The diameter of the sphere having the same volume as the irregular particle.
<i>ESD<sub>50</sub></i>	An equivalent spherical diameter which has 50 % collection efficiency for each Andersen impaction stage.
Gaussian	Refers to the normal distribution; phenomena whose events are "normally" distributed are "Gaussian" distributed.
Inhalable Dust	Dust that is hazardous when deposited anywhere in the respiratory tree including the nose and mouth. It has a 50 % cutoff size of AED 100 $\mu\text{m}$ .
Inverse square law	Any point source of intensity spreads its influence equally in all directions without a limit to its range if there are no reflections or reverberation.
Particulate matter	Particulate Matter is a complex mixture of particles suspended in the air that vary in size and composition. Any solid particles and liquid droplets that are small enough to remain suspended in air.
Penetration Efficiency	The efficiency of particles passed through the filter.
Pinacoid	A plane parallel to two of the crystalline axes.
PM <sub>10</sub>	PM <sub>10</sub> as particulate matter with an AED of 10 $\mu\text{m}$ collected with 50 % efficiency by a PM <sub>10</sub> sampling collection device. However, for convenience in this reference material, the term PM <sub>10</sub> includes all particles having an AED of less than or equal to 10 $\mu\text{m}$ .
PM <sub>2.5</sub>	PM <sub>2.5</sub> as particulate matter with an AED of 2.5 $\mu\text{m}$ collected with 50 % efficiency by a PM <sub>2.5</sub> sampling collection device. However, for convenience in this reference material, the term PM <sub>2.5</sub> includes all particles having an AED of less than or equal to 2.5 $\mu\text{m}$ .
Respirable Dust	Dust that has a 50 % cutoff size of AED 4 $\mu\text{m}$ .
Thoracic Dust	Dust that has a 50 % cutoff size of AED 10 $\mu\text{m}$ .
Triclinic	Having three unequal axes intersecting at oblique angles.

## CHAPTER I

### INTRODUCTION

The most important purpose of this dissertation is to quantify the potential for human exposure of suspended dust from petroleum pipe rattling operations and to compare that potential with consensus guidelines and governmental regulations for the public and for the workers. The petroleum pipe rattling process removes tightly bound scale from the inside surface of tubular petroleum pipes and removes loose corrosion products from external surfaces. To estimate the potential hazard from particulate air pollutants, several types of size selective aerosol samplers were tested.

In a chamber study, polydisperse fly ash particles were generated in the dust chamber with a controlled particle concentration to evaluate the sampling performance of several types of size selective aerosol samplers.

In a field study, the aerosol particles produced by the petroleum pipe rattling operations were collected with several types of size selective aerosol samplers. Petroleum pipes from two oilfields were rattled and sampled to estimate the potential for human exposure to the contaminant airborne particulate matter (PM).

## CHAPTER II

### PERFORMANCE EVALUATION OF SIZE SELECTIVE AEROSOL SAMPLERS

#### A. INTRODUCTION

Quantitative air sampling is used to gain knowledge of human exposure to contaminant particulate matter (PM), a complex mixture of particles suspended in the air that vary in size and composition. The health effects of PM are dependent on their chemical composition and where they are deposited in the respiratory tract. A portion of particles with large aerodynamic equivalent diameters (AEDs) ( $> 10 \mu\text{m}$ ) tend to deposit in the upper airways, and a portion of those with small AEDs ( $\leq 4 \mu\text{m}$ ) tend to deposit in airspace deep in the lungs, while the rest tend to deposit in the pharynx and upper bronchial tree.

In 1993, “Particle Size-Selective Sampling Criteria for Airborne Particulate Matter” were adopted by the American Conference of Governmental Industrial Hygienists (ACGIH) and published as Appendix D of the ACGIH TLV booklet.<sup>(1)</sup> Three particulate mass fractions were defined as inhalable, thoracic, and respirable. Their 50 % cutoff sizes ( $AED_{50}$ ) are  $100 \mu\text{m}$ ,  $10 \mu\text{m}$ , and  $4 \mu\text{m}$ , respectively (See Figure 2-1). These size conventions were co-developed and adopted by the International Organization for Standardization (ISO)<sup>(2)</sup> and the Comité Européen de Normalisation (CEN).<sup>(3)</sup> They are also the sampling size fractions recommended by American Industrial Hygiene Association (AIHA).<sup>(4)</sup>

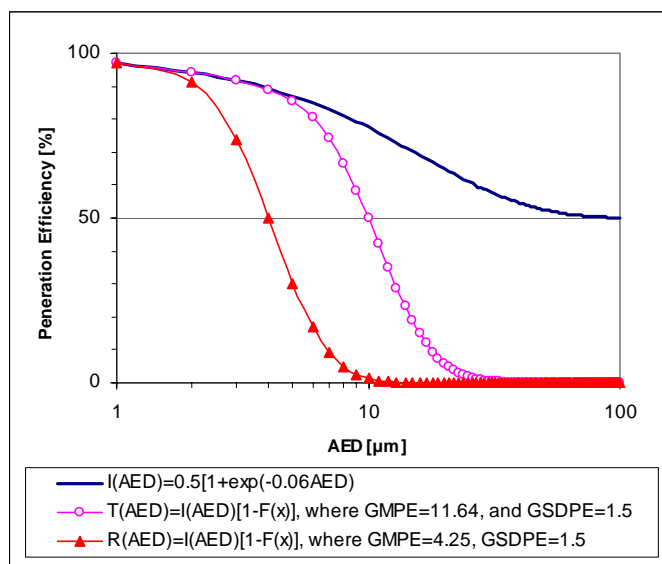


**FIGURE 2-1. ACGIH sampling criteria.** Equation source: Appendix D of the ACGIH TLV booklet.

*I (AED)* = Penetration efficiency of inhaled particles as a function of AED in  $\mu\text{m}$ ;

*T (AED)* = Penetration efficiency of thoracic particles as a function of AED in  $\mu\text{m}$ ;

*R (AED)* = Penetration efficiency of respirable particles as a function of AED in  $\mu\text{m}$ ;

$$x = \frac{\ln(AED) - \ln(GM_{PE})}{\ln(GSD_{PE})};$$

*AED* = Aerodynamic equivalent diameter;

$GM_{PE}$  = Median AED of the penetration efficiency curve;

$GSD_{PE}$  = Slope of penetration efficiency curve;

$F(x)$  = Cumulative probability function of a standardized normal variable,  $x$ .

Independently, the US Environmental Protection Agency (EPA) defined four terms for categorizing PM of different sizes as supercoarse, coarse, fine, and ultrafine with 50 % cutoff AED greater than 10  $\mu\text{m}$ , between 2.5  $\mu\text{m}$  and 10  $\mu\text{m}$ , between 0.1  $\mu\text{m}$  and 2.5  $\mu\text{m}$ , and less than 0.1  $\mu\text{m}$ . Aerosol samplers are available to collect mass fractions called: Total Suspended Particulate Matter (TSP),  $PM_{10}$ ,  $PM_{2.5}$ , Particles less than 0.1  $\mu\text{m}$ , and Condensable Particulate Matter. The EPA defines  $PM_{10}$  as particulate matter with an AED of 10  $\mu\text{m}$  collected with 50 % efficiency by a  $PM_{10}$  sampling



collection device and  $PM_{2.5}$  as particulate matter with an AED of  $2.5 \mu m$  collected with 50 % efficiency by a  $PM_{2.5}$  sampling collection device (See Figure 2-2).<sup>(5)</sup> The performance characteristics of  $PM_{10}$  and  $PM_{2.5}$  are described in Appendix D.

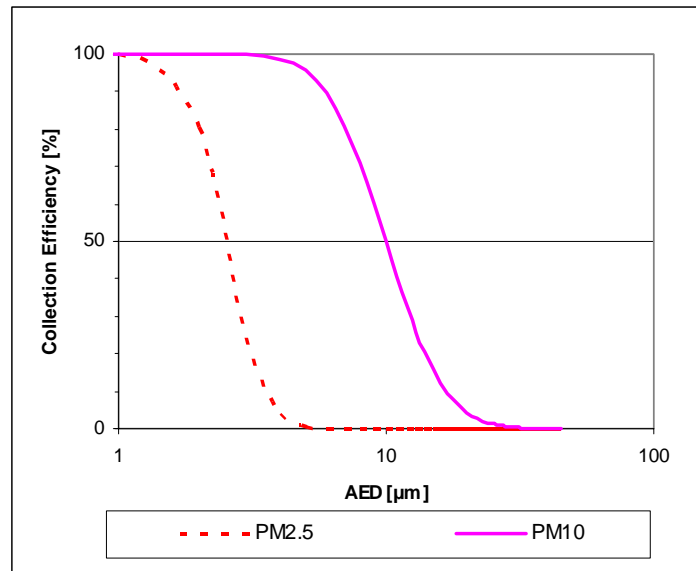


**FIGURE 2-2. EPA regulated PM pollutants.**

Careful comparison of the  $PM_{2.5}$  and  $PM_{10}$  cut curves with the respirable and thoracic curves of ACGIH reveals that the EPA specification has a steeper slope. This means an ideal EPA sampler will collect a larger number of small particles with AED slightly below its cut point and a smaller number of particles with AED slightly above its cut point than an ACGIH sampler (See Figure 2-3).

For example, if the airborne total mass concentration is  $10 \text{ mg/m}^3$  and the PSD of test aerosol is characterized by  $GM_{AED} = 11.8 \mu m$  and  $GSD_{AED} = 2.1$ , then the estimated mass concentration sampled are  $4.0 \text{ mg/m}^3$  for the ACGIH thoracic sampler and  $4.2$

mg/m<sup>3</sup> for the EPA PM<sub>10</sub> sampler. These concentrations are calculated by integrating the PSD of the test aerosol with the collection efficiency curves. The ACGIH sampler may measure slightly less mass than the PM<sub>10</sub> sampler when the PSD of airborne PM is characterized by  $GM_{AED} < 21.3 \mu\text{m}$  with the same  $GSD_{AED} = 2.1$ . While the ACGIH sampler may measure slightly more mass than the PM<sub>10</sub> sampler when the PSD of airborne PM is characterized by  $GM_{AED} \geq 21.3 \mu\text{m}$  with the same  $GSD_{AED} = 2.1$ . A detailed calculation is described in Appendix D-3.

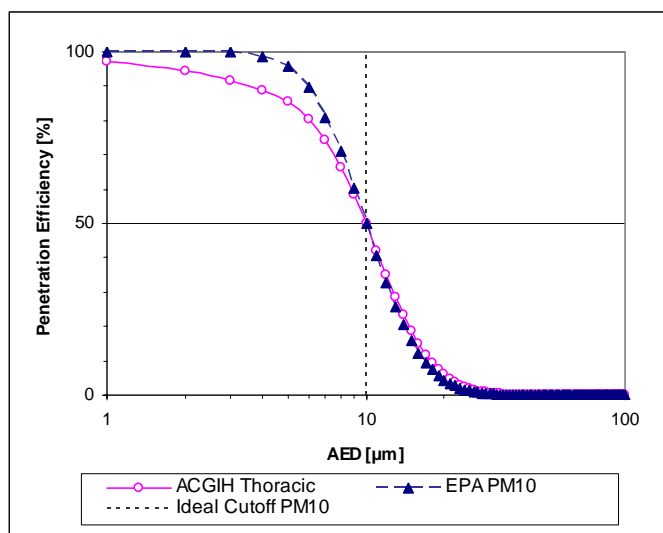


**FIGURE 2-3. ACGIH Thoracic vs. EPA PM<sub>10</sub>.**

National Ambient Air Quality Standards (NAAQS) for PM have been established to minimize the adverse effects of PM on the majority of US residents. The NAAQS established a 24-hour average limit of 150  $\mu\text{g}/\text{m}^3$  and an annual average limit of 50  $\mu\text{g}/\text{m}^3$  for PM<sub>10</sub>, and a 24-hour average limit of 65  $\mu\text{g}/\text{m}^3$  and an annual average limit of

15  $\mu\text{g}/\text{m}^3$  for  $\text{PM}_{2.5}$ .<sup>(6)</sup> In contrast, Occupational Safety and Health Administration (OSHA) Permissible Exposure Limits (PEL) for Particulates Not Otherwise Regulated (PNOR) of respirable fraction and total dust are 5  $\text{mg}/\text{m}^3$  and 15  $\text{mg}/\text{m}^3$ .<sup>(7)</sup> These limits are based on an 8-hour average during a conventional workday. The American Conference of Governmental Industrial Hygienists (ACGIH) Threshold Limit Value (TLV) for Particulates Not Otherwise Classified (PNOC) are 3  $\text{mg}/\text{m}^3$  for respirable particulates and 10  $\text{mg}/\text{m}^3$  for inhalable particulates based on a Time Weighted Average (TWA) of 8-hours per day and five days per week, and apply to particles that are inert, that are not metabolized.<sup>(8)</sup>

To estimate the potential hazard from particulate air pollutants, it is necessary to choose among many different size selective sampling instruments. Six types of aerosol samplers were tested. Three types of aerodynamic size selective aerosol samplers were used, including two Andersen cascade impactors,<sup>(9)</sup> two RespiCon serial virtual impactors,<sup>(10)</sup> and four  $\text{PM}_{10}$  samplers.<sup>(11)</sup> One type of volumetric particle size selective sampler was used, including four TSP samplers<sup>(12)</sup> with particles sized by volume using a coulter counter multisizer (TSP/CCMs). Two types of laser-light scattering particle monitors were used, including two DustTrak<sup>(13)</sup> and two SidePak<sup>(14)</sup> real-time particle number counting photometers.

The goal of the chamber study discussed in this chapter is to evaluate their sampling performances experimentally with total mass concentrations and with mass fractions for the ACGIH/CEN/ISO respirable, thoracic, and inhalable convention. It was expected that the observed differences would lie within the range of uncertainty allowed

by specifications for the samplers. The sampling performances were tested using polydisperse fly ash in a chamber with the following hypotheses:

- 1) There is no significant difference between total dust mass concentrations measured by the size selective aerosol samplers in this study.
- 2) There would be good relationships between the mass fractions from Andersen samplers, RespiCon samplers, and TSP/CCMs for ACGIH/CEN/ISO respirable ( $AED \leq 4 \mu\text{m}$ ) and thoracic ( $AED \leq 10 \mu\text{m}$ ) convention.
- 3) The mass fractions of  $PM_{10}$  and  $PM_{2.5}$  would be determined by multiplying the volume fraction of  $PM_{10}$  and  $PM_{2.5}$  estimated from a TSP/CCM by the scale density and an appropriate shape factor.

### **1. Introduction: Operating Principles of Six Aerosol Samplers**

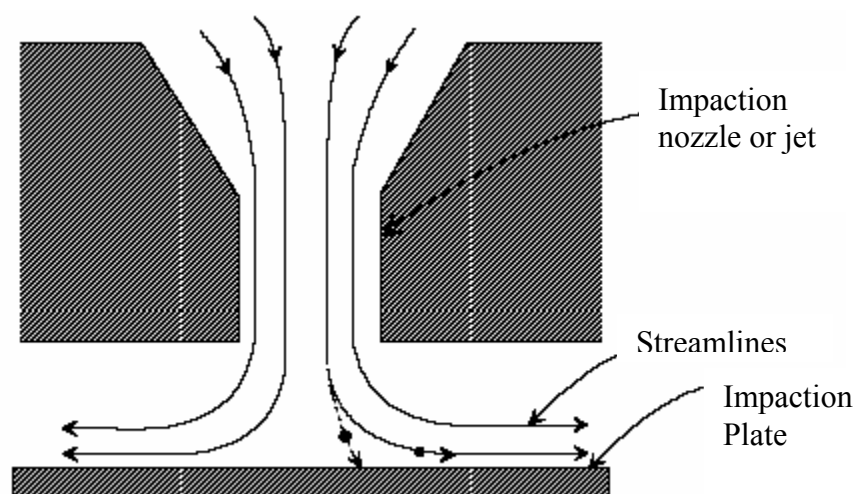
All samplers used in this study depend, in part, on particle classification by means of scaling aerodynamic inertial forces of high velocity particles. In an impactor, the particles are passed through a jet-forming nozzle and the output stream is directed against an impaction plane (real or virtual). The flow turns through a  $90^\circ$  bend in the streamlines. Particles with sufficient inertia are unable to follow the streamlines and impact the collection plane. Large particles reach the collection plane and small particles are carried away with the bypass air flow. Thus, there are two size ranges in the particles: particles larger than the AED of interest are likely to be removed from the aerosol stream by the sampler (Probability of removal  $> 0.5$ ). Those smaller than that size are likely to continue in the bypass air flow to the next stage (Probability of removal

$\leq 0.5$ ). The discussion below shows how the manufactures have implemented this principle in various air sampling geometries.

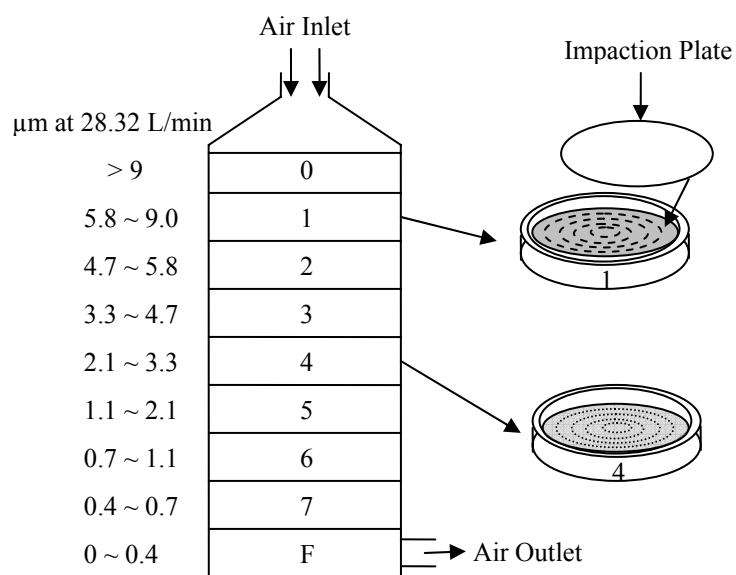
***a) Andersen Sampler***

The Andersen sampler is a one actual cubic foot per minute (1 ACFM; 28.3 L/min) non-viable ambient particle sizing sampler. It is configured as a multi-stage and multi-orifice per stage cascade impactor with stages characterized by round holes of successively smaller diameter. In the first half of the 20th century, impaction was a common method for collecting dust for the evaluation of occupational environments. In the last 50 years, the cascade impactor has been used to measure PSDs by mass.<sup>(15)</sup> All inertial impactors in this study including virtual impactors and the real-time monitors operate on the same principle.

The eight stages of the Andersen cascade impactor are designed and arranged so that the largest particles are aerodynamically impacted onto the first stage, and progressively smaller particles are aerodynamically impacted on successive stages. Stages from 0 to 6 contain 400 round orifices and stage 7 contains 210 round orifices arranged in circular patterns (See Figure 2-4). The orifices are progressively smaller from stage 0 to stage 6, and the jet velocities are progressive larger (see Table 2-1).



(a)



(b)

**FIGURE 2-4. Andersen sampler. (a) Cross sectional view of one orifice,<sup>(16)</sup>**

**(b) Schematic diagram of stacked orifice plates and impactor plates.**

**TABLE 2-1. Dimension of the Andersen Impactor Orifices**

Stage	Orifice diameter [Inch]	Number of orifices	Stage velocity <sup>A</sup> [cm/s <sup>1</sup> ]	Effective cutoff diameter ( $d_{ec}^B$ ) [μm]
0	0.0625	400	60	9
1	0.0465	400	108	5.8
2	0.0360	400	180	4.7
3	0.0280	400	297	3.3
4	0.0210	400	528	2.1
5	0.0135	400	1278	1.1
6	0.0100	400	2329	0.7
7	0.0100	210	4435	0.4

Notes:

<sup>A</sup> Stage velocity at 1 ACFM [28.32 L/min];

<sup>B</sup>  $d_{ec}$  = Effective cutoff diameter (Nominal cutoff diameter when the flow rate is at 1 ACFM [28.32 L/min]).

Large particles, which are expected to be collected in one stage, can bounce off the collection plate and be carried by horizontal flow around the edge of that plate to deposit on subsequent plates. The bounce phenomena, which affect the shape of the PSD estimated from mass per stage, were carefully studied during the latter half of the last century. May<sup>(16)</sup> emphasized the importance of coating the impaction surface with an adhesive substance. In experiments with aerosols of glass beads and polystyrene spheres, Lundgren<sup>(17)</sup> found quantitative collection when the impaction surfaces were coated with high-vacuum silicone grease or some other suitable adhesive material. A similar conclusion was reached by Rao and Whitby.<sup>(18, 19)</sup> Aiache et al.<sup>(20)</sup> studied the performance of different impactors and found that the multi-stage Andersen Cascade impactor (Mark II) exhibited a large variability. Nevertheless, this method continues to be used to obtain detailed information about the aerodynamic PSD of the thoracic and respirable fractions, especially in pharmaceutical air sampling.<sup>(21,22,23,24,25,26)</sup>

In this study, every impaction plate was cleaned and coated with silicone grease so that most deposited particles would remain on the impaction plates and not bounce off, unless the sampler ran too long and became overloaded.

The combination of a constant flow rate and successively smaller diameter orifices increase the jet velocities of sample air as it cascades through the sampler. Progressively smaller particles impact on succeeding stages. Mass per stage is measured gravimetrically. Figure 2-5 shows a PSD curve for each stage as portrayed in the operator's manual. A detailed cutoff size calculation as a function of flow is presented in Appendix E.

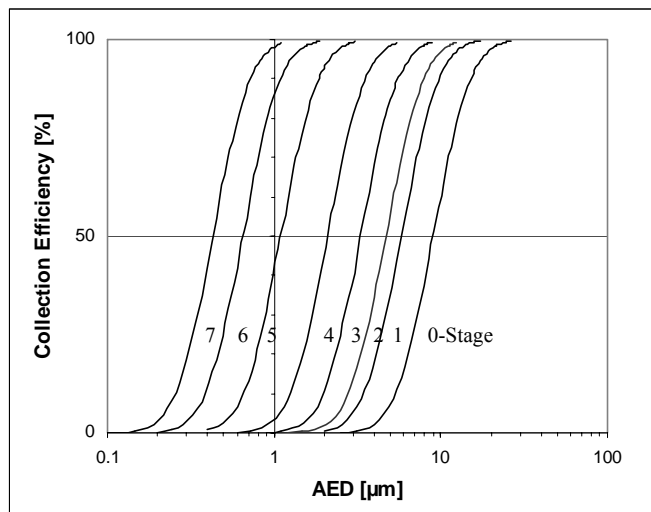


**FIGURE 2-5. Andersen sampler collection efficiency at 1 ACFM (28.32 L/min).**

Source: Andersen sampler's operator manual<sup>(27)</sup>.



***b) RespiCon Sampler***

The RespiCon sampler is a three-stage virtual impactor that simultaneously collects the ACGIH/CEN/ISO size fractions (See Figure 2-1) of respirable, thoracic, and inhalable particulate matter. It was designed by Koch et al.<sup>(28)</sup> Its inlet is symmetric with respect to horizontal wind, and serves to select particles according to the inhalable convention. Its first virtual impactor stage separates out and collects particles with AED  $\leq 4 \mu\text{m}$  (in a second version, the cut point is  $2.5 \mu\text{m}$ ). The second stage collects particles with AED  $\leq 10 \mu\text{m}$ , while the third stage collects the remaining larger particles. The benefits of the virtual impactor include its extended sampling time, its freedom from overloading, and its lack of particle bounce. As designed, the RespiCon virtual impactor captures particles gently with low velocity air through its collection filters. This contrasts with the very high impact velocities that fracture some particles on the impaction plate of traditional impactors.

In a virtual impactor, as described by Marple and Chien<sup>(29)</sup> and TSI, Inc.<sup>(30)</sup>, an aerosol passes through an accelerating nozzle toward a collection probe (See Figure 2-6). Tatum et al.<sup>(31)</sup> conclude that the RespiCon is a useful sampling device for those situations in which it is important to simultaneously collect either personal or area samples for the respirable, thoracic, and inhalable fractions of airborne PM with acceptable precision.

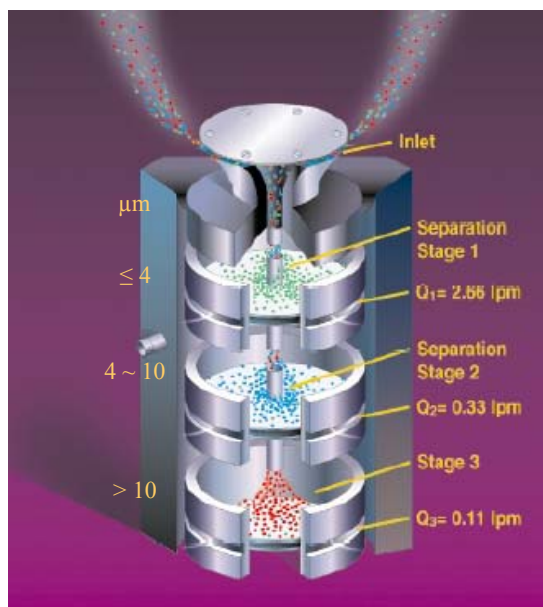


**FIGURE 2-6. Inside schematic diagram of a RespiCon sampler.**

Source: Manufacturer (TSI, Inc.) Brochure<sup>(10)</sup>.

Two models of the RespiCon Particle Samplers were used: one has a first stage 4  $\mu\text{m}$  cutoff size which represents the ISO respirable size fractions, while the other has a first stage 2.5  $\mu\text{m}$  cutoff size which represents the EPA  $\text{PM}_{2.5}$  measurements. The second stage has a 10  $\mu\text{m}$  cutoff and its mass is summed with the first stage for both the ISO thoracic and EPA  $\text{PM}_{10}$  fractions. The sum of three stages provides a usable estimate for the ISO inhalable fraction, the EPA total suspended particulate measurement, and the OSHA total dust PEL. Li et al.<sup>(32)</sup> found that the sampling performance of the RespiCon sampler matched the inhalable convention fairly well in the laboratory with horizontal wind speeds of 0.55 m/s and 1.1 m/s with particles ranging from AED 5  $\mu\text{m}$  to 68  $\mu\text{m}$ .

*c) Total Suspended Particulate Sampler and a Coulter Counter Multisizer*

The flow rate of the low volume TSP sampler (16.7 L/min) was designed by Wanjura et al.<sup>(33)</sup> at Texas A&M University (See Figure 2-7). They called it low volume because standard PM<sub>10</sub> and PM<sub>2.5</sub> samplers operate at much higher flow rates (> 40 ACFM; 1132.7 L/min). They reported that the low volume TSP sampler may be more robust and more accurate than the standard high volume TSP sampler on the basis that they found no significance difference between the two low volume samplers with a t-test, and there was a significant difference detected between two low volume TSPs and a high volume sampler (1416.7 L/min) with an ANOVA test. In this study, the low volume TSP sampler is called the TSP sampler.

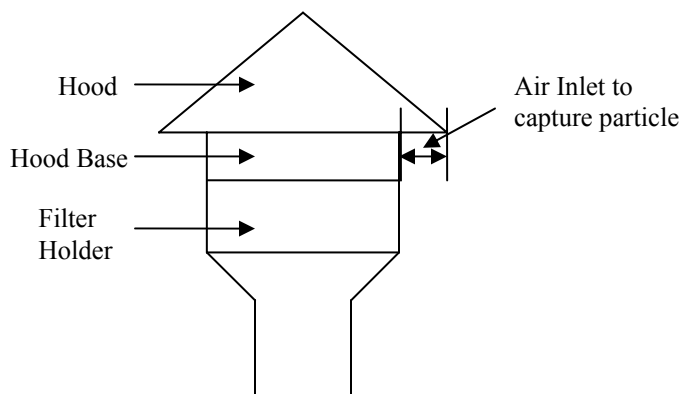


**FIGURE 2-7. Schematic diagram of a TSP sampler.**

#### *d) PM<sub>10</sub> Sampler*

The Graseby-Andersen Federal Reference Method (FRM) PM<sub>10</sub> inlet was used for the EPA approved PM<sub>10</sub> samplers to capture PM less than or equal to an AED 10 µm and to remove PM with AED larger than 10 µm (See Figure 2-8). The PM<sub>10</sub> samplers operated at the flow rate of 16.7 L/min. McFarland et al.<sup>(34)</sup> reported that the PM<sub>10</sub> sampler has an *AED*<sub>50</sub> of 10.2 µm and a slope of 1.41 with liquid aerosols. The FRM performance standard calls for an *AED*<sub>50</sub> of 10 µm ± 0.5 µm and a slope of 1.5 ± 0.1.<sup>(35)</sup>

A detailed analysis of allowed variations in PM<sub>10</sub> collection efficiency is presented in Appendix D. It shows that although the point design should collect 50 % of particles with AED = 10 µm, a sampler that collects between 44 % and 56 % of 10 µm particles is acceptable under the standard. Appendix D shows that the range of allowable PM<sub>10</sub> concentration estimates is significant. In air with total mass concentration of 10 mg/m<sup>3</sup>, the actual concentration of all particles with AED ≤ 10 µm is 4.12 mg/m<sup>3</sup>. A PM<sub>10</sub> sampler with nominal FRM parameters would measure 4.22 mg/m<sup>3</sup>, while other PM<sub>10</sub> samplers with extreme, but acceptable, parameter values would report concentrations between 3.95 mg/m<sup>3</sup> and 4.47 mg/m<sup>3</sup>.

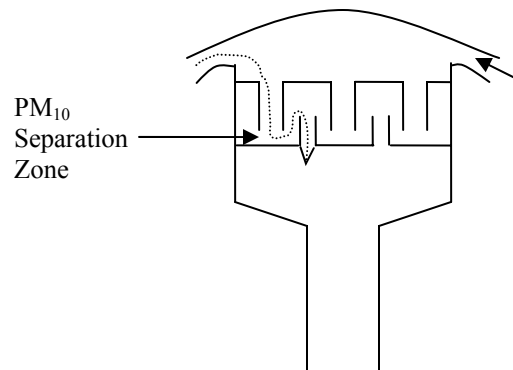


**FIGURE 2-8. Schematic diagram of a PM<sub>10</sub> sampler showing its circularly symmetric inlet and its design as a plate impactor with side walls to minimize particle bounce and subsequent carry through of large particles.**

*e) DustTrak and SidePak Monitors*

The DustTrak and SidePak Aerosol Monitors, from TSI Inc., are portable and battery-operated laser photometers using an optional impactor as a preseparator. Two impactors for the cutoff sizes 10  $\mu\text{m}$  (10  $\mu\text{m}$  inlet) and 2.5  $\mu\text{m}$  (2.5  $\mu\text{m}$  inlet) were used in two DustTrak monitors and two impactors for the cutoff sizes 2.5  $\mu\text{m}$  (2.5  $\mu\text{m}$  inlet) and 1  $\mu\text{m}$  (1  $\mu\text{m}$  inlet) were used in two SidePak monitors (See Figure 2-9). As mentioned in the beginning of introduction, the impaction plate collects particles bigger than a certain size of interest and passes those smaller than that size through the impactor stage for detection. The impactor plates of the DustTrak and SidePak monitors were smeared with a thin layer of grease to minimize bounce. Unfortunately, under conditions of this study, these plates overloaded quickly, so particle bounce is likely.

These monitors measure and record real time airborne PM concentrations reported in milligrams per cubic meter ( $\text{mg}/\text{m}^3$ ). Data were logged into memory at one second intervals during each test. Mass is determined indirectly from the intensity of light scattered by the particles within a fixed sensing volume. The mass concentration scale was calibrated by the manufacturer against a gravimetric measurement using the respirable fraction of standard ISO 12103-1, A1 test dust (Arizona Test Dust). The scale was not calibrated for fly ash used in this study because there is no provision for sampling exhaust air from these devices.



**FIGURE 2-9. Impactors used as size selective pre-filters in real-time monitors.**

**(a) DustTrak, (b) SidePak.**

The pictures of all aerosol samplers used in this study are shown in Figure 2-10.

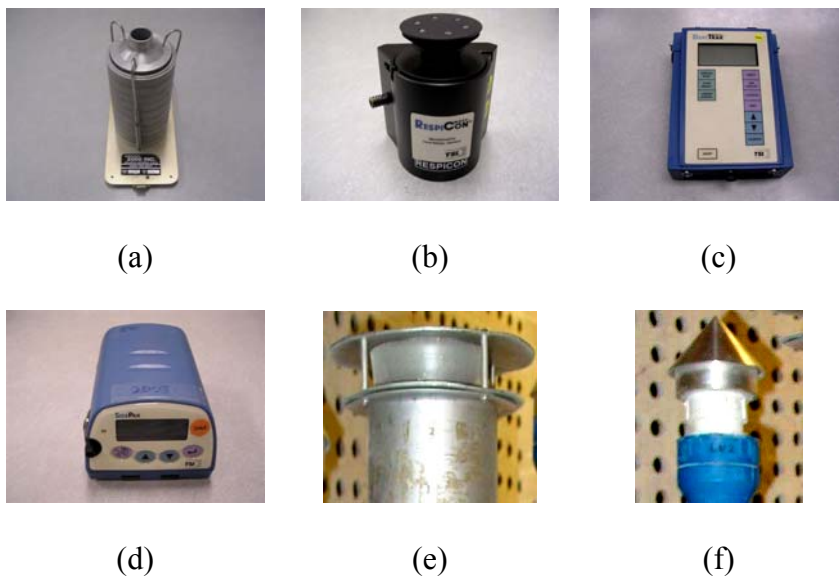


**FIGURE 2-10. Aerosol samplers used in a chamber study. (a) Andersen sampler, (b) RespiCon sampler, (c) DustTrak monitor, (d) SidePak monitor, (e) PM<sub>10</sub> sampler, (f) TSP sampler.**

## 2. Particle Sizing Methods Introduction

In this study, three broad cumulative mass fractions for respirable ( $AED \leq 4 \mu\text{m}$ ), thoracic ( $AED \leq 10 \mu\text{m}$ ), and inhalable ( $AED \leq 100 \mu\text{m}$ ) PM were obtained by RespiCon samplers (one RespiCon captured PM<sub>2.5</sub> rather than the respirable fraction), and were calculated from measurements by Andersen samplers, and by TSP/CCM samplers. These data were compared to each other.

Hinds indicated that lognormal distribution is the most common distribution used for characterizing the particle sizes associated with the aerosol.<sup>(36)</sup> The significance of a lognormal distribution is that the particle size distribution (PSD) can be described in

terms of only two parameters, called the geometric mean ( $GM$ ) and the geometric standard deviation ( $GSD$ ). In this study,  $GM_{AED}$  and  $GSD_{AED}$  represent the median AED of the sample data and the slope of PSD curve.

The Reliasoft Weibull++ program was used to conduct the Goodness of Fit (GOF) test to find the best distribution of airborne fly ash by a TSP/CCM. When the raw data of a TSP/CCM were put into the Weibull++ program, the software ranked for the best distribution of Lognormal and Normal, Exponential 1-parameter, Exponential 2-parameter, Weibull 2-parameter, and Weibull 3-parameter distributions. The results show that the lognormal distribution ranked first at 9 PSDs of 11 PSDs by TSP/CCM, and it ranked two and three one time each when the Weibull 2-parameter distribution was ranked as one.

In this study, the PSD of a TSP/CCM was characterized by a  $GM_{AED}$  and a  $GSD_{AED}$  using Equation 2.1 on the basis of GOF test.

$$GSD = \frac{d_{84.1}}{GM_{AED}} = \frac{GM_{AED}}{d_{15.9}} = \sqrt{\frac{d_{84.1}}{d_{15.9}}} \text{ for the PSD of fly ash} \quad (2.1)$$

where  $d_{84.1}$  = AED corresponding to the 84.1 % of the PSD or 84.1 % of the stage sampling efficiency curve,

$d_{15.9}$  = AED corresponding to the 15.9 % of the PSD or 15.9 % of the stage sampling efficiency curve,

$GM_{AED}$  = Median AED corresponding to the 50 % of the PSD or 50 % of the stage sampling efficiency curve.



The PSD of the Andersen sampler was characterized by a  $GM_{AED}$  and a  $GSD_{AED}$  using Equation 2.3.<sup>(37)</sup> The mass fractions of the first and last impaction stages were neglected in this analysis to obtain best log-probit curve. The log-probit graphs for each test are introduced in Appendix A-8.

$$z = \frac{x - \mu}{\sigma} \hat{=} \frac{\ln(x) - \ln(GM_{AED})}{\ln(GSD_{AED})} \quad (2.2)$$

$$\ln(x) \hat{=} \ln(GSD_{AED}) \times z + \ln(GM_{AED}) \quad (2.3)$$

where  $z$  = Standard normal random variable (Mass fraction),

$x$  = Normal random variable (Aerodynamic equivalent diameter),

$\mu$  = Population mean,

$\sigma$  = Population standard deviation,

$GM_{AED}$  = Sample geometric mean (Median AED of sample data),

$GSD_{AED}$  = Sample geometric standard deviation (Slope of sampling efficiency curve).

A linear regression model was conducted using the least squares estimators to predict the best PSD and prediction interval at 95 % confidence level for Andersen samplers and TSP/CCMs (See Equation 2.4). The Mathematica code used for this analysis is offered in Appendix I-3.

$$\hat{y}_0 - t_{\alpha/2, n-2} \sqrt{\hat{\sigma}^2 \left[ 1 + \frac{1}{n} + \frac{(x_0 - \bar{x})^2}{S_{xx}} \right]} \leq y_0 \leq \hat{y}_0 + t_{\alpha/2, n-2} \sqrt{\hat{\sigma}^2 \left[ 1 + \frac{1}{n} + \frac{(x_0 - \bar{x})^2}{S_{xx}} \right]} \quad (2.4)$$

$$\text{where } \hat{y}_0 = \hat{\beta}_0 + \hat{\beta}_1 x_0, \quad S_{xx} = \sum_{i=1}^n (x_i - \bar{x})^2 = \sum_{i=1}^n x_i^2 - \frac{\left( \sum_{i=1}^n x_i \right)^2}{n},$$

$y_0$  = Future observation of mass fraction,  $\hat{y}_0$  = Estimator of  $y_0$ ,  $x_0$  = new observation,

$\hat{y}_0 = \hat{\beta}_0 + \hat{\beta}_1 x_0$  = Point estimator of the future observation,

$\hat{\beta}_0$  = Estimator of intercept  $\beta_0$ ,  $\hat{\beta}_1$  = Estimator of slope  $\beta_1$ ,  $x_i$  =  $i$ th observation of  $x$ ,

$x$  = AED,  $y$  = Mass fraction,  $n$  = Number of case,  $\bar{x}$  = Mean of AED,  $t$  =  $t$  distribution.

A log-probit analysis was conducted to visualize the collection efficiency of Andersen sampler. The PSD for each stage of Andersen sampler was not tested by a CCM analysis because there was not enough mass to run a CCM.

The CCM was used to find the PSD of the fly ash from TSP samplers. The result of analysis by a TSP/CCM is a histogram of particle volume fraction as a function of equivalent spherical diameter (ESD). An ESD is the diameter of the sphere having the same volume as the irregular particle. The ESD resulting from the PSD by a CCM was converted to an AED using Equation 2.1 using appropriate density ( $2.7 \text{ g/cm}^3$ ) and shape factor ( $\chi = 1$ ). Then, PSDs by TSP/CCMs are expressed in terms of AED. This means that no matter a particle's shape or density, it has the same settling velocity as a unit density sphere ( $\rho_p = 1 \text{ g/cm}^3$ ) with the equivalent AED. In this chapter, all comparisons are based on an AED.

The same dynamic shape factor ( $\chi = 1$ ) for all the different particle size ranges is used because the particle shape was totally spherical when the images of fly ash were obtained from an environmental scanning electron microscopy (ESEM) (See Figure 2-11). Shape factors for non-spherical particles are described more fully in Appendix G.

$$AED = ESD \left[ \frac{\rho_p}{\rho_0 \cdot \chi} \right]^{\frac{1}{2}} \quad (2.5)$$

where  $AED$  = Aerodynamic Equivalent Diameter [ $\mu\text{m}$ ], a calculated estimate,

$ESD$  = Equivalent Spherical Diameter [ $\mu\text{m}$ ], calculated from volume measured by CCM,  
 $\rho_p$  = Particle Density [ $\text{g}/\text{cm}^3$ ],  $\rho_0$  = Unit Density ( $1 \text{ g}/\text{cm}^3$ ),  $\chi$  = Dynamic shape factor ( $\chi$   
 $=1$  for fly ash).

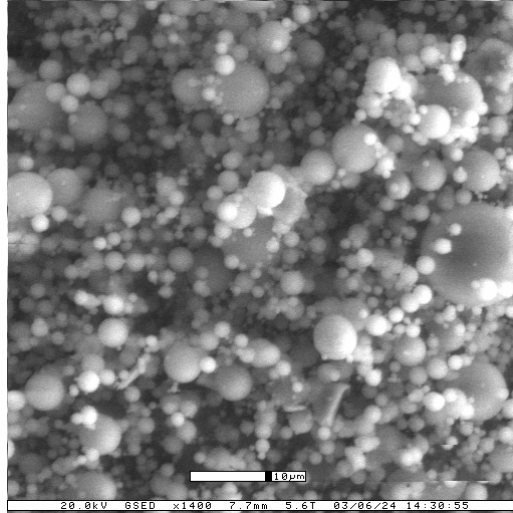


**FIGURE 2-11. The general shape of fly ash.** (Calibration bar =  $10 \mu\text{m}$ ; a RespiCon sampler Stage 1).

The CCM was operated with its  $100 \mu\text{m}$  aperture installed to obtain a PSD from the TSP samplers. The CCM counts the particle size range in terms of ESD ranging from 2 % to 60 % of aperture diameter. In this study, that corresponds to particle sizes measured from ESD  $2 \mu\text{m}$  to ESD  $60 \mu\text{m}$ . Factoring in density and shape factor with Equation 2.1, the equivalent range for the AED is from  $3.3 \mu\text{m}$  to  $99 \mu\text{m}$ .

Thus, the cumulative PSD for the truncated AED  $< 3.3 \mu\text{m}$  was estimated using a  $GM_{AED}$  and a  $GSD_{AED}$  obtained from each TSP/CCM.

When a more detailed analysis of experimental PM samples is needed for the respirable convention, or for  $PM_{2.5}$ , smaller apertures should be installed in the CCM. Because this option was not available during this study, the best fit lognormal density function was used to reconstruct data not sampled in the lower tail for particles with  $AED < 3.3$  micrometer.

### **3. Statistical Analyses Introduction**

In this study, a randomized block procedure (PROC GLM) was conducted using the SAS program to test the null hypothesis that the true population means of the total fly ash concentration measured by two Andersen samplers and four TSP samplers are the same.

The GLM procedure uses the method of least squares to fit general linear models. Among the statistical methods available in PROC GLM are regression, analysis of variance, analysis of covariance, multivariate analysis of variance, and partial correlation. The TUKEY (Tukey's studentized range test) option was selected to find the relationship between samplers. Details are summarized in Appendix C.

## **B. METHODS**

The chamber experiment was conducted in the Center for Agricultural Air Quality Engineering and Science (CAAQES) Processing Lab at Texas A&M University. Polydisperse fly ash particles (bulk density =  $2.7 \text{ g/cm}^3$ ) were generated in the dust chamber with a controlled PM concentration. A  $GM_{BS}$  of  $11.8 \text{ } \mu\text{m}$  and a  $GSD_{BS}$  of 2.1

were measured by a CCM from a bulk sample of the fly ash used in a chamber.  $GM_{BS}$  and  $GSD_{BS}$  represent the median AED of bulk sample and the slope of bulk sample's PSD curve, respectively. The bulk density of  $2.7 \times (1 \pm 3 \%) \text{ g/cm}^3$  was measured by an AccuPyc 1330 pycnometer (Micromeritics Instr. Corp., Norcross, GA).

This chamber was initially designed and built for Pargmann's research.<sup>(38)</sup> Figure 2-12 shows the arrangement of the samplers in the dust chamber. In order to estimate the relationship between the samplers, all six samplers were co-located with the following conditions.

1. The exposure section of the chamber is cubical with a length of 2.4 m on each side.
2. The generated volume flow rate that recirculates through the chamber is  $128 \text{ m}^3/\text{min}$ .
3. The perforated walls, which have 18 % open area, act as airflow straighteners to provide nearly uniformly distributed air across the chamber cross-section. The velocity through the holes is estimated to have been 2.1 m/s, and the velocity through the chamber and past the samplers is estimated to have higher than 0.4 m/s due to partial flow restriction caused by the samplers and the boxes on which some samplers were mounted.
4. Andersen samplers, DustTrak monitors, and SidePak monitors were located at a height of 115 cm above the chamber floor.
5. RespiCon samplers were located at a height of 150 cm above the chamber floor.
6. TSP samplers and  $\text{PM}_{10}$  samplers were located at a height of 160 cm above the chamber floor.

7. The first and second tests were one hour tests. The third test was intended to have two-hour duration, but because of trends toward filter overloading, the PM<sub>10</sub> samplers and TSP samplers were stopped after one hour. Planned two-hour tests were completed with the Andersen samplers, RespiCon samplers, DustTrak monitors, and SidePak monitors.
8. The chamber was cleaned after each test before starting a new experiment with new dust.
9. Teflon filters with a 0.5 µm pore size were used for the RespiCon samplers, PM<sub>10</sub> samplers, and TSP samplers to assure consistency between samplers on both tests.
10. A high-precision analytical balance with its precision ± 10 µg (AG245, Mettler Toledo, Greifensee Switzerland) was used to weigh the filters measured by all samplers. Each filter and plate was weighed three times and the average value was recorded.
11. The required airflows for Andersen, TSP, and PM<sub>10</sub> samplers were controlled with a needle valve using a diaphragm pump with a flow-restricting orifice (Dayton, 4z792). The airflow rate was logged and recorded by a data logger (HOBO H8 RH/Temp/2X External) at 12 second intervals.
12. The orifice meter pressure drop was converted to volumetric flow using Equation 2.6.

$$Q = 5.976 \cdot K \cdot D_o^2 \cdot \sqrt{\frac{\Delta P}{\rho_{air}}} \quad (2.6)$$

$Q$  = Airflow rate through the orifice meter [m<sup>3</sup>/s],  $K$  = flow coefficient of orifice,

$D_o$  = orifice meter [m],  $\Delta P$  = measured pressure drop across the orifice [mmH<sub>2</sub>O], and

$\rho_{air}$  = air density estimated from temperature and pressure [kg/m<sup>3</sup>].

13. Due to a miscalculation of pressure drop, the airflow rates for the Andersen sampler were adjusted to 0.8 ACFM (22.65 L/min) instead of 1 ACFM (28.32 L/min).
14. The airflow rates for RespiCon Samplers were adjusted to 3.11 L/min.
15. The airflow rates for TSP and PM<sub>10</sub> samplers were adjusted to 16.67 L/min.
16. The airflow rates for DustTrak and SidePak monitors were adjusted to 1.7 L/min prior to each experiment using a flow meter provided by the TSI Company. The concentration scale was zeroed with a zero filter prior to each experiment.



**FIGURE 2-12. Experimental setup in a chamber.**

## **C. RESULTS**

### **1. Total Mass Concentration**

The total mass concentrations from Andersen and TSP samplers are arranged in Table 2-2. A randomized block hypothesis test, described below, shows that there is significance difference between the total mass concentration estimated by the Andersen

and by the TSP samplers. Inspection of Table 2-2 shows that in each test, The Andersen data were smaller than any of the TSP data.

**TABLE 2-2. Total Mass Concentration Measured with Andersen and TSP**

**Samplers**

Sampler	Andersen		TSP sampler			
	C1 <sup>A</sup>	C2	T1 <sup>B</sup>	T2	T3	T4
Test 1	29.2 (1.0)	29.5 (1.0)	33.6 (1.9)	34.5 (1.8)	31.6 (2.3)	34.7 (2.4)
Test 2	21.4 (0.7)	21.5 (0.8)	24.0 (1.1)	24.5 (0.9)	25.6 (1.0)	25.2 (0.8)
Test 3	23.5 (0.5)	23.9 (0.5)	25.0 (1.4)	25.7 (2.0)	30.0 (1.7)	30.0 (1.6)

Notes:

Unit: [mg/m<sup>3</sup>]  $\bar{C}$  (SD)<sup>C</sup>

TSP samplers ran for 1 hour run in all three tests.

Andersen samplers ran for 1 hour in tests 1 & 2, and for 2 hour in test 3.

<sup>A</sup> C1 & C2 = Andersen samplers; <sup>B</sup> T1-T4 = TSP samplers; <sup>C</sup>  $\bar{C}$  = Average concentration from 3 times filter measurements; (SD) = Standard deviation were obtained using an error propagation.

$$C = \frac{\text{Mass}}{Q \times T}, \quad \frac{SD_C}{C} = \sqrt{\left( \frac{SD_W^2}{W} + \frac{SD_Q^2}{Q} + \frac{SD_T^2}{T} \right)}$$

where  $C$  = Concentration;  $W$  = Weighing;  $Q$  = Volume flow rate;  $T$  = Time;  $SD$  = Standard deviation.

This subjective conclusion remains apparent after reducing the data to summary descriptive statistics for each type of sampler in each test. The descriptive statistics are summarized in Table 2-3 and in Figure 2-13, below.

Table 2-3 and Figure 2-13 show that Andersen underestimates total mass concentration when compared with the newer design of TSP sampler. This is to be expected as the two samplers have very different inlets and the Andersen sampler has more wall losses.



**TABLE 2-3. Average Mass Concentration Measured with Andersen and TSP Samplers**

Sampler	Andersen n = 2	TSP sampler n = 4
	Mean $\pm$ $SU^A$	Mean $\pm$ $SU$
Test 1	29.4 $\pm$ 2.8	33.6 $\pm$ 8.4
Test 2	21.5 $\pm$ 2.1	24.8 $\pm$ 3.8
Test 3	23.7 $\pm$ 1.4	27.7 $\pm$ 7.2
All data	24.8 $\pm$ 4.7	28.7 $\pm$ 11.1

Notes:

Unit: [mg/m<sup>3</sup>]

$$^A SU = \left( 1.96 \times \frac{SD_C}{\sqrt{n}} \right) = \text{Sampling Uncertainty of mean}$$

where n = the number of cases; 1.96 = z-value for 95 % confidence level;

$SD_C$  = standard deviation of measured concentrations;

$$\frac{SD_C}{\bar{C}_T} = \sqrt{\left( \frac{SE}{\bar{C}_T} \right)^2 + \left( \frac{SD_1}{\bar{C}_1} \right)^2 + \dots + \left( \frac{SD_n}{\bar{C}_n} \right)^2}$$

standard deviation for an error propagation of n samplers

where  $\bar{C}_T$  = Average concentration of n samplers;  $SE$  = standard error of sample mean;

$SD_n$  = Standard deviation of  $n^{\text{th}}$  sampler;  $\bar{C}_n$  = Concentration of  $n^{\text{th}}$  sample.

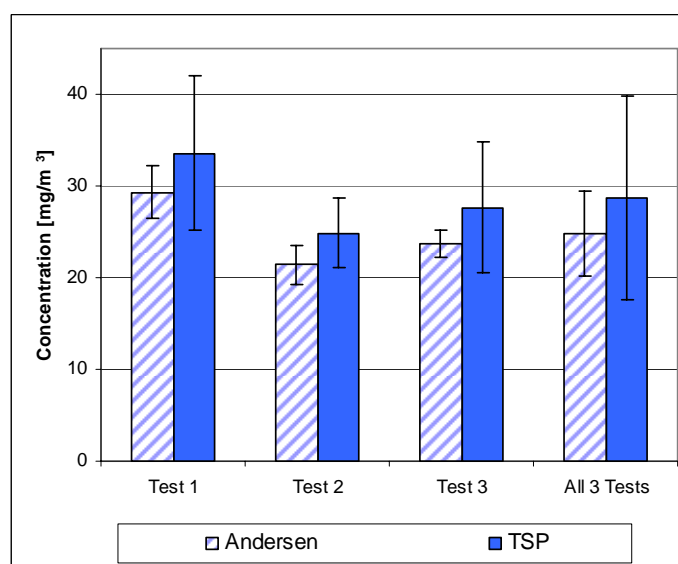


**FIGURE 2-13. Average concentration measured with Andersen and TSP samplers.**

Note: Error bar = Sampling uncertainty of mean.

To confirm the subjective evaluation that the Andersen samplers are systematically biased to report lower concentrations than the TSP samplers, conduct a randomized block test of the hypothesis that these six samplers reported the same mean values for total mass concentration in all three tests. This test was conducted using a PROC general linear model (GLM) in SAS program (SAS Institute Inc., Cary, NC) between two Andersen samplers and four TSP samplers to evaluate the performance of size selective aerosol samplers. The TSP samplers were used for reference samplers in the block design because it, alone among these samplers, was designed to measure total particulate mass.

The Randomized block design was used to test for statistical differences between total concentration estimates of the samplers at 95 % confidence level. The null hypothesis is that the true population mean of the fly ash concentration sampler is the same for all samplers. The hypothesis is based on the implicit assumption that all samplers were exposed to the same concentration during each chamber experiment.

$$H_0: \mu_{C1} = \mu_{C2} = \mu_{T1} = \mu_{T2} = \mu_{T3} = \mu_{T4}$$

$H_A$ : Not all the  $\mu_j$ 's are equal

where  $C1$  &  $C2$  = Andersen samplers;  $T1-T4$  = TSP samplers.

The PROC GLM procedure ( $\alpha = 0.05$ ) rejected the null hypothesis ( $p = 0.0047$ ). Tukey's test shows that there is no significant difference between the same types of sampler. These results show that there is an overlap in Tukey Grouping. Two of four TSP samplers are overlapped. The randomized block code in SAS and its results are described in Appendix C.

The hypothesis test confirms the observation from Table 2-3 and Figure 2-13 that in all three tests the Andersen sampler underestimated the total dust concentration when compared with the TSP sampler. The normalizing factor ( $1.16 \pm 0.01$ ) for the Andersen sampler was obtained from the overall average concentration (See Equation 2.7).

$$\begin{aligned} & \text{Normalizing Factor for Andersen sampler} \\ & = \frac{\text{Overall Average Concentration of TSP sampler}}{\text{Average Concentration of Each Andersen Sampler}} \end{aligned} \quad (2.7)$$

This normalizing factor for the Andersen samplers suggests that there is a  $16 \% \pm 1 \%$  loss of particle mass. This result was consistent with the author's observation after each experiment when the Andersen samplers were cleaned. Many particles were found on the wall and in the holes of the orifice plates for each stage of the Andersen sampler. Additionally, the inlet design of the Andersen may undersample particles with  $AED > 10 \mu\text{m}$  at its operating air velocity of 2.1 m/s.

## 2. Particle Size Distribution

The  $GM_{AED}$  and  $GSD_{AED}$  for the Particle Size Distribution estimated by the Andersen samplers were estimated using the principle of least squares fitting to the log normal cumulative density function (See Table 2-4). The  $GM_{AED}$  and  $GSD_{AED}$  for the PSD estimated by the TSP/CCM samplers were also estimated the same way (See Table 2-5).

**TABLE 2-4. Parameters for Estimated PSD from Andersen Sampler Data**

Test	Test 1		Test 2		Test 3	
	C1 <sup>A</sup>	C2	C1	C2	C1	C2
$GM_{EAED}^B$ [ $\mu\text{m}$ ]	4.7 (0.3)	4.9 (0.3)	4.6 (0.3)	4.7 (0.3)	4.7 (0.2)	4.8 (0.2)
$GSD_{EAED}^C$	1.9 (0.1)	2.0 (0.1)	2.1 (0.1)	1.9 (0.1)	2.1 (0.1)	1.9 (0.1)

Notes:

Unit:  $GM_{EAED}$  (SU) and  $GSD_{EAED}$  (SU)<sup>D</sup><sup>A</sup> C1 & C2 = Andersen samplers.<sup>B</sup>  $GM_{EAED}$  = Estimated median AED of sample data (See Appendix A-8).<sup>C</sup>  $GSD_{EAED}$  = Estimated slope of estimated PSD curve (See Appendix A-8).

$$^D \frac{SD_{GM_{EAED}}}{GM_{EAED} \text{ (or } GSD_{EAED})} = \sqrt{\left(\frac{SD_W}{\bar{W}}\right)^2 + \left(\frac{SD_Q}{\bar{Q}}\right)^2 + \left(\frac{SD_T}{\bar{T}}\right)^2},$$

where  $SD$  = Standard deviation;  $W$  = Weighing;  $Q$  = Volume flow rate;  $T$  = Time; $SD_{GM_{EAED}}$  (or  $SD_{GSD_{EAED}}$ ) = Standard deviation of  $GM_{EAED}$  (or  $GSD_{EAED}$ ). $SU_{GM_{EAED}}$  (or  $SU_{GSD_{EAED}}$ ) = Sampling uncertainty of  $GM_{EAED}$  or  $GSD_{EAED} = 1.96 \times SE$ .**TABLE 2-5. Parameters for Estimated PSD from TSP/CCM Data**

Test	Test 1				Test 2				Test 3		
	T1 <sup>A</sup>	T2	T3	T4	T1	T2	T3	T4	T1	T2	T4
$GM_{EAED}^B$	6.4	7.1	6.6	6.6	6.1	6.6	6.3	7.1	4.9	6.6	8.3
[ $\mu\text{m}$ ]	(1.3)	(1.4)	(1.6)	(1.6)	(1.1)	(1.1)	(1.1)	(1.2)	(1.0)	(1.7)	(1.7)
$GSD_{EAED}^C$	1.8	1.9	1.8	2.0	1.7	1.8	1.8	2.0	1.7	1.9	2.0
	(0.4)	(0.4)	(0.4)	(0.5)	(0.3)	(0.3)	(0.3)	(0.3)	(0.4)	(0.5)	(0.4)

Notes:

Unit:  $GM_{EAED}$  (SU) and  $GSD_{EAED}$  (SU)<sup>D</sup><sup>A</sup> T1-T4 = TSP samplers; T3 in Test 3 = the filter was used to get images by an ESEM.<sup>B</sup>  $GM_{EAED}$  = Estimated median AED of sample data (See Appendix A-5).<sup>C</sup>  $GSD_{EAED}$  = Estimated slope of estimated PSD curve (See Appendix A-5).

$$^D \frac{SD_{GM_{EAED}}}{GM_{EAED} \text{ (or } GSD_{EAED})} = \sqrt{\left(\frac{SD_W}{\bar{W}}\right)^2 + \left(\frac{SD_Q}{\bar{Q}}\right)^2 + \left(\frac{SD_T}{\bar{T}}\right)^2 + \left(\frac{SD_{\rho_p}}{\bar{\rho}_p}\right)^2 + \left(\frac{SD_{\chi}}{\bar{\chi}}\right)^2},$$

where  $SD$  = Standard deviation;  $W$  = Weighing;  $Q$  = Volume flow rate;  $T$  = Time;  $\rho_p$  = Density of particles;  $\chi$  = Shape factor; and  $SD$  = Standard deviation.The equations above were based on the conversion from ESD to AED using  $AED = ESD \left[ \frac{\rho_p}{\rho_0 \cdot \chi} \right]^{1/2}$ where  $AED$  = Aerodynamic equivalent diameter;  $ESD$  = Equivalent spherical diameter; $\rho_0$  = Unit Density ( $1 \text{ g} \cdot \text{cm}^{-3}$ );  $\chi$  = Dynamic shape factor. $SU_{GM_{EAED}}$  (or  $SU_{GSD_{EAED}}$ ) = Sampling uncertainty of  $GM_{EAED}$  or  $GSD_{EAED} = 1.96 \times SE$  $SD_{\rho_p}/\bar{\rho}_p$  and  $SD_{\chi}/\bar{\chi}$  were estimated as  $0.1 \equiv (2.7 \pm 0.2) \text{ g/cm}^3$  and as 0.01 (from ESEM images).

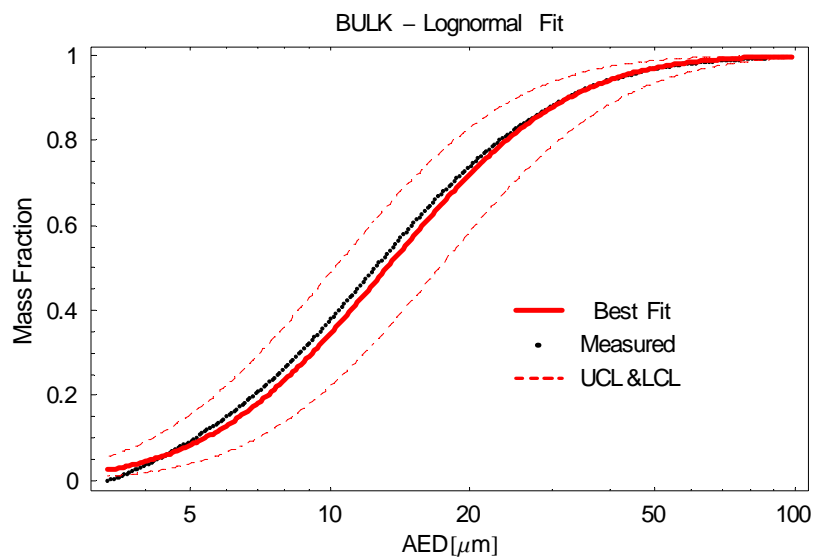
To find the relationship between the Andersen sampler and TSP/CCM for a  $GM_{EAED}$  and a  $GSD_{EAED}$ , the overall averages of  $GM_{EAEDS}$  and  $GSD_{EAEDS}$  from all tests

were calculated as  $4.7 \mu\text{m} \pm 0.2 \mu\text{m}$  and  $2.0 \pm 0.2$  for Andersen sampler and  $6.6 \mu\text{m} \pm 1.6 \mu\text{m}$  and  $1.9 \pm 0.2$  for TSP/CCMs at 95% confidence level. The relationships derived between the two samplers are (See Equations 2.8 and 2.9):

$$GM_{TSP/CCM} = (1.39 \pm 0.67) \times GM_{Andersen} \quad (2.8)$$

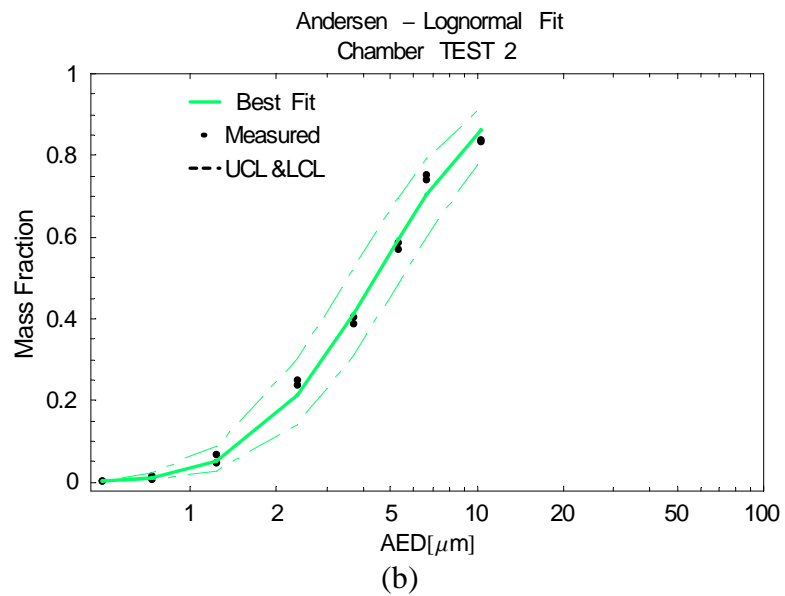
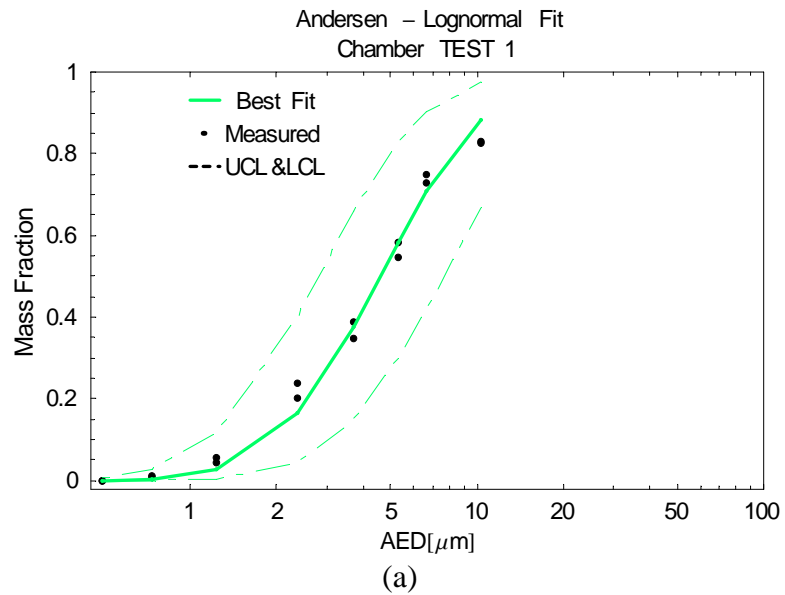
$$GSD_{TSP/CCM} = (0.86 \pm 0.28) \times GSD_{Andersen} \quad (2.9)$$

The best PSD of the bulk sample of fly ash distributed in a chamber was obtained with a log-probit analysis and a regression analysis for prediction interval on a new observation (See Figure 2-14). The true PSDs of the sampled fly ash from Andersen samplers and TSP samplers in the chamber were also obtained (See Figures 2-15 and 2-16). The bulk sample of fly ash has a median AED ( $GM_{BS} = 11.8 \mu\text{m}$ ) and a slope of the bulk sample ( $GSD_{BS} = 2.1$ ).



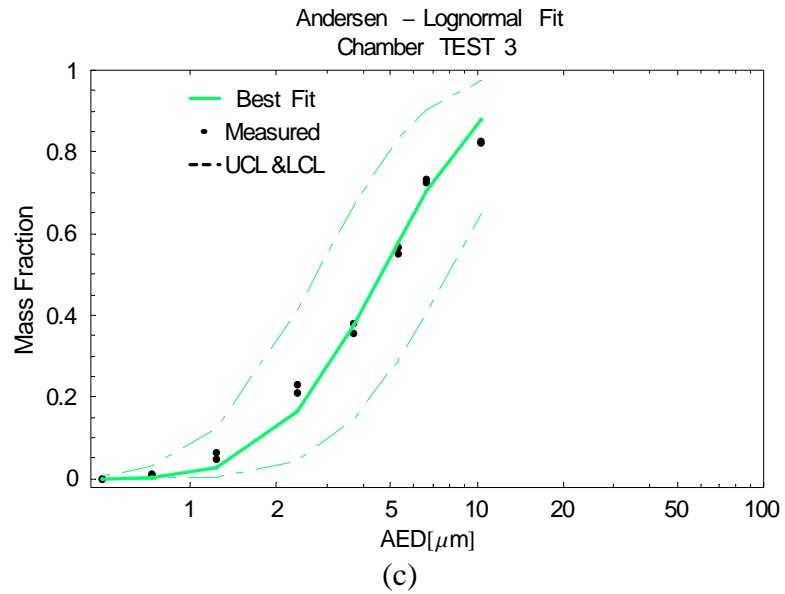
**FIGURE 2-14. PSD of fly ash's bulk sample (See Appendix I-2).**

*Note:* The dashed lines represent the 95 % confidence interval for the fitted curve.

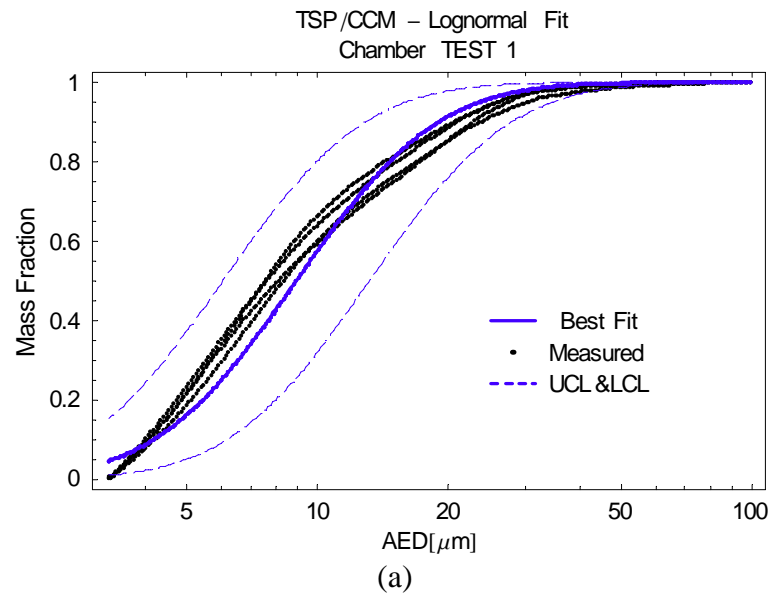


**FIGURE 2-15. PSD of Andersen Sampler (See Appendix I-2) (a) Test 1, (b) Test 2, (c) Test 3.**

*Note:* The dashed lines represent the 95 % confidence interval for the fitted curve.

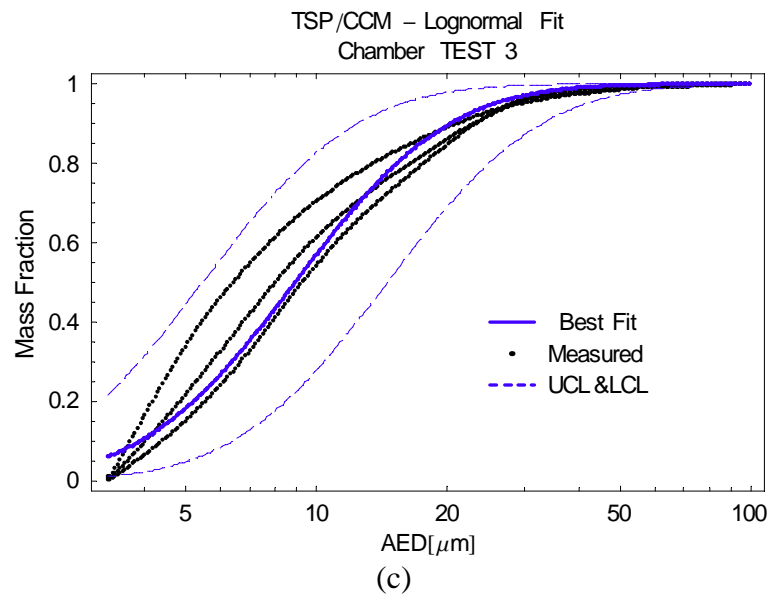
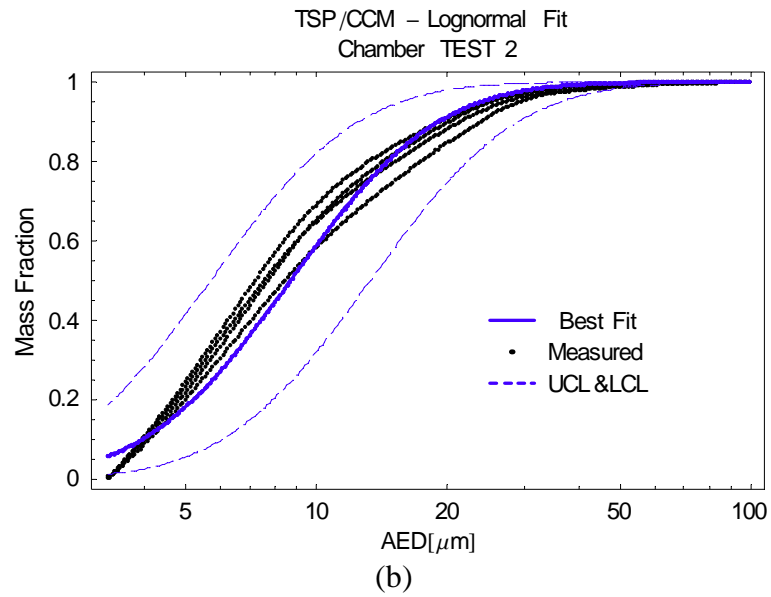


**FIGURE 2-15. Continued.**



**FIGURE 2-16. PSD of TSP/CCM (See Appendix I-2). (a) Test 1, (b) Test 2,  
(c) Test 3.**

*Note:* The dashed lines represent the 95 % confidence interval for the fitted curve.

**FIGURE 2-16. Continued.**



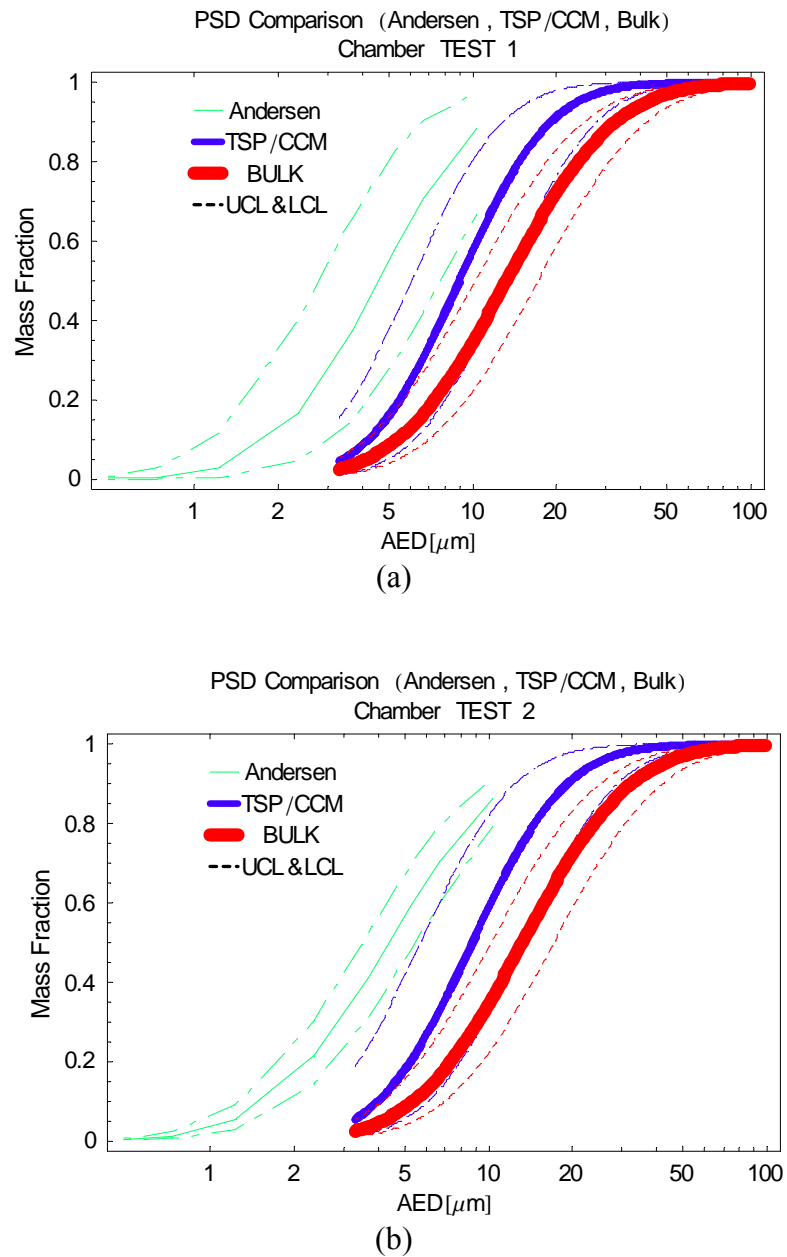


**FIGURE 2-17. PSDs by samplers vs. PSD of fly ash's bulk sample. (a) Test 1, (b) Test 2, (c) Test 3.**

*Note:* The dashed lines represent the 95 % confidence interval for the fitted curve.

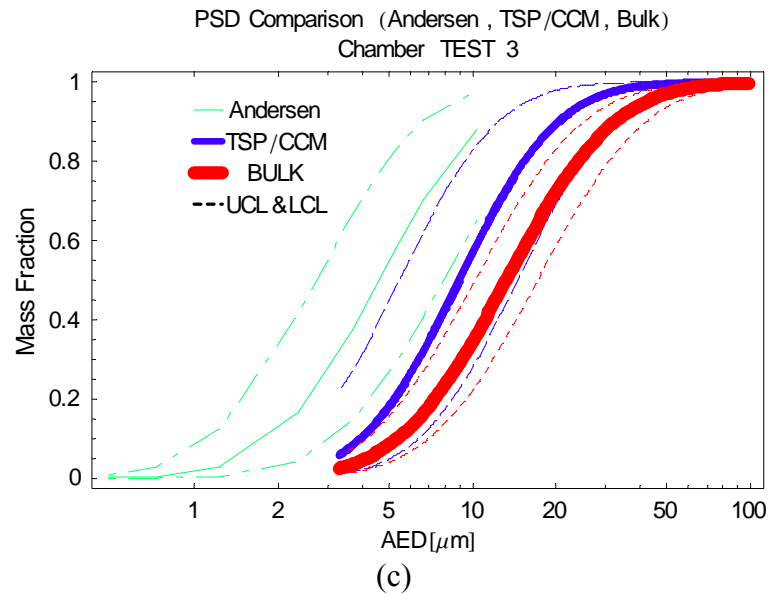


**FIGURE 2-17. Continued.**

To compare the PSDs of aerosol samplers and bulk sample of fly ash, all the PSDs were shown on the same graph (See Figure 2-17). The PSD of bulk fly ash injected into the chamber appears to have a higher number of particles of all sizes than are evident in the PSD measured by the Andersen sampler and that measured by the TSP/CCM. There is a significant difference between the median AEDs of aerosol samplers and  $GM_{BS} = 11.8$  of the bulk fly ash. The reasons for this difference include: particle losses on the walls, the holes in the air straighteners, and the fan blades and feeding nozzle that injects the fly ash.

Figure 2-17 and Equation 2.8 show that there is a difference between the PSD curves of Andersen samplers and those of TSP/CCMs. This difference is consistent with the bounce phenomenon in the Andersen sampler. Mass transport by particle bounce causes the PSD slope to flatten. The Andersen tends to show more mass in small diameter fractions than was present, and to show less mass in large diameter fractions that was present.

### **3. Mass Fractions for the Convention**

The average mass fractions for respirable and thoracic PM were estimated from Andersen samplers and, TSP/CCMs, and RespiCon samplers to estimate sampler sampling efficiency as shown in Table 2-6.

When the average mass fractions of Andersen samplers were compared with those of TSP/CCMs and RespiCon samplers, there were differences. This different mass fraction can be explained by the particle loss on the walls, or any losses in the sampling conditions. This table shows that the Andersen sampler has a bounce phenomenon.

**TABLE 2-6. Average Mass Fractions of Respirable PM and Thoracic PM from Andersen, TSP/CCM, and RespiCon Samplers**

Sampler	Andersen Mean (SD <sup>A</sup> )			TSP sampler Mean (SD)			RespiCon Mean (SD)		
	Test1 n = 2	Test2 n = 2	Test3 n = 2	Test1 n = 4	Test2 n = 4	Test3 n = 4	Test1 n = 1	Test2	Test3 n = 2
Respirable (AED≤4µm; PM <sub>4</sub> )	0.37 (0.04)	0.40 (0.04)	0.37 (0.04)	0.20 (0.08)	0.20 (0.07)	0.23 (0.08)	0.11 (0.02)	-- <sup>B</sup>	0.25 <sup>C</sup> (0.03)
Thoracic (AED≤10µm; PM <sub>10</sub> )	0.83 (0.09)	0.84 (0.10)	0.83 (0.09)	0.73 (0.12)	0.75 (0.19)	0.74 (0.21)	0.81 (0.08)	--	0.67 (0.09)

Notes: <sup>A</sup> SD = Standard deviation for PM<sub>10</sub> and PM<sub>4</sub>.

$$\frac{SD_{PM_{10}}}{\bar{C}_{PM_{10}}} = \sqrt{\left(\frac{SD_{PM_{total}}}{\bar{C}_{PM_{total}}}\right)^2 + \left(\frac{SD_{\rho_p}}{\bar{\rho}_p}\right)^2 + \left(\frac{SD_{\chi}}{\bar{\chi}}\right)^2}, \quad \frac{SD_{PM_4}}{\bar{C}_{PM_4}} = \sqrt{\left(\frac{SD_{PM_{total}}}{\bar{C}_{PM_{total}}}\right)^2 + \left(\frac{SD_{\rho_p}}{\bar{\rho}_p}\right)^2 + \left(\frac{SD_{\chi}}{\bar{\chi}}\right)^2} \text{ for TSP samplers.}$$

where  $C$  = Concentration;  $\rho_p$  = Density of particles;  $\chi$  = Shape factor; and  $SD$  = Standard deviation.

The equations above were based on the conversion from ESD to AED using  $AED = ESD \left[ \frac{\rho_p}{\rho_0 \cdot \chi} \right]^{1/2}$

where  $AED$  = Aerodynamic equivalent diameter;  $ESD$  = Equivalent spherical diameter;  
 $\rho_0$  = Unit Density (1 g/cm<sup>3</sup>);  $\chi$  = Dynamic shape factor.

$SD_{\rho_p} / \bar{\rho}_p$  was estimated as 0.1 = (2.7 ± 0.2) g/cm<sup>3</sup> for fly ash.

The value for  $SD_{\chi} / \bar{\chi}$  was estimated as 0.01 from the images obtained from the ESEM.

$$\frac{SD_{PM_{10}}}{\bar{C}_{PM_{10}}} = \sqrt{\left(\frac{SD_{SF}}{\bar{W}_{SF}}\right)^2 + \left(\frac{SD_{S7}}{\bar{W}_{S7}}\right)^2 + \dots + \left(\frac{SD_{S1}}{\bar{W}_{S1}}\right)^2 + \left(\frac{SD_Q}{\bar{Q}}\right)^2 + \left(\frac{SD_T}{\bar{T}}\right)^2},$$

$$\frac{SD_{PM_4}}{\bar{C}_{PM_4}} = \sqrt{\left(\frac{SD_{SF}}{\bar{W}_{SF}}\right)^2 + \left(\frac{SD_{S7}}{\bar{W}_{S7}}\right)^2 + \left(\frac{SD_{S6}}{\bar{W}_{S6}}\right)^2 + \left(\frac{SD_{S5}}{\bar{W}_{S5}}\right)^2 + \left(\frac{SD_{S4}}{\bar{W}_{S4}}\right)^2 + \left(\frac{SD_Q}{\bar{Q}}\right)^2 + \left(\frac{SD_T}{\bar{T}}\right)^2} \text{ for Andersen samplers.}$$

where  $S_0, S_1, S_2, S_3, S_4, S_5, S_6, S_7, S_F$  = The number of stage. In these calculations, the relative standard deviation for stages 6, 7, and F were above 1 because of a small quantity of mass on these stages. Thus, the relative standard deviation of stages 6, 7, and F were estimated as 0.02.

$$\frac{SD_{PM_{10}}}{\bar{C}_{PM_{10}}} = \sqrt{\left(\frac{SD_{SR1}}{\bar{W}_{SR1}}\right)^2 + \left(\frac{SD_{SR2}}{\bar{W}_{SR2}}\right)^2 + \left(\frac{SD_Q}{\bar{Q}}\right)^2 + \left(\frac{SD_T}{\bar{T}}\right)^2}, \quad \frac{SD_{PM_4}}{\bar{C}_{PM_4}} = \sqrt{\left(\frac{SD_{SR1}}{\bar{W}_{SR1}}\right)^2 + \left(\frac{SD_Q}{\bar{Q}}\right)^2 + \left(\frac{SD_T}{\bar{T}}\right)^2} \text{ for}$$

RespiCon samplers.

where  $S_{R1}$  and  $S_{R2}$  = The number of stage with stage cutoff size 4 µm and 10 µm.

$$\frac{SD_C}{\bar{M}_F} = \sqrt{\left(\frac{SD_1}{\bar{M}_{F1}}\right)^2 + \dots + \left(\frac{SD_n}{\bar{M}_{Fn}}\right)^2} \text{ where } \bar{M}_F = \text{Average mass fraction of n sampler.}$$

$$\frac{SD_C}{\bar{C}_T} = \sqrt{\left(\frac{SE}{\bar{C}_T}\right)^2 + \left(\frac{SD_1}{\bar{C}_1}\right)^2 + \dots + \left(\frac{SD_n}{\bar{C}_n}\right)^2} \text{ standard deviation for an error propagation of n samplers}$$

where  $\bar{C}_T$  = Average concentration of n samplers;  $SE$  = standard error of sample mean;

$SD_n$  = Standard deviation of  $n^{\text{th}}$  sampler;  $\bar{C}_n$  = Concentration of  $n^{\text{th}}$  sample. <sup>B</sup>no measurement;

<sup>C</sup> $n = 1$ ; In RespiCon samplers, two cutoff size for respirable were used. The 2.5 µm inlet is excluded.

In Andersen samplers, the  $AED_{50s}$  for respirable and thoracic PM were decided by the stage cutoff size  $3.7 \mu\text{m}$  and  $10.3 \mu\text{m}$  which are close to respirable ( $AED \leq 4 \mu\text{m}$ ) and thoracic ( $AED \leq 10 \mu\text{m}$ ) convention.

## **D. DISCUSSION**

### **1. Mass Fractions by Aerosol Samplers**

The average concentrations were measured and compared using three types of impactors through three tests (See Table 2-7). The following were expected from the monitors used in this study;

- 1)  $PM_{10}$  concentration of a DustTrak monitor would be same as that of a  $PM_{10}$  sampler and  $PM_{2.5}$  concentration of a DustTrak and SidePak would also be same as that of RespiCon sampler.
- 2)  $PM_{10}$  concentration of a DustTrak monitor would be higher than the  $PM_{2.5}$  concentration of a DustTrak monitor when a median AED of airborne particles is bigger than an AED  $2.5 \mu\text{m}$ . The  $PM_{2.5}$  concentration of a SidePak monitor would be higher than the  $PM_{1.0}$  concentration of a SidePak monitor when a median AED of airborne particles is bigger than  $1.0 \mu\text{m}$ . When a median AED of airborne particles is smaller than AEDs  $1 \mu\text{m}$  and  $2.5 \mu\text{m}$ , similar concentrations would be expected.

**TABLE 2-7. Comparison of the Concentration of Real-time Monitors to the Unbiased Concentrations of Size Selective Samplers**

Sampler	DustTrak (Mean $\pm$ $SU^A$ )		SidePak (Mean $\pm$ $SU$ )		PM <sub>10</sub> Sampler (Mean $\pm$ $SU$ )	RespiCon (Mean $\pm$ $SU$ )
Inlet cutoff size [ $\mu\text{m}$ ]	10 n = 3	2.5 n = 3	2.5 n = 3	1 n = 3	n = 12	Respirable (AED $\leq$ 2.5 $\mu\text{m}$ ) n = 1
Concentration [ $\text{mg}/\text{m}^3$ ]	10.91 $\pm$ 3.00	5.87 $\pm$ 2.84	11.26 $\pm$ 4.10	11.12 $\pm$ 7.44	24.13 $\pm$ 12.19	7.90 $\pm$ 0.8

$$^A C = \frac{\text{Mass}}{Q \times T}, \quad \frac{SD_C}{\bar{C}} = \sqrt{\left(\frac{SD_W}{\bar{W}}\right)^2 + \left(\frac{SD_Q}{\bar{Q}}\right)^2 + \left(\frac{SD_T}{\bar{T}}\right)^2} \text{ for PM}_{10} \text{ and RespiCon samplers}$$

where  $C$  = Concentration;  $W$  = Weighing;  $Q$  = Flow rate;  $T$  = Time; and  $SD$  = Standard deviation.

$$C = \frac{\text{Mass}}{Q \times T}, \quad \frac{SD_C}{\bar{C}} = \sqrt{\left(\frac{SD_Q}{\bar{Q}}\right)^2 + \left(\frac{SD_T}{\bar{T}}\right)^2} \text{ for DustTrak and SidePak real-time monitors}$$

$$\frac{SD_C}{\bar{C}_T} = \sqrt{\left(\frac{SE}{\bar{C}_T}\right)^2 + \left(\frac{SD_1}{\bar{C}_1}\right)^2 + \dots + \left(\frac{SD_n}{\bar{C}_n}\right)^2} \text{ standard deviation for an error propagation of n samplers}$$

where  $\bar{C}_T$  = Average concentration of  $n$  samplers;  $SU$  = Sampling uncertainty =  $1.96 \times SE$ ;

$SDn$  = Standard deviation of  $n^{\text{th}}$  sampler;  $\bar{C}_n$  = Concentration of  $n^{\text{th}}$  sample.

Wu et al.<sup>(39)</sup> and Lehocky et al.<sup>(40)</sup> used a calibration factor for their research showing the benefit of calibrating an DustTrak monitor to dust being measured because it is calibrated using Arizona Test Dust at the factory. The field calibration relates light scattering intensity to aerosol mass concentration (factory sets a calibration factor of 1.00). Thus, the correction factor (2.21, range of 0.86 to 4.59) for fly ash was calculated from the PM<sub>10</sub> concentration of a DustTrak monitor and that of a PM<sub>10</sub> sampler using Equation 2.10. To find the calibration factor, the average concentration of PM<sub>10</sub> samplers was used as a reference concentration because the PM<sub>10</sub> sampler provides a reasonable estimate of the thoracic particulate fraction.

$$\text{Calibration factor for flyash} = \left( \frac{\text{Ref. conc.}}{\text{DustTrak conc.}} \right) \times \text{old calibration factor} \quad (2.10)$$

Also, the calibration factors for DustTrak and SidePak monitors using 2.5  $\mu\text{m}$  inlets were calculated using a respirable ( $\text{AED} \leq 2.5 \mu\text{m}$ ) PM concentration of RespiCon sampler because a RespiCon sampler provides an unbiased estimate of respirable, thoracic, and inhalable fractions. The calibration factors are 1.35, which has a range of 0.91 to 2.61 for a DustTrak monitor, and 0.70, which has a range of 0.51 to 1.10 for a SidePak monitor.

These calibration factors for the chamber study cannot apply to field study because the density and shape of particles in the field is not the same as fly ash. DustTrak and SidePak monitors are useful for obtaining relative particle concentrations against the scattered light.

As seen in Table 2-8, the same 2.5  $\mu\text{m}$  inlets between DustTrak and SidePak monitors reported different mass concentration. The indicated concentration measurement range of a DustTrak is from 0.002  $\text{mg}/\text{m}^3$  to 100  $\text{mg}/\text{m}^3$  (150  $\text{mg}/\text{m}^3$ \*) while that of SidePak is from 0.001  $\text{mg}/\text{m}^3$  to 20  $\text{mg}/\text{m}^3$ . When data were analyzed, there were “invalid” signs instead of the one second interval value of concentration for 6 % of the intervals when using a 2.5  $\mu\text{m}$  inlet SidePak monitor and for 10 % of the intervals when using a 1  $\mu\text{m}$  inlet SidePak monitor. There were no “invalid” signs from DustTrak monitors. These signs are recorded in the SidePak data stream when the values are above the maximum range (20  $\text{mg}/\text{m}^3$ ). This is confirmed because most of these signs occur in intervals during which the DustTrak is reporting the higher concentrations (See Figure 2-18).

---

\* The value of 150  $\text{mg}/\text{m}^3$  is experimental factory range.

Note, from Figure 2-18, that the total mass estimated by DustTrak and SidePak monitors has the same overall shape but has different calibration factors. This means these instruments are useful for measuring relative concentrations over time, but not for absolute concentration measurements.

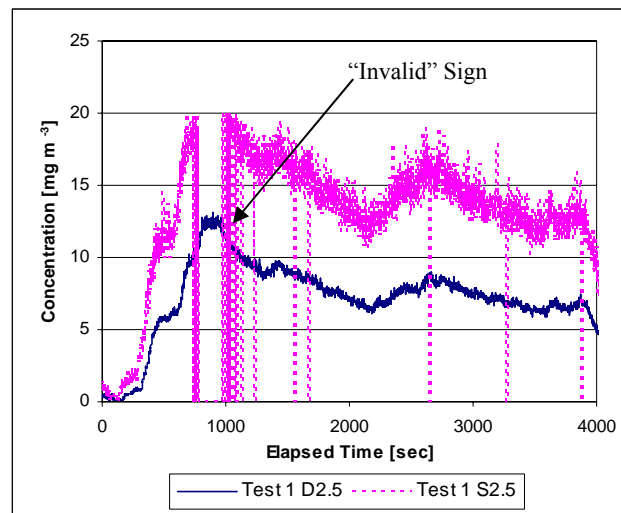


**FIGURE 2-18. Measured concentration by real-time monitor.**

*Note:*  $D_{2.5}$  = 2.5  $\mu\text{m}$  inlet DustTrak;  $S_{2.5}$  = 2.5  $\mu\text{m}$  inlet SidePak.

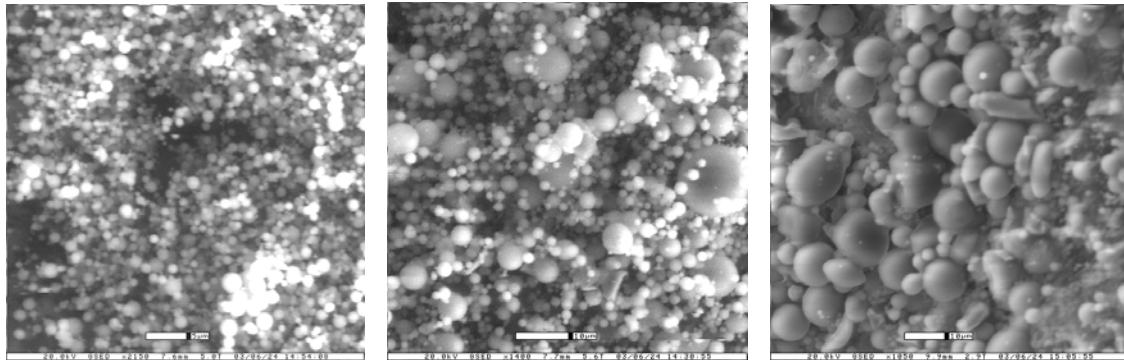
## 2. Microscopic Analysis

The important parameters for characterizing the behavior of PM are particle size, shape, and density. To verify the particle size ranges, the images below were obtained from the filters of RespiCon samplers and TSP samplers using an ESEM at the Microscopy Imaging Center, Texas A&M University.

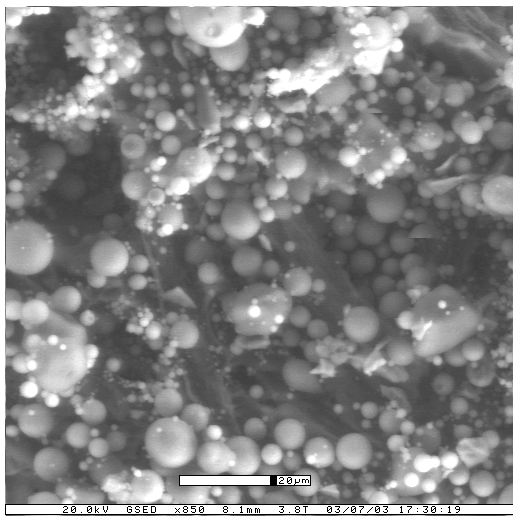
The images were taken from a RespiCon sampler with an AED 2.5  $\mu\text{m}$  cutoff stage and one of TSP samplers. As shown in Figure 2-19, the images of (a), (b), and (c)



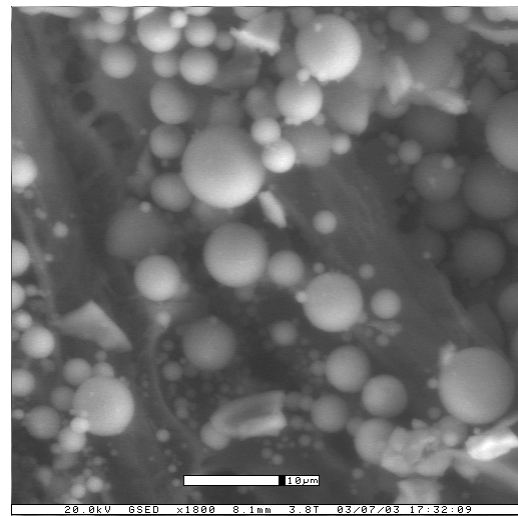
show that the collected particle size from the stages of the RespiCon sampler appears to agree with the cutoff sizes AEDs 2.5  $\mu\text{m}$  and 10  $\mu\text{m}$ . The images (d) and (e) in Figure 2-19 show that a TSP sampler has a various range of particle size.



(a) Calibration bar = 5  $\mu\text{m}$  (b) Calibration bar = 10  $\mu\text{m}$  (c) Calibration bar = 10  $\mu\text{m}$



(d) Calibration bar = 20  $\mu\text{m}$



(e) Calibration bar = 10  $\mu\text{m}$

**FIGURE 2-19. Particle images from a RespiCon sampler and a TSP sampler. (a) RespiCon Stage 1 with 2.5  $\mu\text{m}$  cut-point, (b) RespiCon Stage 2 with 10  $\mu\text{m}$  cut-point, (c) RespiCon Stage 3 with 100  $\mu\text{m}$  cut-point, (d) TSP Sampler, (e) TSP sampler.**

When the images were obtained from the filters, it was noted that the electron beam created electrostatic forces between particles sufficient to cause visible particles displacement between images. These forces may also produce the appearance of clusters or conglomerates on a filter, even though the aerosol may have been sampled as isolated particles from the atmosphere.

Through the images taken by an ESEM, the most of fly ash are shown to have a smooth surface and spherical shape. The shape factor was estimated as one on the basis of ESEM images (See Appendix G). The particle size distributions from the RespiCon samplers are shown to agree with the cutoff of each stage.

## **E. CONCLUSIONS**

The goal of the chamber studies in this chapter was to select air sampling technology that would allow one to estimate the respirable, thoracic, and inhalable fraction of airborne PM as defined by the ACGIH/CEN/ISO standard.

Six sampler technologies were tested by challenging them with uniform density poly-disperse fly ash spheres having a lognormal distribution with estimated parameters of  $GM_{AED} = 11.8 \mu\text{m}$  and  $GS_{AED} = 2.1$ .

None of the sampling techniques, standing alone, provided a complete estimate of particle size distribution and mass concentration in the chamber air. These distributions were therefore estimated by inference from data collected by the various samplers.

The Andersen samplers overestimate mass of small particles due to particle bounce and carryover between stages. It therefore provides a conservative estimate of respirable particulate mass and thoracic particulate mass.

The TSP samplers provide an unbiased estimate of total particulate mass. TSP/CCM provides a reasonable estimate of PM mass for ESD between 2  $\mu\text{m}$  and 60  $\mu\text{m}$ . TSP/CCM provides no information below ESD 2  $\mu\text{m}$  and therefore underestimates respirable and thoracic particulate mass. The conversion from ESD to AED for comparison with exposure standards is imprecise due to the range of particle shapes and densities in the sampled air.

The  $\text{PM}_{10}$  samplers provide a reasonable estimate of the thoracic particulate fraction.

The RespiCon samplers provide an unbiased estimate of respirable, thoracic and inhalable fractions.

The DustTrak and SidePak monitors, with a one stage impactor prefilter, are useful for studying relative particle concentrations, but not for absolute concentrations. These samplers can not be calibrated for absolute particle concentrations in a plume with varying particle shape, composition, and density. The prefilters overload quickly and particle bounce results.

## **CHAPTER III**

### **RISK ASSESSMENT OF PETROLEUM PIPE SCALE FROM A PIPE RATTLING PROCESS**

#### **A. INTRODUCTION**

National Air Ambient Quality Standards (NAAQSs) were set by the Environmental Protection Agency (EPA). In these standards, particulate matter (PM) is defined as a complex mixture of particles suspended in the air that vary in size and composition. PM is regulated to protect public health on the basis of its aerodynamic behavior and 24-hour average concentration.  $PM_{10}$  and  $PM_{2.5}$  are the mass fractions found in size selective samplers that measure PM with aerodynamic equivalent diameter (AED) less than  $10\ \mu\text{m}$  and less than  $2.5\ \mu\text{m}$ , respectively. The standard values for  $PM_{10}$  and  $PM_{2.5}$  are 24 hour average concentrations of  $150\ \mu\text{g}/\text{m}^3$  and  $65\ \mu\text{g}/\text{m}^3$ , and annual arithmetic mean concentrations of  $50\ \mu\text{g}/\text{m}^3$  and  $15\ \mu\text{g}/\text{m}^3$ .<sup>(41)</sup>

Occupational Safety and Health Administration (OSHA) Permissible Exposure Limit (PEL) for Particulates Not Otherwise Regulated (PNOR) are  $5\ \text{mg}/\text{m}^3$  for the respirable fraction ( $\text{AED} \leq 4\ \mu\text{m}$ ) and  $15\ \text{mg}/\text{m}^3$  for total dust.<sup>(7)</sup> These limits are based on averaging the concentration over a conventional 8 hour workday, and are called 8-hour time weighted average (TWA) limits.

The American Conference of Governmental Industrial Hygienists (ACGIH) 8-hr TWA Threshold Limit Value (TLV) for barium sulfate and for Particulates Not Otherwise Classified (PNOC) is offered in two forms: the TLV for respirable particulate

matter (AED  $\leq 4 \mu\text{m}$ ) is  $3 \text{ mg/m}^3$ , and the TLV for inhalable particulate matter (AED  $\leq 100 \mu\text{m}$ ) is  $10 \text{ mg/m}^3$ .<sup>(8)</sup> This applies to insoluble and poorly soluble materials. The pipe scale is primarily a barium sulfate scale. In recent tests, it has been shown that it does not measurably dissolve in body fluids, so it fits the definition of PNOC offered by the ACGIH.<sup>(42)</sup>

Currently accepted limits for PM are summarized in Table 3-1.

**TABLE 3-1. Accepted limits for PM\***

Description	PM <sub>2.5</sub>	PM <sub>4</sub>	PM <sub>10</sub>	PM total
EPA NAAQSs				
Annual arithmetic mean	$15 \mu\text{g/m}^3$	--	$50 \mu\text{g/m}^3$	--
24-hour average	$65 \mu\text{g/m}^3$		$150 \mu\text{g/m}^3$	
ACGIH TLV-TWA	--	$3 \text{ mg/m}^3$	--	$10 \text{ mg/m}^3$
OSHA PEL	--	$5 \text{ mg/m}^3$	--	$15 \text{ mg/m}^3$

Note: \* Year: 2004

The health effects of PM are dependent on several factors including: where they deposit in the respiratory tract, aqueous solubility, Octanol-Water partition coefficient, surface reactivity, and radionuclide content. The particles with large AED ( $> 10 \mu\text{m}$ ) are almost all deposited in the nose and throat. The particles with an AED between  $4 \mu\text{m}$  and  $10 \mu\text{m}$  are deposited primarily in the pharynx, whereas respirable particles (AED  $\leq 4 \mu\text{m}$ ) are able to reach the airspace deep in the lungs.

To evaluate the health hazard of PM in the workplace, three PM fractions for inhalable, thoracic, and respirable convention are used on the basis of 50 % cutoff size at

AEDs of 100  $\mu\text{m}$ , 10  $\mu\text{m}$ , and 4  $\mu\text{m}$ . These size conventions were co-developed and adopted by the ACGIH, the Comité Européen de Normalisation (CEN),<sup>(3)</sup> and the International Organization for Standardization (ISO).<sup>(2)</sup> They are also the sampling size fractions recommended by American Industrial Hygiene Association (AIHA).<sup>(4)</sup>

The petroleum pipe rattling process removes tightly bound scale from the inside surface of tubular petroleum pipes and removes loose corrosion products from external surfaces. The aerosol particles produced by the petroleum pipe rattling operations were collected with several types of size selective aerosol samplers. This study reports results of air samples taken while petroleum pipes from two oilfields were rattled. The aerosol dispersion was produced from the two distinct petroleum pipe scales. No similar detailed, comprehensive study has been found in published literature.

The main objectives of this study are:

1. Measure PM mass concentrations and estimate particle size distributions (PSDs) of two different petroleum pipe scales (Mud Lake and Lake Sand).
2. Compare the measured mass concentrations with accepted standards and guidelines.
3. Provide images using an ESEM to illustrate particle shapes and physical sizes for two different scales.

## **B. METHODS**

The petroleum pipe rattling process was conducted at a remote location on Texas A&M University's Riverside Campus, a former WWII bomber base. Two tubular rattling machines, approximately 3 m wide and 24 m long, were installed on a geotextile

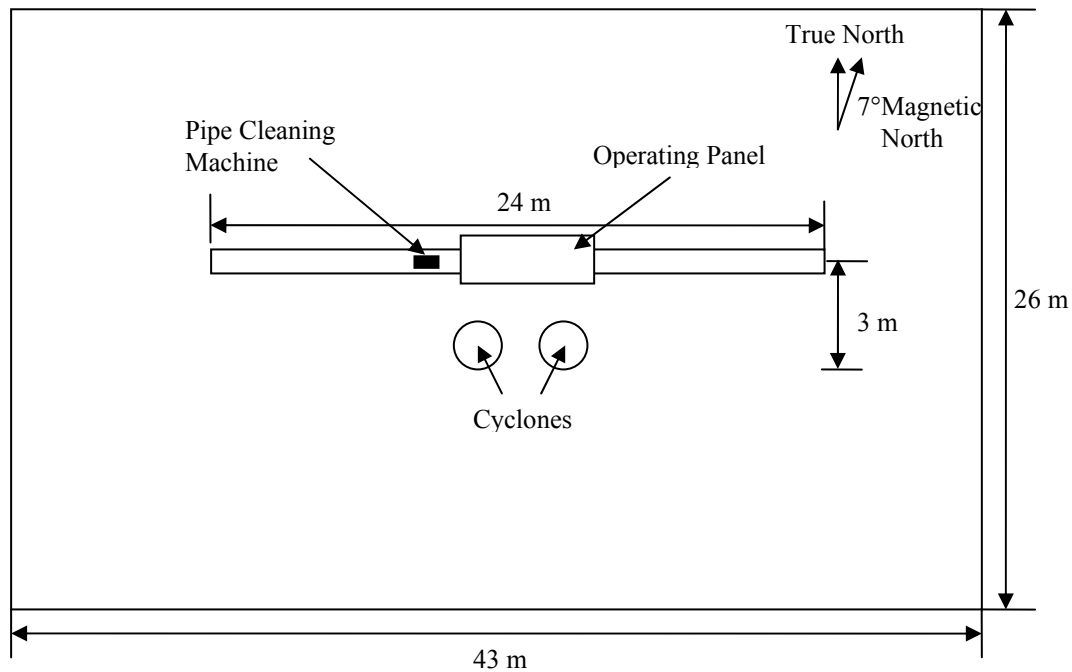
covered pad site having dimensions of 26 m × 43 m (See Figure 3-1). All pipes tested for pipe rattling operations have a same length of 30 ft (9.14 m).

Tests were conducted under a variety of weather conditions. Meteorological data were measured and saved on a 10-minute duty cycle using a Davis Vantage Pro (Davis Instruments, Hayward, CA) wireless weather station that was installed on the roof of the administrative trailer 10 m above the ground, high enough to ensure unimpeded acquisition of local weather data. Meteorological data, including wind speed and direction, temperature, barometric pressure, and rainfall on each day were also obtained on one hour cycles from the nearest National Oceanic and Atmospheric Administration (NOAA) reporting station, located at Easterwood Airport (NOAA designation, CLL), located approximately 8 miles ESE of the pad site.



(a)

**FIGURE 3-1. Pipe rattling process. (a) Pipe rattling process, (b) Field floor plan.**



(b)

**FIGURE 3-1. Continued.**

Two Andersen samplers, two RespiCon samplers, and four Total Suspended Particulate samplers analyzed by a Coulter counter multisizer (TSP/CCM) were used to estimate the aerodynamic PSD. In TSP/CCMs, an AED is calculated from the measured particle volume, expressed as an equivalent spherical diameter (ESD).

An AED is the diameter of the unit density ( $1 \text{ g/cm}^3$ ) sphere that has the same settling velocity as the observed particle. The cumulative mass fractions of  $\text{PM}_{10}$  and  $\text{PM}_4$  were determined by multiplying the volume fraction of  $\text{PM}_{10}$  and  $\text{PM}_4$  estimated by a CCM.

Four  $\text{PM}_{10}$  samplers were also used to measure the  $\text{PM}_{10}$  concentration.



DustTrak and SidePak monitors were used to measure the second to second variation in real time aerosol concentration. In this study, these concentrations are considered to be relative measures of scattered light intensity, not as a true mass concentration because the real-time monitors were not calibrated for the scale.

In order to estimate respirable, thoracic, and inhalable fractions from each 1 m, 2 m, and 3 m distance, the size selective aerosol samplers and real-time monitors were co-located with the following conditions (See Figure 3-2).

During the each experiment, there were variable conditions such as differing sampling locations, heights, wind speeds, wind dispersions, emission rates, and turbulence. Under these conditions, the following sampling and measurement protocol was used to obtain comparable results:

1. The workplace was a bermed field covered with a reinforced, black, impermeable geotextile liner that extended about 3 m beyond the outside border of the berm.
2. A 1 m by 1 m by 0.5 m deep sump was constructed at the low point of the bermed area to gather rain water and to collect any particles that settled on the liner.
3. A sump pumping system and six-stage water filter was installed and connected to portable tanks to hold filtered waste water used to clean the geotextile after each experiment, and to hold any rain water accumulated on the pad site, until chemical analysis showed it safe for disposal to a municipal treatment plant.
4. The first and second tests had durations of 191 and 93 minutes, respectively.
5. The petroleum pipes were rattled with a restored Hub City Iron Works pipe-cleaning machine (PCM-13375; Hub City Inc., Aberdeen, SD 57402).

6. Andersen samplers were located at a height of 60 cm on the first day and 120 cm on the second day.
7. DustTrak and SidePak monitors were located at a height of 120 cm and the data were saved at one second intervals.
8. RespiCon samplers were located at a height of 150 cm. TSP samplers and PM<sub>10</sub> samplers were located at the height of 150 cm.
9. Teflon filters with a 0.5  $\mu\text{m}$  pore size were used in the PM<sub>10</sub>, TSP, and RespiCon samplers as a filter media.
10. The particles that fell out of the air onto the pad were collected after each test day and the pad plus all equipment were cleaned.
11. A high-precision analytical balance with a limit of detection of 0.01 mg (AG245, Mettler Toledo, Greifensee Switzerland) was used to weigh the filters of TSP and PM<sub>10</sub> samplers. A Mettler Toledo AE 100 with a limit of detection of 0.1 mg was used to weigh the particles on the impaction plate of Andersen samplers.
12. The filters and plates were weighed three times before and after each experiment inside a temporary office set up at the experimental site.
13. The required airflows for TSP and PM<sub>10</sub> samplers were set at 16.7 L/min with a needle valve in series with a diaphragm pump and the flow was monitored continuously with an orifice flow meter (Dayton, 4z792). The airflow rate was logged and recorded by a data logger (HOBO H8 RH/Temp/2X External) at 12 second intervals.
14. The orifice meter pressure drop was converted using Equation 2.1.

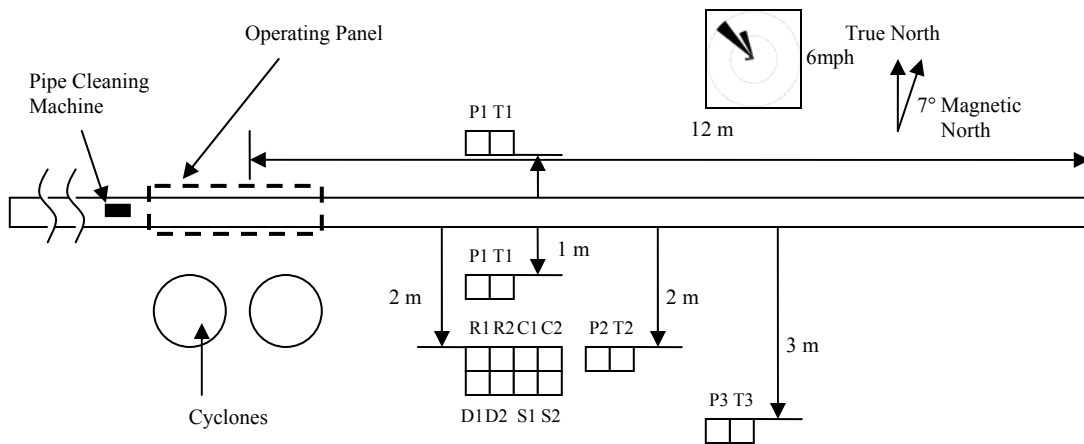
$$Q = 5.976 \cdot K \cdot D_o^2 \cdot \sqrt{\Delta P / \rho_a} \quad (3.1)$$

where  $Q$  = Airflow rate through the orifice meter [ $\text{m}^3/\text{s}$ ];  $K$  = flow coefficient;

$D_o$  = orifice meter [m];  $\Delta P$  = pressure drop cross the orifice [ $\text{mmH}_2\text{O}$ ]; and

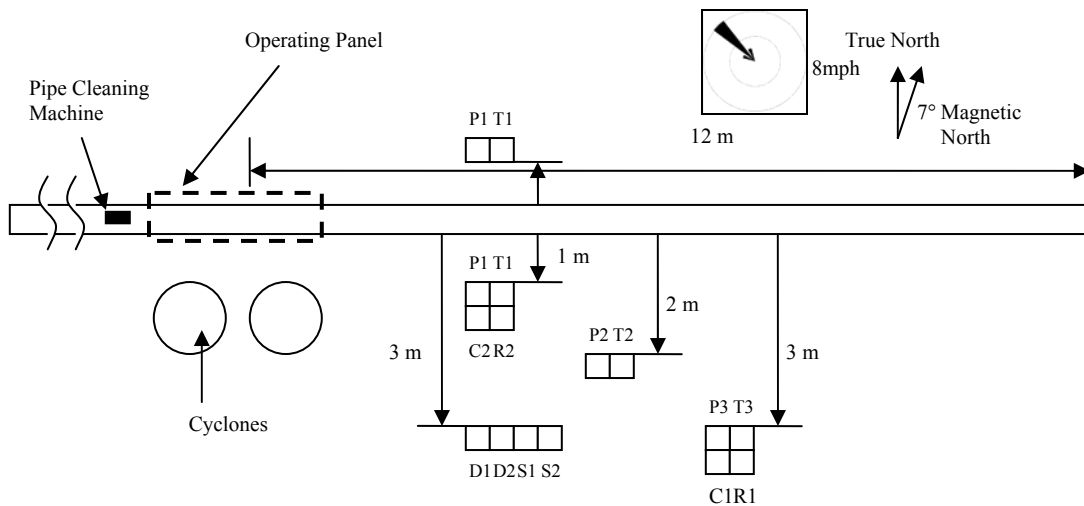
$\rho_a$  = air density [ $\text{kg}/\text{m}^3$ ].

15. The airflow rates for Andersen samplers were adjusted to 1 ACFM (28.32 L/min) and this flow was checked before and after each test using the flow meter.
16. The airflow rates for RespiCon Samplers were adjusted to 3.11 L/min before each test and checked after each test using a flow meter provided by the TSI Company.
17. The airflow rates for DustTrak and SidePak monitors were adjusted to 1.7 L/min prior to each experiment using a flow meter provided by the TSI Company. The particle concentration scale was zeroed with air passing through a zero filter prior to each experiment.
18. The operator and helper wore coveralls, goggles, disposable masks, disposable earplugs, gloves, safety hats, and safety boots.
19. The positioning of the aerosol samplers was determined by wind direction from the weather monitor plus visual monitoring of the wind conditions with a smoke generator (F-100 Performance Fog Generator; Light Wave Research/High End Systems, Austin, TX 78758), whose plume is visible in videos recorded during the experiments.
20. The dispersion of the smoke was a visual indication of the median wind direction and the degree of variability of the wind direction.



Notes: C1 & C2 = Andersen samplers;  
 R1 = RespiCon sampler with a 4  $\mu\text{m}$  and 10  $\mu\text{m}$  cut-points; R2 = RespiCon sampler with a 2.5  $\mu\text{m}$  and 10  $\mu\text{m}$  cut-points;  
 T1-T4 = Total suspended particulate samplers; P1-P4 = PM<sub>10</sub> samplers;  
 D1 = DustTrak monitor used a 10  $\mu\text{m}$  inlet; D2 = DustTrak monitor used a 2.5  $\mu\text{m}$  inlet;  
 S1 = SidePak monitor used a 2.5  $\mu\text{m}$  inlet; S2 = SidePak monitor used a 1  $\mu\text{m}$  inlet.

(a)



Notes: All samplers' conditions are the same as in field test 1.  
 D1 & D2 = DustTrak monitors (a 1  $\mu\text{m}$  inlet module was used for each monitor)

(b)

**FIGURE 3-2. Aerosol sampler setup for field tests 1 and 2 with wind rose.**

**(a) Field test 1 (Mud Lake pipe), (b) Field test 2 (Lake Sand pipe).**

## **C. RESULTS**

### **1. Mass Concentration**

As shown in Table 3-2, comparable total mass concentrations in the petroleum pipe rattling process were found between Andersen samplers and TSP samplers located at the same distance from the centerline of scale source through overall experiments. The mass concentration of each sampler has individual standard deviation because there were uncertainties from the mass weighed, the volume flow rate of pump, and the time collecting particles.

The total mass concentrations from Andersen, RespiCon, and TSP samplers are displayed with their confidence interval at 95 % confidence level (See Figure 3-3).

Interestingly, the highest concentrations were found from the TSP sampler and the PM<sub>10</sub> sampler located at 2 m distance from the centerline of the pipe machine, not at 1 m distance. This result is not consistent with a simple inverse square law model of concentration vs. distance (See Figure 3-4). It is consistent with a Gaussian plume model whose centerline passes beneath the sampler at 1 m distance from the pipe, as illustrated in Figures 3-5 and Figure 3-19.

**TABLE 3-2. Measured Concentrations from Each Aerosol Sampler by Distance**

Field test 1 (Mud Lake 13 pipes) Total Test Time: 191 minutes

Distance From Source	TSP <sup>A</sup> [150] <sup>E</sup>	C1 <sup>B</sup> [60]	C2 <sup>B</sup> [60]	R1 <sup>C</sup> [150]	R2 <sup>D</sup> [150]
1 m	12.7 (0.5) <sup>F</sup>	-- <sup>G</sup>	--	--	--
2 m	12.9 (0.5)	12.5 (1.3)	12.4 (1.5)	16.7 (1.4)	13.7 (1.2)
3 m	1.6 (0.1)	--	--	--	--
Upwind 1m	0.35 (0.02)	--	--	--	--

Unit: [mg/m<sup>3</sup>]  $\bar{C}$  (SD)

Field test 2 (Lake Sand 17 pipes) Total Test Time: 93 minutes

Distance From Source	TSP [150]	C [120]	R [150]
1 m	8.1 (1.5)	8.2 (0.8)	18.6 <sup>D</sup> (3.1)
2 m	11.5 (2.1)	--	--
3 m	5.8 (1.0)	4.6 (0.9)	10.6 <sup>C</sup> (1.5)
Upwind 1m	0.57 (0.1)	--	--

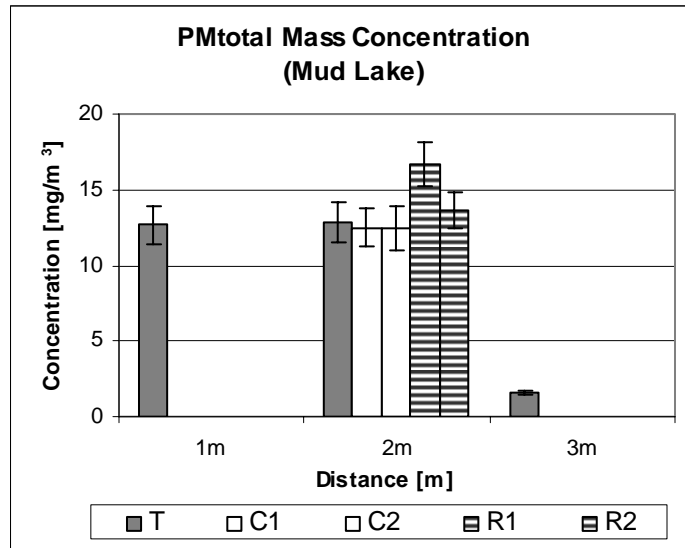
Notes: Unit: [mg/m<sup>3</sup>]  $\bar{C}$  (SD)<sup>H</sup>

Total Test Time represents all the time elapsed from the start to the finish during a sampling day.

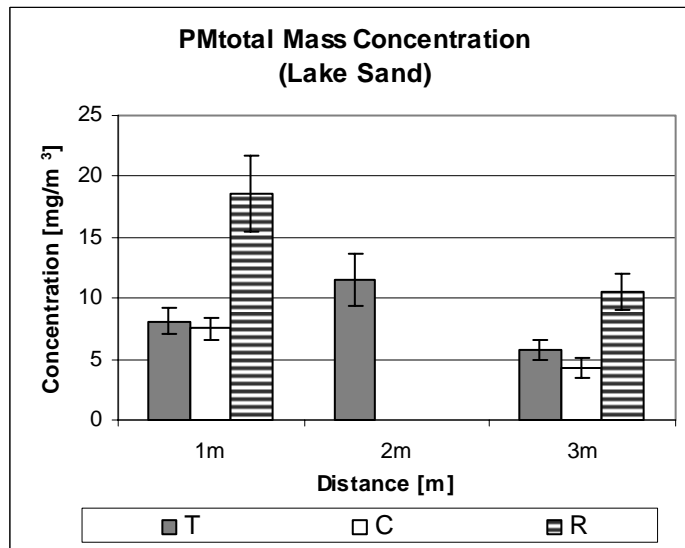
<sup>A</sup>TSP = Total Suspended Particulate samplers; <sup>B</sup>C1 and C2 = Andersen samplers; <sup>C</sup>R1 = RespiCon Sampler with 4  $\mu$ m and 10  $\mu$ m cut-points; <sup>D</sup>R2 = RespiCon sampler with 2.5  $\mu$ m and 10  $\mu$ m cut-points; <sup>E</sup>[ ] = The height of each sampler's inlet in cm; <sup>F</sup>( ) = Inlet size for the cutoff of interest in  $\mu$ m; <sup>G</sup>No measurement; <sup>H</sup> $\bar{C}$  = Average concentration from 3 times filter measurements, SD = Standard deviation were obtained using an error propagation.

$$C = \frac{\text{Mass}}{Q \times T}, \quad \frac{SD_C}{\bar{C}} = \sqrt{\left(\frac{SD_W}{\bar{W}}\right)^2 + \left(\frac{SD_Q}{\bar{Q}}\right)^2 + \left(\frac{SD_T}{\bar{T}}\right)^2} \text{ for TSP, Andersen, and RespiCon samplers.}$$

where C = Concentration; W = Weighing; Q = Flow rate; T = Time; and SD = Standard deviation.



(a)



(b)

**FIGURE 3-3. Total mass concentration by distance. (a) Mud Lake pipe,**

**(b) Lake Sand pipe.**

*Note:* (a) Plotted data = TSP sampler [150 cm], Andersen sampler [60 cm], RespiCon sampler [150 cm], (b) Plotted data = TSP sampler [150 cm], Andersen sampler [120 cm], RespiCon sampler [150 cm]. [ ] = The height of sampler's inlet in cm.

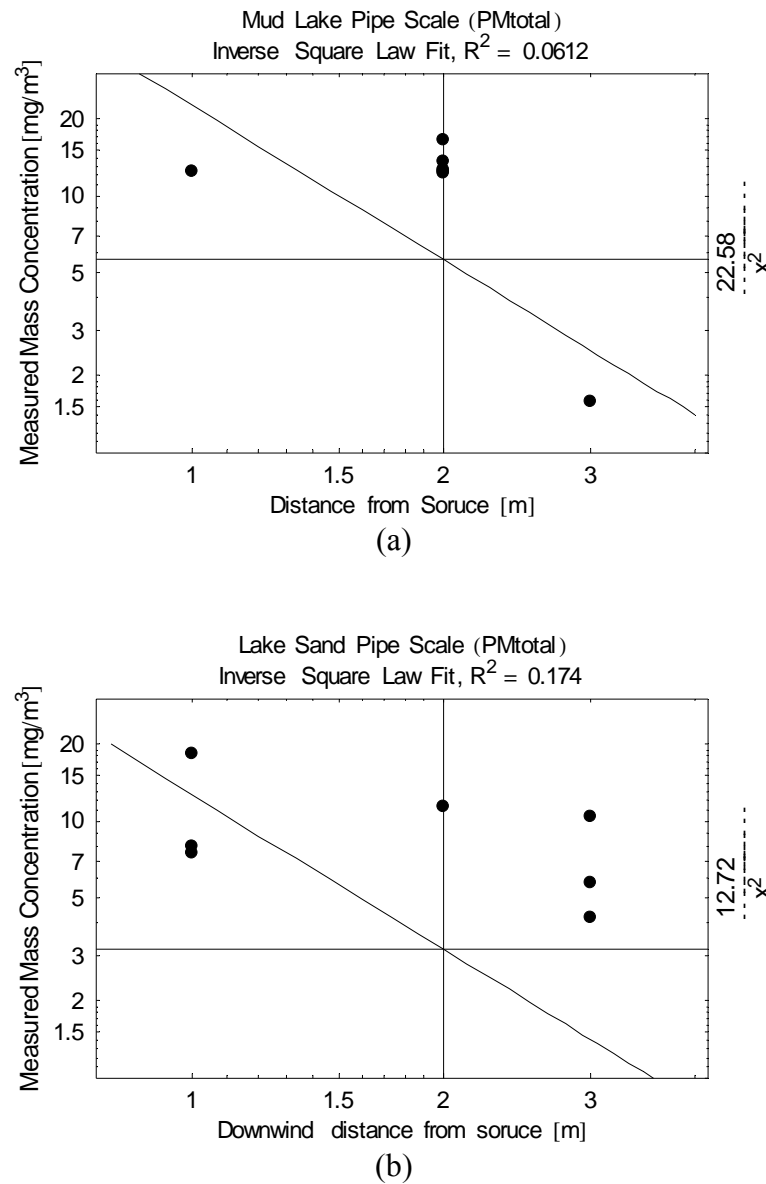


**FIGURE 3-4. Minimum mean square error fit showing unsuitability of the Inverse Square Law as a model for PM<sub>Total</sub> data. (a) Mud Lake pipe, (b) Lake Sand pipe.**

*Note:* (a) Plotted data = TSP sampler [150 cm], Andersen sampler [60 cm], RespiCon sampler [150 cm], (b) Plotted data = TSP sampler [150 cm], Andersen sampler [120 cm], RespiCon sampler [150 cm]. [ ] = The height of sampler's inlet in cm.



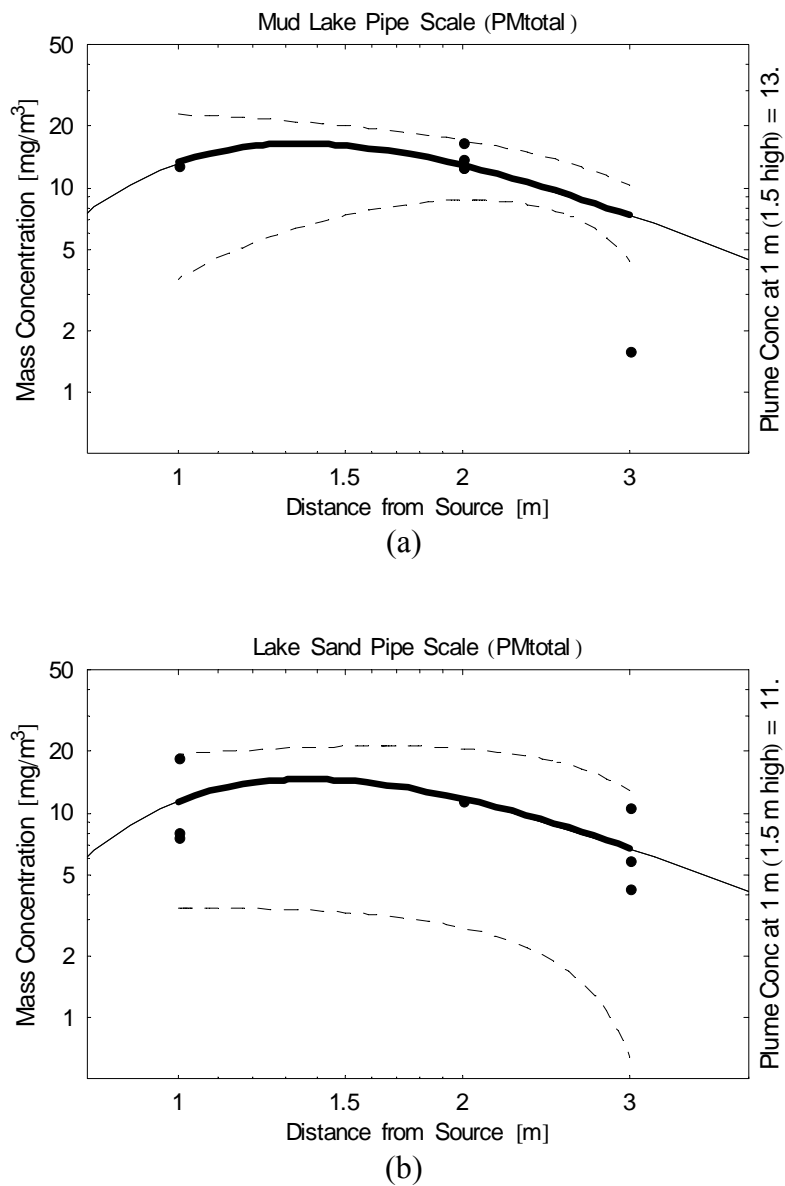


**FIGURE 3-5. Minimum mean square error fit showing Gaussian Point Source**

**Model fit to PM<sub>Total</sub> data. (a) Mud Lake ( $R^2 = 0.21$ ), (b) Lake Sand ( $R^2 = 0.27$ ).**

*Note:* (a) Plotted data = TSP sampler [150 cm], Andersen sampler [60 cm], RespiCon sampler [150 cm], (b) Plotted data = TSP sampler [150 cm], Andersen sampler [120 cm], RespiCon sampler [150 cm]. [ ] = The height of sampler's inlet in cm. Dashed lines = 95 % confidence interval (Multiple values occur at each distance. There is only one predicted value at each distance. To find confidence intervals on the fitted curve, it is sufficient to retain the concentrations of TSP samplers, representing predicted data at 1 m, 2 m, and 3 m, respectively).

In Figure 3-5, the bold line shows the nonlinear fit to a Gaussian point source model. It represents the plume centerline concentration of  $PM_{10}$ . The Mathematica NonlinearFit procedure was used to find the best fit of plume model. The Gaussian line source model was not applied to the NonlinearFit procedure because there is no horizontal dispersion coefficient in that model. The parameters were estimated by matching the concentrations measured with aerosol samplers (See Mathematica Codes in I-3).

## 2. Particle Shape and Density Influence Estimated AED

The images of front and back of a filter were examined to understand the shape of accumulated particles in Figure 3-6.

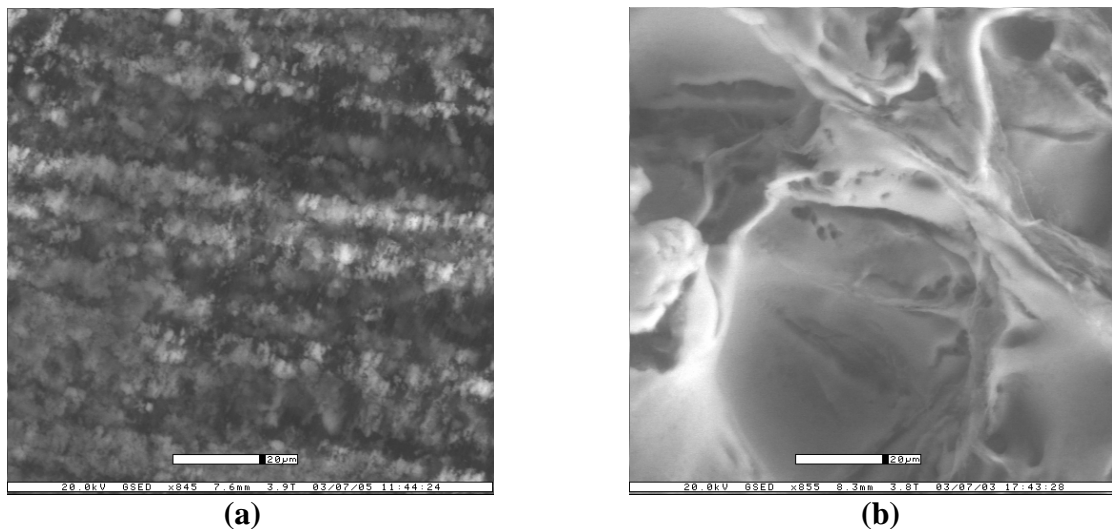


**FIGURE 3-6. The front and back images of Teflon filter. (a) Front (Calibration bar = 20  $\mu\text{m}$ ), (b) Back (Calibration bar = 20  $\mu\text{m}$ ).**

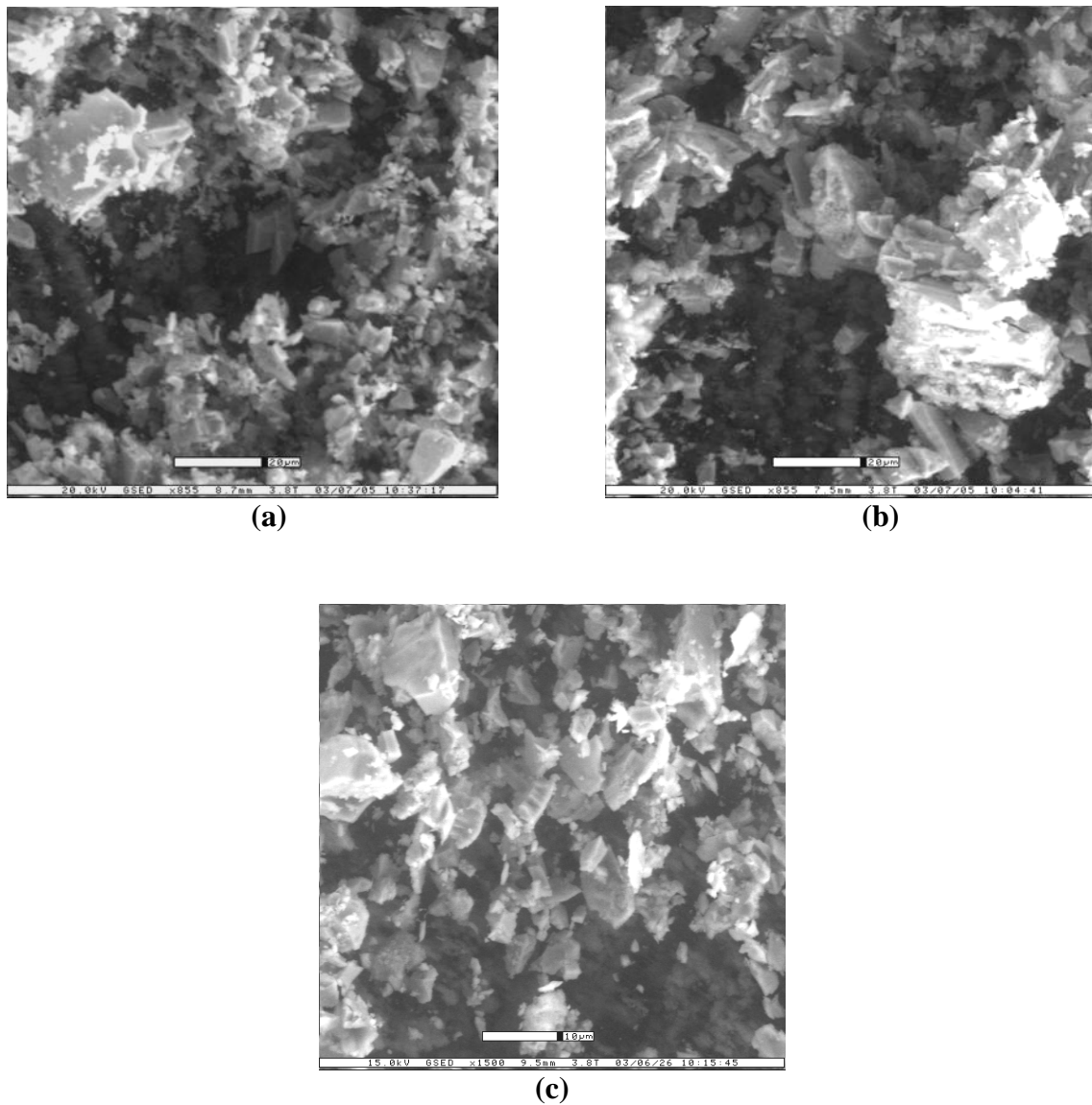


**FIGURE 3-7. The images of Mud Lake scale. (a) TSP sampler (Calibration bar = 20  $\mu\text{m}$ ), (b) PM10 sampler (Calibration bar = 20  $\mu\text{m}$ ), (c) RespiCon sampler stage 2 (Calibration bar = 10  $\mu\text{m}$ ).**

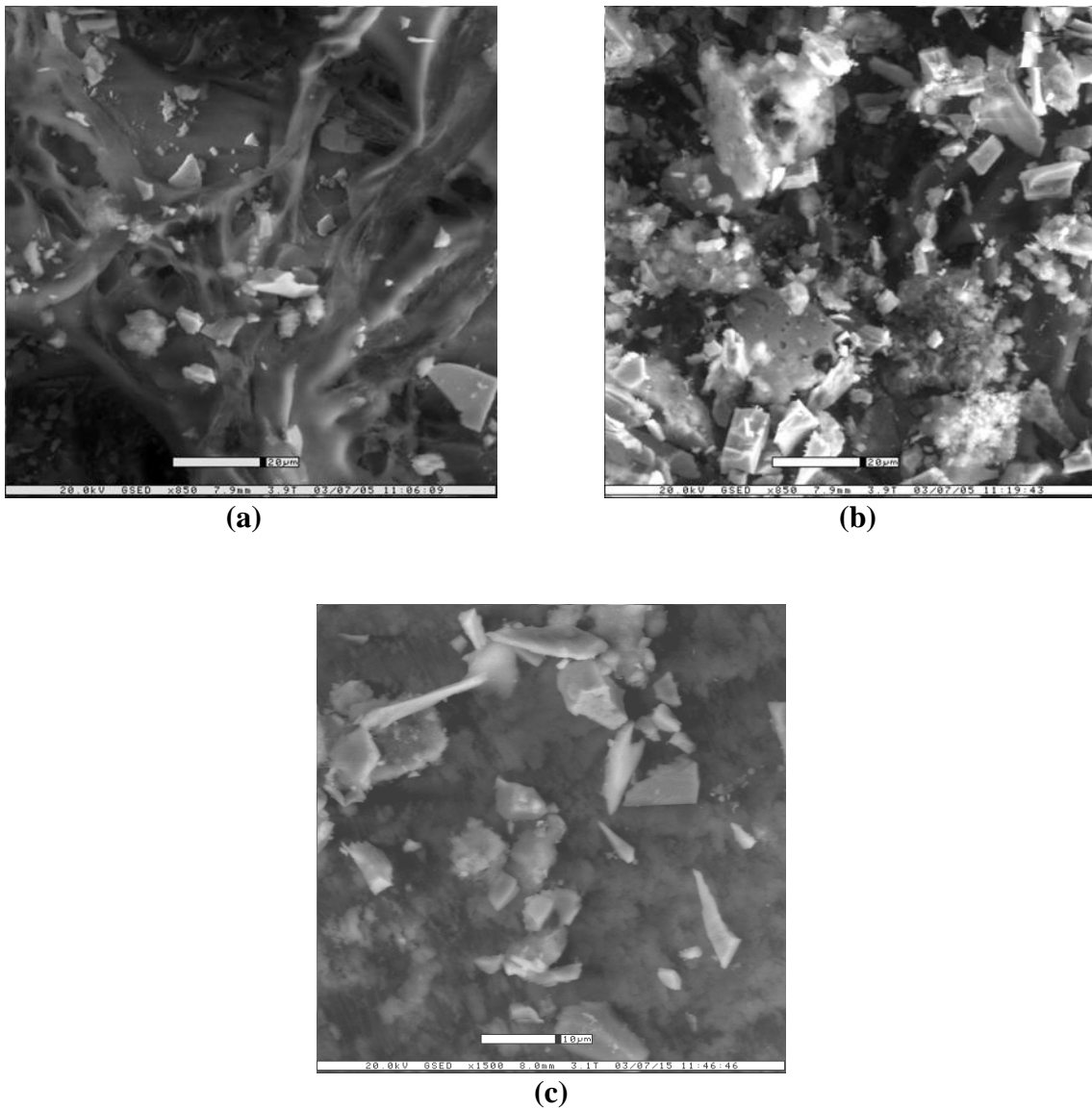


**FIGURE 3-8. The images of Lake Sand scale. (a) TSP sampler (Calibration bar = 20  $\mu\text{m}$ ), (b) PM10 sampler (Calibration bar = 20  $\mu\text{m}$ ), (c) RespiCon sampler stage 2 (Calibration bar = 10  $\mu\text{m}$ ).**

The scale images of Mud Lake and Lake Sand were provided in Figures 3-7 and 3-8. Through the ESEM images, the scale of Mud Lake is shown to have an irregular shape and many holes with dark and brown color and the scale of Lake Sand has a regular shape and a clear angled surface with bright and grey color. The shape factor ( $\chi = 1.57 \pm 0.08$ ) was estimated from particle shapes modeled as orthorhombic crystals in which the orthogonal dimensions are 1: 1: 2 (Between 1: 1: 1.5 and 1: 1: 2.5). A more detailed shape factor calculation is presented in Appendix G.

The American Society for Testing and Materials (ASTM) U.S. Standard Sieve Series were used as following: Opening size of 297  $\mu\text{m}$  with a mesh number of 50 and opening size of 105  $\mu\text{m}$  with a mesh number of 140 (E. H. SARGENT and CO., Chicago, IL). The measured density of scale passing through Mesh 140 was  $(3.46 \pm 0.3) \text{ g} \cdot \text{cm}^{-3}$  for Mud Lake pipe scale and  $(3.04 \pm 0.3) \text{ g/cm}^3$  for Lake Sand pipe scale and for scale dust passing through mesh 50 was  $(3.41 \pm 0.3) \text{ g/cm}^3$  for Mud Lake pipe scale and  $(3.13 \pm 0.3) \text{ g/cm}^3$  for Lake Sand pipe scale. In this study, the measured density of general sample was  $(3.35 \pm 0.3) \text{ g/cm}^3$  for Mud Lake scale and  $(2.43 \pm 0.3) \text{ g/cm}^3$  for Lake Sand scale. The density of general sample was used to convert ESD to AED in this study.

Five grams of finely ground scale was put into a tared graduated cylinder. A balance (AE100, Mettler Toledo, Greifensee, Switzerland) with a maximum detection of 25 g was used to weigh the sample. Then, deionized water was added, keeping track of the amount added, until 10 mL total volume is reached. At that point, the sample was agitated to make sure all the air bubbles were out. Then, the deionized water was added to make up for the lost volume again. In the end, it was found that the 5 g of Mud Lake

scale plus 8.51 mL of water occupied 10 mL. For example, the Mud Lake scale had a volume of 1.49 ml ( $\text{cm}^3$ ) and its density was  $5 \text{ g} / 1.49 \text{ mL} = 3.35 \text{ g/mL (g/cm}^3\text{)}$ .

When the images of petroleum pipe scale were taken using an ESEM, many clusters or conglomerates were found on the filters (See Figure 3-9).

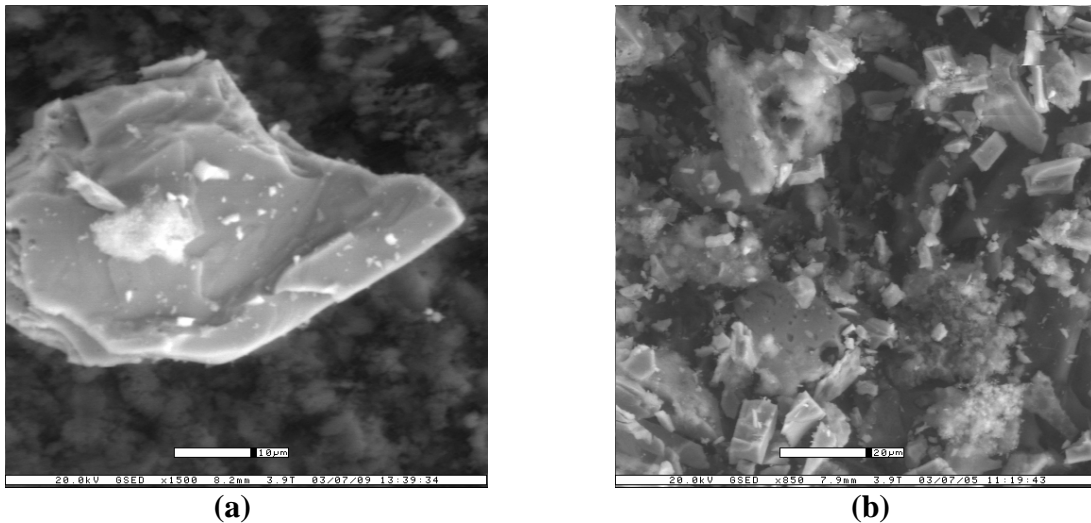


**FIGURE 3-9. Electrostatic and cluster (Lake Sand). (a) RespiCon (Calibration bar = 10  $\mu\text{m}$ ), (b) TSP (Calibration bar = 20  $\mu\text{m}$ ).**

During the petroleum pipe rattling process, a deposition mapping experiment was conducted to obtain a deposition “footprint” using 1118 Petri dishes (100 mm diameter  $\times$  18 mm deep). These were placed on a 1 m grid over the area (26  $\times$  43 array) as shown in Figure 3-10.

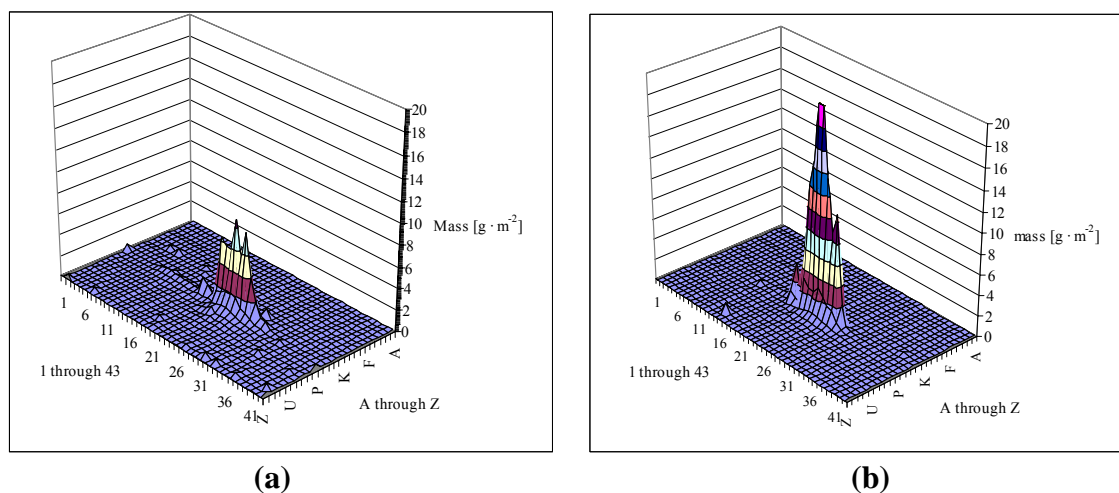


**FIGURE 3-10. Deposition mapping. (a) Mud Lake, (b) Lake Sand.**

The mapping shows that the mass percentages collected in the Petri dishes within 3 m downwind distance from the centerline, N, are 73 % and 84 % and the those within 1m upwind distance form the centerline are 11 % and 12 % from the both scales (See Table 3-3).<sup>(43)</sup>

**TABLE 3-3. Measured Mass Fraction of Settled Dust within 3 m Distance from the Centerline of Source**

Wind dir.	Upwind			Centerline	Downwind			Overall <sup>B</sup>
Distance from the centerline [m]	3	2	1	0	1	2	3	
Collected Mass fraction <sup>A</sup> (Mud Lake)	0.00	0.02	0.11	0.50	0.13	0.06	0.04	0.86
Collected Mass fraction (Lake Sand)	0.00	0.01	0.12	0.67	0.12	0.03	0.01	0.96

Notes:

<sup>A</sup>Mass fraction = Total mass at each distance / Overall settled mass. Total mass at each distance were calculated from 43 Petri dishes of each line.

<sup>B</sup>Overall mass fraction was calculated from 1118 Petri dishes.

When the images of scales were taken from the Petri dishes located at 3 m distance from the centerline of scale source, most of particles are bigger than 50  $\mu\text{m}$ . This means that in this study, the PSD for suspended aerosol able to be transported by the wind is dominated by particles smaller than ESD of 50  $\mu\text{m}$ .

Hinds<sup>(15)</sup> defined aerosol as a suspension of solid or liquid particles in a gas which have a range from 0.001 to 100  $\mu\text{m}$ . Turner<sup>(44)</sup> defined aerosol as particles smaller than about 20  $\mu\text{m}$ .

From the particles collected in the Petri dishes, several colors of particles were found. To verify the shapes of these particles, four different color groups were photographed with an ESEM. To get images of two interesting colors of particles which were deposited into the Petri dishes on both tests, the following procedures were followed for the four different color groups:

1. One of particles from each group was selected for imaging using a pin.
2. The images with magnification  $\times 250$  and  $\times 350$  (Calibration bar = 50  $\mu\text{m}$ ) from each group were obtained to compare each with other. In a small particle size range (brighter particles), the additional images were obtained with magnitude  $\times 850$  (Calibration bar = 20  $\mu\text{m}$ ).



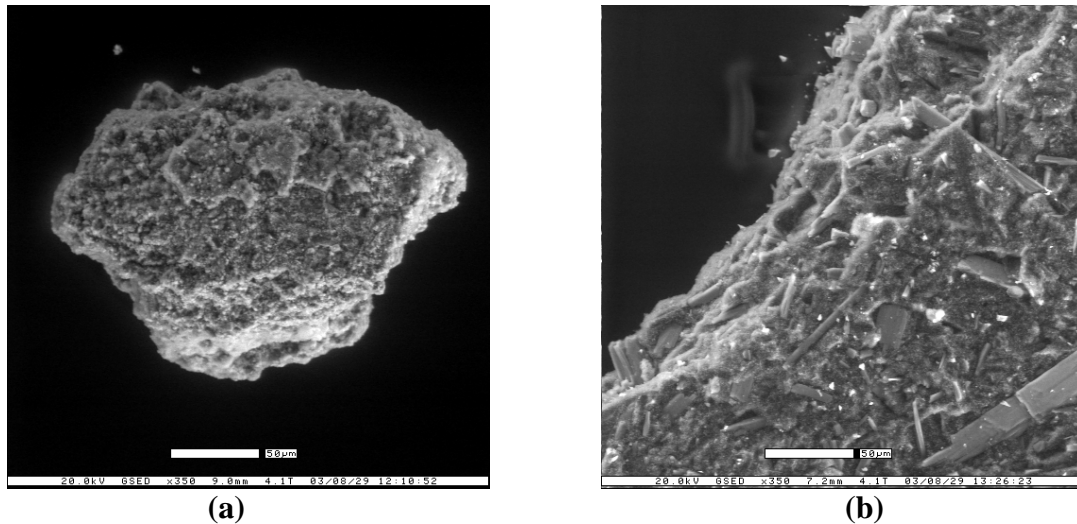


**FIGURE 3-11. The images of black and gray particle. (a) Mud Lake (Calibration bar = 50  $\mu\text{m}$ ), (b) Lake Sand (Calibration bar = 50  $\mu\text{m}$ ).**

*Notes:* The images of particle a) and b) are similar to rust. These particles were obtained at 1 m distance away from the centerline in each test.

In the Mud Lake particles, the black particles were assumed to arise from rust in the petroleum pipes. In the Lake Sand particles, the gray particles have two different sides, the grey side of particles and the darker sides of the gray side. The darker side was assumed as rust attached with the particles (See Figure 3-11). Both images were obtained from the Petri dish 1 m away from the centerline in each test.

### 3. Particle Size Distribution

The Andersen samplers and TSP/CCMs provide PSDs for two different scales. The PSD of each sampler above was plotted one by one to show the measured mass fraction (See Figures 3-12 and 3-13).

The Goodness of Fit (GOF) test was conducted to find the best distribution of airborne scales from TSP/CCMs using the Reliasoft Weibull++ program. The software ranked quality of fit for Lognormal and Normal, Exponential 1-parameter, Exponential 2-parameter, Weibull 2-parameter, and Weibull 3-parameter distributions.

The results show that the lognormal distribution was ranked as one for five of six TSP/CCMs' samples, and it ranked second when the Weibull 2-parameter distribution is ranked as one in one of six TSP/CCMs' samples. For uniformity, the lognormal model was used for all. The estimated PSD is then characterized with a  $GM_{AED}$  and a  $GSD_{AED}$  for Andersen samplers and another for TSP/CCMs.

The best PSDs and confidence intervals for Mud Lake and Lake Sand scales distributed in the air were obtained from Andersen samplers and TSP/CCMs using a log-probit analysis and a linear regression analysis (See Equations 2.4 and 2.5).

To compare the PSD of an Andersen sampler with that of a TSP/CCM, the PSDs were plotted in the same graph (See Figure 3-14).

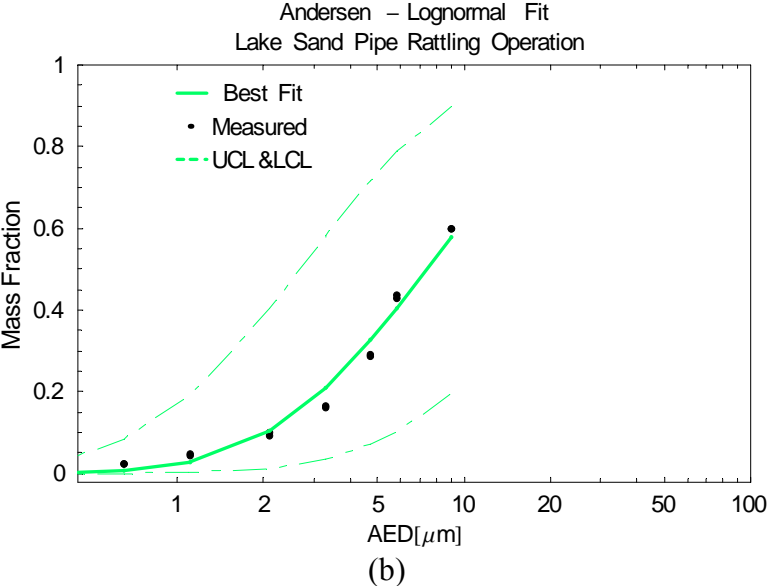
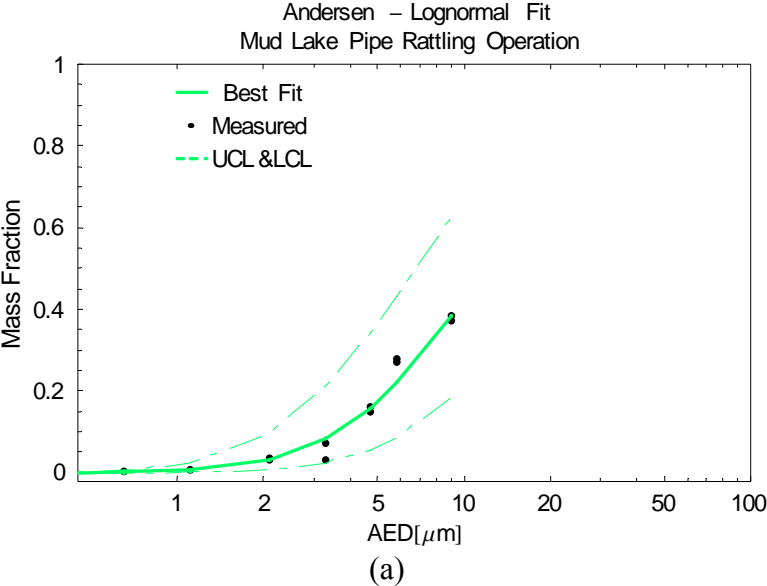


**FIGURE 3-12. PSD of Andersen Sampler (Field test). (a) Mud Lake pipe, (b) Lake Sand pipe.**

*Note:* The dashed lines represent the 95 % confidence interval for the fitted curve.

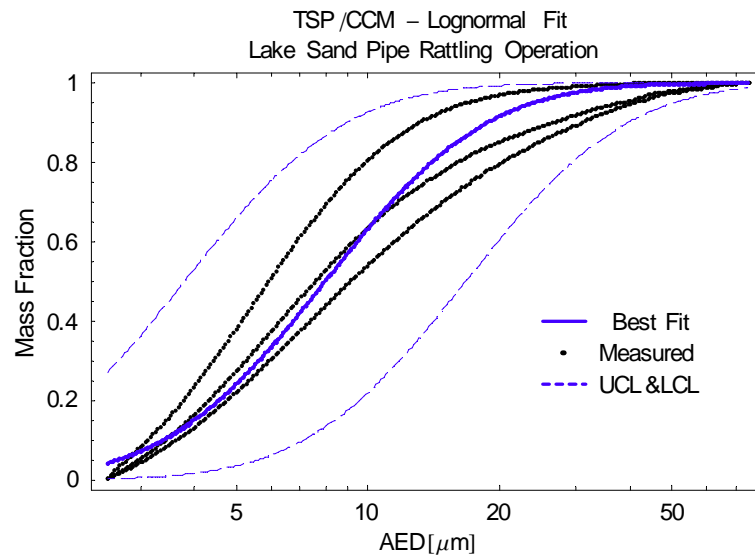
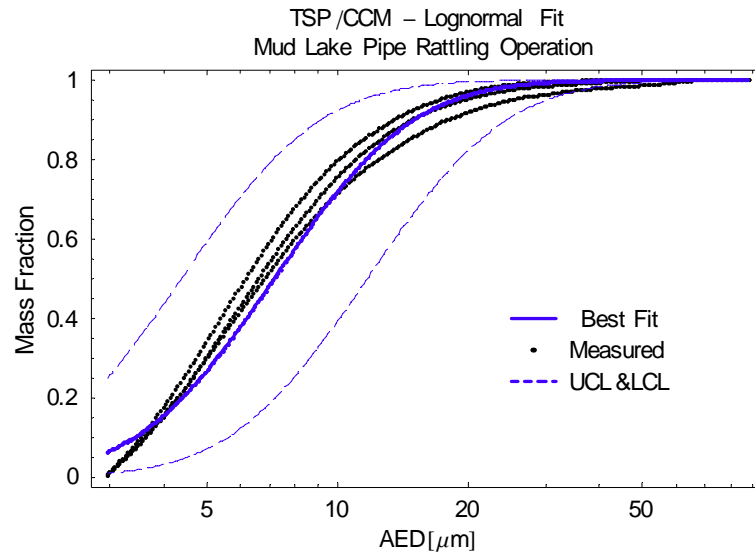


**FIGURE 3-13. PSD of TSP/CCM (Field test). (a) Mud Lake pipe, (b) Lake Sand pipe.**

*Note:* The dashed lines represent the 95 % confidence interval for the fitted curve.

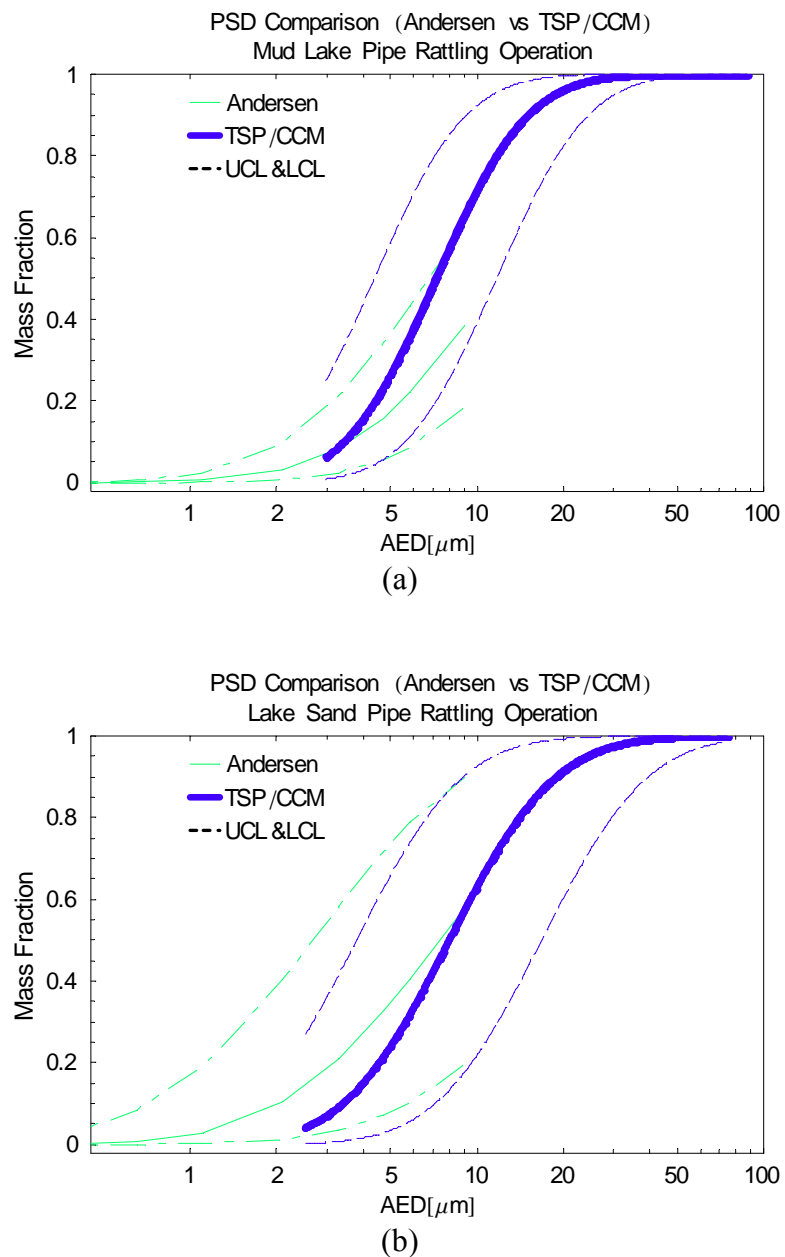


**FIGURE 3-14. PSD comparison, showing that the fitted PSD for the Andersen and the TSP/CCM analyses are consistent with one another. (a) Mud Lake with acceptable fit, (b) Lake Sand with better fit**

*Note:* The dashed lines represent the 95 % confidence interval for the fitted curve.

In Figure 3-14, there is reasonable overlap between the 95% confidence intervals associated with the PSD estimated from the Andersen Samples and that estimated from the TSP/CCM samples. As expected from the chamber studies, the Andersen slope appears to be a bit flatter than that of the TSP/CCM. As both PSDs are uncertain, the best interpretation of the data is that the portion of the PSD for small particle sizes estimated by the Andersen samples is consistent with the portion of the PSD for larger particle sizes estimated by the TSP/CCM data, within the estimated uncertainty of the data.

The  $GM_{AED}$  and  $GSD_{AED}$  for the PSD of the Andersen samplers were estimated using the principle of least squares fitting to the log normal cumulative density function (See Table 3-4). The  $GM_{AED}$  and  $GSD_{AED}$  for the PSD of the TSP/CCM samplers were also estimated the same way (See Table 3-5).

**TABLE 3-4. Parameters for Estimated PSD from Andersen Sampler Data**

Test	Field test 1 (Mud Lake)		Field test 2 (Lake Sand)	
	C1 <sup>A</sup>	C2	C1	C2
$GM_{EAED}$ <sup>B</sup> [μm]	7.1 (1.6)	6.7 (1.6)	6.2 (2.4)	6.2 (1.4)
$GSD_{EAED}$ <sup>C</sup>	2.4 (0.5)	2.1 (0.5)	3.0 (1.2)	3.0 (0.7)

Notes:

Unit:  $GM_{EAED}$  (SU) and  $GSD_{EAED}$  (SU)<sup>D</sup>

The  $GM_{AED}$  and  $GSD_{AED}$  of an Andersen sampler were estimated from log-probit analysis (See Appendix B-5).

<sup>A</sup> C1 & C2 = Andersen samplers; <sup>B</sup>  $GM_{EAED}$  = Estimated median AED of sample data;

<sup>C</sup>  $GSD_{EAED}$  = Estimated slope of PSD curve.

$$^D \frac{SD_{GM_{EAED}}}{GM_{EAED} \text{ (or } GSD_{EAED})} = \sqrt{\left(\frac{SD_W}{\bar{W}}\right)^2 + \left(\frac{SD_Q}{Q}\right)^2 + \left(\frac{SD_T}{T}\right)^2},$$

where  $SD$  = Standard deviation;  $W$  = Weighing;  $Q$  = Volume flow rate;  $T$  = Time;

$SD_{GMEaed}$  (or  $SD_{GSDEaed}$ ) = Standard deviation of  $GM_{EAED}$  (or  $GSD_{EAED}$ ).

$SU_{GMEaed}$  (or  $SU_{GSDEaed}$ ) = Sampling uncertainty of  $GM_{EAED}$  or  $GSD_{EAED} = 1.96 \times SE$ .

**TABLE 3-5. Parameters for Estimated PSD from TSP/CCM data**

Test	Field test 1 (Mud Lake)			Field test 2 (Lake Sand)		
	T1 <sup>A</sup>	T2	T3	T1	T2	T3
$GM_{EAED}^B$ [ $\mu\text{m}$ ]	5.9 (1.4)	5.5 (1.4)	5.9 (1.4)	7.9 (4.4)	5.4 (2.9)	6.5 (3.3)
$GSD_{EAED}^C$	1.7 (0.4)	1.6 (0.4)	1.8 (0.4)	2.3 (1.3)	1.7 (0.9)	2.1 (1.1)

Notes:

Unit:  $GM_{EAED}$  (SU) and  $GSD_{EAED}$  (SU)<sup>D</sup>The  $GM_{EAED}$  and  $GSD_{EAED}$  of a TSP/CCM were estimated from log-probit analysis (See Appendix B-5).<sup>A</sup> T1-T3 = TSP samplers;

The T4 sampler is excluded for lack of data; it had insufficient dust to run a CCM for a PSD.

<sup>B</sup>  $GM_{EAED}$  = Estimated median AED of sample data;<sup>C</sup>  $GSD_{EAED}$  = Estimated slope of PSD curve.

$$^D \frac{SD_{GM_{EAED}}}{GM_{EAED} \text{ (or } GSD_{EAED})} = \sqrt{\left(\frac{SD_W}{\bar{W}}\right)^2 + \left(\frac{SD_Q}{\bar{Q}}\right)^2 + \left(\frac{SD_T}{\bar{T}}\right)^2 + \left(\frac{SD_{\rho_p}}{\bar{\rho}_p}\right)^2 + \left(\frac{SD_{\chi}}{\bar{\chi}}\right)^2},$$

where  $SD$  = Standard deviation;  $W$  = Weighing;  $Q$  = Volume flow rate;  $T$  = Time;  $\rho_p$  = Density of particles;  $\chi$  = Shape factor; and  $SD$  = Standard deviation. $SU_{GMEAEAD}$  (or  $SU_{GSDEAEAD}$ ) = Sampling uncertainty of  $GM_{EAED}$  or  $GSD_{EAED}$  =  $1.96 \times SE$ . $SD_{\rho_p}/\bar{\rho}_p$  and  $SD_{\chi}/\bar{\chi}$  were estimated as 0.1 and as 0.05 (from ESEM images).

#### 4. PM<sub>10</sub> and PM<sub>4</sub> mass concentration

The PM<sub>10</sub> concentrations by PM<sub>10</sub> samplers were compared with the mass concentration for thoracic concentrations (AED  $\leq 10 \mu\text{m}$ ) estimated by RespiCon samplers. In Andersen samplers, the concentrations of PM<sub>10</sub> and PM<sub>4</sub> were estimated from the stage cutoff AED  $\leq 9 \mu\text{m}$  and AED  $\leq 3.3 \mu\text{m}$ . In TSP/CCMs, the concentrations of PM<sub>10</sub> and PM<sub>4</sub> were estimated from the converted AEDs. RespiCon samplers provide unbiased mass fraction for PM<sub>10</sub> and PM<sub>4</sub>.

Tables 3-6 and 3-7 show mass concentration and mass fraction from each size selective aerosol sampler for respirable (called PM<sub>4</sub>) and thoracic (called PM<sub>10</sub>) fractions. The estimated PM<sub>10</sub> concentrations in Table 3-6 were used to find best fit for Gaussian plume model. The vertical and horizontal coefficients,  $\sigma_y$  and  $\sigma_z$ , and an emission rate for a Gaussian plume model are estimated to find an attainment area for the public.

**TABLE 3-6. Mass Concentrations for Respirable and Thoracic PM**

## Field test 1 (Mud Lake 13 pipes)

Sampler	T <sup>A</sup> 1m <sup>E</sup> [150] <sup>F</sup>	T 2m [150]	T 3m [150]	C <sup>B</sup> 2m [60]	C 2m [60]	R <sup>C</sup> 2m (4μm) <sup>G</sup> [150]	R 2m (2.5μm) [150]	P <sup>D</sup> 1m [150]	P 2m [150]	P 3m [150]
PM <sub>4</sub>	2.9 (0.3)	3.4 (0.4)	0.4 (0.1)	<u>0.4</u> <sup>H</sup> (0.01)	<u>0.9</u> (0.1)	2.7 (0.1)	1.4 (0.1)	-- <sup>I</sup>	--	--
PM <sub>10</sub>	10.5 (1.2)	11.3 (1.4)	1.3 (0.1)	<u>4.8</u> <sup>H</sup> (0.5)	<u>4.6</u> (0.6)	6.40 (0.4)	3.64 (0.7)	2.8 (0.1)	5.1 (0.7)	--

Unit: [mg/m<sup>3</sup>]  $\bar{C}$  (SD)<sup>J</sup>

## Field Test 2 (Lake Sand 17 pipes)

Description	T 1m [150]	T 2m [150]	T 3m [150]	C 1m [120]	C 3m [120]	R 1m (2.5μm) [150]	R 3m (4μm) [150]	P 1m [150]	P 2m [150]	P 3m [150]
PM <sub>4</sub>	1.6 (0.4)	3.5 (0.7)	1.4 (0.3)	<u>1.4</u> (0.1)	<u>0.7</u> (0.1)	2.6 (0.4)	0.9 (0.1)	--	--	--
PM <sub>10</sub>	4.9 (1.1)	10.0 (2.1)	4.2 (0.8)	<u>4.9</u> (0.5)	<u>2.7</u> (0.5)	6.6 (0.5)	3.6 (0.4)	2.2 (0.4)	2.7 (0.5)	1.6 (0.3)

Unit: [mg/m<sup>3</sup>]  $\bar{C}$  (SD)

Notes:

<sup>A</sup>T = Total suspended particulate samplers by a CCM; <sup>B</sup>C = Andersen samplers;<sup>C</sup>R = RespiCon samplers; <sup>D</sup>P = PM<sub>10</sub> samplers; <sup>E</sup> 1m, 2m, and 3m = the distance from the source [m];<sup>F</sup>[ ] = The height of each sampler's inlet in cm; <sup>G</sup>(μm) = cutoff size for first stage;<sup>H</sup> $\bar{C}$  = The mass fractions for PM<sub>4</sub> and PM<sub>10</sub> based on the stage cutoff AED 3.3 μm and 9 μm of Andersen sampler; <sup>I</sup>-- = No measurement by a CCM for the PM<sub>10</sub> sampler;<sup>J</sup> $\bar{C}$  = Average concentration from 3 times filter measurements; SD = Standard deviation were obtained using an error propagation.

$$\frac{SD_{PM_{10}}}{\bar{C}_{PM_{10}}} = \sqrt{\left(\frac{SD_{PM_{total}}}{\bar{C}_{PM_{total}}}\right)^2 + \left(\frac{SD_{\rho_p}}{\bar{\rho}_p}\right)^2 + \left(\frac{SD_{\chi}}{\bar{\chi}}\right)^2}, \quad \frac{SD_{PM_4}}{\bar{C}_{PM_4}} = \sqrt{\left(\frac{SD_{PM_{total}}}{\bar{C}_{PM_{total}}}\right)^2 + \left(\frac{SD_{\rho_p}}{\bar{\rho}_p}\right)^2 + \left(\frac{SD_{\chi}}{\bar{\chi}}\right)^2} \text{ for TSP samplers.}$$

where C = Concentration;  $\rho_p$  = Density of particles;  $\chi$  = Shape factor; and SD = Standard deviation.The equations above were based on the conversion from ESD to AED using  $AED = ESD \left[ \frac{\rho_p}{\rho_0 \cdot \chi} \right]^{1/2}$ 

where AED = Aerodynamic Equivalent Diameter; ESD = Equivalent Spherical Diameter;

 $\rho_0$  = Unit Density (1 g · cm<sup>-3</sup>);  $\chi$  = Dynamic shape factor. $SD_{\rho_p} / \bar{\rho}_p = 0.1$  because the measured density were (3.4 ± 0.3) g · cm<sup>3</sup> for Mud Lake scale and(2.4 ± 0.2) g · cm<sup>3</sup> for Lake Sand scale.The value for  $SD_{\chi} / \bar{\chi}$  was estimated as 0.1 from the images obtained from the ESEM for both scales.

$$\frac{SD_{PM_{10}}}{\bar{C}_{PM_{10}}} = \sqrt{\left(\frac{SD_{S_F}}{\bar{W}_{S_F}}\right)^2 + \left(\frac{SD_{S_7}}{\bar{W}_{S_7}}\right)^2 + \dots + \left(\frac{SD_{S_1}}{\bar{W}_{S_1}}\right)^2 + \left(\frac{SD_Q}{\bar{Q}}\right)^2 + \left(\frac{SD_T}{\bar{T}}\right)^2},$$

$$\frac{SD_{PM_4}}{\bar{C}_{PM_4}} = \sqrt{\left(\frac{SD_{S_F}}{\bar{W}_{S_F}}\right)^2 + \left(\frac{SD_{S_7}}{\bar{W}_{S_7}}\right)^2 + \left(\frac{SD_{S_6}}{\bar{W}_{S_6}}\right)^2 + \left(\frac{SD_{S_5}}{\bar{W}_{S_5}}\right)^2 + \left(\frac{SD_{S_4}}{\bar{W}_{S_4}}\right)^2 + \left(\frac{SD_Q}{\bar{Q}}\right)^2 + \left(\frac{SD_T}{\bar{T}}\right)^2} \text{ for Andersen samplers.}$$

where S<sub>0</sub>, S<sub>1</sub>, S<sub>2</sub>, S<sub>3</sub>, S<sub>4</sub>, S<sub>5</sub>, S<sub>6</sub>, S<sub>7</sub>, S<sub>F</sub> = The number of stages.

In these calculations, the relative standard deviation for stages 6, 7, and F were above 1 because of small quantity of mass on these stages. Thus, the relative standard deviation of stages 6, 7, and F were estimated as 0.02.



**TABLE 3-7. Mass Fractions for Respirable and Thoracic PM**

## 1) Field test 1 (Mud Lake 13 pipes)

Sampler	T <sup>A</sup> 1m <sup>D</sup> [150] <sup>E</sup>	T 2m [150]	T 3m [150]	C <sup>B</sup> 2m [60]	C 2m [60]	R <sup>C</sup> 2m (4µm) <sup>F</sup> [150]	R 2m (2.5µm) [150]
PM <sub>4</sub>	0.23 (0.03)	0.26 (0.03)	0.25 (0.03)	<u>0.03</u> <sup>G</sup> (0.00)	<u>0.07</u> (0.01)	0.16 (0.01)	0.10 (0.01)
PM <sub>10</sub>	0.83 (0.10)	0.88 (0.10)	0.81 (0.09)	<u>0.38</u> <sup>G</sup> (0.04)	<u>0.37</u> (0.04)	0.38 (0.03)	0.27 (0.02)

Note:

Unit: [mg/m<sup>3</sup>]  $\bar{C}$  (SD)<sup>A</sup>T = Total Suspended Particulate samplers by a CCM; <sup>B</sup>C = Andersen samplers;<sup>C</sup>R = RespiCon samplers; <sup>D</sup>1 m, 2 m, and 3 m = the distance from the source;<sup>E</sup>[ ] = The height of each sampler's inlet in cm; <sup>F</sup>(µm) = cutoff size for first stage;<sup>G</sup>    = The mass fractions for PM<sub>4</sub> and PM<sub>10</sub> based on the stage cutoff AED 3.3 µm and 9 µm of Andersen sampler.

## 2) Field test 2 (Lake Sand 17 pipes)

Description	T 1m [150]	T 2m [150]	T 3m [150]	C 1m [120]	C 3m [120]	R 1m (2.5µm) [150]	R 3m (4µm) [150]
PM <sub>4</sub>	0.20 (0.04)	0.30 (0.06)	0.25 (0.05)	<u>0.16</u> (0.03)	<u>0.16</u> (0.11)	0.08 (0.01)	0.14 (0.02)
PM <sub>10</sub>	0.61 (0.13)	0.87 (0.19)	0.72 (0.14)	<u>0.6</u> (0.06)	<u>0.6</u> (0.11)	0.34 (0.06)	0.35 (0.05)

Unit: [mg/m<sup>3</sup>]**5. Risk Assessment**

To find the attainment area for the general public, one starts by deciding how to conduct risk assessment. From TSP sampler data in Table 3-2 and PM<sub>10</sub> sampler data in Table 3-6, the highest mass concentrations were observed from the aerosol samplers located at a 2 m distance from the centerline source. Two video cameras were used to record the pipe rattling research on the ground and at the height of 10 m on each experiment day. The recorded DVDs of pipe rattling operations show that most of

plume passed beneath the sampler at 1 m for most of each test and that the plume engulfed the samplers at 2 and 3 meters.

Figure 3-15 shows that the PM<sub>10</sub> concentrations from Andersen, RespiCon, and TSP/CCM, and PM<sub>10</sub> samplers are not consistent with a simple inverse square law model of concentration vs. distance.

The Gaussian plume model was used for predicting the distance from the centerline to the proximate edge of the attainment area for the NAAQS 24 hour average limit of 0.15 mg/m<sup>3</sup> for the public. The Mathematica NonlinearFit procedure was used to find the best fit of plume model. Parameters of the plume model were estimated to obtain a best fit in the minimum mean square error sense.

In NonlinearFit procedure, the estimated parameters were: emission rate (ER [mg/s]), horizontal dispersion coefficient ( $\sigma_y = ay + by \cdot x$ ), vertical dispersion coefficient ( $\sigma_z = az + bz \cdot x$ ), and effective height ( $H [m] = h$  (pipe location height) +  $\Delta h$  (average plume height from the pipe location)). The  $ay$  and  $az$  was assumed to have 0 value. A height of the receptor the ground is modeled as 1.5 m to simulate human breathing zone. Average wind speed measured on the ground was applied to this model as  $(2.2 \pm 1.1)$  m/s for Mud Lake pipe rattling process and  $(3.2 \pm 0.5)$  m/s for Lake Sand pipe rattling process. The values of best parameters of  $ER$ ,  $by$ ,  $bz$ , and  $H$  are introduced for the public exposure standard and for the worker exposure standard in Appendix I-1. The Mathematica code used for this non-linear data analysis reproduced in Appendix I-3. The Gaussian dispersion model is summarized in Appendix H.

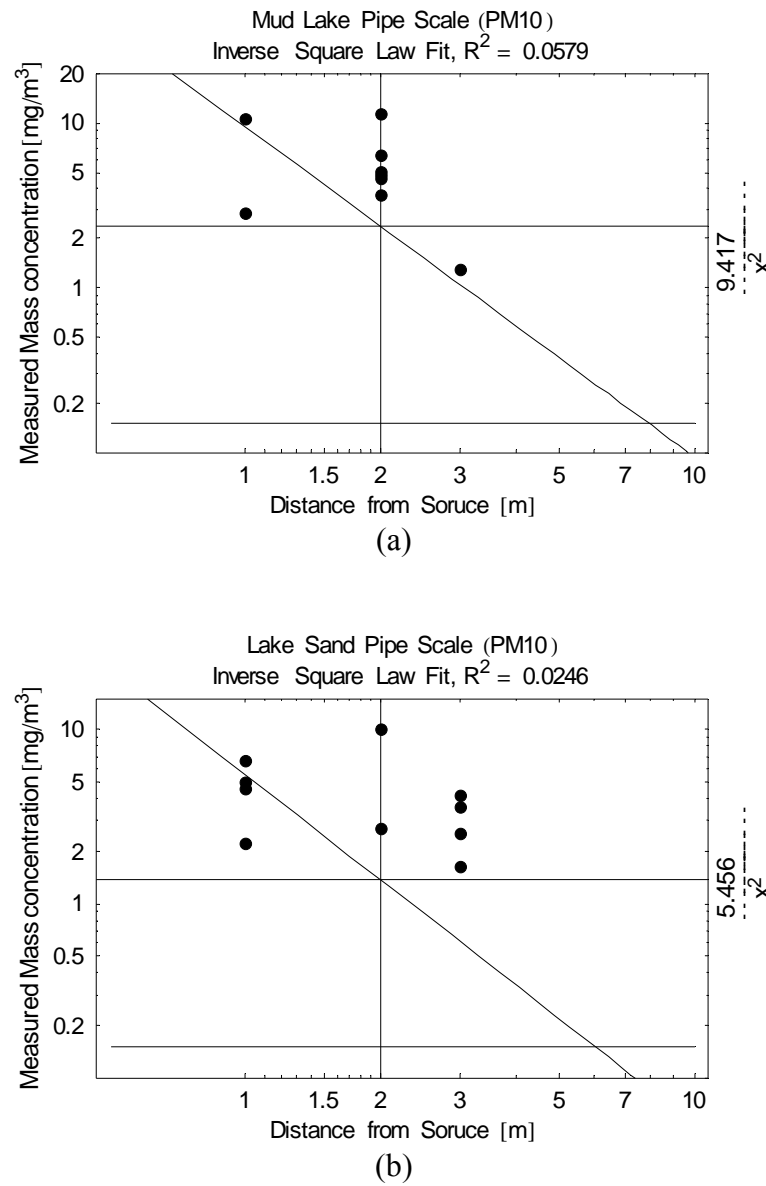


**FIGURE 3-15. Minimum mean square error fit showing unsuitability of the Inverse Square Law as a model for  $\text{PM}_{10}$  data. (a) Mud Lake pipe ( $R^2 = 0.06$ ), (b) Lake Sand pipe ( $R^2 = 0.02$ ).**

*Note:* Plotted data = Estimated  $\text{PM}_{10}$  concentrations of TSP, Andersen, and RespiCon samplers; Measured concentrations of  $\text{PM}_{10}$  samplers.

With the estimated parameters, the plume centerline concentrations for  $PM_{10}$   $PM_{Total}$  were shown in Figures 3-16 and 3-17. The maximum concentrations were found between 1.3 m and 1.5 m for Mud Lake and Lake Sand pipe rattling operation.

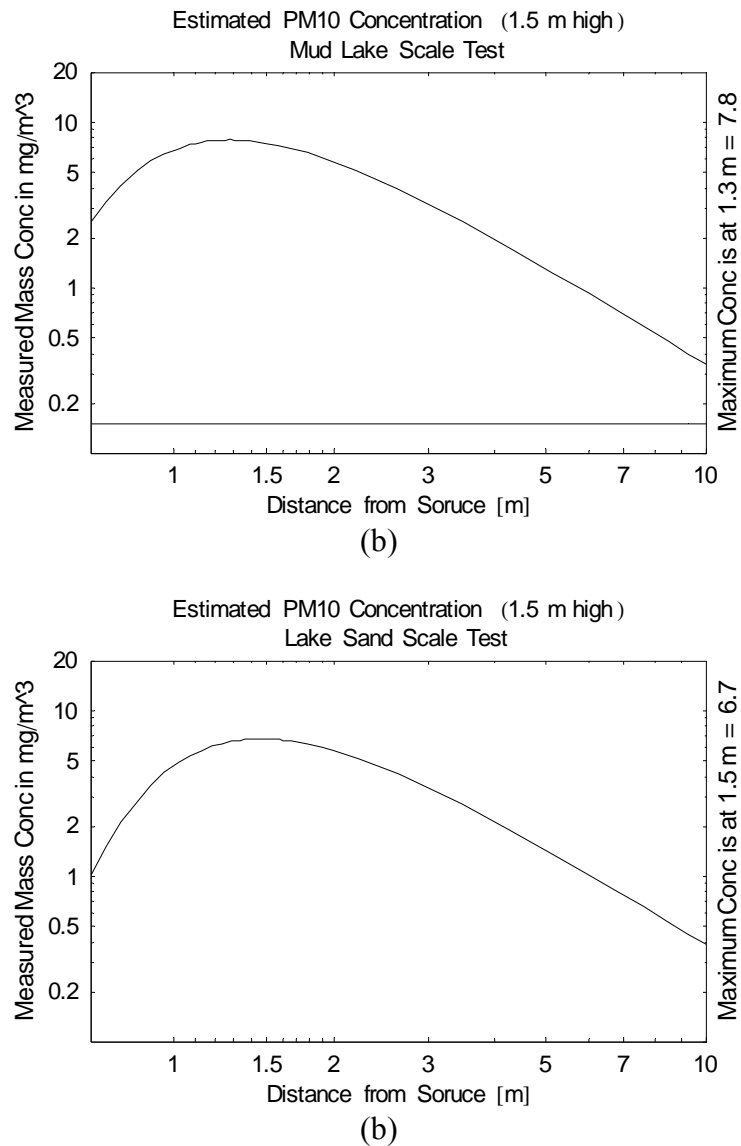


**FIGURE 3-16. Plume centerline concentrations of  $PM_{10}$  showing maximum concentration between 1 m and 2 m distance from the source. (a) Mud Lake pipe, (b) Lake Sand pipe.**

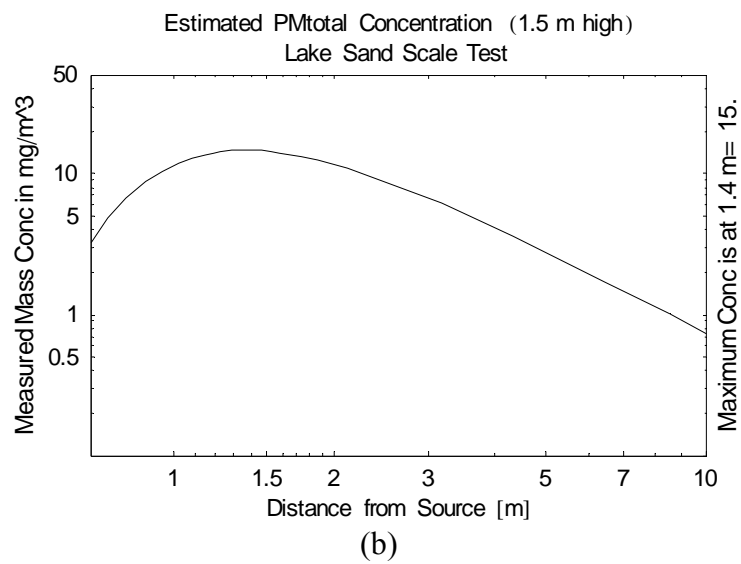
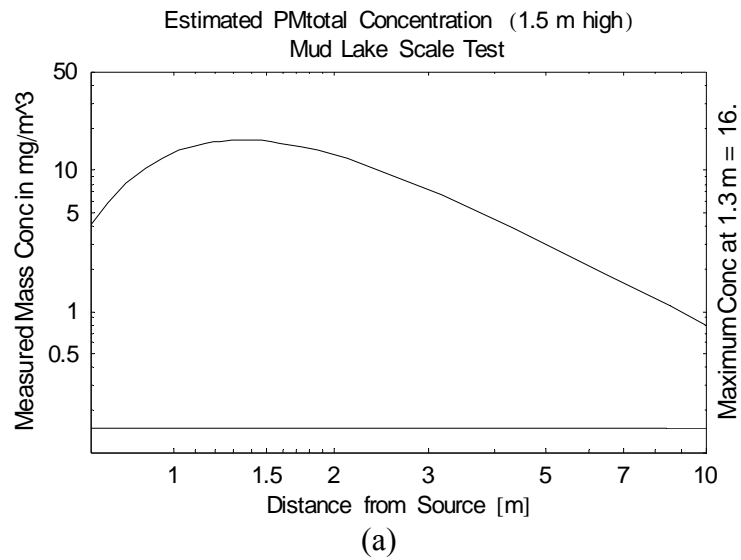


**FIGURE 3-17. Plume centerline concentrations of PM<sub>Total</sub> showing maximum concentration between 1 m and 2 m distance from the source. (a) Mud Lake pipe, (b) Lake Sand pipe**

To obtain the attainment area on the basis of NAAQS, the  $PM_{10}$  concentrations in Table 3-6 were fitted to the Gaussian plume model and that was plotted with the  $0.15 \text{ mg/m}^3$ , NAAQS 24-hour average limit. Figure 3-18 shows that the attainment area starts about 20 m from the estimated centerline concentration of  $PM_{10}$  source for Mud Lake and Lake Sand pipe scales.

The pipe rattling operations did not allow measurement of 8-hour and 24-hour TWA concentrations. The total measurement time is 191 minutes for Mud Lake petroleum pipes and 93 minutes for Lake Sand petroleum pipes. No standards or guidelines were found for short-term exposures as a result of a literature search among PELs, TLVs, and NAAQSs. The 24-hour concentration for NAAQS is overstated by a factor of 3 when the pipe rattling operations is considered as 8-hour measurement. Available data suggest that the NAAQS attainment area for unlimited public access starts at distances of about 9 m for Mud Lake pipe scale and about 10 m for a Lake Sand pipe scale (See Figure 3-18).

Figures 3-18 and 3-19 show that the estimated plume centerline concentrations from a Gaussian plume model are consistent with the concentrations measured by size selective aerosol sampler at the height of breathing zone.

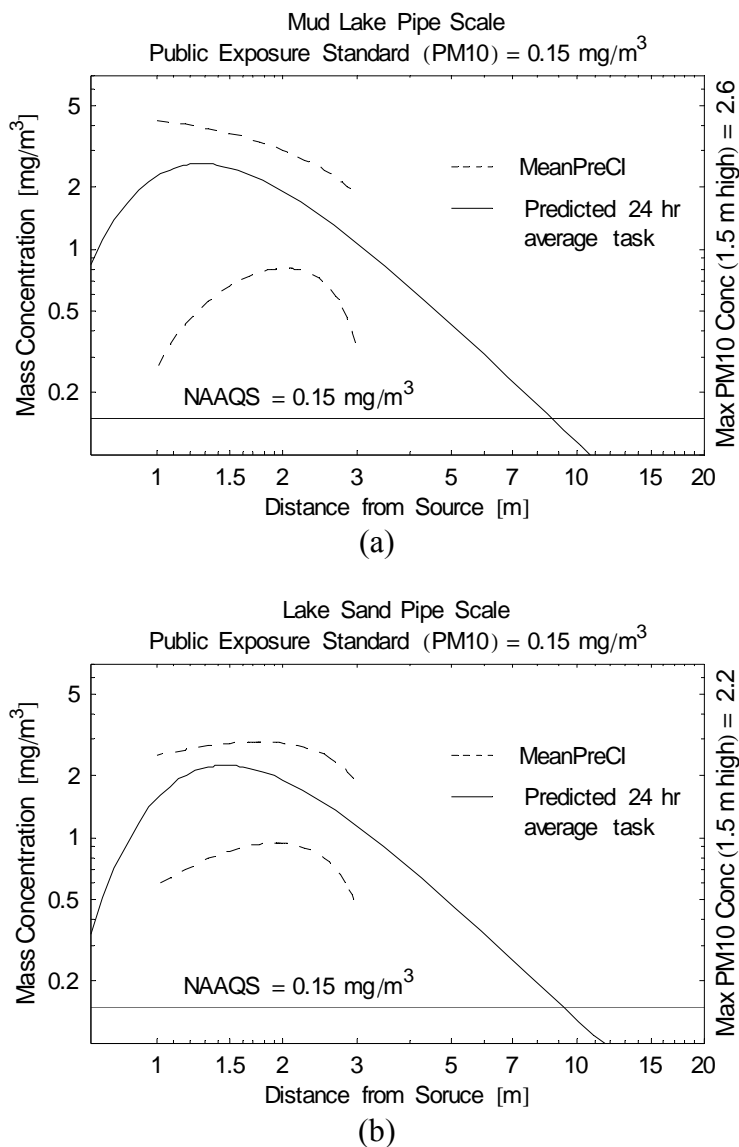


**FIGURE 3-18. Nonlinear fit of Gaussian plume model to task average exposures compared with the NAAQS used for the public exposure standard. (a) Mud Lake pipe, (b) Lake Sand pipe.**

*Notes:* Plotted data = Estimated PM<sub>10</sub> Concentrations of TSP, Andersen, and RespiCon samplers; Measured concentrations of PM<sub>10</sub> samplers.  
The line for a predicted 24-hour average task was estimated by the factor (8-hour / 24-hour) at the height of 1.5 m receptor for human breathing zone.

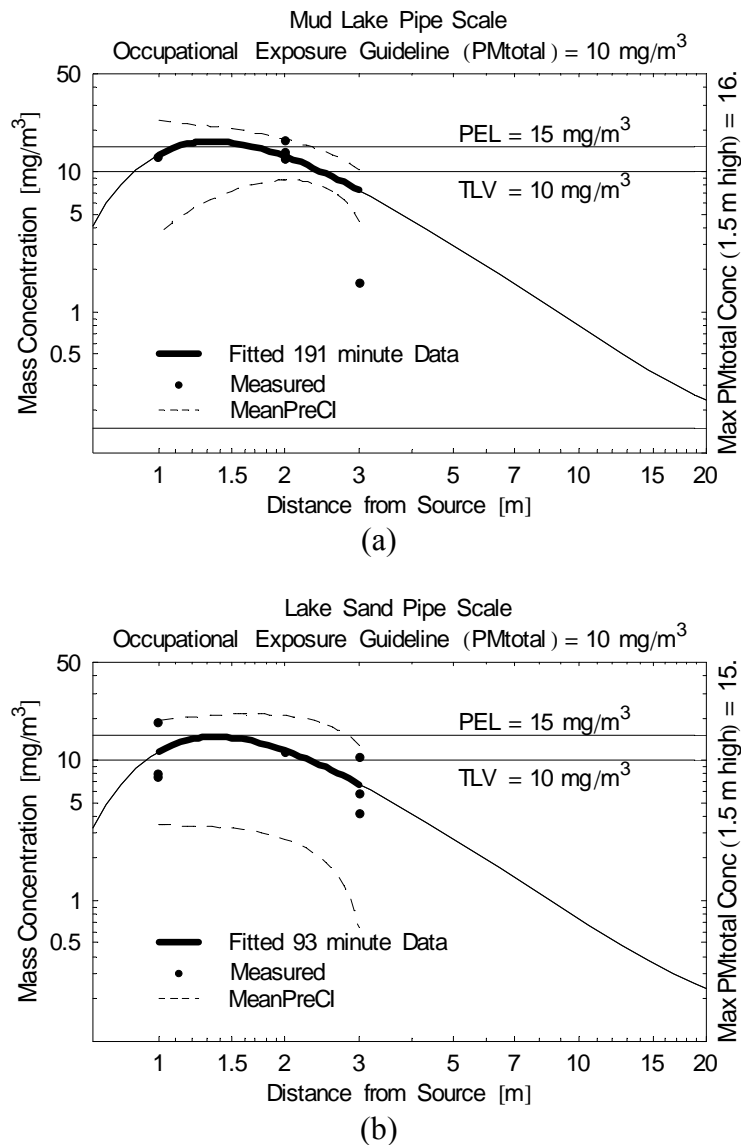


**FIGURE 3-19. Nonlinear fit of the Gaussian plume model to task average exposures compared with the TLV used for the occupational exposure guideline.**

**(a) Mud Lake pipe ( $R^2 = 0.21$ ), (b) Lake Sand pipe ( $R^2 = 0.27$ ).**

*Note:* Plotted data = Measured PM<sub>Total</sub> concentrations of TSP, Andersen, RespiCon samplers. The line for a fitted 191-minute and 93-minute average tasks surrogates for 8-hour TWA. The line for a fitted 8-hour average task was estimated for PM<sub>Total</sub> concentrations at the height of 1.5 m receptor for human breathing zone.



To obtain the attainment area for the worker on the basis of ACGIH guideline, the total mass concentrations in Table 3-2 was plotted with the TLV-TWA  $10 \text{ mg/m}^3$ . Figure 3-19 shows that the attainment area for the worker is estimated to start 4 m from the estimated centerline concentration of total PM source for both scales on the basis of upper confidence limit about the mean. No respirator needs to be worn beyond this distance to keep the inhaled dust concentration below the TLV.

#### D. DISCUSSION

The highest concentrations were found from the TSP sampler and the  $\text{PM}_{10}$  sampler located at 2 m distance from the centerline of the cleaning machine, the dust source (See Table 3-2). These results can be explained by the height of samplers that were located at a height of 1.5 m which is above the estimated effective heights from the Mud Lake and Lake Sand pipe rattling operations ( $H \equiv 1.3 \text{ m}$ ; see Appendix I) and is not in the particle dispersion region at 1 m receptor distance sometimes (See Figure 3-20).

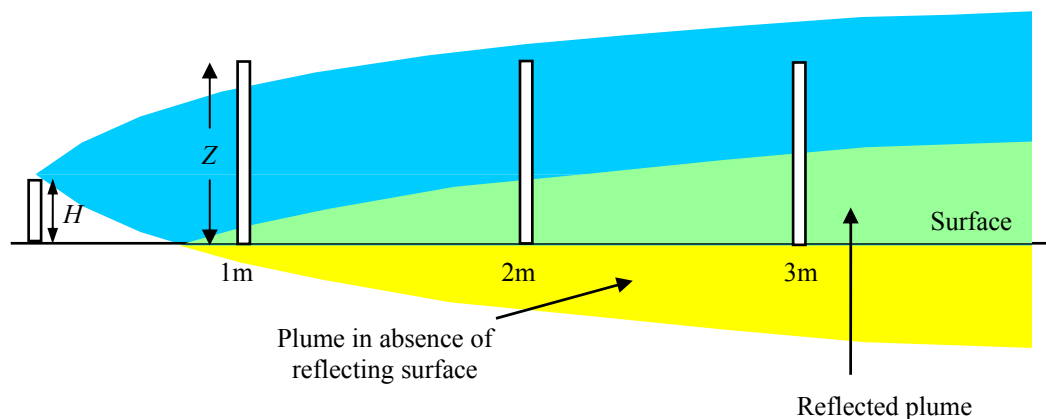


**FIGURE 3-20. Plume dispersion by distance.**

## E. CONCLUSIONS

Six sampler technologies were used to evaluate airborne dust concentrations released from oilfield pipe rattling operations. The task sampled was the removal of scale deposited on the inner wall of the pipe before it was removed from service in a producing well. The pipe cleaning machine removed rust and corrosion products as well as scale from used oilfield pipe and casing joints. The resulting dust cloud contains a mixture of particles ranging in maximum dimension from a few cm to a few  $\mu\text{m}$ , and ranging in density from  $2 \text{ g/cm}^3$  to  $4 \text{ g/cm}^3$ . Only those particles with dimensions smaller than  $50 \mu\text{m}$  were carried by the wind. Larger particles fell on the geotextile fabric laid beneath the machine for these tests. These precipitated particles and chunks of scale and corrosion were collected at the end of each test.

Appropriate data from each sampler was combined with appropriate data from other samplers to estimate both the occupational exposure patterns and the environmental exposure patterns. The test duration was limited by the quantity of pipe available for cleaning. The Lake Sand pipe required 191 operating minutes for cleaning 13 pipe joints. The Mud Lake pipe required 93 operating minutes for cleaning 17 pipe joints. Many of the samplers were operating near their lower limit of detection. Spatially, the data are sparse, and this chapter contains a transparent attempt at error propagation to report all measured concentrations with an estimate of their 95 % confidence limits.

The attainment area was found using a plume model with parameters estimated by minimum mean square error fitting algorithms. The measured mass concentration of

the aerosol samplers shows that the inverse square law is not applicable to the data of pipe rattling process for finding an attainment area. The recorded DVD video also shows that the plume passed beneath the sampler at 1 m for most of each test.

It is estimated that workers who remain within 1 m of the machine centerline have TWA exposure opportunity with  $< (13.3 \pm 9.7) \text{ mg/m}^3$  for the Mud Lake pipe scale and  $< (11.4 \pm 9.7) \text{ mg/m}^3$  for the Lake Sand pipe scale depending on the wind direction relative to the worker's position. At distances more than 4 m downwind from the machine centerline, observed and predicted dust concentrations were below the TWA-TLV  $10 \text{ mg/m}^3$  for the total dust samples in both scales based on upper confidence limit about the each mean concentration.

It is estimated that nearly all dust particles with  $\text{ESD} > 50 \text{ }\mu\text{m}$  fall on the ground within 3 meters of the machine. Available data suggest that the NAAQS attainment area for unlimited public access starts at distances from the source of about 9 m for Mud Lad pipe scale and about 10 m for Lake Sand pipe scale. Because this estimate is based on an extrapolation to distances beyond measured data, its precision remains to be verified in future studies.

## CHAPTER IV

### CONCLUSIONS

The images of fly ash and two oilfield scales were obtained using an environmental scanning electron microscope to illustrate particle shapes. This information is important in that the visual particle size distribution was introduced through the several types of size selective aerosol sampler.

From the two types of scale sampled from the petroleum pipe rattling operations, the attainment area was found using a Gaussian point source model with parameters estimated by minimum mean square error fitting algorithms. The measured concentration and the recorded DVD video both show that the plume passed beneath the sampler located at the distance of 1 m from PM source for most of each test, and that the concentration at breathing zone height (1.5 m) was maximum at or near 2 meters downwind from the source. The Gaussian point source model fits this overall pattern better than a simple inverse square law model and better than the Gaussian line source model.

In this study, Gaussian point source model used to identify distances to “safe” zones for the public and the workers is consistent with the measured data by aerosol samplers. However, the attainment area for the public was estimated by an extrapolation of a model to distances beyond measured data. These estimates for Mud Lake and Lake Sand are point estimates. Their uncertainty interval of this attainment area remains to be verified with a measurement at 9 m and 10 m from the source in the future study.

## REFERENCES

1. **American Conference of Governmental Industrial Hygienists (ACGIH):** *Threshold Limit Values for Chemical Substances and Physical Agents and Biological Exposure Indices*. Cincinnati, OH: ACGIH, 1995.
2. **International Organization for Standardization (ISO):** *Air Quality Particle Size Fraction Definition for Health-Related Sampling (ISOCD7708)*. Geneva: ISO, 1992.
3. **Comité Européen de Normalisation (CEN):** *Workplace Atmosphere: Size Fraction Definitions for Measurement of Airborne Particles in the Workplace (CEN Standard EN 481)*. Brussels: CEN, 1992.
4. **American Industrial Hygiene Association (AIHA):** *Particle Size Selective Aerosol Sampling in the Workplace*. Fairfax, VA: AIHA, 1996.
5. National primary and secondary ambient air quality standards for particulate matter *Code of Federal Regulations* Title 40, Part 50.7. 1987.
6. National primary and secondary ambient air quality standards *Code of Federal Regulations* Title 40, Part 50. 1999.
7. **Occupational Safety and Health Administration (OSHA):** *Code of Federal Regulations 1910.1000, Table Z-1*. Washington, DC: OSHA, 1995. Available at [http://www.osha.gov/dts/chemicalsampling/data/CH\\_259640.html](http://www.osha.gov/dts/chemicalsampling/data/CH_259640.html).
8. **American Conference of Governmental Industrial Hygienists (ACGIH):** *Threshold Limit Values for Chemical Substances and Physical Agents and Biological Exposure Indices*. Cincinnati, OH: ACGIH, 1995.
9. **Thermo Electron Co.:** Andersen Sampler model 20-800. Smyrna, GA.
10. **TSI, Inc.:** RESPICON™ Particle Sampler Models 801132 (4.0 µm) and 801586 (2.5 µm). St. Paul, MN.
11. **Thermo Electron Co.:** Graseby-Andersen Federal Reference Method PM10 pre-separator. Smyrna, GA.
12. **Wanjura, J. D., C. B. Parnell, B. W. Shaw, and R. E. Lacey:** The design and evaluation of a low-volume total suspended particulate (TSP) sampler. In *Proceedings of the 2003 Beltwide Cotton Production Conferences on National Cotton Council*, Memphis, TN, 2003.

13. **TSI Inc.:** DUSTTRAK™ Aerosol monitor model 8520. Shoreview, MN.
14. **TSI Inc.:** SIDEPAK™ Aerosol monitor model AM510. Shoreview, MN.
15. **Hinds, W.C.:** *Aerosol Technology Properties, Behavior, and Measurement of Airborne Particles*. New York: John Wiley & Sons, Inc, 1999.
16. **May, K.R.:** The cascade impactor: An instrument for sampling coarse particles. *J. Sci. Instrm.* 22:187-195 (1945).
17. **Lundgren, D.A.:** An aerosol sampler for determination of particle concentration as a function of size and time. *JAPCA* 17:225-229 (1967).
18. **Rao, A.K., and K. T. Whitby:** Non-ideal collection characteristics of inertial impactors-I. Single-stage impactor and solid particles. *Journal of Aerosol Science* 9(2): 77-86 (1978).
19. **Rao, A.K., and K. T. Whitby:** Non-ideal collection characteristics of inertial impactors—II. Cascade impactors. *Journal of Aerosol Science* 9(2): 87-100 (1978).
20. **Aiache, J.M., H. Bull, D. Ganderton, P. Haywood, B. Olsson, and P.Wright:** Inhalations: collaborative study on the measurement of the fine particle dose using inertial impactors. *Pharmeuropa* 5:386-389 (1993).
21. **Srichana, T., G.P. Martin, and C. Marriott:** On the relationship between drug and carrier deposition from dry powder inhalers in vitro. *International Journal of Pharmaceutics* 167:13-23 (1998).
22. **Podczeck, F.:** Optimization of the operation conditions of an Andersen-Cascade impactor and the relationship to centrifugal adhesion measurements to aid the development of dry powder inhalations. *International Journal of Pharmaceutics* 149:51-61 (1997).
23. **Stein S. W.:** Size distribution measurements of metered dose inhalers using Andersen Mark II cascade impactors. *International Journal of Pharmaceutics* 186:43-52 (1999).
24. **Marple, V.A., D.L. Roberts, F.J. Romay, N.C. Miller, K.G. Truman, M.V. Oort, et al.:** Next generation pharmaceutical impactor. Part 1: Design. *J. Aerosol Med.* 16:283-299 (2003).

25. **Marple, V.A., B.A. Olson, K. Santhanakrishnan, J.P. Mitchell, S.C. Murray, and B.L. Hudson-Curtis:** Next generation pharmaceutical impactor (a new impactor for pharmaceutical inhaler testing). Part II: archival calibration. *J. Aerosol Med.* 16:301–324 (2003).
26. **Mitchell, J.P., and M.W. Nagel;** Cascade impactors for the size characterization of aerosols from medical inhalers: their uses and limitations. *J. Aerosol Med.* 16(4):341-377 (2003).
27. **Thermo Electron Co.:** Operating manual for Andersen 2000 ambient particle sizing sampler. Smyrna, GA: Thermo Andersen Co. (1977).
28. **Koch, W., W. Dunkhorst, and H. Lodding:** Design and performance of a new personal aerosol monitor. *Aerosol Science and Technology* 31:231-246 (1999).
29. **Marple, V.A., and C.M. Chien:** Virtual impactors: A theoretical study. *Environ. Sci. Technol.* 14:976–985 (1980).
30. **TSI, Inc.:** *Health and Safety Application Note ITI-051 How A Virtual Impactor Works.* St. Paul, MN.: TSI, Inc., 1997.
31. **Tatum, V., A.E. Ray, and D. Rovell-Rixx:** Performance of the RespiCon personal aerosol sampler in forest products industry workplaces. *Am. Ind. Hyg. Assoc. J.* 63:311–316 (2002).
32. **Li, S.N., D.A. Lundgren, and D. Rovell-Rixx:** Evaluation of six inhalable aerosol samplers. *Am. Ind. Hyg. Assoc. J.* 61(4):506-516 (2000).
33. **Wanjura, J. D., C.B. Parnell, B.W. Shaw, and R.E. Lacey:** Design and Evaluation of a Low Volume Total Suspended Particulate Sampler. In *the Proceedings of the Beltwide Cotton Conferences on National Cotton Council* Nashville, TN. (2003).
34. **McFarland, A. R., and C. A. Ortiz:** Evaluation of prototype PM-10 inlets with cyclonic fractionators. In *Proceedings of the 76th Annual Meeting and Exposition on Air Pollution Control Association*, Atlanta, GA, 1983.
35. National Ambient Air Quality Standards for Particulate Matter *Code of Federal Regulations* Title 40, Part 53. 2000.
36. **Hinds, W.C.:** *Aerosol Technology Properties, Behavior, and Measurement of Airborne Particles.* New York: John Wiley & Sons, Inc, 1999.
37. **Rock, J. C.:** *Occupational Air Sampling Strategies.* In *Air Sampling Instruments*, 8th edition. Cincinnati OH: ACGIH. 1995. pp. 19-44.

38. **Pargmann, A.R., C.B. Parnell, Jr. and B.W. Shaw:** Performance Characteristics of PM<sub>2.5</sub> Samplers in the Presence of Agricultural Dusts. Paper No. 014008, presented at the 2001 ASAE Annual International Meeting in Sacramento, CA, 2001.
39. **Wu, Y., J. Hao, L. Fu, Z. Wang, and U. Tang:** Vertical and horizontal profiles of airborne particulate matter near major roads in Macao, China. *Atmospheric Environment* 36(31):4907-4918 (2002).
40. **Lehocky, A.H., and P.L. Williams:** Comparison of respirable samplers to direct-reading Real-Time Aerosol monitor for measuring coal dust, *Am. Ind. Hyg. Assoc. J.* 57(11):1013-1018 (1996).
41. **U.S. Environmental Protection Agency (EPA):** National ambient air quality standards (NAAQSs). [Standard] Washington, DC: USEPA, 2004.
42. **Rabbe, O.G.:** Studies of the solubility of naturally-occurring radionuclides in petroleum pipe scale. In *Proceedings of the 29th Midyear Topical Meeting of the Health Physics Society* Madison, WI: Medical Physics Publishing; 121-128 (1996).
43. **I. S. Hamilton, M. G. Arno, J. C. Rock, R. O. Berry, J. W. Poston, J. R. Cezeaux, and J-M. Park;** Radiological Assessment of Petroleum Pipe Scale from Pipe-Rattling Operations. *Health Phys.* 87(4):382-97 (2004).
44. **Turner, D.B.:** *Workbook of Atmospheric Dispersion Estimates.* Cincinnati, OH: U.S. Department of Health, Education, and Welfare Public Health Service, (1970).



## APPENDIX A

### CHAMBER STUDY RESULTS USING FLY ASH

This appendix is to provide the mass concentrations and mass fractions measured from each aerosol sampler. The measured mass fractions are estimated for the ACGIH/CEN/ISO\* respirable ( $AED \leq 4 \mu\text{m}$ ), thoracic ( $AED \leq 10 \mu\text{m}$ ), and inhalable ( $AED \leq 100 \mu\text{m}$ ) convention.

The followings are terms in the tables below.

C1 & C2 = Andersen samplers;

R1 = RespiCon sampler used a  $4 \mu\text{m}$  cut-point for first stage, R2 = RespiCon sampler used a  $2.5 \mu\text{m}$  cut-point for first stage;

T1 – T4 = TSP samplers;

P1 – P4 = PM10 samplers;

D1 = DustTrak monitor used a  $10 \mu\text{m}$  inlet module, D2 = used a  $2.5 \mu\text{m}$  inlet module;

S1 = SidePak monitor used a  $2.5 \mu\text{m}$  inlet module, S2 = used a  $1 \mu\text{m}$  inlet module;

$SU = \text{Standard error} = 1.96 \times SE$  (A.1)

where  $SU = \text{Sampling uncertainty of sample mean}$ ;  $1.96 = z\text{-value for } 95 \% \text{ confidence interval}$ .  $SE = (SD/\sqrt{n})$  where  $SE = \text{Standard error}$ ;  $SD = \text{standard deviation of sample}$ ;

$n = \text{the number of cases}$ ;

---

\* American Conference of Governmental Industrial Hygienists (ACGIH)  
Comité Européen de Normalisation (CEN)  
International Organization for Standardization (ISO)

$$RSU [\%] = \text{Relative sampling uncertainty} = \frac{2 \cdot SU}{\text{Measured concentration}} \times 100 \quad (\text{A.2})$$

AED = Aerodynamic Equivalent Diameter; An AED is a diameter of the unit density (1 g/cm<sup>3</sup>) sphere that has the same settling velocity as the particle of interest. It standardizes the inertial and aerodynamic behavior for both shape and density.

ESD = Equivalent Spherical Diameter; It is a diameter of the sphere having the same volume as the irregular particle of interest.

### A-1. Andersen Chamber Study Results

**TABLE A-1. Estimated Mass Concentrations from Andersen Sampler Measurements (Chamber)**

Stage	F	7	6	5	4	3	2	1	0	Total Con.
Size range <sup>A</sup> (AED μm)	< 0.5	0.5 ~ 0.7	0.7 ~ 1.2	1.2 ~ 2.3	2.3 ~ 3.7	3.7 ~ 5.2	5.2 ~ 6.7	6.7 ~ 10.3	>10.3	
Test 1 (C1)	0.00	0.15	1.50	5.28	4.44	5.63	4.82	2.40	4.97	29.18
Test 1 (C2)	0.01	0.27	1.00	4.67	4.36	5.86	5.31	2.92	5.13	29.52
Test 2 (C1)	0.08	0.24	1.13	3.94	3.27	3.90	3.59	1.86	3.43	21.43
Test 2 (C2)	0.03	0.11	0.86	4.07	3.25	3.94	3.67	1.96	3.58	21.48
Test 3 (C1)	0.01	0.24	1.21	3.90	3.58	4.35	3.89	2.21	4.06	23.45
Test 3 (C2)	0.00	0.14	0.96	3.95	3.48	4.59	4.16	2.39	4.22	23.90
<i>Mean</i>	0.02	0.19	1.11	4.30	3.73	4.71	4.24	2.29	4.23	24.83
<i>SD</i>	0.03	0.07	0.23	0.56	0.53	0.84	0.69	0.38	0.70	3.65
<i>Min</i>	0.00	0.11	0.86	3.90	3.25	3.90	3.59	1.86	3.43	21.43
<i>Max</i>	0.08	0.27	1.50	5.28	4.44	5.86	5.31	2.92	5.13	29.52
<i>SU</i>	0.02	0.05	0.18	0.45	0.43	0.67	0.55	0.30	0.56	3.57
<i>RSU</i>	214%	54%	33%	21%	23%	29%	26%	27%	27%	28.8%

Notes: <sup>A</sup> Particle size range at 0.8 ACFM (22.65 L/min). unit: [mg/m<sup>3</sup>]  
A mass of each stage was measured with a Mettler Toledo AG245 balance having a limit of detection of 0.01 mg.

**TABLE A-2. Estimated Mass Concentrations for a Respirable, Thoracic, and Inhalable Convention from Andersen Sampler Data in TABLE A-1 above (Chamber)**

Description	Test 1		Test 2		Test 3	
	C1	C2	C1	C2	C1	C2
	Mean (SD) <sup>B</sup>	Mean (SD)	Mean (SD)	Mean (SD)	Mean (SD)	Mean (SD)
Respirable <sup>A</sup>	11.37	10.3	8.66	8.33	8.94	8.54
(AED ≤ 3.7 μm)	(0.13)	(0.1)	(0.22)	(0.07)	(0.12)	(0.05)
Thoracic <sup>A</sup>	24.2	24.39	18.01	17.9	19.39	19.69
(AED ≤ 10.1 μm)	(0.78)	(0.68)	(0.88)	(0.65)	(0.62)	(0.50)
Inhalable	29.18	29.52	21.43	21.48	23.45	23.9
(AED ≤ 100 μm)	(0.95)	(0.84)	(1.05)	(0.86)	(0.76)	(0.62)

Note:

Unit: [mg/m<sup>3</sup>]

<sup>A</sup> The 50 % cutoff sizes for respirable and thoracic PM are 3.7 μm and 10.1 μm at 0.8 ACFM (22.65 L/min).

<sup>B</sup> Mean = Average concentration from 3 times filter measurements, SD = Standard deviation were obtained using an error propagation.

$$\frac{SD_{PM_4}}{\bar{C}_{PM_4}} = \sqrt{\left(\frac{SD_{SF}}{\bar{W}_{SF}}\right)^2 + \left(\frac{SD_{S7}}{\bar{W}_{S7}}\right)^2 + \left(\frac{SD_{S6}}{\bar{W}_{S6}}\right)^2 + \left(\frac{SD_{S5}}{\bar{W}_{S5}}\right)^2 + \left(\frac{SD_{S4}}{\bar{W}_{S4}}\right)^2 + \left(\frac{SD_Q}{\bar{Q}}\right)^2 + \left(\frac{SD_T}{\bar{T}}\right)^2},$$

$$\frac{SD_{PM_{10}}}{\bar{C}_{PM_{10}}} = \sqrt{\left(\frac{SD_{SF}}{\bar{W}_{SF}}\right)^2 + \left(\frac{SD_{S7}}{\bar{W}_{S7}}\right)^2 + \dots + \left(\frac{SD_{S1}}{\bar{W}_{S1}}\right)^2 + \left(\frac{SD_Q}{\bar{Q}}\right)^2 + \left(\frac{SD_T}{\bar{T}}\right)^2}, \text{ and}$$

$$\frac{SD_{PM_{total}}}{\bar{C}_{PM_{total}}} = \sqrt{\left(\frac{SD_{SF}}{\bar{W}_{SF}}\right)^2 + \left(\frac{SD_{S7}}{\bar{W}_{S7}}\right)^2 + \dots + \left(\frac{SD_{S1}}{\bar{W}_{S1}}\right)^2 + \left(\frac{SD_{S0}}{\bar{W}_{S0}}\right)^2 + \left(\frac{SD_Q}{\bar{Q}}\right)^2 + \left(\frac{SD_T}{\bar{T}}\right)^2} \text{ for Andersen samplers.}$$

where  $S_0, S_1, S_2, S_3, S_4, S_5, S_6, S_7, S_F$  = The number of stage. In these calculations, the relative standard deviation for stages 6, 7, and F were above 1 because of a small quantity of mass on these stages. Thus, the relative standard deviation of stages 6, 7, and F were estimated as 0.02.

The particle mass concentration  $C$  (mg/m<sup>3</sup>) in each size fraction was estimated using the following equations. The estimates have approximately the proper cut points, but may have different slope factors than called for in the mass fraction convention.

$$C_{Respirable} = (m_F + m_7 + m_6 + m_5 + m_4) \times 10^3 / V \quad (\text{A.4})$$

$$C_{Thoracic} = (m_F + m_7 + m_6 + m_5 + m_4 + m_3 + m_2 + m_1) \times 10^3 / V \quad (\text{A.5})$$

$$C_{Inhalable} = (m_F + m_7 + m_6 + m_5 + m_4 + m_3 + m_2 + m_1 + m_0) \times 10^3 / V \quad (\text{A.6})$$

where  $m_0, m_1, m_2, m_3, m_4, m_5, m_6, m_7, m_F$  = particle mass deposited on each filter stage

$V$  = sampled volume at each stage =  $Q \times ts$

$Q$  = major flow at each stage (L/min)

$ts$  = sample time (min)

## A-2. RespiCon Chamber Study Results

**TABLE A-3. Mass Concentrations for a Respirable, Thoracic, and Inhalable Convention Estimated from RespiCon Measurements (Chamber)**

Description	Test 1		Test 2		Test 3	
	R1 <sup>A</sup> Mean (SD) <sup>C</sup>	R2 <sup>B</sup> Mean (SD)	R1 Mean (SD)	R2 Mean (SD)	R1 Mean (SD)	R2 Mean (SD)
Respirable (AED ≤ 2.5 μm)	-- <sup>D</sup>	--	--	--	--	7.90 (0.37)
Respirable (AED ≤ 4 μm)	2.38 (0.34)	--	--	--	4.10 (0.16)	--
Thoracic (AED ≤ 10 μm)	16.91 (2.50)	--	--	--	11.30 (0.64)	20.95 (1.38)
Inhalable (AED ≤ 100 μm)	20.75 (3.24)	--	--	--	16.29 (1.14)	31.94 (2.60)

Note: RespiCon samplers were located at the height of 150 cm. Unit: [mg/m<sup>3</sup>]

<sup>A</sup> R1 = RespiCon sampler with 4 μm and 10 μm cut-points stages; <sup>B</sup> R2 = RespiCon sampler with 2.5 μm and 10 μm cut-points stages;

<sup>C</sup> Mean = Average concentration from 3 times filter measurements, SD = Standard deviation were obtained using an error propagation.

$$\frac{SD_{PM_4}}{\bar{C}_{PM_4}} = \sqrt{\left(\frac{SD_{St1}}{\bar{W}_{St1}}\right)^2 + \left(\frac{SD_Q}{\bar{Q}}\right)^2 + \left(\frac{SD_T}{\bar{T}}\right)^2} \text{ and}$$

$$\frac{SD_{PM_{10}}}{\bar{C}_{PM_{10}}} = \sqrt{\left(\frac{SD_{St1}}{\bar{W}_{St1}}\right)^2 + \left(\frac{SD_{St2}}{\bar{W}_{St2}}\right)^2 + \left(\frac{SD_Q}{\bar{Q}}\right)^2 + \left(\frac{SD_T}{\bar{T}}\right)^2} \text{ for RespiCon samplers.}$$

where  $St1$  = The number of stage with cut-point 2.5 μm or 4 μm,  $St2$  = The number of stage with cut-point 10 μm.

<sup>D</sup> No measurement.

The particle mass concentration  $C$  (mg/m<sup>3</sup>) in each size fraction was determined using the following equations. (Equation Source: RespiCon sampler's User Guide)

$$C_{Respirable} = m_1 \times 10^3 / V_1 \quad (\text{A.7})$$

$$C_{Thoracic} = (m_1 + m_2) \times 10^3 / V_2 \quad (\text{A.8})$$

$$C_{Inhalable} = (m_1 + m_2 + m_3) \times 10^3 / V_3 \quad (\text{A.9})$$

where  $m_1, m_2, m_3$  = particle mass deposited on each filter stage

$V_1$  = sampled volume at stage one =  $Q_1 \times ts$

$V_2$  = sampled volume at stages one and two =  $(Q_1 + Q_2) \times ts$

$V_3$  = sampled volume at stages one, two and three =  $(Q_1 + Q_2 + Q_3) \times ts$

$Q_1, Q_2, Q_3$  = volume flow at each stage (L/min) ( $Q_1 = 2.667, Q_2 = 0.333, Q_3 = 0.111$ )

$ts$  = sample time (min)

### A-3. DustTrak Chamber Study Results (summary statistics)

**TABLE A-4. Relative Mass Concentrations from DustTrak Measurements (Chamber)**

Description	Test 1		Test 2		Test 3	
	D1 (10 $\mu\text{m}$ ) <sup>A</sup>	D2 (2.5 $\mu\text{m}$ )	D1 (10 $\mu\text{m}$ )	D2 (2.5 $\mu\text{m}$ )	D1 (10 $\mu\text{m}$ )	D2 (2.5 $\mu\text{m}$ )
<i>Mean</i>	11.94	7.18	9.42	4.67	11.38	5.78
<i>Max</i>	23.99	13.06	14.49	7.17	21.75	12.60
<i>Min</i>	0.27	0.08	0.03	0.02	0.01	0.01
<i>SD</i>	4.29	2.65	3.57	1.83	4.38	2.50
No. of Points <sup>B</sup>	4054	4054	3894	3894	7547	7547
<i>SU</i>	0.13	0.08	0.11	0.06	0.10	0.06
<i>RSU (%)</i>	2%	2%	2%	2%	2%	2%

Notes: <sup>A</sup> ( ) = AED size of impactor prefilter

Unit: [mg/m<sup>3</sup>]<sup>C</sup>

<sup>B</sup>No. of Points = the number of logged data.

<sup>C</sup>These units are printed on scale of instrument and are not calibrated to the fly ash density in this study. These data should be considered reliable only as a relative measure of scattered light, not as a true mass.

#### A-4. SidePak Chamber Study Results (Summary Statistics)

**TABLE A-5. Relative Mass Concentrations from SidePak Measurements (Chamber)**

Description	Test 1		Test 2		Test 3	
	S1 (2.5 $\mu\text{m}$ ) <sup>A</sup>	S2 (1 $\mu\text{m}$ )	S1 (2.5 $\mu\text{m}$ )	S2 (1 $\mu\text{m}$ )	S1 (2.5 $\mu\text{m}$ )	S2 (1 $\mu\text{m}$ )
<i>Mean</i>	12.97	14.30	9.36	7.73	11.44	11.32
<i>Max</i>	20.00	20.00	18.91	14.69	19.99	20.00
<i>Min</i>	0.09	0.08	0.02	0.02	0.25	0.02
<i>SD</i>	4.34	4.96	3.55	3.15	4.30	4.57
No. of Points <sup>B</sup>	3774	3583	3890	3889	7128	6815
<i>SU</i>	0.14	0.16	0.11	0.10	0.10	0.11
<i>RSU (%)</i>	2%	2%	2%	3%	2%	2%

Notes: <sup>A</sup>( ) = AED inlet size of impactor prefilter.

Unit: [mg/m<sup>3</sup>]<sup>C</sup>

<sup>B</sup>No. of Points = the number of logged data.

<sup>C</sup>These units are printed on scale of instrument and are not calibrated to the fly ash density in this study. These data should be considered reliable only as a relative measure of scattered light, not as a true mass.

## A-5. TSP Chamber Study Results

**TABLE A-6. Estimated TSP/CCM Volume Percentile (Chamber)**

ESD	AED	Volume % <sup>A</sup>										
		Test 1				Test 2				Test 3		
Unit: [μm]		T1 <sup>B</sup>	T2	T3	T4	T1	T2	T3	T4	T1	T2	T4
2.0	3.3 <sup>C</sup>	10.95	9.43	9.81	10.71	10.59	9.46	11.18	9.73	16.97	10.84	6.57
2.03	3.33	11.55	9.88	10.35	11.23	11.23	10.04	11.80	10.26	17.98	11.45	6.97
2.05	3.37	12.19	10.38	10.93	11.80	11.93	10.65	12.46	10.82	19.09	12.09	7.40
:	:	:	:	:	:	:	:	:	:	:	:	:
2.44	<b>4.01<sup>D</sup></b>	21.33	17.50	19.22	19.99	21.60	19.25	21.76	18.71	33.74	20.82	13.28
:	:	:	:	:	:	:	:	:	:	:	:	:
2.98	4.90	33.40	27.36	30.63	31.38	34.16	30.47	33.74	29.01	<u>49.92</u>	31.80	33.40
:	:	:	:	:	:	:	:	:	:	:	:	:
3.73	6.14	47.93	40.58	45.69	45.49	<u>49.68</u>	44.66	48.22	41.84	64.76	45.13	3.73
3.78	6.22	48.78	41.40	46.60	46.28	50.61	45.52	49.07	42.59	65.52	45.92	3.78
3.83	6.30	<u>49.61<sup>E</sup></u>	42.24	47.52	47.08	51.54	46.40	<u>49.94</u>	43.37	66.27	46.73	3.83
3.89	6.39	50.45	43.07	48.45	47.87	52.48	47.27	50.80	44.14	67.02	47.54	3.89
3.94	6.47	51.31	43.89	49.39	48.64	53.40	48.15	51.68	44.92	67.75	48.35	3.94
3.99	6.56	52.13	44.74	<u>50.33</u>	49.43	54.33	49.03	52.52	45.70	68.49	49.15	3.99
4.04	6.65	52.95	45.56	51.26	<u>50.21</u>	55.26	<u>49.92</u>	53.37	46.47	69.22	<u>49.95</u>	4.04
4.10	6.73	53.76	46.39	52.17	50.99	56.18	50.80	54.20	47.23	69.93	50.76	4.10
4.15	6.82	54.58	47.24	53.07	51.74	57.11	51.68	55.05	47.99	70.63	51.56	4.15
4.21	6.92	55.39	48.07	54.02	52.50	58.02	52.55	55.89	48.77	71.32	52.38	4.21
4.27	7.01	56.23	48.91	54.94	53.24	58.93	53.43	56.73	49.55	72.02	53.20	4.27
4.32	7.10	57.03	<u>49.75</u>	55.89	53.98	59.82	54.31	57.56	<u>50.32</u>	72.70	53.97	4.32
4.38	7.20	57.83	50.60	56.80	54.71	60.74	55.19	58.39	51.08	73.38	54.79	4.38
4.44	7.29	58.64	51.43	57.72	55.40	61.66	56.06	59.21	51.84	74.06	55.57	4.44
:	:	:	:	:	:	:	:	:	:	:	:	:
5.00	8.22	65.50	58.86	65.65	61.62	69.41	63.87	66.35	58.54	79.77	62.53	49.54
5.07	8.33	66.23	59.64	66.50	62.28	70.23	64.71	67.09	59.25	80.37	63.25	<u>50.34</u>
5.14	8.44	66.94	60.45	67.30	62.92	71.03	65.53	67.85	59.94	80.97	63.98	51.17
:	:	:	:	:	:	:	:	:	:	:	:	:
6.11	<b>10.03<sup>D</sup></b>	<b>64.55</b>	<b>60.60</b>	<b>66.86</b>	<b>60.01</b>	<b>69.66</b>	<b>65.83</b>	<b>65.23</b>	<b>58.84</b>	<b>70.91</b>	<b>61.87</b>	<b>54.95</b>
6.19	10.17	65.14	61.24	67.50	60.54	70.27	66.50	65.84	59.47	71.38	62.51	55.68
:	:	:	:	:	:	:	:	:	:	:	:	:

Notes: T3 in Test 3 = The filter was used to get images by ESEM.

<sup>A</sup> Volume % = Obtained by a CCM. <sup>B</sup> T1-T12 = TSP Sampler data, 4 sets in each of 3 chamber tests.

<sup>C</sup> The PSD less than an AED 3.3 μm was estimated from a median AED of sampling efficiency and a slope of sampling efficiency measured by each TSP/CCM because an AED 3.3 μm is the smallest particle size that a CCM can count with a 100 μm orifice aperture.

<sup>D</sup> AED 4 μm, 10 μm = Respirable, Thoracic cutoff size.

<sup>E</sup> \_ = 50% Cumulative Volume.

**TABLE A-7. Estimated Mass Concentrations for a Respirable, Thoracic, and Inhalable Convention from TSP/CCMs (Chamber)**

Description	Test 1				Test 2				Test 3			
	T1	T2	T3	T4	T1	T2	T3	T4	T1	T2	T3	T4
Respirable <sup>4</sup> (AED ≤ 4 μm)	7.17	6.04	6.08	6.93	5.19	4.72	5.57	4.72	8.43	5.35	-- <sup>B</sup>	3.98
Thoracic (AED ≤ 10 μm)	25.37	24.16	24.26	24.51	19.27	18.47	19.54	17.30	21.95	18.70	--	18.43
Inhalable (AED ≤ 100μm)	33.60	34.51	31.65	34.66	24.02	24.53	25.58	25.23	24.98	25.72	30.00	29.96

Notes:

Unit: [mg/m<sup>3</sup>]

These concentrations of TSP samplers were estimated from the volume % by a coulter counter multisizer (CCM).

<sup>4</sup>In the respirable concentration, the PSD less than an AED 3.3 μm was estimated from a median AED of sampling efficiency and a slope of sampling efficiency measured by each TSP/CCM because an AED 3.3 μm is the smallest particle size that a CCM can count with a 100 μm orifice aperture.

<sup>4</sup> No measurement



**A-6. Bulk sample of dust for Chamber Study, volume percentile by CCM**

**TABLE A-8. Estimated Bulk Sample Volume Percentile (Chamber)**

ESD	AED	Volume % <sup>A</sup>
Unit: [ $\mu\text{m}$ ]		Bulk <sup>B</sup>
2.03	3.33	3.37
2.05	3.37	3.61
2.08	3.42	3.85
2.11	3.47	4.10
2.14	3.51	4.35
2.17	3.56	4.60
2.19	3.61	4.86
2.22	3.65	5.13
2.25	3.70	5.40
2.28	3.75	5.68
2.31	3.80	5.96
2.35	3.85	6.24
2.38	3.91	6.53
2.41	3.96	6.83
2.44	<b>4.01<sup>C</sup></b>	7.12
:		
:		
6.02	9.90	40.69
6.11	<b>10.03<sup>C</sup></b>	41.40
6.19	10.17	42.09
6.27	10.30	42.83
6.35	10.44	43.56
6.44	10.58	44.28
6.52	10.72	45.01
:		
:		
7.07	11.61	49.40
7.16	11.77 <sup>D</sup>	50.16
7.26	11.92	50.91
7.35	12.08	51.67
7.45	12.24	52.39
:		
:		

Notes: <sup>A</sup> Volume % = Obtained by a CCM.

<sup>B</sup> Bulk = Bulk sample of fly ash.

<sup>C</sup> AED 4  $\mu\text{m}$ , 10  $\mu\text{m}$  = Respirable, Thoracic cutoff size.

<sup>D</sup> \_ = 50% Cumulative volume.



### A-8. Estimated $GM_{AED}$ and $GSD_{AED}$ of Andersen sampler by Log Probit Analysis of Chamber Study Data

A log probit analysis is an application of the lognormal distribution to obtain particle size distribution by the use of log-probability graphs. A log probability plot can be constructed by plotting the logarithm of diameter versus the probit of the cumulative percentages. It gives geometric mean and geometric standard deviation as shown in equation 1-3. When the data of Andersen sampler were analyzed, the mass fractions of Andersen sampler's first and last stages deviate from the expected the straight line. Thus, the mass fractions of the first and last impaction stages were neglected for purposes of finding the best fit straight line to obtain best log probit curve. This is justified because the Andersen inlet is known to violate the inhalable size selection criteria and because the last stage collected insufficient mass for reliable weighing.

$$z = \frac{x - \mu}{\sigma} \hat{=} \frac{\ln(x) - \ln(GM_{AED})}{\ln(GSD_{AED})} \quad (A.1)$$

$$\ln(x) \hat{=} \ln(GSD_{AED}) \times z + \ln(GM_{AED}) \quad (A.2)$$

$z$  = Standard normal random variable (Mass fraction),

$x$  = Normal random variable (Aerodynamic equivalent diameter),

$\mu$  = Population mean,

$\sigma$  = Population standard deviation,

$GM_{AED}$  = Sample geometric mean (Median AED of sample data),

$GSD_{AED}$  = Sample geometric standard deviation (Slope of PSD curve).

**TABLE A-12. Mass Fraction Estimated from Each Stage of Andersen Sampler (Chamber)**

Stage	Cutoff AED [ $\mu\text{m}$ ]	Test 1		Test 2		Test 3	
		C1	C2	C1	C2	C1	C2
0	10.1	0.820	0.826	0.840	0.833	0.827	0.824
1	6.5	0.739	0.727	0.753	0.742	0.732	0.723
2	5.3	0.576	0.547	0.586	0.571	0.566	0.549
3	3.7	0.385	0.349	0.404	0.388	0.381	0.357
4	2.4	0.235	0.201	0.252	0.236	0.228	0.211
5	1.2	0.056	0.043	0.068	0.047	0.062	0.046
6	0.7	0.005	0.010	0.015	0.007	0.011	0.006
7	0.5	0.000	0.000	0.004	0.001	0.001	0.000

**TABLE A-13. Standard Normal Random Variables from the Mass Fraction Estimated in TABLE A-12 above (Chamber)**

Stage	Cutoff AED [ $\mu\text{m}$ ]	Test 1		Test 2		Test 3	
		C1	C2	C1	C2	C1	C2
0	10.1	0.915	0.939	0.995	0.967	0.941	0.929
1	6.5	0.639	0.604	0.686	0.650	0.620	0.593
2	5.3	0.191	0.119	0.217	0.180	0.167	0.124
3	3.7	-0.292	-0.388	-0.242	-0.285	-0.303	-0.366
4	2.4	-0.724	-0.837	-0.670	-0.718	-0.744	-0.801
5	1.2	-1.590	-1.714	-1.494	-1.678	-1.537	-1.683
6	0.7	-2.577	-2.344	-2.174	-2.480	-2.306	-2.512
7	0.5	-5.199	-3.342	-2.692	-3.008	-3.278	-5.199

*Notes:* The values of standard normal random variables are calculated using a NORMINV function as NORMINV(Mass Fraction,0,1) in Microsoft Excel.

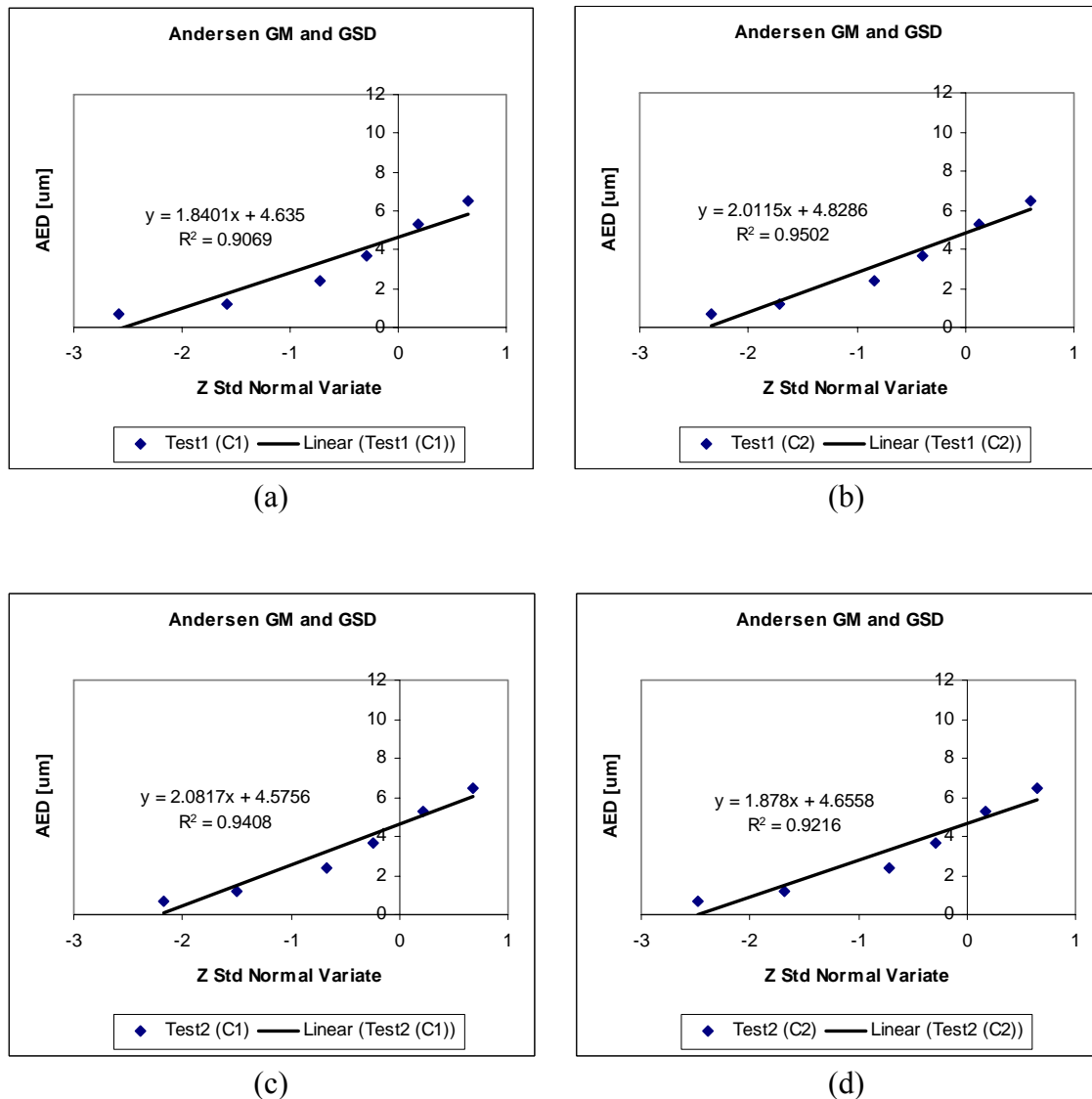
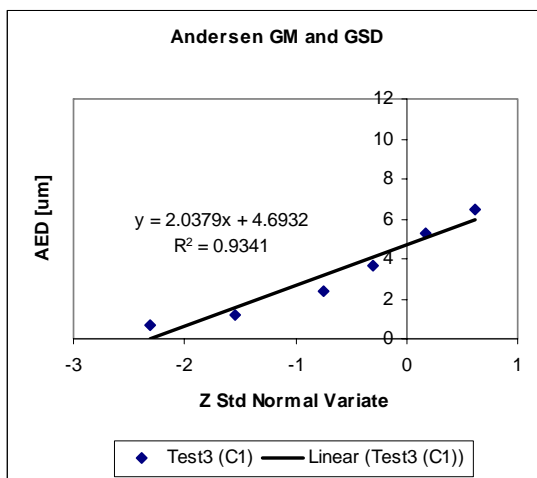
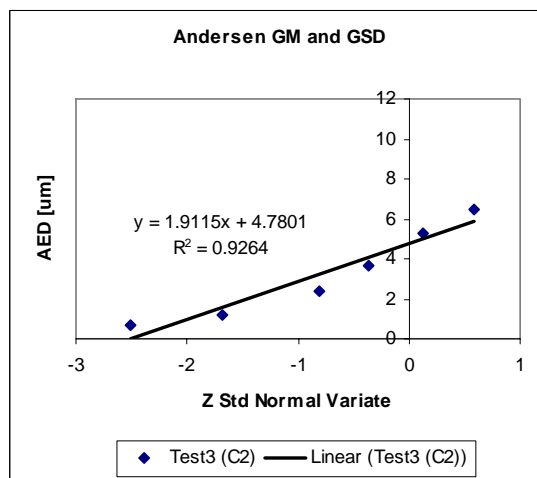


**FIGURE A-1. Estimated  $GM_{AED}$  and  $GSD_{AED}$  of the Andersen sampler (Chamber). (a) C1 in test 1, (b) C2 in test 1, (c) C1 in test 2, (d) C2 in test 2, (e) C1 in test 3, (f) C2 in test 3.**

*Note:* The mass fractions of the first and last impaction stages were neglected from TABLE A-13 to obtain best log probit curve.



(e)



(f)

FIGURE A-1. Continued.

## APPENDIX B

### PIPE RATTLING STUDY RESULTS

The petroleum pipe rattling operations discussed in this dissertation were conducted using two different pipe scales (Field test 1 for Mud Lake and Field test 2 for Lake Sand). The mass concentrations for an ACGIH/CEN/ISO convention were arranged for the comparison with the accepted standard and guideline from each size selective aerosol sampler.

The measured concentrations by DustTrak and SidePak monitors are considered relative measures useful for observing time variation as they were not calibrated for different petroleum pipe scales.

#### B-1. Andersen Field Study Results

**TABLE B-1. Measured Mass Concentration of Each Stage of Andersen Samplers (Field)**

Stage <sup>A</sup>	F	7	6	5	4	3	2	1	0	Total Con.
Size Range <sup>B</sup> ( $\mu\text{m}$ )	< 0.4	0.4 ~ 0.7	0.7 ~ 1.1	1.1 ~ 2.1	2.1 ~ 3.3	3.3 ~ 4.7	4.7 ~ 5.8	5.8 ~ 9.0	> 9.0	
Field test 1 (C1)	0.01	0.02	0.04	0.32	0.00	1.48	1.61	1.32	7.72	12.51
Field test 1 (C2)	0.00	0.01	0.07	0.35	0.46	1.12	1.34	1.29	7.80	12.44
Field test 2 (C1)	0.05	0.06	0.08	0.21	0.29	0.54	0.62	0.69	1.70	4.23
Field test 2 (C2)	0.00	0.16	0.21	0.38	0.49	0.92	1.06	1.29	3.04	7.56

Notes:

<sup>A</sup> A mass of each stage was measured with a Mettler Toledo AE 100 balance having a limit of detection of 0.1 mg.

<sup>B</sup> Particle size range at 1 ACFM (28.32 L/min)

Unit: [mg/m<sup>3</sup>]

**TABLE B-2. Estimated Mass Concentrations for a Respirable, Thoracic, and Inhalable Convention from Andersen Sampler Data in TABLE B-1 above (Field)**

Description	Field test 1 <sup>B</sup>		Field test 2 <sup>C</sup>	
	C1	C2	C1	C2
	Mean (SD) <sup>D</sup>	Mean (SD)	Mean (SD)	Mean (SD)
Respirable or PM <sub>4</sub> (AED ≤ 3.3 μm) <sup>A</sup>	0.39 (0.01)	0.89 (0.06)	0.70 (0.13)	1.23 (0.12)
Thoracic or PM <sub>10</sub> (AED ≤ 9 μm) <sup>A</sup>	4.80 (0.51)	4.64 (0.55)	2.53 (0.52)	4.52 (0.48)
Inhalable or PM <sub>total</sub> (AED ≤ 100 μm)	12.51 (1.34)	12.44 (1.48)	4.23 (0.88)	7.56 (0.80)

Notes:

Unit: [mg/m<sup>3</sup>]

<sup>A</sup>The 50 % cutoff sizes for Respirable and thoracic PM are 3.3 μm and 9 μm at 1 ACFM (28.32 L/min).

<sup>B</sup>In Field test 1, C1, C2 were located at 2m from the centerline of source.

<sup>C</sup>In Field test 2, C1 was located at 3m and C2 was at 1m from the centerline of source.

<sup>D</sup>Mean = Average concentration from 3 times filter measurements, SD = Standard deviation were obtained using an error propagation.

$$\frac{SD_{PM_4}}{\bar{C}_{PM_4}} = \sqrt{\left(\frac{SD_{SF}}{\bar{W}_{SF}}\right)^2 + \left(\frac{SD_{S7}}{\bar{W}_{S7}}\right)^2 + \left(\frac{SD_{S6}}{\bar{W}_{S6}}\right)^2 + \left(\frac{SD_{S5}}{\bar{W}_{S5}}\right)^2 + \left(\frac{SD_{S4}}{\bar{W}_{S4}}\right)^2 + \left(\frac{SD_Q}{\bar{Q}}\right)^2 + \left(\frac{SD_T}{\bar{T}}\right)^2},$$

$$\frac{SD_{PM_{10}}}{\bar{C}_{PM_{10}}} = \sqrt{\left(\frac{SD_{SF}}{\bar{W}_{SF}}\right)^2 + \left(\frac{SD_{S7}}{\bar{W}_{S7}}\right)^2 + \dots + \left(\frac{SD_{S1}}{\bar{W}_{S1}}\right)^2 + \left(\frac{SD_Q}{\bar{Q}}\right)^2 + \left(\frac{SD_T}{\bar{T}}\right)^2}, \text{ and}$$

$$\frac{SD_{PM_{total}}}{\bar{C}_{PM_{total}}} = \sqrt{\left(\frac{SD_{SF}}{\bar{W}_{SF}}\right)^2 + \left(\frac{SD_{S7}}{\bar{W}_{S7}}\right)^2 + \dots + \left(\frac{SD_{S1}}{\bar{W}_{S1}}\right)^2 + \left(\frac{SD_{S0}}{\bar{W}_{S0}}\right)^2 + \left(\frac{SD_Q}{\bar{Q}}\right)^2 + \left(\frac{SD_T}{\bar{T}}\right)^2} \text{ for Andersen samplers.}$$

where S<sub>0</sub>, S<sub>1</sub>, S<sub>2</sub>, S<sub>3</sub>, S<sub>4</sub>, S<sub>5</sub>, S<sub>6</sub>, S<sub>7</sub>, S<sub>F</sub> = The number of stage. In these calculations, the relative standard deviation for stages 6, 7, and F were above 1 because of a small quantity of mass on these stages. Thus, the relative standard deviation of stages 6, 7, and F were estimated as 0.02.



## B-2. RespiCon Field Study Results

**TABLE B-3. Mass Concentrations for a Respirable, Thoracic, and Inhalable Convention Estimated from RespiCon Measurements (Field)**

Description	Field test 1 <sup>A</sup>		Field test 2 <sup>B</sup>	
	R1 <sup>C</sup> Mean (SD) <sup>E</sup>	R2 <sup>D</sup> Mean (SD)	R1 Mean (SD)	R2 Mean (SD)
Respirable (AED ≤ 2.5 μm)	--	1.37 (0.08)	--	2.62 (0.35)
Respirable (AED ≤ 4 μm)	2.69 (0.10)	--	0.85 (0.09)	--
Thoracic (AED ≤ 10 μm)	6.40 (0.45)	3.64 (0.28)	3.60 (0.44)	6.61 (1.02)
Inhalable (AED ≤ 100 μm)	16.69 (1.37)	13.70 (1.17)	10.56 (1.49)	18.61 (3.09)

Notes:

Unit: [mg · m<sup>-3</sup>]

<sup>A</sup>In Field test 1, R1, R2 were located at 2m from the centerline of source.

<sup>B</sup>In Field test 2, R1 was located at 3m and R2 was at 1m from the centerline of source.

<sup>C</sup> R1 = RespiCon sampler with 4 μm and 10 μm cut-points stages; <sup>D</sup> R2 = RespiCon sampler with 2.5 μm and 10 μm cut-points stages;

<sup>E</sup> Mean = Average concentration from 3 times filter measurements, SD = Standard deviation were obtained using an error propagation.

$$\frac{SD_{PM_4}}{\bar{C}_{PM_4}} = \sqrt{\left(\frac{SD_{SR1}}{\bar{W}_{SR1}}\right)^2 + \left(\frac{SD_Q}{\bar{Q}}\right)^2 + \left(\frac{SD_T}{\bar{T}}\right)^2} \text{ and}$$

$$\frac{SD_{PM_{10}}}{\bar{C}_{PM_{10}}} = \sqrt{\left(\frac{SD_{SR1}}{\bar{W}_{SR1}}\right)^2 + \left(\frac{SD_{SR2}}{\bar{W}_{SR2}}\right)^2 + \left(\frac{SD_Q}{\bar{Q}}\right)^2 + \left(\frac{SD_T}{\bar{T}}\right)^2} \text{ for RespiCon samplers.}$$

where  $SR1$  = The number of stage with a cut-point 2.5 μm or 4 μm,  $SR2$  = The number of stage with a cut-point 10 μm.

### B-3. DustTrak Field Study Results (Summary Statistics)

**TABLE B-4. Relative Mass Concentrations from DustTrak Measurements (Field)**

Description	Field test 1 <sup>A</sup>		Field test 2 <sup>B</sup>	
	D1 (10 µm) <sup>C</sup>	D2 (2.5 µm)	D1 (1 µm)	D2 (1 µm)
<i>Mean</i>	3.61	0.83	0.16	0.23
<i>Max</i>	238.74	57.98	32.84	36.89
<i>Min</i>	0.01	0.02	0.02	0.03
<i>SD</i>	12.17	2.72	0.94	1.19
No. of Points <sup>D</sup>	11393	11223	6044	6044
<i>SU</i>	0.22	0.05	0.02	0.03
<i>RSU (%)</i>	12%	12%	30%	26%

Notes:

Unit: [mg/m<sup>3</sup>]<sup>E</sup>

<sup>A</sup>In a field test 1, D1 and D2 were located at 2m from the centerline of source;

<sup>B</sup>In a field test 2, D1 and D2 were located at 3m from the centerline of source;

<sup>C</sup>( ) = AED inlet size of impactor prefilter; <sup>D</sup>No. of Points = the number of logged data;

<sup>E</sup>These units are printed on scale of instrument and are not calibrated to the petroleum pipe scale. These data are considered as a relative measure of scattered light intensity, not as a true mass.

### B-4. SidePak Field Study Results (Summary Statistics)

**TABLE B-5. Relative Mass Concentrations from SidePak Measurements (Field)**

Description	Field test 1 <sup>A</sup>		Field test 2 <sup>B</sup>	
	S1 (2.5 µm) <sup>A</sup>	S2 (1 µm)	S1 (2.5 µm)	S2 (1 µm)
<i>Mean</i>	2.12	1.24	1.52	0.62
<i>Max</i>	19.98	19.97	19.72	19.98
<i>Min</i>	0.94	0.10	1.02	0.12
<i>SD</i>	2.73	2.72	1.68	1.64
No. of Points <sup>D</sup>	12807	12811	5960	5952
<i>SU</i>	0.05	0.05	0.04	0.04
<i>RSU (%)</i>	4 %	8 %	6 %	13 %

Notes:

Unit: [mg/m<sup>3</sup>]<sup>E</sup>

<sup>A</sup>In a field test 1, S1 and S2 were located at 2m from the centerline of source.

<sup>B</sup>In a field test 2, S1 and S2 were located at 3m from the centerline of source.

<sup>C</sup>( ) = AED inlet size of impactor prefilter.; <sup>D</sup>No. of Points = the number of logged data.

<sup>E</sup>These units are printed on scale of instrument and are not calibrated to the petroleum pipe scale. These data are considered as a relative measure of scattered light intensity, not as a true mass.

## B-5. TSP Field Study Results

**TABLE B-6. Estimated TSP/CCM Volume Percentile (Field)**

Description		Volume % <sup>A</sup>						
ESD	AED	Field test 1 (Mud Lake)			AED	Field test 2 (Lake Sand)		
Unit: [ $\mu\text{m}$ ]		T1 <sup>B</sup>	T2	T3	Unit:[ $\mu\text{m}$ ]	T1	T2	T3
2.0	2.9*	7.14	7.87	9.04	2.50*	6.50	6.41	8.06
2.03	2.96	7.66	8.48	9.63	2.52	6.80	7.00	8.39
:								
2.75	<b>4.02<sup>C</sup></b>	<b>23.09</b>	<b>26.20</b>	<b>25.30</b>	3.42	14.65	21.29	18.15
:								
3.23	4.71	33.35	37.66	35.13	<b>4.01</b>	<b>20.01</b>	<b>30.41</b>	<b>24.89</b>
:								
3.78	5.53	44.69	<u>49.84</u>	45.56	4.71	26.29	40.76	32.69
:								
4.04	5.91	<u>49.53<sup>D</sup></u>	54.98	<u>50.11</u>	5.03	29.16	45.33	36.15
:								
4.32	6.31	54.31	60.00	54.51	5.38	32.08	<u>49.95</u>	39.71
:								
5.21	7.60	67.14	72.89	66.28	6.48	40.65	62.73	<u>49.86</u>
:								
6.35	9.28	79.00	84.26	77.12	7.90	<u>49.99</u>	75.20	60.52
:								
6.88	<b>10.05<sup>C</sup></b>	<b>83.12</b>	<b>87.93</b>	<b>80.91</b>	8.56	53.71	79.69	64.56
:								
8.07	11.79	90.04	94.05	87.40	<b>10.04</b>	<b>60.95</b>	<b>87.36</b>	<b>71.99</b>
:								

*Notes:*

<sup>A</sup> Volume % = Obtained by an CCM; <sup>B</sup> T1-T12 = TSP Samplers.

<sup>C</sup> AED 4  $\mu\text{m}$ , 10  $\mu\text{m}$  = Respirable, Thoracic cutoff size.

<sup>D</sup> = 50 % Cumulative Volume.

\*Each PSD less than an AED 2.9  $\mu\text{m}$  (Mud Lake) and 3.3  $\mu\text{m}$  (Lake Sand) was estimated from a median AED of sampling efficiency and a slope of sampling efficiency measured by each TSP/CCM because AEDs 2.9  $\mu\text{m}$  and 3.3  $\mu\text{m}$  are the smallest particle size that a CCM can count with a 100  $\mu\text{m}$  orifice aperture in this study.

**TABLE B-7. Estimated Mass Fractions for a Respirable, Thoracic, and Inhalable Convention from TSP/CCMs (Field)**

Description	Field test 1 (Mud Lake)			Field test 1 (Lake Sand)		
	T1	T2	T3	T1	T2	T3
Respirable <sup>A</sup> ( $\leq 4 \mu\text{m}$ )	0.23	0.26	0.25	0.20	0.30	0.25
Thoracic ( $\leq 10 \mu\text{m}$ )	0.83	0.88	0.81	0.61	0.87	0.72
Inhalable ( $\leq 100 \mu\text{m}$ )	1	1	1	1	1	1

Note: <sup>A</sup> Each PSD less than an AED 2.9  $\mu\text{m}$  (Mud Lake) and 3.3  $\mu\text{m}$  (Lake Sand) was estimated from a median AED of sampling efficiency and a slope of sampling efficiency measured by each TSP/CCM because AEDs 2.9  $\mu\text{m}$  and 3.3  $\mu\text{m}$  are the smallest particle size that a CCM can count with a 100  $\mu\text{m}$  orifice aperture in this study.

**B-6. Estimated  $GM_{AED}$  and  $GSD_{AED}$  of Andersen sampler by Log Probit Analysis**

When the data of Andersen sampler were analyzed, the mass fractions of Andersen sampler's first and last stages are not in the straight line. Thus, the mass fractions of the first and last impaction stages were neglected in this analysis to obtain best log probit curve.

**TABLE B-8. Mass Fraction Measured from Each Stage of Andersen Sampler (Field)**

Stage	Cutoff AED [ $\mu\text{m}$ ]	Field test 1		Field test 2	
		C1	C2	C1	C2
0	9.00	0.383	0.373	0.598	0.598
1	5.80	0.278	0.269	0.435	0.427
2	4.70	0.150	0.162	0.289	0.287
3	3.30	0.032	0.071	0.163	0.165
4	2.10	0.032	0.035	0.094	0.100
5	1.10	0.006	0.006	0.044	0.049
6	0.65	0.003	0.001	0.025	0.022
7	0.43	0.000	0.000	0.011	0.000

**TABLE B-9. Standard Normal Random Variables from the Mass Fraction Measured in TABLE B-8 above (Field)**

Stage	Cutoff AED [ $\mu\text{m}$ ]	Field test 1		Field test 2	
		C1	C2	C1	C2
0	9.00	-0.297	-0.324	0.248	0.248
1	5.80	-0.588	-0.616	-0.163	-0.185
2	4.70	-1.038	-0.988	-0.555	-0.563
3	3.30	-1.859	-1.466	-0.984	-0.975
4	2.10	-1.859	-1.816	-1.318	-1.280
5	1.10	-2.518	-2.489	-1.705	-1.652
6	0.65	-2.807	-3.090	-1.963	-2.022
7	0.43	-5.199	-4.265	-2.290	-4.265

*Notes:* The values of standard normal random variables are calculated using a NORMINV function as NORMINV(Mass Fraction,0,1) in Microsoft Excel.

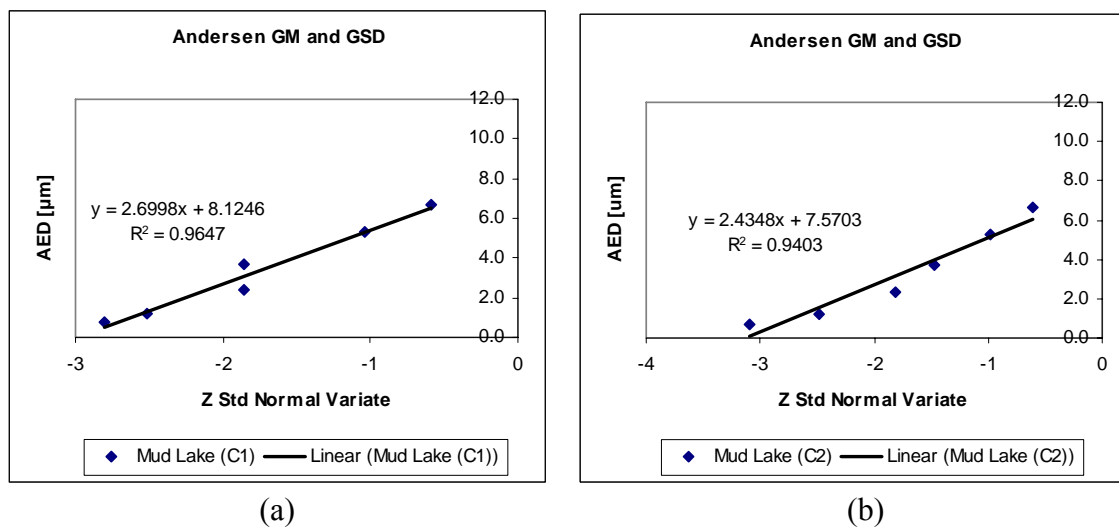


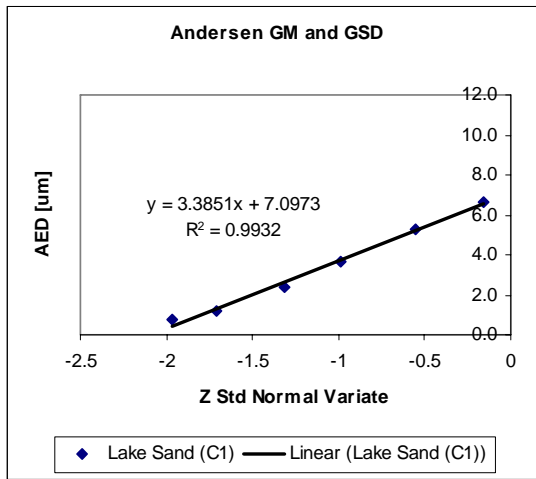
**FIGURE B-1. Estimated  $GM_{AED}$  and  $GSD_{AED}$  of the Andersen sampler (Field). (a)**

**C1 in field test 1, (b) C2 in field test 1, (c) C1 in field test 2, (d) C2 in field test 2.**

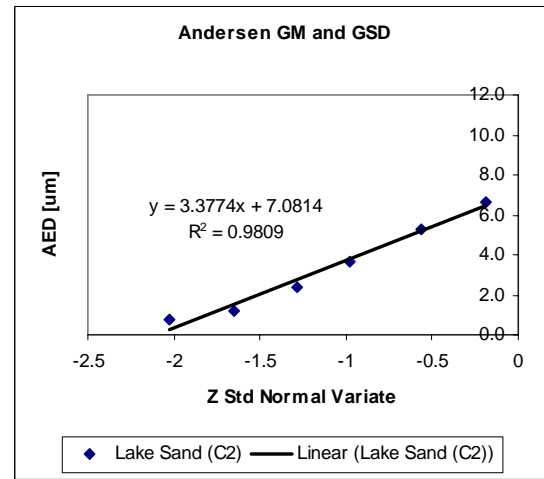
*Notes:* The mass fractions of the first and last impaction stages were neglected from TABLE B-9 to obtain best log probit curve.

C1 and C2 in a field test 1 were located at 2 m distance away from the centerline source.

C1 and C2 in a field test 2 were located at 3 m and 1 m distance from the centerline source respectively.



(c)



(d)

**FIGURE B-1. Continued.**

## APPENDIX C

### RANDOMIZED BLOCK DESIGN

This section documents the SAS procedures for a randomized block analysis in the chamber study. Arial font is used for the code and Times New Roman font is used for results.

#### C-1. SAS Procedures

```

DATA Chamber;
  INPUT sampler $ block $ con @@;
CARDS;
C1 Test1 29.2 C2 Test1 29.5 T1 Test1 33.6 T2 Test1 34.5 T3 Test1 31.6 T4 Test1 34.7
C1 Test2 21.4 C2 Test2 21.5 T1 Test2 24.0 T2 Test2 24.5 T3 Test2 25.6 T4 Test2 25.2
C1 Test3 23.5 C2 Test3 23.9 T1 Test3 25.0 T2 Test3 25.7 T3 Test3 30.0 T4 Test3 30.0
;

PROC SORT DATA=Chamber;
  BY sampler block;

PROC PRINT DATA=Chamber;
  VAR sampler block con;
  TITLE 'Mass Concentration by Aerosol Samplers';

PROC GLM DATA=Chamber;
  CLASS sampler block;
  MODEL con=sampler block;
  MEANS sampler/TUKEY;
  OUTPUT OUT=output R=resid P=predict;
  TITLE2 'Randomized Block Design';

```

#### C-2. Results

Mass Concentration by Aerosol Samplers  
Randomized Block Design

The GLM Procedure

Class Level Information

Class	Levels	Values
sampler	6	C1 C2 T1 T2 T3 T4
block	3	Test1 Test2 Test3
Number of observations		18

Mass Concentration by Aerosol Samplers  
Randomized Block Design

The GLM Procedure

Dependent Variable: con

Source	DF	Sum of Squares	Mean Square	F Value	Pr > F
Model	7	295.8988889	42.2712698	21.12	<.0001
Error	10	20.0188889	2.0018889		
Corrected Total	17	315.9177778			

R-Square	Coeff Var	Root MSE	con Mean
0.936633	5.161707	1.414881	27.41111

Source	DF	Type I SS	Mean Square	F Value	Pr > F
sampler	5	69.8644444	13.9728889	6.98	0.0047
block	2	226.0344444	113.0172222	56.46	<.0001

Source	DF	Type III SS	Mean Square	F Value	Pr > F
sampler	5	69.8644444	13.9728889	6.98	0.0047
block	2	226.0344444	113.0172222	56.46	<.0001



Mass Concentration by Aerosol Samplers  
Randomized Block Design

The GLM Procedure

Tukey's Studentized Range (HSD) Test for con

NOTE: This test controls the Type I experimentwise error rate, but it generally has a higher Type II error rate than REGWQ.

Alpha	0.05
Error Degrees of Freedom	10
Error Mean Square	2.001889
Critical Value of Studentized Range	4.91202
Minimum Significant Difference	4.0125

Means with the same letter are not significantly different. Means with different letters are different, but there is visible overlap between concentrations estimated by Andersen (C1 & C2) and TSP (T3 & T4) samplers.

Tukey Grouping	Mean	N	sampler
A	29.967	3	T4
A			
A	29.067	3	T3
A			
B A	28.233	3	T2
B A			
B A	27.533	3	T1
B			
B	24.967	3	C2
B			
B	24.700	3	C1

## Mass Concentration by Aerosol Samplers

Obs	sampler	block	con
1	C1	Test1	29.2
2	C1	Test2	21.4
3	C1	Test3	23.5
4	C2	Test1	29.5
5	C2	Test2	21.5
6	C2	Test3	23.9
7	T1	Test1	33.6
8	T1	Test2	24.0
9	T1	Test3	25.0
10	T2	Test1	34.5
11	T2	Test2	24.5
12	T2	Test3	25.7
13	T3	Test1	31.6
14	T3	Test2	25.6
15	T3	Test3	30.0
16	T4	Test1	34.7
17	T4	Test2	25.2
18	T4	Test3	30.0

## APPENDIX D

### PERFORMANCE CHARACTERISTICS OF A PM<sub>10</sub> SAMPLER

#### D-1. Overviews of Collection Efficiency

Hinds<sup>(1)</sup> indicated that the lognormal distribution is the most common distribution used for characterizing the particle sizes associated with the aerosol. The significance of a lognormal distribution is that the particle size distribution (PSD) can be described in terms of two parameters: a geometric mean ( $GM$ ) and a geometric standard deviation ( $GSD$ ). Equation D.1 shows the probability density function (PDF) for the lognormal distribution which represents the particle size distribution.

$$f(AED, GM_{AED}, GSD_{AED}) = \frac{1}{AED \cdot \ln(GSD_{AED}) \cdot \sqrt{2\pi}} \cdot \exp\left[-\frac{1}{2} \cdot \frac{(\ln(AED) - \ln(GM_{AED}))^2}{(\ln(GSD_{AED}))^2}\right] \quad (D.1)$$

where  $f(AED, GM_{AED}, GSD_{AED})$  = The lognormal probability density function for sample data;

$AED$  = Aerodynamic equivalent diameter;

$GM_{AED}$  = Median AED of sample data;

$GSD_{AED}$  = slope of PSD curve.

Equation D.1 applies to particle size distribution where  $GSD_{AED}$  is greater than 1.0. The fraction of the total particles  $dAED$  having particle diameters between  $AED$  and  $AED + dAED$  is

$$df = f(AED, GM_{AED}, GSD_{AED})dAED \quad (D.2)$$

where  $dAED$  = a differential interval of particle size. The area under the density distribution curve is

$$\int_0^{\infty} f(AED, GM_{AED}, GSD_{AED}) dAED = 1.0 \quad (D.3)$$

The area under the PDF may be estimated for particle sizes ranging from zero to infinity as shown in Equation D.3 or between given AEDs  $a$  and  $b$  in Equation D.4. The area under the PDF curve between two AEDs  $a$  and  $b$  equals the fraction of particles whose AEDs fall within this interval, which can be expressed as

$$f_{ab}(a, b, GM_{AED}, GSD_{AED}) = \int_a^b f(AED, GM_{AED}, GSD_{AED}) dAED \quad (D.4)$$

The lognormal distribution is useful for describing the behavior of size selective air samplers. Equations D.5 and D.6 illustrate the use of the cumulative distribution function of the lognormal distribution to represent air sampler size selective collection efficiency and penetration efficiency, respectively.

Cumulative sampler collection efficiency and penetration efficiency are defined as below.

Collection efficiency =  $F(a, GM_{AED}, GSD_{AED}) =$

$$\int_0^a \left[ \frac{1}{AED \cdot \ln(GSD_{AED}) \cdot \sqrt{2\pi}} \cdot \exp \left[ -\frac{1}{2} \cdot \frac{(\ln(AED) - \ln(GM_{AED}))^2}{(\ln(GSD_{AED}))^2} \right] \right] dAED \quad (D.5)$$

where  $F(a, GM_{AED}, GSD_{AED})$  = the fraction of the particles having AEDs less than  $a$ .

Penetration efficiency =

$$1 - \int_0^{\infty} \left[ \frac{1}{AED \cdot \ln(GSD_{AED}) \cdot \sqrt{2\pi}} \cdot \exp \left[ -\frac{1}{2} \cdot \frac{(\ln(AED) - \ln(GM_{AED}))^2}{(\ln(GSD_{AED}))^2} \right] \right] dAED \quad (D.6)$$

## D-2. PM<sub>10</sub> Sampler Vs PM<sub>2.5</sub> Sampler

The US Environmental Protection Agency (EPA) defines the 50 % cut size for a PM<sub>10</sub> sampler as a median AED ( $GM_{AED}$ ) of  $10 \mu\text{m} \pm 0.5 \mu\text{m}$  and the 50 % cut size for a PM<sub>2.5</sub> sampler as a median AED of  $2.5 \mu\text{m} \pm 0.2 \mu\text{m}$  in 40CFR53. No slope values for the sampler are listed in EPA's 40CFR53 or any other current EPA standard.

The Federal Reference Method (FRM) performance standard for PM<sub>10</sub> sampler is a cut size of a median AED of  $10 \mu\text{m} \pm 0.5 \mu\text{m}$  and a slope of  $1.5 \pm 0.1$  using an equations 1 and 2 (See Figure D-1).<sup>(2)</sup> EPA intended for the PM<sub>2.5</sub> sampler to have a "sharp cut" or represent a true concentration of PM<sub>2.5</sub> in EPA's 40CFR53. This means that the slope would be equal to 1.0. It is difficult to design a sampler with a sharp cut from an engineering standpoint. Buch<sup>(3)</sup> suggested that the performance characteristics for PM<sub>2.5</sub> sampler is a median AED of  $2.5 \mu\text{m} \pm 0.2 \mu\text{m}$  and a slope =  $1.3 \pm 0.03$  (See Figure D-2). Figures D-1 and D-2 illustrate the efficiency ranges for PM<sub>10</sub> and PM<sub>2.5</sub> samplers. When comparing collection efficiencies, the acceptable ranges are 44 % to 56 % for PM<sub>10</sub> sampler and 36 % to 63 % for PM<sub>2.5</sub> sampler for benchmark spherical particles of  $10 \mu\text{m}$  and  $2.5 \mu\text{m}$ , respectively (See Tables D-1 and D-2).

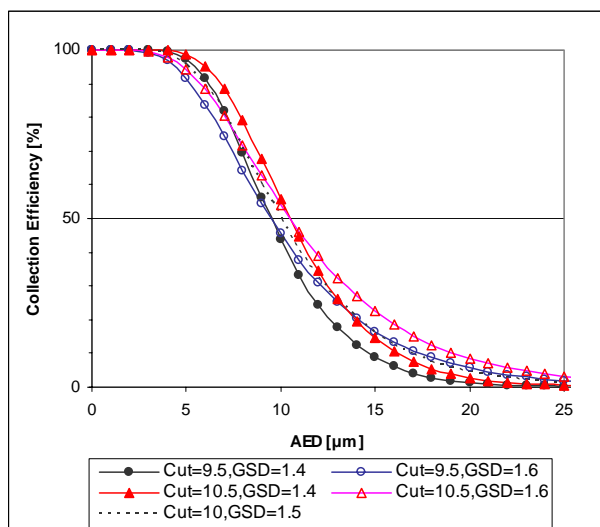


**FIGURE D-1. Penetration efficiency usable region for a  $PM_{10}$  sampler with parameters falling in the acceptable range as defined by FRM.**

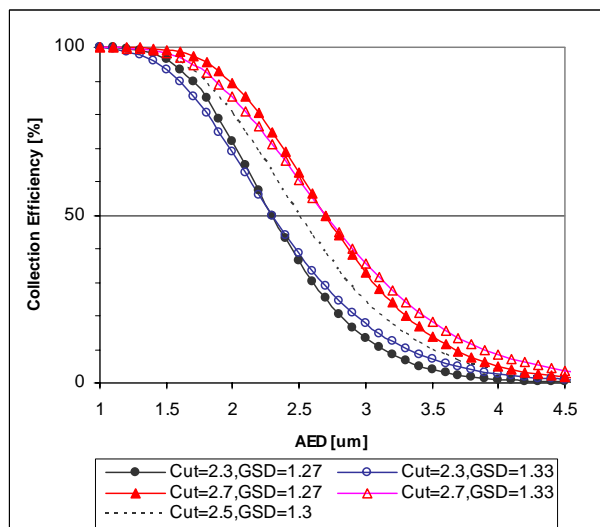


**FIGURE D-2. Penetration efficiency usable region for  $PM_{2.5}$  sampler with parameters falling into the acceptable range.**

**TABLE D-1. Penetration Efficiency of PM<sub>10</sub> Sampler**

AED [μm]	$GM_{AED}^A$	Slope	$GM_{AED}$	Slope	$GM_{AED}$	Slope	$GM_{AED}$	Slope
	9.5	1.4	9.5	1.6	10.5	1.4	10.5	1.6
	Collection Efficiency <sup>B</sup>	Penetration Efficiency <sup>C</sup>	Collection Efficiency	Penetration Efficiency	Collection Efficiency	Penetration Efficiency	Collection Efficiency	Penetration Efficiency
0	1.25E-254	1	1.2E-131	1	4.73E-259	1	6.44E-134	1
1	1.109E-11	1	8.341E-07	0.9999992	1.391E-12	1	2.824E-07	0.9999997
2	1.821E-06	0.9999982	0.0004579	0.9995421	4.148E-07	0.9999996	0.0002093	0.9997907
3	0.0003065	0.9996935	0.0070936	0.9929064	9.835E-05	0.9999017	0.0038445	0.9961555
4	0.0050734	0.9949266	0.0328543	0.9671457	0.0020639	0.9979361	0.0200194	0.9799806
5	0.0282216	0.9717784	0.0860266	0.9139734	0.0137254	0.9862746	0.0572165	0.9427835
6	0.0860109	0.9139891	0.1641062	0.8358938	0.0481376	0.9518624	0.116893	0.883107
7	0.1820452	0.8179548	0.2579291	0.7420709	0.1140924	0.8859076	0.1941553	0.8058447
8	0.3047661	0.6952339	0.3573183	0.6426817	0.2094904	0.7905096	0.281437	0.718563
9	0.4361694	0.5638306	0.4542084	0.5457916	0.3234267	0.6765733	0.3714643	0.6285357
10	0.5605818	<b>0.4394182<sup>D</sup></b>	0.5434518	<b>0.4565482</b>	0.4423535	<b>0.5576465</b>	0.4586608	<b>0.5413392</b>
11	0.6684755	0.3315245	0.6224493	0.3775507	0.5549818	0.4450182	0.5394221	0.4605779
12	0.756255	0.243745	0.6904228	0.3095772	0.6542636	0.3457364	0.6118359	0.3881641
13	0.824382	0.175618	0.7477261	0.2522739	0.7372027	0.2627973	0.6752329	0.3247671
14	0.8754307	0.1245693	0.7953218	0.2046782	0.803723	0.196277	0.7297592	0.2702408
15	0.9126875	0.0873125	0.8344297	0.1655703	0.8554374	0.1445626	0.7760369	0.2239631
16	0.9393454	0.0606546	0.8663138	0.1336862	0.8946881	0.1053119	0.8149249	0.1850751
17	0.9581383	0.0418617	0.8921645	0.1078355	0.9239323	0.0760677	0.8473608	0.1526392
18	0.971241	0.028759	0.913043	0.086957	0.9454117	0.0545883	0.8742662	0.1257338
19	0.9803028	0.0196972	0.9298628	0.0701372	0.9610154	0.0389846	0.8964947	0.1035053
20	0.9865335	0.0134665	0.9433922	0.0566078	0.9722562	0.0277438	0.9148066	0.0851934
21	0.9908006	0.0091994	0.9542667	0.0457333	0.9803028	0.0196972	0.9298628	0.0701372
22	0.9937154	0.0062846	0.9630062	0.0369938	0.9860362	0.0139638	0.9422271	0.0577729
23	0.9957038	0.0042962	0.9700322	0.0299678	0.9901078	0.0098922	0.9523744	0.0476256
24	0.9970596	0.0029404	0.9756849	0.0243151	0.9929929	0.0070071	0.9607008	0.0392992
:								
:								

Notes: <sup>A</sup> $GM_{AED}$  = Median AED of PM<sub>10</sub> or PM<sub>2.5</sub> sample.

<sup>B</sup>Collection efficiency = LOGNORMDIST(AED, ln(AED<sub>50</sub>), ln(slope)) in Microsoft Excel.

<sup>C</sup>Penetration efficiency = 1-Cumulative collection efficiency.

<sup>D</sup>Bold values indicate the collection efficiency ranges for AED<sub>50</sub> for PM<sub>10</sub> sampler at AED 10 μm.

**TABLE D-2. Penetration Efficiency of PM<sub>2.5</sub> Sampler**

AED [ $\mu\text{m}$ ]	$GM_{AED}^A$	Slope	$GM_{AED}$	Slope	$GM_{AED}$	Slope	$GM_{AED}$	Slope
	2.3	1.27	2.3	1.33	2.7	1.27	2.7	1.33
	Collection Efficiency	Penetration Efficiency	Collection Efficiency	Penetration Efficiency	Collection Efficiency	Penetration Efficiency	Collection Efficiency	Penetration Efficiency
0.1	1.293E-39	1	2.023E-28	1	1.481E-43	1	3.399E-31	1
0.2	8.21E-25	1	5.439E-18	1	6.493E-28	1	3.537E-20	1
0.3	7.847E-18	1	4.583E-13	1	1.914E-20	1	6.556E-15	1
0.4	1.256E-13	1	4.293E-10	1	6.793E-16	1	1.071E-11	1
0.5	8.585E-11	1	4.368E-08	1	8.595E-13	1	1.675E-09	1
0.6	9.442E-09	1	1.227E-06	0.9999988	1.559E-10	1	6.669E-08	0.9999999
0.7	3.229E-07	0.9999997	1.514E-05	0.9999849	8.124E-09	1	1.103E-06	0.9999989
0.8	4.974E-06	0.999995	0.0001065	0.9998935	1.798E-07	0.9999998	9.978E-06	0.99999
0.9	4.327E-05	0.9999567	0.0005007	0.9994993	2.149E-06	0.9999979	5.849E-05	0.9999415
1	0.0002463	0.9997537	0.0017465	0.9982535	1.622E-05	0.9999838	0.000248	0.999752
1.1	0.0010144	0.9989856	0.0048486	0.9951514	8.605E-05	0.999914	0.00082	0.99918
1.2	0.0032451	0.9967549	0.0112644	0.9887356	0.0003459	0.9996541	0.0022305	0.9977695
:								
:								
2	0.2793624	0.7206376	0.3120369	0.6879631	0.1046343	0.8953657	0.1463223	0.8536777
2.1	0.351747	0.648253	0.3748637	0.6251363	0.1465259	0.8534741	0.1890908	0.8109092
2.2	0.4262312	0.5737688	0.4380665	0.5619335	0.1957722	0.8042278	0.2363398	0.7636602
2.3	0.5	0.5	0.5	0.5	0.2511605	0.7488395	0.2869719	0.7130281
2.4	0.5706625	0.4293375	0.5593172	0.4406828	0.3110836	0.6889164	0.339798	0.660202
2.5	0.6363999	<b>0.3636001<sup>B</sup></b>	0.6150033	<b>0.3849967</b>	0.3737302	<b>0.6262698</b>	0.3936304	<b>0.6063696</b>
:								
:								

Notes: <sup>A</sup> $GM_{AED}$  = Median AED of PM<sub>10</sub> or PM<sub>2.5</sub> sample.

<sup>B</sup>Bold Values indicate the collection efficiency ranges for AED<sub>50</sub> for PM<sub>2.5</sub> sampler at AED 2.5  $\mu\text{m}$ .

### D-3. Mathematica<sup>(4)</sup> Code for PDF of random variables

This section documents the Mathematica Codes developed and used for PSD analysis. Times New Roman font is used for the code and Italic Arial font is used for non-executing comments.



(\*\*\*\*\* Content-type: application/mathematica \*\*\*\*\*  
 CreatedBy='Mathematica 5.0'

### Mathematica-Compatible Notebook

*This notebook can be used with any Mathematica-compatible application, such as Mathematica, MathReader or Publicon. The data for the notebook starts with the line containing stars above.*

*To get the notebook into a Mathematica-compatible application, do one of the following:*

- \* Save the data starting with the line of stars above into a file with a name ending in .nb, then open the file inside the application;*
- \* Copy the data starting with the line of stars above to the clipboard, then use the Paste menu command inside the application.*

*Data for notebooks contains only printable 7-bit ASCII and can be sent directly in email or through ftp in text mode. Newlines can be CR, LF or CRLF (Unix, Macintosh or MS-DOS style).*

*NOTE: If you modify the data for this notebook not in a Mathematica-compatible application, you must delete the line below containing the word CacheID, otherwise Mathematica-compatible applications may try to use invalid cache data.*

*For more information on notebooks and Mathematica-compatible applications, contact Wolfram Research:*

*web: <http://www.wolfram.com>  
 email: [info@wolfram.com](mailto:info@wolfram.com)  
 phone: +1-217-398-0700 (U.S.)*

*Notebook reader applications are available free of charge from Wolfram Research.*

\*\*\*\*\*)

(\*CacheID: 232\*)

(\*NotebookFileLineBreakTest  
 NotebookFileLineBreakTest\*)  
 (\*NotebookOptionsPosition[ 13620, 385]\*)

```
(*NotebookOutlinePosition[ 14263, 407]*)
(* CellTagsIndexPosition[ 14219, 403]*)
(*WindowFrame->Normal*)
```

```
Notebook[{
```

```
Cell[CellGroupData[{
Cell["<\
The FRM PM10 performance standard calls for an AED50 of 10 \[Micro]m \
\[PlusMinus] 0.5 \[Micro]m and a slope of 1.5 \[PlusMinus] 0.1. \
>", "Subsection"],
```

```
Cell[TextData[{
"Ref: ",
StyleBox[".\[OpenCurlyDoubleQuote]National Ambient Air Quality Standards \
for Particulate Matter\[CloseCurlyDoubleQuote] ",
FontFamily->"Times New Roman"],
StyleBox["Code of Federal Regulations",
FontFamily->"Times New Roman",
FontSlant->"Italic"],
StyleBox[" Title 40, Part 53. 2000.",
FontFamily->"Times New Roman"]
}], "Subsubsection"]
}, Open ]],
```

```
Cell[CellGroupData[{
```

```
Cell["<\
Input data, lognormal PSD and Lognormal Collection Efficiency Curve.\
>", "Subsection"],
```

```
Cell[BoxData[
\(<< Statistics`ContinuousDistributions`\)], "Input"],
```

```
Cell[BoxData[{
\ (Clear[gm, gs, GM, GS, lnd, AED, aed]), "\[IndentingNewLine]",
\ (lnd[gm_, gs_] :=
LogNormalDistribution[Log[gm], Log[gs]]), "\[IndentingNewLine]",
\ (PSD[AED_] \ = \ PDF[lnd[GM, GS], AED]), "\[IndentingNewLine]",
\ (PM10CE[AED_] = 1 - CDF[lnd[CP, Slope], AED])}], "Input"],
```

```
Cell[CellGroupData[{
```

Cell["<

In an environment with a total mass concentration of  $\text{tot mg/m}^3$  and a PSD as indicated above, the PM10 sampler will collect approximately the following

mass:

>", "Subsubsection"],

Cell[BoxData[

$$\text{(samplemass)} = \int_0^{\infty} (5 \text{ GS} \text{ GM}) \text{PM10CE[AED]} \text{ PSD[AED]} \text{ [DifferentialD]AED}$$
), "Text"]

}, Open ]],

Cell[CellGroupData[{

Cell["<

This integral does not have a closed form solution, but it can be integrated numerically. If the airborne total mass concentration is  $10 \text{ mg/m}^3$ , and the PSD is characterized by  $\text{GM} = 11.8 \mu\text{m}$  and  $\text{GS} = 2.1$ , then the equation can be integrated for the central and both extreme values of the FRM

specification to find the range of measurements expected from samplers that comply with the allowed variation in the FRM. The various combinations of median and slope are represented below with n for negative limit and p for positive limit: thus, spmn indicates a sample taken with sampler whose slope is at the positive limit, 1.6, and whose cut point is at the negative limit,

9.5.

>", "Subsubsection"],

Cell[BoxData[

$$\text{(psd[AED]} = \text{PSD[AED]} / \{ \text{GM} \text{ [Rule]} 11.8, \text{ GS} \text{ [Rule]} 2.1 \}$$
), "Input"],

Cell[BoxData[

$$\text{(truePM10conc} = \text{NIntegrate}[10 \text{ psd[AED], \{AED, 0, 10\}}]$$
), "Input"]

}, Open ]],

Cell[CellGroupData[{

Cell[TextData[{

"Both the slope and the cut point are allowed a reasonable tolerance. Thus, among acceptable PM-10 samplers, there is an allowed uncertainty in measuring PM-10 for an atmosphere with PSD having "

Cell[BoxData[

$$\text{(TraditionalForm} \text{ GM\_AED} = \text{ (11.8 } \mu\text{m} \text{ and } \text{ GS\_AED} = \text{ 2.1)}$$
),

", as shown below."  
 }], "Subsubsection"],

```
Cell[BoxData[
  \(\text{okPM10conc} = \{\text{smpPM10conc} \ = \
    \text{NIntegrate}[\ \{(\
      \text{PM10CE}[\text{AED}] /. \{\text{CP} \[\text{Rule}] 10.5,
        \text{Slope} \[\text{Rule}] 1.6\}\}\ \{(\text{10} \ \text{psd}[\text{AED}])\}, \{\text{AED}, 0,
        5 \ 11.8 \ 2.1\}], \[\text{IndentingNewLine}]\text{smpPM10conc} \ = \
      \text{NIntegrate}[\ \{(\
        \text{PM10CE}[\text{AED}] /. \{\text{CP} \[\text{Rule}] 10.5,
          \text{Slope} \[\text{Rule}] 1.4\}\}\ \{(\text{10} \ \text{psd}[\text{AED}])\}, \{\text{AED}, 0,
          5 \ 11.8 \ 2.1\}], \[\text{IndentingNewLine}]\text{nominalPM10conc} =
        \text{NIntegrate}[\ \{(\
          \text{PM10CE}[\text{AED}] /. \{\text{CP} \[\text{Rule}] 10, \text{Slope} \[\text{Rule}] 1.5\}\}\}\ \{(\text{10}
            \ \text{psd}[\text{AED}])\}, \{\text{AED}, 0,
            5 \ 11.8 \ 2.1\}], \[\text{IndentingNewLine}]\text{smpnPM10conc} =
          \text{NIntegrate}[\ \{(\
            \text{PM10CE}[\text{AED}] /. \{\text{CP} \[\text{Rule}] 9.5,
              \text{Slope} \[\text{Rule}] 1.6\}\}\}\ \{(\text{10} \ \text{psd}[\text{AED}])\}, \{\text{AED}, 0,
              5 \ 11.8 \ 2.1\}], \[\text{IndentingNewLine}]\text{snmpPM10conc} =
            \text{NIntegrate}[\ \{(\
              \text{PM10CE}[\text{AED}] /. \{\text{CP} \[\text{Rule}] 9.5,
                \text{Slope} \[\text{Rule}] 1.4\}\}\}\ \{(\text{10} \ \text{psd}[\text{AED}])\}, \{\text{AED}, 0,
                5 \ 11.8 \ 2.1\}\} // \text{Reverse}\}], \text{"Input"}
        ], \text{Open} ]],
```

```
Cell[CellGroupData[{
```

```
Cell["\<
Let the 90% confidence interval be the largest allowed difference between \
samplers.\
\>", "Subsubsection"],
```

```
Cell[BoxData[{
  \(\{\{\text{snmnPM10conc} - \{\text{smpPM10conc}, \text{snmpPM10conc}\},
    \text{smpnPM10conc} - \{\text{smpPM10conc}, \text{snmpPM10conc}\} // \text{Abs}\} //
    \text{Flatten}\}, \[\text{IndentingNewLine}]",
  \(\text{ci} = \text{Max}[\%]\)\}, \text{"Input"}
}, \text{Open} ]],
```

```
Cell[CellGroupData[{
```

```
Cell["\<
```



```
Cell[BoxData[
  \(\Plot[
    10\ psd[AED] {sm[AED], snmn[AED], spmp[AED]} // Evaluate, {AED, 0,
    30}\ ;\)\), "Input"]
  ], Open ]],
```

```
Cell[TextData[{
  "In summary, given an atmospheric dust concentration of 10 mg/m3 on the \
  basis of total mass, with a PSD characterized as LogNormal with ",
  Cell[BoxData[
    \(\TraditionalForm\`GM\_AED\)\)],
  "= 11.8 \[Mu]m and ",
  Cell[BoxData[
    \(\TraditionalForm\`GS\_AED\)\)],
  "= 2.1, the true value of PM10 is 4.12 mg/m3. A PM10 sampler which \
  operated with FRM parameters will report 4.22 mg.m3 and PM10 samplers which \
  operates in the FRM allowed parameter space will report values between 3.95 \
  and 4.47 mg/m3. \n Assuming this range is the 90% confidence region \
  for production samplers operating under field conditions, the estimated PM10 \
  concentration would be 0.422 times the TSP concentration with a standard \
  deviation of 0.016. In a chamber test, I would expect this sort of variation \
  between PM10 samplers, even if they all experienced exactly the same \
  concentration. If a larger variation were observed, then either one or more \
  PM10 samplers are operating outside the range specified above, or they are "
  }], "Subsubsection"]
  ], Open ]],
```

```
Cell[CellGroupData[{
```

```
Cell["Next, repeat these estimates for an ACIGH thoracic sampler.", \
  "Subsection"],
```

```
Cell[CellGroupData[{
```

```
Cell["<\
  The sampling efficiency curves for the inhalable, thoracic and respirable \
  conventions are expressed in terms of the Standard Normal Distribution \
  Function, F[x].\
  >", "Subsubsection"],
```

```
Cell[BoxData[
  \(\F[x_] = CDF[NormalDistribution[0, 1], x]\)\), "Input"],
```

```
Cell[BoxData[{
```

```

\(\SI[d_] :=
  0.5 \((1 + \[ExponentialE]^\((-0.06)\ d))\), \
"\[IndentingNewLine]",
\(\ST[d_] :=
  \SI[d] \((1 - F[x])\) /
  x \[Rule] \ Log[d/11.64]/Log[1.5]\), "\[IndentingNewLine]",
\(\SR[d_] :=
  \SI[d] \((1 - F[x])\) / x \[Rule] \ Log[d/4.25]/Log[1.5]\)}, "Input"
}, Open ]],

Cell[CellGroupData[{

Cell["\<
Verify that the 50% cut point for thoracic is 10 um and for respirable is 4 \
um. \
\>", "Subsubsection"],

Cell[BoxData[
\(\FindRoot[ST[d] \[Equal] 0.5, {d, 10}]\)], "Input"],

Cell[BoxData[
\(\FindRoot[SR[d] \[Equal] 0.5, {d, 4}]\)], "Input"
}, Open ]],

Cell[CellGroupData[{

Cell["\<
Show the samling efficiency curves for the respirable,thoracic and inhalable \
fractions.\
\>", "Subsubsection"],

Cell[BoxData[
\(\Plot[{SI[d], ST[d], SR[d]}, {d, 0, 30}, Frame \[Rule] True,
  FrameLabel \[Rule] {"\<AED in um\>", "\<Sampling Efficiency\>", "\< \
ISO Resp 4 um, Thor 10 um, Inhal 100 um\>", "\<\>"},
  ImageSize \[Rule] 72*7, \
  TextStyle \[Rule] {FontFamily -> "\<Arial\>",
    FontSize \[Rule] 14};)\)], "Input"
}, Open ]],

Cell[CellGroupData[{

Cell["\<
Show the distribution of particles sampled with four samplers, Respirable, \

```

Thoracic, Inhalable, Total Suspended PM. \

```
\>", "Subsubsection"],

Cell[BoxData[
  \(\Plot[{1.0, SI[d], ST[d], SR[d]} psd[d] // Evaluate, {d, 0, 30},
    Frame \[Rule] True,
    FrameLabel \[Rule] {"\<AED in um\>", "\<Mass Density \>", "\< ISO \
Resp 4 um, Thor 10 um, Inhal 100 um, Total\>", "\<\>"},
    ImageSize \[Rule] 72*7, \
    TextStyle \[Rule] {FontFamily -> "\<Arial\>",
      FontSize \[Rule] 14};\)\), "Input"
], Open ]],
```

```
Cell[CellGroupData[{
```

```
Cell["\<
What mass concentration will be reported by each of these four samplers? \
Integrate numerically from d = 0 to d = 5*GM*GS = 123.9 um.
Note: 5*GM is five standard deviations from the median in the \
\>", "Subsubsection"],
```

```
Cell[BoxData[{
  \(\totalmass\ = \
    10\ NIntegrate[
      psd[d], {d, 0, 11.8*2.1*5};\)\), "\[IndentingNewLine]",
  \(\inhalablemass =
    10\ NIntegrate[
      psd[d]\ SI[d], {d, 0, 11.8*2.1*5};\)\), "\[IndentingNewLine]",
  \(\thoracicmass\ = \
    10\ \ NIntegrate[
      psd[d]\ ST[d], {d, 0, 11.8*2.1*5};\)\), "\[IndentingNewLine]",
  \(\respirablemass =
    10\ \ NIntegrate[
      psd[d]\ SR[d], {d, 0, 11.8*2.1*5};\)\), "\[IndentingNewLine]",
  \(\TableForm[{{ "\<totalmass\>", "\<inhalablemass\>", "\<thoracicmass\>", "\
\<respirablemass\>"}, {totalmass, inhalablemass, thoracicmass,
    respirablemass}}]\)\), "Input"
], Open ]],
```

```
Cell[CellGroupData[{
```

```
Cell[TextData[{
  "In the test atmosphere used for these estimates { psd[d] with ",
  Cell[BoxData[
```



```

\ (TraditionalForm\`GM\_AED\ = \ (11.8\ um\ and\ GS\_AED\ = \
2.1\))],
"}, the nominal PM10 and thoracic fractions are different from one another \
and from the true mass \[LessEqual] 10 um AED. Due to their finite slopes, \
both PM10 and thoracic samplers collect some particles larger than 10 um and \
miss some that are smaller than 10 um AED. The net result is that both \
overestimate the true mass for particles with AEC \[LessEqual] 10 um. "
}], "Subsubsection"],

```

```

Cell[BoxData[
\ ({{"\<thoracic conc>", "\<truePM10conc>", "\<nominalPM10conc>", \
"\<MinPM10Conc>", \ "\<MaxPM10conc>"}, {thoracicmass, truePM10conc, \
nominalPM10conc, smnPM10conc, \
smpmPM10conc} \*"\< mg \!(m\^(-3))\>"} //
TableForm\)], "Input"],

```

```

Cell[BoxData[{
\ (GM = 21.3; GS = 2.1;), "\[IndentingNewLine]",
\ ({{truePM10conc = NIntegrate[10\ psd[AED], {AED, 0, 10}], \
nominalPM10conc = \
NIntegrate[\ ( ( \
PM10CE[AED] /. {CP \[Rule] 10, Slope \[Rule] 1.5} ) \) \ ( (10 \
psd[AED] ) \), {AED, 0, \
5\ GM\ GS}], \[IndentingNewLine]ACGIHthoracicconc\ = \
NIntegrate[\ ( ( \ ST[d] ) \) \ ( (10 \ psd[d] ) \), {d, 0, \
5\ GM\ GS} ] ; ) \), "\[IndentingNewLine]",
\ ({{"\<truePM10conc>", "\<nominalPM10conc>", "\<ACGIH thoracic \
conc>"}, {truePM10conc, nominalPM10conc, \
ACGIHthoracicconc} \*"\< mg \!(m\^(-3))\>"} //
TableForm\)], "Input"
}, Open ]]
}, Open ]]
},
FrontEndVersion->"5.0 for Microsoft Windows",
ScreenRectangle->{{0, 1024}, {0, 693}},
WindowSize->{496, 535},
WindowMargins->{{0, Automatic}, {Automatic, 0}}
]

```

```

(*****
Cached data follows. If you edit this Notebook file directly, not
using Mathematica, you must remove the line containing CachedID at
the top of the file. The cache data will then be recreated when
you save this file from within Mathematica.

```

\*\*\*\*\*)

```
(*CellTagsOutline
CellTagsIndex->{}
*)
```

```
(*CellTagsIndex
CellTagsIndex->{}
*)
```

```
(*NotebookFileOutline
Notebook[{
```

```
Cell[CellGroupData[{
Cell[1776, 53, 168, 3, 56, "Subsection"],
Cell[1947, 58, 391, 10, 29, "Subsubsection"]
}, Open ]],
```

```
Cell[CellGroupData[{
Cell[2375, 73, 98, 2, 38, "Subsection"],
Cell[2476, 77, 71, 1, 30, "Input"],
Cell[2550, 80, 316, 5, 90, "Input"],
```

```
Cell[CellGroupData[{
Cell[2891, 89, 194, 4, 46, "Subsubsection"],
Cell[3088, 95, 130, 2, 44, "Text"]
}, Open ]],
```

```
Cell[CellGroupData[{
Cell[3255, 102, 732, 11, 114, "Subsubsection"],
Cell[3990, 115, 101, 2, 30, "Input"],
Cell[4094, 119, 86, 1, 30, "Input"]
}, Open ]],
```

```
Cell[CellGroupData[{
Cell[4217, 125, 370, 8, 63, "Subsubsection"],
Cell[4590, 135, 1168, 21, 230, "Input"]
}, Open ]],
```

```
Cell[CellGroupData[{
Cell[5795, 161, 118, 3, 29, "Subsubsection"],
Cell[5916, 166, 210, 4, 70, "Input"]
}, Open ]],
```

```
Cell[CellGroupData[{  
Cell[6163, 175, 152, 3, 29, "Subsubsection"],  
Cell[6318, 180, 71, 1, 43, "Input"]  
}, Open ]],
```

```
Cell[CellGroupData[{  
Cell[6426, 186, 75, 0, 29, "Subsubsection"],  
Cell[6504, 188, 303, 6, 70, "Input"],  
Cell[6810, 196, 309, 6, 70, "Input"],  
Cell[7122, 204, 315, 6, 70, "Input"]  
}, Open ]],
```

```
Cell[CellGroupData[{  
Cell[7474, 215, 123, 3, 29, "Subsubsection"],  
Cell[7600, 220, 136, 3, 30, "Input"]  
}, Open ]],  
Cell[7751, 226, 1081, 18, 148, "Subsubsection"]  
}, Open ]],
```

```
Cell[CellGroupData[{  
Cell[8869, 249, 83, 1, 38, "Subsection"],
```

```
Cell[CellGroupData[{  
Cell[8977, 254, 197, 4, 46, "Subsubsection"],  
Cell[9177, 260, 73, 1, 30, "Input"],  
Cell[9253, 263, 325, 8, 71, "Input"]  
}, Open ]],
```

```
Cell[CellGroupData[{  
Cell[9615, 276, 116, 3, 29, "Subsubsection"],  
Cell[9734, 281, 70, 1, 30, "Input"],  
Cell[9807, 284, 69, 1, 30, "Input"]  
}, Open ]],
```

```
Cell[CellGroupData[{  
Cell[9913, 290, 122, 3, 29, "Subsubsection"],  
Cell[10038, 295, 354, 6, 90, "Input"]  
}, Open ]],
```

```
Cell[CellGroupData[{  
Cell[10429, 306, 152, 3, 46, "Subsubsection"],  
Cell[10584, 311, 388, 7, 90, "Input"]  
}, Open ]],
```

```
Cell[CellGroupData[{
Cell[11009, 323, 232, 4, 63, "Subsubsection"],
Cell[11244, 329, 704, 15, 270, "Input"]
}, Open ]],
```

```
Cell[CellGroupData[{
Cell[11985, 349, 595, 10, 131, "Subsubsection"],
Cell[12583, 361, 294, 5, 112, "Input"],
Cell[12880, 368, 712, 13, 232, "Input"]
}, Open ]]
}, Open ]]
}
]
*)
```

```
(*****
End of Mathematica Notebook file.
*****)
```

## APPENDIX D REFERENCES

---

1. **Hinds, W.C.:** *Aerosol Technology Properties, Behavior, and Measurement of Airborne Particles*. New York: John Wiley & Sons, Inc, 1999.
- 2 National Ambient Air Quality Standards for Particulate Matter *Code of Federal Regulations* Title 40, Part 53. 2000.
3. **Buch,U.M.;** *Performance analysis of the cascade impactor, the federal reference method PM2.5 sampler and the improved sampler*. Thesis, Texas A&M University, College Station, TX.
4. **Wolfram Research, Inc.:** Mathematica 5.0 Champaign, IL.

## APPENDIX E

### CUTOFF SIZE CALCULATION (ANDERSEN SAMPLER)

#### ABBREVIATIONS

$AED_{50}$	An aerodynamic equivalent diameter which has 50 % collection efficiency for size selective aerosol sampler.
AED	The diameter of the unit density ( $\rho_P = 1 \text{ g/cm}^3$ ) sphere that has the same settling velocity as the particle.
$B$	Mobility of particle [cm/s/dyn]
$C_{AED}$	Cunningham correction factor of aerodynamic equivalent diameter $AED$ , a dimensionless number
$C_{AED50}$	Cunningham correction factor corresponding to $AED_{50}$
$C_P$	Cunningham correction factor of particle $d_P$
$C_{P50}$	Cunningham correction factor corresponding to $d_{P50}$
$d_{EC}$	Effective cutoff diameter [ $\mu\text{m}$ ] (Nominal cutoff diameter when the flow rate is at 1 ACFM [28.32 L/min])
$d_c$	Diameter of the round jet [cm]
$d_P$	Particle diameter [cm]
$D_P$	Particle diameter [ $\mu\text{m}$ ]
$d_{P50}$	Impactor stage cutoff size in particle diameter [cm]
$m$	Mass of particle [g]
$M.W.$	Molecular weight of particle [g]
$P$	Absolute pressure [ $Pa$ ]
$S$	Stopping distance [cm]

$\psi$	Dimensionless inertial parameter
$\psi_{50}$	Dimensionless parameter corresponding to the 50th percentile of the stage collection efficiency (0.1444 by Ranz and Wong)
$V_o$	Aerosol (Stage) velocity [cm/s]
$\mu$	Dynamic viscosity (poise) [g/cm/s]
$\rho_o$	Unit density (1 g/cm <sup>3</sup> )
$\rho_P$	Particle density [g/cm <sup>3</sup> ]
$\lambda$	Mean free path [ $\mu$ m]
$\tau$	Relaxation time [s]

### **E-1. Overview of Cutoff Size Calculation**

In this study, the Andersen sampler collected particles with two flow rates: 0.8 ACFM (22.65 L/min) for a chamber study and 1.0 ACFM (28.32 L/min) for a field study. In the chamber study, non-viable ambient Andersen samplers were adjusted to 0.8 ACFM (22.65 L/min) instead of 1 ACFM (28.32 L/min) because of a miscalculation of pressure drop. Thus, the goal of this appendix is to illustrate the cutoff size on each stage of an Andersen sampler according to the flow rate.

### **E-2. Cutoff Size Calculation**

The cutoff size can be characterized by a dimensionless parameter ( $\psi$ ) in Equation E.1. Fundamental work in inertial impaction theory was conducted in the early 1950's by Ranz and Wong <sup>(1)</sup>, Marple and Liu. <sup>(2)</sup>

The Andersen operator manual provides the cutoff size based on Equation E.1. Original measurements were based on glycerol, with density = 1.26 g/cm<sup>3</sup>, as an aerosol media. Those spherical droplets were used to determine the inertial parameter for a round jet impactor. Ranz and Wong measured  $\psi_{50} = 0.1444$  used in the calculations below.

The impactor stage performance is governed by the dimensionless parameter,  $\Psi$ .  $\Psi$  is defined as the ratio of the stopping distance of a particle to a characteristic length of the round jet. From this equation, the cutoff size of the particles collected on each stage increases as the volume flow rate decreases and as the particle density decreases.

$$\psi = \frac{S}{d_c} = \frac{\tau V_o}{d_c} = \frac{C_p \rho_p V_o (d_p)^2}{18 \mu d_c} \quad (\text{E.1})$$

where  $\psi$  = Dimensionless inertial parameter;  $S$  = Stopping distance [cm];

$\rho_p$  = Particle density [g/cm<sup>3</sup>];  $V_o$  = Aerosol (Stage) velocity [cm/s];  $d_p$  = Particle diameter [cm];  $\mu$  = Dynamic viscosity (poise) [g/cm/s],  $1.8 \times 10^{-4}$  g/cm/s at 20 °C and 1 atm;  $d_c$  = Diameter of the round jet [cm];

$$\tau = \text{relaxation time[s]} = m \times B = \rho_p \cdot \frac{\pi (d_p)^3}{6} \cdot \left( \frac{C_p}{3\pi\mu d_p} \right) = \frac{C_p \rho_p (d_p)^2}{18\mu}; \quad (\text{E.2})$$

where  $m$  = Mass of particle [g];  $B$  = Mobility of particle [cm/s/dyn];

$C_p$  = Cunningham correction factor for the smallest particles  $d_p$ ,

$$C_p = \left( 1 + \frac{0.16 \times 10^{-4}}{d_p} \right) \quad (\text{E.3})$$

Ranz and Wong used a Cunningham correction factor (Equation E.3) which is the empirical correction factor at normal temperature and pressure and it only depends on spherical particle size. Actually, the pressure and temperature influences the mean free path, which affects Cunningham correction. Equation E.4 was reported by Allen and Raabe<sup>(3)</sup> using parameters, mean free path and particle diameter.

Equations E.3 and E.4 show almost same values between  $C_p$  (Ranz & Wong) and  $C_p$  (Allen & Raabe) for particles bigger than or equal to 0.1  $\mu\text{m}$ . This is illustrated in Table E-1. The values of  $C_p$  (Ranz & Wong) for 0.1  $\mu\text{m}$  and 1  $\mu\text{m}$  particles at STP (20 °C and 1 atm) are 2.6 and 1.16. This means that the particles settle 260 % and 16 % faster than predicted by Stokes' Law without this size dependent correction factor.

$$C_p = 1 + \frac{2\lambda}{D_p} \left( 1.257 + 0.4 \exp\left(-\frac{1.1D_p}{2\lambda}\right) \right) \quad (\text{E.4})$$

$$\lambda = \frac{2\mu}{P \sqrt{\left(\frac{8M.W.}{\pi RT}\right)}} \quad (\text{E.5})$$

where  $\lambda$  = Mean free path (0.066  $\mu\text{m}$  at STP, 20 °C and 1 atm) [ $\mu\text{m}$ ];

$D_p$  = Particle diameter [ $\mu\text{m}$ ];  $M.W.$  = Molecular weight of particle [g];

$P$  = Absolute pressure in Pa.

The Cunningham correction factor is necessary for small particles because the particles are so small that they slip between the molecules.<sup>(4)</sup> As shown in Table E-1, the correction factor is small compared with typical measurement uncertainty for particles larger than 2  $\mu\text{m}$ .



**TABLE E-1. Cunningham Correction Factor Comparison in Air at 298 K and 1 atm**

$d_p$ or $D_p$ [ $\mu\text{m}$ ]	$C_p$ (Ranz & Wong)	$C_p$ (Allen and Raabe)
0.001	161.00	218.85
0.002	81.00	109.50
0.005	33.00	43.90
0.1	2.60	2.76
0.2	1.80	1.84
0.5	1.32	1.33
1	1.16	1.17
2	1.08	1.08
5	1.03	1.03
10	1.02	1.02
20	1.01	1.01
50	1.00	1.00
100	1.00	1.00

Ranz and Wong determined the inertial impaction parameter ( $\psi = 0.1444$ ) using glycerol as an aerosol media with a particle density of  $1.2 \text{ g/cm}^3$ . They defined the ( $\psi = 0.1444$ ) by averaging the difference between the maximum Stokes number and the minimum Stokes number indicated by the experimental curves.

In this appendix,  $\Psi_{50}$ ,  $d_{P50}$ , and  $C_{50}$  are used as appropriate parameters to calculate the cutoff size for each stage from Equation E.1.

$$\psi_{50} = \frac{C_{P50} \rho_p V_o (d_{P50})^2}{18 \mu d_c} \quad (\text{E.6})$$

where  $\psi_{50}$  = Dimensionless parameter corresponding to the 50<sup>th</sup> percentile of the stage collection efficiency ( $\psi_{50} = 0.1444$  by Ranz and Wong);

$d_{P50}$  = Impactor stage cutoff size in particle diameter [cm];

$\mu$  = Dynamic viscosity (poise) [g/cm/s],  $1.8 \times 10^{-4}$  g/cm/s at 20 °C and 1 atm;

$C_{P50}$  = Cunningham correction factor corresponding to  $d_{P50}$

Substituting E.6 into equation E.2, the  $d_{P50}$  is shown to be a function of five observable parameters:  $\rho_p$ ,  $V_o$ ,  $\mu$ ,  $d_c$ , and  $\psi_{50}$ .

$$d_{P50} = \frac{-0.16 \times 10^{-4} \rho_p V_o + \sqrt{(0.16 \times 10^{-4} \rho_p V_o)^2 + 72 \rho_p V_o \mu d_c \psi_{50}}}{2 \rho_p V_o} \quad (\text{E.7})$$

An  $AED_{50}$  with non standard density becomes

$$AED_{50} = d_{P50} [\rho_p]^{1/2} \quad (\text{E.8})$$

where  $\rho_p$  = Particle density [ $\text{g}/\text{cm}^3$ ].

Table E-2 shows higher  $AED_{50}$  at lower volume flow rate. The ratio represents the cut-point adjustment factor for each stage of an Andersen sampler at 0.8 ACFM (22.65 L/min) with same STP (20 °C, 1 atm). The ratio was calculated using an equation in the notes of Table E-2 and almost same ratios are shown at different densities 1  $\text{g}/\text{cm}^3$  and 2.7  $\text{g}/\text{cm}^3$ .

when  $d_{EC}$ , effective cutoff diameter [ $\mu\text{m}$ ] (Nominal cutoff diameter when the flow rate is at 1 ACFM [28.32 L/min]), in Table E-3 is compared with  $AED_{50}$  at 1 ACFM in Table E-2, the Andersen Sampler does not operate completely like the Ranz Wong model. Most of the orifices in the Andersen sampler are in a field of horizontal outflow. Therefore, the Ranz Wong equation does not predict the observed cut points. The cut-point adjustment factors with the density of fly ash (2.7  $\text{g}/\text{cm}^3$ ) were multiplied

to  $d_{EC}$  for obtaining the  $AED_{50}$ s of the Andersen sampler at 0.8 ACFM as shown Table E-3. The cutoff diameters with a unit density at 0.8 ACFM (22.65 L/min) are AEDs 10.1  $\mu\text{m}$ , 6.5  $\mu\text{m}$ , 5.3  $\mu\text{m}$ , 3.7  $\mu\text{m}$ , 2.4  $\mu\text{m}$ , 1.2  $\mu\text{m}$ , 0.7  $\mu\text{m}$ , and 0.5  $\mu\text{m}$  from 0 stage to 7 stage of the Andersen sampler.

In a field study, the Andersen cascade impactor separates particles by AED. In a dust cloud, the PM has differing densities and the physical diameters are different among particles as shown in Figures 3-7 and 3-8 in Chapter III.

**TABLE E-2. Stage Cutoff Size as a Function of Density and Flow Rate**

Stage	$AED_{50} [\mu\text{m}]^4$				Ratio <sup>B</sup> at 1 g/cm <sup>3</sup>	Ratio at 2.7 g/cm <sup>3</sup>
	At 1 ACFM, 1 g/cm <sup>3</sup>	At 1 ACFM, 2.7 g/cm <sup>3</sup>	At 0.8 ACFM, 1 g/cm <sup>3</sup>	At 0.8 ACFM, 2.7 g/cm <sup>3</sup>		
0	11.08	11.03	12.40	12.35	1.12	1.12
1	7.08	7.03	7.93	7.88	1.12	1.12
2	4.80	4.75	5.38	5.33	1.12	1.12
3	3.27	3.22	3.66	3.61	1.12	1.12
4	2.10	2.05	2.35	2.30	1.12	1.13
5	1.04	1.00	1.18	1.13	1.13	1.13
6	0.64	0.59	0.72	0.68	1.13	1.14
7	0.44	0.40	0.50	0.46	1.14	1.15

Notes:

<sup>A</sup>  $AED_{50}$  was calculated using Equations E.7 and E.8.  $AED_{50} = d_{p50} [\rho_p]^{1/2}$ ;

$$d_{p50} = \frac{-0.16 \times 10^{-4} \rho_p V_o + \sqrt{(0.16 \times 10^{-4} \rho_p V_o)^2 + 72 \rho_p V_o \mu d_c \psi_{50}}}{2 \rho_p V_o}$$

where  $d_{p50}$  = Particle cutoff diameter [cm];  $\rho_p$  = Particle density [g/cm<sup>3</sup>];

$$V_o = Q/A = \text{Aerosol (Stage) velocity [cm/s]} = Q / \left( \frac{\pi d_c^2}{4} \times \text{Number of orifice} \right);$$

$\mu$  = Dynamic viscosity (poise) [g/cm/s],  $1.8 \times 10^{-4}$  g/cm/s at 20 °C and 1 atm;  $\psi_{50} = 0.1444$ ;

$d_c$  = Diameter of the round jet [cm];  $\rho_p$  = Particle density [g/cm<sup>3</sup>].

$$\text{Ratio}^B = \text{Cut-point Adjustment Factor} = \frac{AED_{50} \text{ at } 0.8 \text{ ACFM}}{AED_{50} \text{ at } 1 \text{ ACFM}}$$

**TABLE E-3. Dimension of the Andersen Sampler Orifices**

Stage	Orifice diameter [Inch]	Number of orifices	At 1 ACFM, $d_{EC}^A$ [ $\mu\text{m}$ ]	At 0.8 ACFM, $AED_{50}^B$ [ $\mu\text{m}$ ]
0	0.0625	400	9	10.1
1	0.0465	400	5.8	6.5
2	0.0360	400	4.7	5.3
3	0.0280	400	3.3	3.7
4	0.0210	400	2.1	2.4
5	0.0135	400	1.1	1.2
6	0.0100	400	0.7	0.7
7	0.0100	210	0.4	0.5

Note:

<sup>A</sup>Effective cutoff diameter [ $\mu\text{m}$ ] (Nominal cutoff diameter when the flow rate is at 1 ACFM [28.32 L/min])

<sup>B</sup> $AED_{50}$  at 0.8 ACFM (22.65 L/min) = An aerodynamic equivalent diameter which has 50 % collection efficiency.

## APPENDIX E REFERENCES

1. **Ranz, W.E., and J.B. Wong;** Jet impactors for determining the particle size distribution of aerosols. *Arch. Ind. Hyg. Occup. Med.* 5:464-477 (1952).
2. **Marple, V.A., and B.Y. Liu;** Characteristics of laminar jet impactors. *Environ. Sci. Technol.* 648-654 (1974).
3. **Allen, M.D., and O.G., Raabe;** Reevaluation of Millikan's oil drop data for the motion of small particle in air. *J. Aerosol Sci.*, 13, 537-547 (1982).
4. **Hinds, W.C.:** *Aerosol Technology Properties, Behavior, and Measurement of Airborne Particles.* New York: John Wiley & Sons, Inc, 1999.

## APPENDIX F

### PARTICLE SIZE DISTRIBUTION MODELS

#### F-1. Overview of Particle Size Distribution

The probability density function (PDF) is an important way of characterizing distributed quantities such as a particle size. Here, the PDF for particle size is called the particle size distribution (PSD). It can be extended by analogy to any other distributed quantity such as shape, density, mass, or velocity.

The goals of this appendix are:

- 1) To understand PSD characteristics when represented as a function of a particle's aerodynamic equivalent diameter (AED), projected area (PA), surface area (SA), volume, equivalent spherical diameter (ESD), and mass.
- 2) To predict mass fractions for the ACGIH/CEN/ISO\* respirable, thoracic, and inhalable convention from the PSD for ESD.

The two parameters  $GM_{AED}$  and  $GSD_{AED}$  were estimated from the particle volume histogram of the bulk flyash used as the challenge material for comparing the behavior of various size selective aerosol samplers. The histogram was produced using the Coulter Counter Multisizer (CCM) which measures the change in electrical conductivity of a carrier solution due to volume displacement as a particle passes through an orifice with 100  $\mu\text{m}$  diameter.

---

\* American Conference of Governmental Industrial Hygienists (ACGIH);  
Comité Européen de Normalisation (CEN);  
International Organization for Standardization (ISO).

Through the PSD characteristics and Mathematica procedures below, the particle fractions for the respirable, thoracic, and inhalable convention were found as 7.2 %, 41.2 %, and 99.8 % from PDFs of a particle's AED, PA, SA, volume, ESD, and mass, based on the parameters for the AED PDF: median =  $GM_{AED} = 11.8 \mu\text{m}$  and slope =  $GSD_{AED} = 2.1$ .

## F-2. PSD characteristics

Let two random variables be related by  $Y = \ln X$  or equivalently, by  $X = e^Y$  and assume that  $Y$  is Gaussian with a mean of  $\bar{Y}$  and a standard deviation of  $\sigma_y$ . It is clear that whenever the random variable  $X$  lies between  $x$  and  $x + dx$ , the random variable  $Y$  will lie between  $y$  and  $y + dy$ . Since the probabilities of these events are  $f_X(x) dx$  and  $f_Y(y) dy$ , one can write  $f_X(x) dx = f_Y(y) dy$  from which the desired probability density function of  $X$ , denoted by  $f_X(x)$ , becomes

$$f_X(x) = f_Y(y) \left| \frac{dy}{dx} \right| \quad (\text{F.1})$$

To complete the transformation indicated in Equation F.1, it is sufficient to express both  $y$  and  $dy/dx$  in terms of  $x$ . Because  $Y = \ln X$ , it follows that:

$$\frac{dy}{dx} = \frac{1}{x}, \text{ and } \frac{dx}{dy} = x$$

Substitute these expressions into Equation F.1. For  $f_X(x)$  to be a PDF, it must be true that  $0 < f_X(x) \leq 1$  for all values of  $x$ . To achieve this, use the absolute value of the term  $(1/x)$ .

$$f_X(x) = \left| \frac{1}{x} \right| f_Y(y) = \left| \frac{1}{x} \right| f_Y(\ln x) \quad (\text{F.2})$$

Recall that  $Y$  is a random variable characterized by a Gaussian distribution.

$$f_Y(y) = \frac{1}{\sqrt{2\pi}\sigma_Y} \exp\left[-\frac{(y-\bar{Y})^2}{2\sigma_Y^2}\right] \quad (\text{F.3})$$

In equation F.3, substitute  $y = \ln(x)$ ,  $\sigma_Y = \ln(GSD_X)$  and  $Y = \ln(GM_X)$  to find the useful representation of the PDF for the lognormally distributed random variable,  $X$ , shown in Equation F.4.

$$f_X(x) = \frac{1}{x \cdot \ln(GSD_X) \cdot \sqrt{2\pi}} \exp\left[-\frac{(\ln(x) - \ln(GM_X))^2}{2 \cdot (\ln(GSD_X))^2}\right] \text{ if } x > 0 \quad (\text{F.4})$$

$$= 0 \quad x \leq 0$$

$$\frac{1}{AED \cdot \ln(GSD_{AED}) \cdot \sqrt{2\pi}} \cdot \exp\left[-\frac{1}{2} \cdot \frac{(\ln(AED) - \ln(GM_{AED}))^2}{(\ln(GSD_{AED}))^2}\right]$$

For assessing inhalation risk,  $X$  is the  $AED$  and  $Y$  is Gaussian with a mean of  $\ln(GM_{AED})$  and a standard deviation of  $\ln(GSD_{AED})$ . After making these substitutions, Equation F.5 is the PDF for an AED as below.

$$f_{AED}(AED) = \frac{1}{AED \cdot \ln(GSD_{AED}) \cdot \sqrt{2\pi}} \exp\left[-\frac{(\ln(AED) - \ln(GM_{AED}))^2}{2 \cdot (\ln(GSD_{AED}))^2}\right] \quad (\text{F.5})$$

where  $GM_{AED}$  = Geometric Mean of the AED;  $GSD_{AED}$  = Geometric Standard Deviation of the AED.

Using the same steps, one can derive the PDF for projected area (PA) of a spherical particle as in Equations F.6 leading to Equation F.7.

$$PA = \frac{\pi AED^2}{4}, \quad AED = \sqrt{\frac{4PA}{\pi}}$$

$$\begin{aligned}
\frac{dPA}{dAED} &= \frac{\pi AED}{2}, \quad \frac{dAED}{dPA} = \frac{2}{\pi AED} \\
f_{PA}(PA) &= f_{AED}(AED) \frac{dAED}{dPA} \\
&= f_{AED}\left(\sqrt{\frac{4PA}{\pi}}\right) \frac{2}{\pi AED} \\
&= f_{AED}\left(\sqrt{\frac{4PA}{\pi}}\right) \frac{2}{\pi \sqrt{\frac{4PA}{\pi}}} \\
&= f_{AED}\left(\sqrt{\frac{4PA}{\pi}}\right) \frac{1}{\sqrt{\pi PA}} \\
&= f_{AED}\left(\sqrt{\frac{4PA}{\pi}}\right) \frac{1}{\sqrt{\pi PA}}
\end{aligned} \tag{F.6}$$

Applying Equation F.6 to Equation F.5 yields

$$f_{PA}(PA) = \frac{1}{2 \cdot PA \cdot \ln(GSD_{PA}) \cdot \sqrt{2\pi}} \exp \left[ -\frac{\left( \ln \left( 2\sqrt{\frac{PA}{\pi}} \right) - \ln(GM_{PA}) \right)^2}{2 \cdot (\ln(GSD_{PA}))^2} \right] \tag{F.7}$$

where  $GM_{PA}$  = Geometric Mean of the PA;  $GSD_{PA}$  = Geometric Standard Deviation of the PA.

The PDF for spherical particle by surface area is

$$\begin{aligned}
SA &= \pi AED^2, \quad AED = \sqrt{\frac{SA}{\pi}} \\
\frac{dSA}{dAED} &= 2\pi AED, \quad \frac{dAED}{dPA} = \frac{1}{2\pi AED}
\end{aligned}$$



$$f_{SA}(SA) = \frac{1}{2 \cdot SA \cdot \ln(GSD_{SA}) \cdot \sqrt{2\pi}} \exp \left[ -\frac{\left( \ln \left( \sqrt{\frac{SA}{\pi}} \right) - \ln(GM_{SA}) \right)^2}{2 \cdot (\ln(GSD_{SA}))^2} \right] \quad (F.8)$$

where  $GM_{SA}$  = Geometric Mean of the SA;  $GSD_{SA}$  = Geometric Standard Deviation of the SA.

The PDF for a spherical particle by volume is

$$VOL = \frac{\pi}{6} AED^3, \quad AED = \left( \frac{6}{\pi} \right)^{1/3} (VOL)^{1/3}$$

$$\frac{dVOL}{dAED} = \frac{\pi AED^2}{2}, \quad \frac{dAED}{dVOL} = \frac{2}{\pi AED^2}$$

$$f_{VOL}(VOL) = \frac{1}{3 \cdot VOL \cdot \ln(GSD_{VOL}) \cdot \sqrt{2\pi}} \exp \left[ -\frac{\left( \ln \left( \left( \frac{6}{\pi} \right)^{1/3} (VOL)^{1/3} \right) - \ln(GM_{VOL}) \right)^2}{2 \cdot (\ln(GSD_{VOL}))^2} \right] \quad (F.9)$$

where  $GM_{VOL}$  = Geometric Mean of the VOL;  $GSD_{VOL}$  = Geometric Standard Deviation of the VOL.

The PDF for an ESD is

$$AED = ESD \sqrt{\frac{\rho_P}{\rho_P \cdot \chi}}, \quad \frac{dAED}{dESD} = \sqrt{\frac{\rho_P}{\rho_P \cdot \chi}}$$

Apply to Equation F.5:

$$f_{ESD}(ESD) = \frac{1}{ESD \cdot \ln(GSD_{ESD}) \cdot \sqrt{2\pi}} \exp \left[ -\frac{\left( \ln \left( ESD \cdot \sqrt{\frac{\rho_p}{\rho_p \cdot \chi}} \right) - \ln(GM_{ESD}) \right)^2}{2 \cdot (\ln(GSD_{ESD}))^2} \right] \quad (F.10)$$

where  $GM_{ESD}$  = Geometric Mean of the ESD;  $GSD_{ESD}$  = Geometric Standard Deviation of the ESD;  $\rho_p$  = Particle density;  $\rho_0$  = Unit density (1 g/cm<sup>3</sup>);  $\chi$  = Dynamic shape factor.

### F-3. Mathematica<sup>(1)</sup> Code for PDF of Random Variables

This section documents the Mathematica Codes developed and used for PSD analysis. Times New Roman font is used for the code and Italic Arial font is used for non-executing comments.

```
(***** Content-type: application/mathematica *****)
      CreatedBy='Mathematica 5.0'
```

*Mathematica-Compatible Notebook*

*This notebook can be used with any Mathematica-compatible application, such as Mathematica, MathReader or PubIcon. The data for the notebook starts with the line containing stars above.*

*To get the notebook into a Mathematica-compatible application, do one of the following:*

- \* Save the data starting with the line of stars above into a file with a name ending in .nb, then open the file inside the application;*
- \* Copy the data starting with the line of stars above to the clipboard, then use the Paste menu command inside the application.*

*Data for notebooks contains only printable 7-bit ASCII and can be*

sent directly in email or through ftp in text mode. Newlines can be CR, LF or CRLF (Unix, Macintosh or MS-DOS style).

NOTE: If you modify the data for this notebook not in a Mathematica-compatible application, you must delete the line below containing the word CacheID, otherwise Mathematica-compatible applications may try to use invalid cache data.

For more information on notebooks and Mathematica-compatible applications, contact Wolfram Research:

web: <http://www.wolfram.com>

email: [info@wolfram.com](mailto:info@wolfram.com)

phone: +1-217-398-0700 (U.S.)

Notebook reader applications are available free of charge from Wolfram Research.

\*\*\*\*\*)

(\*CacheID: 232\*)

(\*NotebookFileLineBreakTest  
NotebookFileLineBreakTest\*)  
(\*NotebookOptionsPosition[ 8393, 223]\*)  
(\*NotebookOutlinePosition[ 9147, 251]\*)  
(\* CellTagsIndexPosition[ 9076, 245]\*)  
(\*WindowFrame->Normal\*)

Notebook[{  
Cell["<<Statistics`ContinuousDistributions`", "Input",  
CellTags->"S6.0.1"],

Cell[BoxData[  
 \(\pdfaed[aed\_] = \

$$\text{PDF}[\text{LogNormalDistribution}[\text{Log}[gm], \text{Log}[gs]], aed]\), "Input"],$$

Cell[BoxData[  
 \(\solpa = \(\text{Solve}[pa == \[\Pi] \((\ aed/2)\)^2,

$$aed]\)[\{2}\]), "Input"],$$

Cell[BoxData[  
 \(\{dpadaed = \[\text{PartialD}]\\_aed\((\ \[\Pi] \((\ aed/2)\)^2)\),

daeddpa = 1/dpadaed}]], "Input"],

Cell[BoxData[  
 \(\pdfpa[pa\_] \ = \ \((pdfaed[aed] daeddpa)) / . solpa)\), "Input"],

Cell[BoxData[  
 \(\pagraph =  
 Plot[\((pdfpa[pa] / . {gm \[Rule] \ 4, gs \[Rule] \ 2.2})\), {pa, 0,  
 20.0}, Frame \[Rule] True,  
 FrameLabel \[Rule] \ {"\<Projected Area>", "\<pdfpa>"},  
 TextStyle \[Rule] \ (FontFamily \[Rule] "\<Arial>");\)\), "Input"],

Cell[BoxData[  
 \(\aedgraph =  
 Plot[pdfaed[aed] / . {gm \[Rule] \ 4, gs \[Rule] \ 2.2}, {aed, 0,  
 20. }, Frame \[Rule] True,  
 FrameLabel \[Rule] \ {"\<AED>", "\<pdfaed>"},  
 TextStyle \[Rule] \ (FontFamily \[Rule] "\<Arial>");\)\), "Input"],

Cell[BoxData[  
 \(\[Integral]\_2\%3\((pdfaed[aed] / . {gm \[Rule] \ 4,  
 gs \[Rule] \ 2.2})\)) \[DifferentialD]aed)\), "Input"],

Cell[BoxData[  
 \(\[Integral]\_ \ (\[Pi] \ ((2))\^2/4)\% \ (\[Pi] \ ((3))\^2/4)\((pdfpa[  
 pa] / . {gm \[Rule] \ 4,  
 gs \[Rule] \ 2.2})\)) \[DifferentialD]pa)\), "Input"],

Cell[BoxData[  
 \(\{\[Pi] \ ((2. /2))\^2, \ \[Pi] \ ((3. /2))\^2\}\), "Input"],

Cell[BoxData[  
 \(\solsa = \(\Solve[sa == \[Pi] \ ((\ aed))\^2, aed]\)\[([2])\]), "Input"],

Cell[BoxData[  
 \(\{dsadaed = \[PartialD]\_aed\((\ \[Pi] \ ((\ aed))\^2)\),  
 daeddsa = 1/dsadaed}\)\), "Input"],

Cell[BoxData[  
 \(\pdfsa[sa\_] \ = \ \((pdfaed[aed] daeddsa)) / . solsa)\), "Input"],

Cell[BoxData[  
 \(\sagraph =  
 Plot[\((pdfsa[sa] / . {gm \[Rule] \ 4, gs \[Rule] \ 2.2})\), {sa, 0,

```
20.0}, Frame [Rule] True,
FrameLabel [Rule] \ {"<Surface Area>", "<pdfsa>"},
TextStyle [Rule] \ (FontFamily [Rule] "<Arial>");\)), "Input"],
```

```
Cell[BoxData[
\ (solvol = \ (Solve[vol \ [Equal] \ ((\ [Pi] \ ((\ aed)) \ ^3/6)),
aed)] \ \ ([2]) \)], "Input"],
```

```
Cell[BoxData[
\ ({dvoldaed = \ [PartialD] \ _aed \ ((\ [Pi] \ ((\ aed)) \ ^3/6)),
daeddvolaed = 1/dvoldaed} \)], "Input"],
```

```
Cell[BoxData[
\ (pdfvol[vol_] \ = \ ((pdfaed[aed] daeddvolaed)) /. solvol)], "Input"],
```

```
Cell[BoxData[
\ ((volgraph =
Plot[(pdfvol[vol] /. {gm [Rule] \ 4, gs [Rule] \ 2.2})), {vol,
0, 20.0}, Frame [Rule] True,
FrameLabel [Rule] \ {"<Volume>", "<pdfvol>"},
TextStyle [Rule] \ (FontFamily [Rule] "<Arial>");\)), "Input"],
```

```
Cell[BoxData[
\ ((Show[
GraphicsArray[{aedgraph, pagraph, sagraph, volgraph}];\)), "Input"],
```

```
Cell[BoxData[
\ ([Integral] \ _2 \ %3 \ ((pdfaed[aed] /. {gm [Rule] \ 4,
gs [Rule] \ 2.2}))) \ [DifferentialD]aed)], "Input"],
```

```
Cell[BoxData[
\ ([Integral] \ \ ([Pi] \ ((2)) \ ^2/4) \ % \ ([Pi] \ ((3)) \ ^2/4) \ ((pdfpa[
pa] /. {gm [Rule] \ 4,
gs [Rule] \ 2.2}))) \ [DifferentialD]pa)], "Input"],
```

```
Cell[BoxData[
\ ([Integral] \ \ ([Pi] \ ((2)) \ ^2) \ % \ ([Pi] \ ((3)) \ ^2) \ ((pdfsa[
sa] /. {gm [Rule] \ 4,
gs [Rule] \ 2.2}))) \ [DifferentialD]sa)], "Input"],
```

```
Cell[BoxData[
\ ([Integral] \ \ ([Pi] \ ((2)) \ ^3/6) \ % \ ([Pi] \ ((3)) \ ^3/6) \ ((pdfvol[
vol] /. {gm [Rule] \ 4,
gs [Rule] \ 2.2}))) \ [DifferentialD]vol)], "Input"],
```

```

Cell[BoxData[
  \{solesd =
    Solve[aed \[Equal] \((esd \@ \(\[Rho]_p \^ \(\[Rho]_0) \
\[Chi])\))\), aed]\], "Input"],

Cell[BoxData[
  \({daeddesd = \[PartialD]_esd \((esd \@ \(\[Rho]_p \^ \(\[Rho]_0) \
\[Chi])\))\)}\}], "Input"],

Cell[BoxData[
  \{pdfesd[esd_] = \((pdfaed[aed] daeddesd) / . solesd)\}, "Input"],

Cell[BoxData[
  \(\[Rho]_p = 1; \[Rho]_0 = 1; \[Chi] = 1;\)], "Input"],

Cell[BoxData[
  \(\{esdgraph =
    Plot[\((pdfesd[esd] / . {gm \[Rule] \ 11.8,
      gs \[Rule] \ 2.1}\)), {esd, 0, 25.0}, Frame \[Rule] True,
    FrameLabel \[Rule] \ {"<ESD>", "<pdfesd>"},
    TextStyle \[Rule] \ (FontFamily \[Rule] "<Arial>")\;\)], "Input"],

Cell[BoxData[
  \({taed = {\[Integral]_0%4 \((pdfaed[aed] / . {gm \[Rule] \ 11.8,
    gs \[Rule] \
    2.1}\)) \[DifferentialD]aed, \
\[Integral]_0%10 \((pdfaed[aed] / . {gm \[Rule] \ 11.8,
    gs \[Rule] \
    2.1}\)) \[DifferentialD]aed, \
\[Integral]_0%100 \((pdfaed[aed] / . {gm \[Rule] \ 11.8,
    gs \[Rule] \ 2.1}\)) \[DifferentialD]aed}}\)], "Input",
  FontFamily->"Courier New"],

Cell[BoxData[
  \({tpa = {\[Integral]_ \(\[Pi] \ \((0)\)^2/4)\% \(\[Pi] \ \
\((4)\)^2/4)\} \((pdfpa[pa] / . {gm \[Rule] \ 11.8,
    gs \[Rule] \
    2.1}\)) \[DifferentialD]pa, \[Integral]_ \(\[Pi] \ \((0)\
\)^2/4)\% \(\[Pi] \ \((10)\)^2/4)\} \((pdfpa[pa] / . {gm \[Rule] \ 11.8,
    gs \[Rule] \
    2.1}\)) \[DifferentialD]pa, \[Integral]_ \(\[Pi] \ \((0)\
\)^2/4)\% \(\[Pi] \ \((100)\)^2/4)\} \((pdfpa[pa] / . {gm \[Rule] \ 11.8,
    gs \[Rule] \ 2.1}\)) \[DifferentialD]pa}}\)], "Input",

```

```

FontFamily->"Courier New"],

Cell[BoxData[
  \({tsa = {\[Integral]_ \(\[Pi] \((0)\)^2)\% \(\[Pi] \
\((4)\)^2)\((pdfsa[sa] /. {gm \[Rule] \ 11.8,
    gs \[Rule] \
    2.1}) \[DifferentialD]sa, \[Integral]_ \(\[Pi] \((0)\
\)\)^2)\% \(\[Pi] \((10)\)^2)\((pdfsa[sa] /. {gm \[Rule] \ 11.8,
    gs \[Rule] \
    2.1}) \[DifferentialD]sa, \[Integral]_ \(\[Pi] \((0)\
\)\)^2)\% \(\[Pi] \((100)\)^2)\((pdfsa[sa] /. {gm \[Rule] \ 11.8,
    gs \[Rule] \ 2.1}) \[DifferentialD]sa} \)}, "Input",
  FontFamily->"Courier New"],

Cell[BoxData[
  \({tvol = {\[Integral]_ \(\[Pi] \((0)\)^3/6)\% \(\[Pi] \
\((4)\)^3/6)\((pdfvol[vol] /. {gm \[Rule] \ 11.8,
    gs \[Rule] \
    2.1}) \[DifferentialD]vol, \[Integral]_ \(\[Pi] \
\((0)\)^3/6)\% \(\[Pi] \((10)\)^3/6)\((pdfvol[vol] /. {gm \[Rule] \ 11.8,
    gs \[Rule] \
    2.1}) \[DifferentialD]vol, \[Integral]_ \(\[Pi] \
\((0)\)^3/6)\% \(\[Pi] \((100)\)^3/6)\((pdfvol[
    vol] /. {gm \[Rule] \ 11.8,
    gs \[Rule] \ 2.1}) \[DifferentialD]vol} \)}, "Input",
  FontFamily->"Courier New"]
}],
FrontEndVersion->"5.0 for Microsoft Windows",
ScreenRectangle->{{0, 1024}, {0, 693}},
WindowSize->{1016, 666},
WindowMargins->{{0, Automatic}, {Automatic, 0}}
]

(*****
Cached data follows. If you edit this Notebook file directly, not
using Mathematica, you must remove the line containing CacheID at
the top of the file. The cache data will then be recreated when
you save this file from within Mathematica.
*****)

(*CellTagsOutline
CellTagsIndex->{
  "S6.0.1"->{
    Cell[1754, 51, 76, 1, 30, "Input",

```

```

    CellTags->"S6.0.1"}
  }
*)

```

```

(*CellTagsIndex
CellTagsIndex->{
  {"S6.0.1", 8984, 238}
}
*)

```

```

(*NotebookFileOutline
Notebook[{
Cell[1754, 51, 76, 1, 30, "Input",
  CellTags->"S6.0.1",
Cell[1833, 54, 108, 2, 30, "Input"],
Cell[1944, 58, 105, 2, 31, "Input"],
Cell[2052, 62, 119, 2, 31, "Input"],
Cell[2174, 66, 84, 1, 30, "Input"],
Cell[2261, 69, 298, 5, 50, "Input"],
Cell[2562, 76, 286, 5, 50, "Input"],
Cell[2851, 83, 140, 2, 42, "Input"],
Cell[2994, 87, 195, 3, 48, "Input"],
Cell[3192, 92, 80, 1, 31, "Input"],
Cell[3275, 95, 92, 1, 31, "Input"],
Cell[3370, 98, 117, 2, 31, "Input"],
Cell[3490, 102, 84, 1, 30, "Input"],
Cell[3577, 105, 296, 5, 50, "Input"],
Cell[3876, 112, 119, 2, 31, "Input"],
Cell[3998, 116, 122, 2, 31, "Input"],
Cell[4123, 120, 88, 1, 30, "Input"],
Cell[4214, 123, 295, 5, 50, "Input"],
Cell[4512, 130, 106, 2, 30, "Input"],
Cell[4621, 134, 140, 2, 42, "Input"],
Cell[4764, 138, 195, 3, 48, "Input"],
Cell[4962, 143, 191, 3, 47, "Input"],
Cell[5156, 148, 198, 3, 48, "Input"],
Cell[5357, 153, 128, 3, 52, "Input"],
Cell[5488, 158, 116, 2, 52, "Input"],
Cell[5607, 162, 88, 1, 30, "Input"],
Cell[5698, 165, 74, 1, 30, "Input"],
Cell[5775, 168, 299, 5, 50, "Input"],
Cell[6077, 175, 478, 9, 76, "Input"],
Cell[6558, 186, 602, 10, 90, "Input"],
Cell[7163, 198, 590, 10, 88, "Input"],

```



```
Cell[7756, 210, 633, 11, 90, "Input"]  
}  
]  
*)
```

```
(*****  
End of Mathematica Notebook file.  
*****)
```

## APPENDIX F REFERENCE

- 
1. **Wolfram Research, Inc.:** Mathematica 5.0 Champaign, IL.

## APPENDIX G

### SHAPE FACTOR REVIEW

#### G-1. Overview of Shape Factor

This appendix provides an overview of the dynamic shape factor ( $\chi$ ) for the petroleum pipe scale from pipe rattling operations. The standard equations for aerodynamic drag and settling velocity are based on spherical particles and laminar flow. Examples of spherical particles include: liquid droplets and solids condensed from vapors (metal fume in welding, fly ash from furnaces). Most particles from drilling, grinding, and crushing operations are non-spherical, including the dust from pipe rattling. The shape of a particle affects its drag force and settling velocity (See Equations G.1 and G.2). The dynamic shape factor,  $\chi$ , is a largely empirical correction factor which is applied to Stokes law to explain the effect of shape on particle motion. Stokes law has a wide application to the study of occupational aerosols because of low relative velocities between small particles and workplace air. Stokes law is applicable to the Stokes region where the particle Reynolds number is less than 1.0.

$$Re = \frac{\rho_{air} V d_p}{\mu} \quad (G.1)$$

where  $\rho_{air}$  = Density of air;  $V$  = Relative velocity between particle and gas;  $\mu$  = air viscosity and  $d_p$  = Spherical Particle diameter.

Stokes law is

$$F_D = 3\pi\mu V d_p \text{ for } Re < 1 \text{ and spherical particles} \quad (G.2)$$

where  $F_D =$  Drag force.

An equivalent spherical diameter (ESD) is the diameter of the sphere having the same volume as an irregular particle. Use of  $ESD$  as appropriate when Equation G.2 is used to represent irregular shaped particles because it is the diameter of the sphere having the same volume, and the same mass, as the irregular particle. The drag force depends on particle shape as well as particle volume. A shape factor is added to Equation G.2 to arrive at equation G.3, appropriate for non-spherical particles.

$$F_D = 3\pi\mu V \cdot ESD \cdot \chi \quad (G.3)$$

$$\chi = \frac{F_D}{3\pi\mu V \cdot ESD}$$

where  $ESD =$  Equivalent spherical diameter;  $\chi =$  Dynamic shape factor.

The dynamic shape factor is defined to be the ratio of the volume of a circumscribed sphere to the volume of an irregular crystal.<sup>(1)</sup>

$$\chi = \left( \frac{\text{Volume of a circumscribed sphere}}{\text{Volume of a crystal}} \right)^{1/3} \quad (G.4)$$

For purposes of illustrating the typical size of the dynamic shape factor, consider an orthorhombic crystal in which the three orthogonal dimensions may be unequal.

Visualize the orthorhombic crystal to be inscribed in a sphere that touches all of its vertices. The crystal's major diagonal is equal to the diameter of the sphere. Assume that the lengths of the sides are  $a \mu\text{m}$ ,  $b \mu\text{m}$ , and  $c \mu\text{m}$ . The diameter of the circumscribed sphere is found by applying the theorem of Pythagoras:  $d^2 = a^2 + b^2 + c^2$ . The volume of the crystal is  $a b c$ . The volume of the circumscribed sphere is:

$$\frac{\pi d^3}{6} = \frac{\pi(a^2 + b^2 + c^2)^{3/2}}{6} \quad (\text{G.5})$$

The dynamic shape factor is the cube root of the ratio of these two volumes and can be expressed entirely in terms of the three lengths of the crystal sides:

$$\chi = \left( \frac{\text{Volume of a circumscribed sphere}}{\text{Volume of a crystal}} \right)^{1/3} = \left( \frac{(a^2 + b^2 + c^2)^{3/2}}{a b c} \right)^{1/3} \times \left( \frac{\pi}{6} \right)^{1/3} \quad (\text{G.6})$$

This equation can be used to show a reasonable range for values of the shape factor when dust particles are approximately orthorhombic in nature.

**TABLE G-1. Dynamic shape factor for a cube and orthorhombic crystals**

a	b	c	Dynamic shape factor ( $\chi$ )
1	1	1	1.40
1	1	2	1.57
1	1	3	1.85
1	1	4	2.15
1	2	1	1.57
1	2	2	1.52
1	2	3	1.66
1	2	4	1.85
1	3	1	1.85
1	3	2	1.66
1	3	3	1.69
1	3	4	1.80
1	4	1	2.15
1	4	2	1.85
1	4	3	1.80
1	4	4	1.84

Because dust particles from pipe rattling are variable in density, size, shape, and aspect ratio, it is reasonable to believe that they have individual shape factors. Using an Environmental Scanning Electron Microscope (ESEM), it is estimated that most of the dust particles released during pipe rattling have a triclinic pinacoidal shape with a length to width ratio of approximately 1 to 2. From the argument above, it follows that the shape factors for nearly orthorhombic dust particles range from about 1.40 to about 2.15.

#### **APPENDIX G REFERENCE**

---

1. **Hinds, W.C.:** *Aerosol Technology Properties, Behavior, and Measurement of Airborne Particles*. New York: John Wiley & Sons, Inc, 1999.

## APPENDIX H

### GAUSSIAN DISPERSION MODEL

#### H-1. Overviews of Gaussian Dispersion Model

In this study, the Gaussian dispersion model was used to find an attainment area for the workers and for the public because it adequately represented the most distinguishable features of suspended airborne contaminant concentration of pipe rattling process. The Gaussian dispersion model has a double Gaussian distribution based on horizontal wind (in the downwind direction) with standard deviations of plume concentration distributions in the horizontal and vertical directions of  $\sigma_y$  and  $\sigma_z$ . Equation H.1 shows Gaussian distribution in the horizontal plane perpendicular to the x-axis with a horizontal standard deviation ( $\sigma_y$ ) of plume concentration distribution. Equation H.2 shows Gaussian distribution in the vertical plane to the x-axis with a vertical standard deviation ( $\sigma_z$ ) of plume concentration distribution. Equation H.3 shows the double Gaussian distribution by the combination of horizontal and vertical planes to the x-axis. The dispersion coefficients,  $\sigma_y$  and  $\sigma_z$  are functions of downwind distance ( $x$ ) at  $(x,0,H)$  as horizontal dispersion coefficient ( $\sigma_y = ay + by \cdot x$ ) and vertical dispersion coefficient ( $\sigma_z = ax + bz \cdot x$ ).

$$f(y) = \frac{1}{\sqrt{2\pi}\sigma_y} \cdot \exp\left(-\frac{1}{2}\left(\frac{y-\mu_y}{\sigma_y}\right)^2\right) \quad (\text{H.1})$$

$$f(z) = \frac{1}{\sqrt{2\pi}\sigma_z} \cdot \exp\left(-\frac{1}{2}\left(\frac{z-\mu_z}{\sigma_z}\right)^2\right) \quad (\text{H.2})$$

$$f(y) \cdot f(z) = \frac{1}{2\pi\sigma_y\sigma_z} \cdot \exp\left(-\frac{1}{2}\left(\frac{y}{\sigma_y}\right)^2\right) \cdot \left\{ \left[ \exp\left(-\frac{(z-H)^2}{2\sigma_z^2}\right) + \exp\left(-\frac{(z+H)^2}{2\sigma_z^2}\right) \right] \right\}$$

at  $(x, 0, H)$  (H.3)

Equation H.4 is given here in a form that predicts the steady state concentration at a point  $(x, y, z)$  located downwind from the source. Some general relationships are in this equation. That is, 1) the downwind concentration at any location is directly proportional to the emission rate ( $ER$ ), and 2) the downwind, ground-level concentration is generally inversely proportional to wind speed.

$$C(x, y, z, H) = \frac{ER}{2\pi\sigma_y\sigma_z u} \cdot \left[ \exp\left(-\frac{y^2}{2\sigma_y^2}\right) \cdot \left\{ \left[ \exp\left(-\frac{(z-H)^2}{2\sigma_z^2}\right) + \exp\left(-\frac{(z+H)^2}{2\sigma_z^2}\right) \right] \right\} \right] \quad (\text{H.4})$$

where  $C$  = Average Steady state concentration at a point  $(x, y, z)$  [ $\text{mg}/\text{m}^3$ ]

$ER$  = Average emission rate [ $\text{mg}/\text{s}$ ];  $u$  = Average wind speed on the ground [ $\text{m}/\text{s}$ ];

$\sigma_y, \sigma_z$  = Horizontal and Vertical dispersion coefficients [ $\text{m}$ ];

$y$  = Horizontal distance from the plume centerline [ $\text{m}$ ];

$z$  = Height of the receptor above the ground [ $\text{m}$ ];

$H$  = Effective height [ $\text{m}$ ] =  $h$  (pipe location height) +  $\Delta h$  (average plume height from the pipe location).

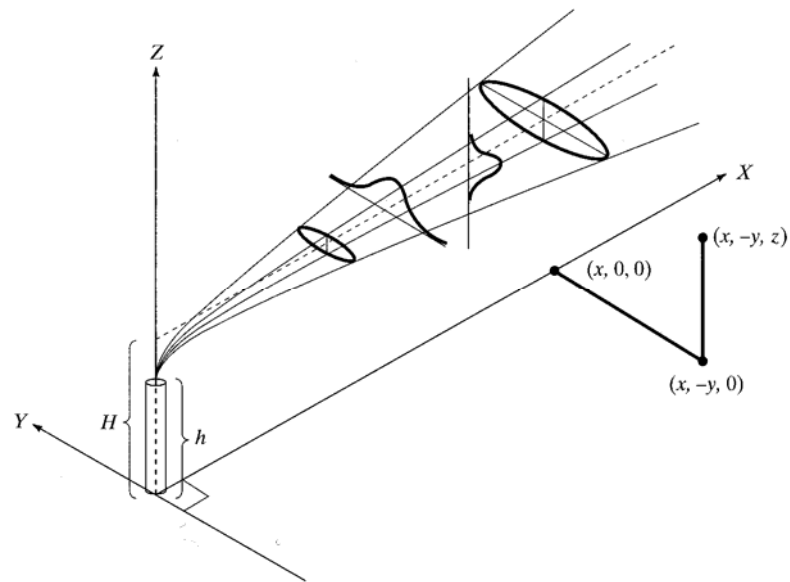


**FIGURE H-1. Coordinate system showing Gaussian distributions in the horizontal and vertical.** Source: Turner's Workbook of Atmospheric Dispersion Estimates (1970).

A quantitative method for estimating the dispersion coefficients was introduced by Pasquill and Gifford in 1961. These dispersion estimates were adopted by the U.S. Public Health Service (Turner 1970) and have been widely used. The values of adopted  $\sigma_y$  and  $\sigma_z$  are representative for a sampling time of about 10 minutes at downwind distances of 0.1 to several tens of kilometers. For estimation of longer time periods, Hino suggest power law for averaging times between 10-minute and 5-hour.

## H-2. Methods

In this study, vertical and horizontal coefficients,  $\sigma_y$  and  $\sigma_z$ , and an emission rate for a Gaussian plume model are estimated for the best fit from the measured



concentrations. The  $\sigma_y$  and  $\sigma_z$  introduced by Pasquill<sup>(1)</sup> and Gifford<sup>(2)</sup> are not applicable at short distance ( $< 100$  m).

Two video cameras were used to record the pipe rattling research on the ground and at the height of 10 m each experiment day. The pictures of a pipe rattling process were taken to provide the information about the plume dispersion at the each side (See Figure H-2).

The effective height, H, was estimated as 1 m because the pipe end height was estimated as 0.5 m and the plume rise also estimated as 0.5 m using the DVD video (see H-2 (c), below). A height of the receptor above the ground is modeled as 1.5 m to simulate human breathing zone. Average wind speed measured on the ground was applied to this model as  $(2.2 \pm 1.1)$  m/s for Mud Lake pipe rattling process and  $(3.2 \pm 0.5)$  m/s for Lake Sand pipe rattling process. These estimates were used as starting values for a Nonlinear mean squared regression of measured data against the plume model as a representation of the concentration expected within about 20 m of the machine centerline.

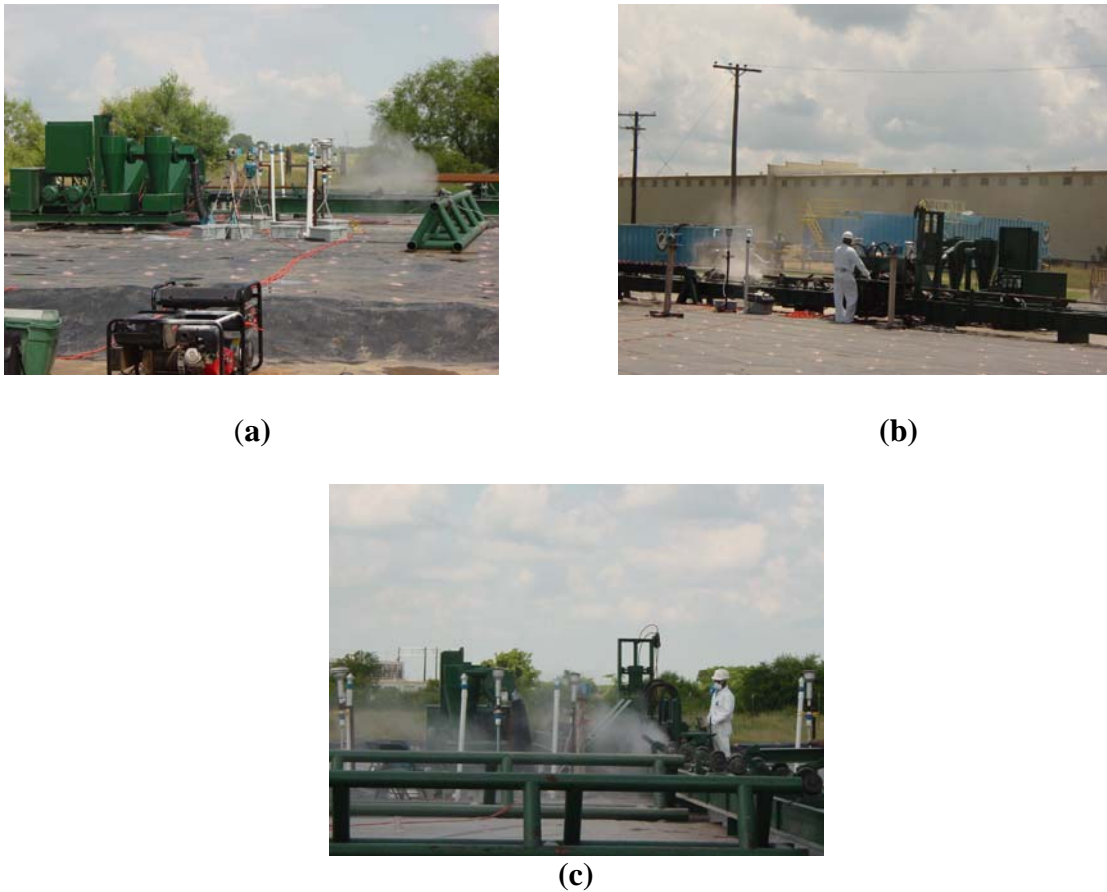


**FIGURE H-2. The images of particle dispersion. (a) Front, (b) Back, (c) Side.**

#### **APPENDIX H REFERENCES**

1. **Pasquill, F.:** The Estimation of the Dispersion of Windborne Material. *Meteorological Magazine* 90(1063): (1961).
2. **Gifford F.A.:** Uses of routine meteorological observations for estimating atmospheric dispersion. *Nuclear Safety* 2(4): (1961).

## APPENDIX I

### LINEAR AND NONLINEAR FIT

#### I-1. Overview of Linear and Nonlinear Fit Analysis

This appendix documents the Mathematica<sup>(1)</sup> Codes developed and used for data analysis. Times New Roman font is used for the code and Italic Arial font is used for non-executing comments. Section I-2 contains the code used to fit the particle size distributions from the Andersen multi-stage cascade impactor and from the TSP/CCM by estimating the lognormal parameters, *GM* and *GSD*. Section I-3 contains the NonlinearFit code used to estimate the confidence interval about a nonlinear fit of estimated average concentration data to a Gaussian plume model.

In section I-3, the Mathematica NonlinearFit procedure was used to find the best fit of plume model. Parameters for a Gaussian plume model are followings;

$$C(x, y, z, H) = \frac{ER}{2\pi\sigma_y\sigma_z u} \cdot \left[ \exp\left(-\frac{y^2}{2\sigma_y^2}\right) \cdot \left\{ \left( \exp\left(-\frac{(z-H)^2}{2\sigma_z^2}\right) + \exp\left(-\frac{(z+H)^2}{2\sigma_z^2}\right) \right) \right\} \right] \quad (\text{I.1})$$

where  $C$  = Average Steady state concentration at a point  $(x, y, z)$  [mg/m<sup>3</sup>]

$ER$  = Average emission rate [mg/s];  $u$  = Average wind speed on the ground [m/s];

$\sigma_y, \sigma_z$  = Horizontal and Vertical dispersion coefficients [m];

$y$  = Horizontal distance from the plume centerline [m];

$z$  = Height of the receptor above the ground [m];

$H$  = Effective height [m] =  $h$  (pipe location height) +  $\Delta h$  (average plume height from the pipe location).

The parameters were estimated by matching the concentrations measured with aerosol samplers (See Mathematica Codes in I-3). In section I-3, the estimated parameters were Emission rate (ER), horizontal dispersion coefficient ( $\sigma_y = ay + by x$ ), vertical dispersion coefficient ( $\sigma_z = az + bz x$ ), and effective height ( $H$ ). A height of the receptor above the ground is modeled as 1.5 m to simulate human breathing zone. Average wind speed measured on the ground was applied to this model as  $(2.2 \pm 1.1)$  m/s for Mud Lake pipe rattling process and  $(3.2 \pm 0.5)$  m/s for Lake Sand pipe rattling process.

The values of best parameters of  $by$ ,  $bz$ , and  $H$  were estimated as  $(0.13 \pm 0.05)$  m,  $(0.09 \pm 0.04)$  m, and  $(1.34 \pm 0.03)$  m with an estimated  $PM_{10}$  ER of 5.2 mg/s for Mud Lake pipe rattling operations and  $(0.09 \pm 0.04)$  m,  $(0.10 \pm 0.02)$  m, and  $(1.30 \pm 0.01)$  m with an estimated  $PM_{10}$  ER of as 6.6 mg/s for Lake Sand pipe rattling operation, respectively. These values were used to find the attainment area for the public standard exposure by comparison with National Ambient Air Quality Standards (NAAQS). For the worker exposure standard, the values of best parameters of  $by$ ,  $bz$ , and  $H$  were estimated as  $(0.10 \pm 0.03)$  m,  $(0.08 \pm 0.02)$  m, and  $(1.35 \pm 0.01)$  m with an estimated  $PM_{Total}$  ER of 8.5 mg/s for Mud Lake pipe rattling operations and  $(0.07 \pm 0.05)$  m,  $(0.09 \pm 0.03)$  m, and  $(1.33 \pm 0.01)$  m with an estimated  $PM_{Total}$  ER of as 8.9 mg/s for Lake Sand pipe rattling operation, respectively.

**I-2. Particle Size Distribution with Prediction Confidence Intervals (TSP/CCM data in Test 1)**

```
(***** Content-type: application/mathematica *****
      CreatedBy='Mathematica 5.0'
```

*Mathematica-Compatible Notebook*

*This notebook can be used with any Mathematica-compatible application, such as Mathematica, MathReader or Publicon. The data for the notebook starts with the line containing stars above.*

*To get the notebook into a Mathematica-compatible application, do one of the following:*

- \* Save the data starting with the line of stars above into a file with a name ending in .nb, then open the file inside the application;*
- \* Copy the data starting with the line of stars above to the clipboard, then use the Paste menu command inside the application.*

*Data for notebooks contains only printable 7-bit ASCII and can be sent directly in email or through ftp in text mode. Newlines can be CR, LF or CRLF (Unix, Macintosh or MS-DOS style).*

*NOTE: If you modify the data for this notebook not in a Mathematica-compatible application, you must delete the line below containing the word CacheID, otherwise Mathematica-compatible applications may try to use invalid cache data.*

*For more information on notebooks and Mathematica-compatible applications, contact Wolfram Research:*

*web: <http://www.wolfram.com>*

*email: [info@wolfram.com](mailto:info@wolfram.com)*

*phone: +1-217-398-0700 (U.S.)*

*Notebook reader applications are available free of charge from Wolfram Research.*

```
*****)
```

(\*CacheID: 232\*)

```
(*NotebookFileLineBreakTest
NotebookFileLineBreakTest*)
(*NotebookOptionsPosition[ 15088, 481]*)
(*NotebookOutlinePosition[ 15846, 509]*)
(* CellTagsIndexPosition[ 15774, 503]*)
(*WindowFrame->Normal*)
```

```
Notebook[{
Cell[BoxData[{
  \(<< Statistics`ContinuousDistributions`), "\[IndentingNewLine]",
  \(<< Statistics`DescriptiveStatistics`), "\[IndentingNewLine]",
  \(<< Graphics`Graphics`), "\[IndentingNewLine]",
  \(<< Statistics`LinearRegression`), "\[IndentingNewLine]",
  \(<< Graphics`MultipleListPlot`), "\[IndentingNewLine]",
  \(<< Graphics`FilledPlot`)}], "Input"],

Cell[BoxData[
  \ (Clear[LStvf, LStz, LStaed, LStzpred, LStucl, LStlcl, \ LStf]), "Input"],
```

```
Cell["\<\
LakeSand Pipe Rattling Data on June 16, 2003 (4 TSP/CCMs)
(AED, T1m, T2m, T3m) \
\>", "Text"],
```

```
Cell["\<\
data={2.52,0.30,0.59,0.33,
2.56,0.61,1.20,0.68,
2.59,0.92,1.81,1.03,
2.62,1.23,2.40,1.39,
2.66,1.54,2.99,1.76,
2.69,1.84,3.57,2.14,
2.73,2.15,4.15,2.52,
2.77,2.46,4.74,2.90,
2.80,2.78,5.33,3.29,
2.84,3.10,5.92,3.69,
2.88,3.42,6.51,4.09,
2.92,3.75,7.10,4.51,
2.96,4.08,7.70,4.92,
3.00,4.42,8.32,5.35,
3.04,4.76,8.93,5.79,
3.08,5.11,9.54,6.23,
```

3.12,5.46,10.18,6.68,  
3.16,5.82,10.82,7.13,  
3.20,6.19,11.47,7.60,  
3.25,6.57,12.13,8.08,  
3.29,6.95,12.80,8.57,  
3.33,7.34,13.48,9.06,  
3.38,7.73,14.17,9.56,  
3.42,8.15,14.88,10.09,  
3.47,8.57,15.60,10.62,  
3.51,8.97,16.28,11.12,  
3.56,9.37,16.97,11.63,  
3.61,9.81,17.71,12.17,  
3.66,10.25,18.46,12.73,  
3.71,10.69,19.22,13.30,  
3.76,11.14,19.99,13.86,  
3.81,11.60,20.78,14.44,  
3.86,12.07,21.57,15.04,  
3.91,12.55,22.37,15.63,  
3.96,13.02,23.18,16.22,  
4.01,13.50,24.00,16.83,  
4.07,14.00,24.82,17.44,  
4.12,14.50,25.66,18.06,  
4.18,15.01,26.51,18.69,  
4.23,15.53,27.34,19.32,  
4.29,16.05,28.20,19.97,  
4.35,16.57,29.06,20.62,  
4.41,17.10,29.93,21.28,  
4.46,17.63,30.81,21.94,  
4.52,18.17,31.69,22.60,  
4.58,18.72,32.58,23.27,  
4.65,19.24,33.47,23.95,  
4.71,19.78,34.35,24.63,  
4.77,20.36,35.24,25.32,  
4.83,20.93,36.14,26.01,  
4.90,21.49,37.07,26.70,  
4.97,22.08,37.99,27.39,  
5.03,22.66,38.91,28.08,  
5.10,23.24,39.84,28.77,  
5.17,23.80,40.77,29.47,  
5.24,24.39,41.69,30.21,  
5.31,24.98,42.60,30.93,  
5.38,25.58,43.53,31.65,  
5.45,26.18,44.44,32.38,  
5.52,26.79,45.34,33.11,

5.60,27.39,46.28,33.84,  
5.67,28.00,47.22,34.55,  
5.75,28.61,48.14,35.27,  
5.82,29.21,49.05,35.99,  
5.90,29.82,49.98,36.71,  
5.98,30.43,50.89,37.43,  
6.06,31.06,51.79,38.16,  
6.14,31.67,52.72,38.90,  
6.22,32.29,53.63,39.62,  
6.31,32.90,54.53,40.34,  
6.39,33.53,55.43,41.08,  
6.48,34.15,56.32,41.79,  
6.56,34.78,57.21,42.52,  
6.65,35.41,58.13,43.24,  
6.74,36.04,59.01,43.98,  
6.83,36.66,59.90,44.71,  
6.92,37.27,60.78,45.45,  
7.01,37.90,61.60,46.17,  
7.11,38.53,62.43,46.85,  
7.20,39.16,63.25,47.54,  
7.30,39.79,64.09,48.26,  
7.40,40.41,64.91,48.98,  
7.50,41.00,65.69,49.68,  
7.60,41.61,66.45,50.37,  
7.70,42.23,67.22,51.07,  
7.80,42.87,68.01,51.77,  
7.90,43.48,68.79,52.45,  
8.01,44.09,69.56,53.15,  
8.12,44.73,70.34,53.81,  
8.23,45.33,71.07,54.48,  
8.34,45.96,71.80,55.14,  
8.45,46.59,72.54,55.82,  
8.56,47.21,73.27,56.50,  
8.67,47.81,73.98,57.14,  
8.79,48.45,74.67,57.77,  
8.91,49.05,75.34,58.41,  
9.03,49.68,75.98,59.06,  
9.15,50.29,76.65,59.66,  
9.27,50.88,77.26,60.26,  
9.39,51.45,77.92,60.86,  
9.52,52.07,78.54,61.50,  
9.65,52.68,79.14,62.13,  
9.78,53.25,79.77,62.79,  
9.91,53.87,80.36,63.38,



10.04,54.45,80.95,63.93,  
10.17,55.00,81.55,64.50,  
10.31,55.57,82.08,65.08,  
10.45,56.17,82.65,65.65,  
10.59,56.74,83.19,66.21,  
10.73,57.30,83.68,66.74,  
10.87,57.85,84.15,67.26,  
11.02,58.40,84.63,67.81,  
11.17,58.95,85.13,68.34,  
11.32,59.50,85.57,68.85,  
11.47,60.04,86.01,69.37,  
11.62,60.58,86.49,69.85,  
11.78,61.10,86.88,70.34,  
11.93,61.66,87.31,70.89,  
12.09,62.18,87.75,71.36,  
12.25,62.72,88.16,71.85,  
12.42,63.26,88.55,72.27,  
12.58,63.83,88.94,72.74,  
12.75,64.39,89.30,73.18,  
12.92,64.92,89.66,73.55,  
13.10,65.46,90.05,73.99,  
13.27,65.95,90.41,74.45,  
13.45,66.45,90.78,74.89,  
13.63,66.93,91.11,75.33,  
13.81,67.46,91.42,75.76,  
14.00,67.96,91.70,76.14,  
14.18,68.45,92.01,76.53,  
14.37,68.95,92.32,76.95,  
14.56,69.43,92.61,77.37,  
14.76,69.96,92.88,77.79,  
14.96,70.47,93.16,78.22,  
15.16,70.90,93.42,78.61,  
15.36,71.35,93.69,79.01,  
15.56,71.80,93.91,79.43,  
15.77,72.26,94.18,79.77,  
15.98,72.72,94.37,80.11,  
16.20,73.19,94.58,80.45,  
16.41,73.66,94.77,80.74,  
16.63,74.05,94.96,81.07,  
16.86,74.46,95.11,81.37,  
17.08,74.90,95.28,81.72,  
17.31,75.36,95.42,82.06,  
17.54,75.76,95.60,82.42,  
17.78,76.17,95.74,82.75,

18.01,76.54,95.90,83.02,  
18.26,76.99,96.09,83.29,  
18.50,77.49,96.28,83.58,  
18.75,77.90,96.47,83.96,  
19.00,78.26,96.61,84.18,  
19.25,78.61,96.77,84.40,  
19.51,79.05,96.89,84.67,  
19.77,79.46,96.97,84.94,  
20.03,79.82,97.09,85.24,  
20.30,80.16,97.17,85.51,  
20.57,80.53,97.28,85.78,  
20.85,80.89,97.47,86.01,  
21.13,81.23,97.57,86.26,  
21.41,81.61,97.66,86.55,  
21.70,81.86,97.72,86.76,  
21.99,82.12,97.83,86.94,  
22.28,82.48,97.93,87.15,  
22.58,82.85,98.01,87.42,  
22.88,83.18,98.12,87.61,  
23.19,83.58,98.20,87.95,  
23.50,83.94,98.28,88.19,  
23.81,84.28,98.38,88.44,  
24.13,84.61,98.44,88.62,  
24.45,84.98,98.46,88.80,  
24.78,85.17,98.55,88.95,  
25.11,85.46,98.60,89.19,  
25.45,85.80,98.67,89.46,  
25.79,86.23,98.69,89.57,  
26.13,86.53,98.77,89.82,  
26.48,86.85,98.80,89.98,  
26.84,87.23,98.87,90.16,  
27.19,87.52,98.87,90.40,  
27.56,87.70,98.91,90.66,  
27.93,88.01,98.93,90.94,  
28.30,88.25,99.00,91.11,  
28.68,88.60,99.05,91.45,  
29.06,88.76,99.08,91.67,  
29.45,89.10,99.19,91.80,  
29.85,89.30,99.27,91.98,  
30.24,89.50,99.27,92.12,  
30.65,89.83,99.30,92.36,  
31.06,90.15,99.30,92.52,  
31.47,90.51,99.40,92.75,  
31.90,90.86,99.43,92.95,

32.32,91.08,99.47,93.15,  
32.75,91.32,99.50,93.31,  
33.19,91.64,99.50,93.42,  
33.64,91.89,99.54,93.70,  
34.09,92.11,99.54,93.94,  
34.54,92.24,99.59,94.06,  
35.00,92.53,99.68,94.16,  
35.47,92.80,99.72,94.29,  
35.95,93.11,99.77,94.47,  
36.43,93.21,99.88,94.72,  
36.91,93.51,99.88,94.83,  
37.41,93.76,99.93,94.99,  
37.91,94.05,99.93,95.11,  
38.42,94.43,99.93,95.20,  
38.93,94.43,99.93,95.29,  
39.45,94.64,99.93,95.47,  
39.98,94.85,99.93,95.56,  
40.51,95.25,100.00,95.66,  
41.05,95.30,100.00,95.92,  
41.60,95.39,100.00,96.25,  
42.16,95.59,100.00,96.36,  
42.72,95.65,100.00,96.59,  
43.29,95.76,100.00,96.96,  
43.87,95.93,100.00,97.08,  
44.46,96.22,100.00,97.22,  
45.06,96.53,100.00,97.42,  
45.66,96.65,100.00,97.49,  
46.27,96.85,100.00,97.64,  
46.89,97.06,100.00,97.64,  
47.51,97.06,100.00,97.72,  
48.15,97.36,100.00,97.80,  
48.79,97.59,100.00,97.89,  
49.45,97.59,100.00,97.89,  
50.11,97.59,100.00,97.99,  
50.78,97.59,100.00,98.18,  
51.46,97.69,100.00,98.18,  
52.15,97.69,100.00,98.39,  
52.84,98.08,100.00,98.51,  
53.55,98.18,100.00,98.51,  
54.27,98.40,100.00,98.62,  
54.99,98.40,100.00,98.75,  
55.73,98.40,100.00,98.88,  
56.47,98.64,100.00,98.88,  
57.23,98.64,100.00,98.88,

```

57.99,98.64,100.00,99.02,
58.77,98.78,100.00,99.18,
59.55,98.92,100.00,99.18,
60.35,98.92,100.00,99.18,
61.16,99.07,100.00,99.18,
61.98,99.07,100.00,99.53,
62.80,99.24,100.00,99.53,
63.65,99.58,100.00,99.53,
64.50,99.76,100.00,99.73,
65.36,99.76,100.00,99.73,
66.23,99.76,100.00,99.73,
67.12,99.76,100.00,99.73,
68.02,99.76,100.00,99.73,
68.93,99.76,100.00,99.73,
69.85,99.76,100.00,99.73,
70.78,100.00,100.00,100.00,
71.73,100.00,100.00,100.00,
72.69,100.00,100.00,100.00,
73.66,100.00,100.00,100.00,
74.65,100.00,100.00,100.00};

```

```

\
\>", "Input"],

```

```

Cell[BoxData[{
  \(\text{nd} = \text{Length}[\text{data}]\), "\[IndentingNewLine]",
  \(\text{nd}/4\)}], "Input"],

```

```

Cell[BoxData[{
  \(\text{AED} = \text{Take}[\text{data}, \{1, \text{nd}, 4\}];\)\), "\[IndentingNewLine]",
  \(\text{TSP1} = \text{Take}[\text{data}, \{2, \text{nd}, 4\}];\)\), "\[IndentingNewLine]",
  \(\text{TSP2} = \text{Take}[\text{data}, \{3, \text{nd}, 4\}];\)\), "\[IndentingNewLine]",
  \(\text{TSP3} = \text{Take}[\text{data}, \{4, \text{nd}, 4\}];\)\)}, "Input"],

```

```

Cell[BoxData[{
  \(\text{LStvf} = \{\{\text{TSP1}, \text{TSP2}, \text{TSP3}\} // \text{Flatten}\)/
  100. ;\)\), "\[IndentingNewLine]",
  \(\text{LStaed} = \{\text{AED}, \text{AED}, \text{AED}\} // \text{Flatten};\)\), "\[IndentingNewLine]",
  \(\text{temp} = \{\{\text{LStaed}, \text{LStvf}\} // \text{Transpose}\} // \text{Sort}\} //
  \text{Transpose};\)\), "\[IndentingNewLine]",
  \(\text{LStaed} = \text{temp}[\{1\}];\)\), "\[IndentingNewLine]",
  \(\text{LStvf} = \text{temp}[\{2\}];\)\)}, "Input"],

```

```

Cell[BoxData[{
  \(\text{nd} = \text{Length}[\text{LStaed}];\)\), "\[IndentingNewLine]",

```

```

\(\LStaed =
  Table[Which[LStaed[\([kk]\)] \[LessEqual] 0,
    LStaed[\([kk]\)] = 0.00001, 0 < LStaed[\([kk]\)],
    LStaed[\([kk]\)] = LStaed[\([kk]\)]], {kk, 1,
    nd};\)\), "\[IndentingNewLine]",
\(\(nd = Length[LStvf];\)\), "\[IndentingNewLine]",
\(\LStvf =
  Table[Which[LStvf[\([kk]\)] \[LessEqual] 0,
    LStvf[\([kk]\)] = 0.00001, LStvf[\([kk]\)] \[GreaterEqual] 1,
    LStvf[\([kk]\)] = 0.99999, 0 < LStvf[\([kk]\)] < 1,
    LStvf[\([kk]\)] = LStvf[\([kk]\)]], {kk, 1, nd};\)\)}, "Input"],

Cell[BoxData[
  \(\LStz\ = \ Quantile[NormalDistribution[0, 1], LStvf];\)\), "Input"],

Cell[BoxData[
  \(\Min[LStvf]\), "Input"],

Cell[BoxData[
  \(\{\Log[LStaed], LStz\} // Transpose;\)\), "Input"],

Cell[CellGroupData[{

Cell["Variables in use:  LStaed, LStvf, LStz", "Subsubsection"],

Cell[BoxData[
  \(\LStreg =
    Regress[\{Log[LStaed], LStz\} // Transpose, \{1, z\}, z,
    RegressionReport \[Rule] \{BestFit, SummaryReport,
    SinglePredictionCITable,
    ParameterConfidenceRegion};\)\), "Input"],

Cell["\<
\{LStaedobs, LStzpred, LStse, LStci\} =
  Transpose[(SinglePredictionCITable /. LStreg)[[1]]];\
\>", "Input",
  CellTags->"S6.3.1"],

Cell[BoxData[{
  \(\LStzlc\ = Map[First, LStci];\)\), "\[IndentingNewLine]",
  \(\LStzuc\ = \ Map[Last, LStci];\)\), "\[IndentingNewLine]",
  \(\LStf[z_]\ = \ BestFit /. LStreg;\)\)}, "Input"],

Cell["\<

```

```
Take[LStucl,4];
Take[LStlcl,4];\
\>", "Text"]
}, Open ]],
```

```
Cell[CellGroupData[{
```

```
Cell["\<\
Active variables: LStvf, LStz, LStaed, LStzpred, LStucl, LStlcl \
LStf[z]\
\>", "Subsubsection"],
```

```
Cell[BoxData[
```

```
\(\(DisplayTogether[\[IndentingNewLine]LogLinearListPlot[{LStaed, LStz} //
Transpose],\[IndentingNewLine]LogLinearListPlot[{LStaed,
LStzpred} //
Transpose],\[IndentingNewLine]LogLinearListPlot[{LStaed,
LStzucl} //
Transpose],\[IndentingNewLine]LogLinearListPlot[{LStaed,
LStzlcl} // Transpose]\ ,\[IndentingNewLine]Frame \[Rule]
True, \[IndentingNewLine]FrameLabel \[Rule] \{"\<AED\>", "\<Z from \
Volume Fraction\>"}, \[IndentingNewLine]ImageSize \[Rule]
7.5*72, \[IndentingNewLine]TextStyle \[Rule] {FontFamily -> \
"\<Arial\>", FontSize \[Rule] 14}\[IndentingNewLine]\ \ ];\)\), "Input"],
```

```
Cell[BoxData[
```

```
\({vf = 0.6, \ \ zvf = Quantile[NormalDistribution[0, 1], vf],
CDF[NormalDistribution[0, 1], zvf]}\), "Input"],
```

```
Cell[BoxData[{
```

```
\(zq[p_] :=
Quantile[NormalDistribution[0, 1], p]\), "\[IndentingNewLine]",
\(\(pz[z_] := CDF[NormalDistribution[0, 1], z]\), "\[IndentingNewLine]",
\(\)\), "Input"],
```

```
Cell[BoxData[
```

```
\(\(tlakesand =
DisplayTogether[\[IndentingNewLine]LogLinearListPlot[{LStaed,
pz[LStz]} // Transpose,
PlotStyle \[Rule]
PointSize[
0.006]],\[IndentingNewLine]LogLinearListPlot[{LStaed,
pz[LStzpred]} // Transpose,
PlotStyle \[Rule] {Hue[0.71], Thickness[0.007]}, \
```

```

PlotJoined [Rule]
  True], \[IndentingNewLine]LogLinearListPlot[{LStaed,
    pz[LStzuc1]} // Transpose,
PlotStyle [Rule] {Hue[0.71], Thickness[0.001],
  Dashing[{.03, .01]}], \
PlotJoined [Rule]
  True], \[IndentingNewLine]LogLinearListPlot[{LStaed,
    pz[LStzlc1]} // Transpose,
PlotStyle [Rule] {Hue[0.71], Thickness[0.001],
  Dashing[{.03, .01]}], \
PlotJoined [Rule] True] \ , \[IndentingNewLine]Frame [Rule]
  True, \[IndentingNewLine]FrameLabel [Rule] \ \({ "\<AED>", \
"\<Volume Fraction>" // Reverse}), \[IndentingNewLine]ImageSize [Rule]
  7.5*72, \[IndentingNewLine]TextStyle [Rule] {FontFamily -> \
"\<Arial>", FontSize [Rule] 14} \[IndentingNewLine] \ \ ];\)), "Input",

```

```

Cell[BoxData[
  \(\(DisplayTogether[\[IndentingNewLine]ListPlot[\({LStaed, pz[LStz]} //
    Reverse) //
  Transpose], \[IndentingNewLine]ListPlot[\({LStaed, pz[LStzpred]} //
    Reverse) //
  Transpose], \[IndentingNewLine]ListPlot[\({LStaed, pz[LStzuc1]} //
    Reverse) //
  Transpose], \[IndentingNewLine]ListPlot[\({LStaed, pz[LStzlc1]} //
    Reverse) // Transpose] \ , \[IndentingNewLine]Frame [Rule]
  True, \[IndentingNewLine]FrameLabel [Rule] \ \({ "\<AED>", \
"\<Volume Fraction>" // Reverse}), \[IndentingNewLine]ImageSize [Rule]
  7.5*72, \[IndentingNewLine]TextStyle [Rule] {FontFamily -> \
"\<Arial>", FontSize [Rule] 14} \[IndentingNewLine] \ \ ];\)), "Input",

```

```

Cell[BoxData[
  \(\(DisplayTogether[\[IndentingNewLine]ListPlot[{LStaed, pz[LStz]} \ //
    Transpose], \[IndentingNewLine]ListPlot[{LStaed, pz[LStzpred]} \ //
    Transpose], \[IndentingNewLine]ListPlot[{LStaed, pz[LStzuc1]} \ //
    Transpose], \[IndentingNewLine]ListPlot[{LStaed, pz[LStzlc1]} \ //
    Transpose] \ , \[IndentingNewLine]Frame [Rule]
  True, \[IndentingNewLine]FrameLabel [Rule] \ { "\<AED>", "\<Volume \
Fraction>" }, \[IndentingNewLine]ImageSize [Rule]
  7.5*72, \[IndentingNewLine]TextStyle [Rule] {FontFamily -> \
"\<Arial>", FontSize [Rule] 14} \[IndentingNewLine] \ \ ];\)), "Input",

```

```

Cell[BoxData[
  \({A, B} // Reverse}), "Input"
], Open ]]

```

```

},
FrontEndVersion->"5.0 for Microsoft Windows",
ScreenRectangle->{{0, 1024}, {0, 693}},
WindowSize->{504, 308},
WindowMargins->{{0, Automatic}, {24, Automatic}}
]

```

```

(*****
Cached data follows. If you edit this Notebook file directly, not
using Mathematica, you must remove the line containing CacheID at
the top of the file. The cache data will then be recreated when
you save this file from within Mathematica.
*****)

```

```

(*CellTagsOutline
CellTagsIndex->{
  "S6.3.1"->{
    Cell[10666, 380, 139, 4, 48, "Input",
      CellTags->"S6.3.1"]}
  }
*)

```

```

(*CellTagsIndex
CellTagsIndex->{
  {"S6.3.1", 15679, 496}
}
*)

```

```

(*NotebookFileOutline
Notebook[{
  Cell[1754, 51, 383, 6, 130, "Input"],
  Cell[2140, 59, 93, 1, 50, "Input"],
  Cell[2236, 62, 103, 3, 52, "Text"],
  Cell[2342, 67, 6318, 258, 4638, "Input"],
  Cell[8663, 327, 90, 2, 50, "Input"],
  Cell[8756, 331, 272, 4, 90, "Input"],
  Cell[9031, 337, 413, 7, 110, "Input"],
  Cell[9447, 346, 658, 12, 230, "Input"],
  Cell[10108, 360, 90, 1, 30, "Input"],
  Cell[10201, 363, 43, 1, 30, "Input"],
  Cell[10247, 366, 70, 1, 30, "Input"],

  Cell[CellGroupData[{
    Cell[10342, 371, 66, 0, 29, "Subsubsection"],

```



```
Cell[10411, 373, 252, 5, 90, "Input"],
Cell[10666, 380, 139, 4, 48, "Input",
  CellTags->"S6.3.1"],
Cell[10808, 386, 207, 3, 70, "Input"],
Cell[11018, 391, 55, 3, 52, "Text"]
}, Open ]],
```

```
Cell[CellGroupData[{
Cell[11110, 399, 122, 3, 46, "Subsubsection"],
Cell[11235, 404, 722, 11, 210, "Input"],
Cell[11960, 417, 136, 2, 50, "Input"],
Cell[12099, 421, 199, 4, 70, "Input"],
Cell[12301, 427, 1254, 23, 390, "Input"],
Cell[13558, 452, 787, 12, 270, "Input"],
Cell[14348, 466, 671, 9, 210, "Input"],
Cell[15022, 477, 50, 1, 30, "Input"]
}, Open ]]
}
]
*)
```

```
(*****
End of Mathematica Notebook file.
*****)
```

### **I-3. Nonlinear Fit Code with Prediction Confidence Intervals to Estimate an Attainment Area (Public Exposure of PM<sub>10</sub>)**

```
(***** Content-type: application/mathematica *****
CreatedBy='Mathematica 5.0'
```

#### *Mathematica-Compatible Notebook*

*This notebook can be used with any Mathematica-compatible application, such as Mathematica, MathReader or Publicon. The data for the notebook starts with the line containing stars above.*

*To get the notebook into a Mathematica-compatible application, do one of the following:*

*\* Save the data starting with the line of stars above into a file with a name ending in .nb, then open the file inside the application;*

*\* Copy the data starting with the line of stars above to the clipboard, then use the Paste menu command inside the application.*

*Data for notebooks contains only printable 7-bit ASCII and can be sent directly in email or through ftp in text mode. Newlines can be CR, LF or CRLF (Unix, Macintosh or MS-DOS style).*

*NOTE: If you modify the data for this notebook not in a Mathematica-compatible application, you must delete the line below containing the word CacheID, otherwise Mathematica-compatible applications may try to use invalid cache data.*

*For more information on notebooks and Mathematica-compatible applications, contact Wolfram Research:*

*web: <http://www.wolfram.com>*

*email: [info@wolfram.com](mailto:info@wolfram.com)*

*phone: +1-217-398-0700 (U.S.)*

*Notebook reader applications are available free of charge from Wolfram Research.*

*\*\*\*\*\*)*

*(\*CacheID: 232\*)*

*(\*NotebookFileLineBreakTest  
NotebookFileLineBreakTest\*)*

*(\*NotebookOptionsPosition[ 22658, 565]\*)*

*(\*NotebookOutlinePosition[ 23415, 593]\*)*

*(\* CellTagsIndexPosition[ 23343, 587]\*)*

*(\*WindowFrame->Normal\*)*

Notebook[{

Cell[CellGroupData[{

Cell["NonlinearFit of LS and ML data", "Section",  
FontSize->12],



```

5.053};\)), "[IndentingNewLine]",
\(\(MLsd10 = {1.239, 1.351, 0.150, 0.513, 0.550, 0.455, 0.283, 0.130,
0.677};\)), "\n",
\(\(MLdis10\ = {1, 2, 3, 2, 2, 2, 2, 1, 2};\)), "[IndentingNewLine]",
\(\(MLpdat = Transpose[{MLdis10, MLpm10}];\)), "[IndentingNewLine]",
\(\(ml[x_] = Fit[MLpdat, {\ x\^(-2)}, x]\)), "Input",

Cell[BoxData[
\(\(mlreg = Regress[MLpdat, {\ x\^(-2)}, x]\)), "Input",

Cell[BoxData[{
\(\(MLfitplot =
LogLogPlot[{0.15, ml[x]}, {x, 0.5, 10},
DisplayFunction \[Rule] Identity,
AxesOrigin \[Rule] {2, 9.41722/4}, Axes \[Rule] True,
PlotRange \[Rule] {0.1, 20}];\)), "[IndentingNewLine]",
\(\(MLdataplot =
LogLogListPlot[MLpdat, PlotStyle \[Rule] {PointSize[0.02]},
PlotRange \[Rule] \ {0.1, 10}, {0.1, 15}},
DisplayFunction \[Rule] Identity];\)), "[IndentingNewLine]",
\(\(Show[MLfitplot, MLdataplot, DisplayFunction \[Rule] $DisplayFunction,
Frame \[Rule] True, \
FrameLabel \[Rule] \ {"<Distance from centerline [m]>", \
\*"\"<Measured Mass concentration [mg/!(m^3)]>\""}, \*"\"<Inverse \
Square Law Fit for Mud Lake, \!(R^2) = >\"\"
NumberForm[RSquared /. mlreg, 3], \ NumberForm[ml[x], 4]},
ImageSize \[Rule] 72*7,
TextStyle \[Rule] {FontFamily -> "<Arial>",
FontSize \[Rule] \ 14}];\)), "Input"
}, Open ]],

Cell[CellGroupData[{
Cell["<\
Clearly, the inverse square law is a poor fit to the field data. \
It was observed that the plume passed beneath the sampler at 1 m for most of \
each test. Therefore, nonlinear fit capability was used to find the best \
fit plume model with four parameters: emission rate, sigma y , sigma z and \
H.
sigma y and sigma z are functions of distance along the centerline, x. \
Therefore, they must be parameterized before the NonLinearFit process starts. \
It is sufficient over the range of interest, for them to be modelled by a \
linear function.\
>", "Subsubsection"],

```

```
Cell[BoxData[{
  \({\[\Sigma]y\ = \ ay + \ by\ x, \ \[\Sigma]z\ = \ az\ + \ bz\ x, H,
  ER}; Clear[Conc, con, x, y, z]), "\[IndentingNewLine]",
  \(\text{Conc}[x_, y_,
  z_] := \(\text{ER}\sqrt{2\ \[\Pi]}\ \[\Sigma]y\ \[\Sigma]z\ u\ \text{Sin}[\[\Theta]]\))
  \(\text{Exp}[(-y^2)\sqrt{2\ \[\Sigma]y^2}] \(\text{Exp}[(-((z - H))^2)\sqrt{2\ \
  \[\Sigma]z^2}] +
  \(\text{Exp}[(-((z + H))^2)\sqrt{2\ \[\Sigma]z^2}]\))\), "\
  \[IndentingNewLine]",
  \(\text{con}[x_, y_, z_] =
  \(\text{Conc}[x, y, z] /. \{u \[\Rule] 3, \[\Theta] \[\Rule] \[\Pi]/2,
  H \[\Rule] 1\}\}), "Input"],
```

```
Cell[BoxData[
  \(\text{Plot}[
  \(\text{con}[x, 0, 1.61] /. \{\[\Theta] \[\Rule] \[\Pi]/2, u \[\Rule] \ 3,
  ER \[\Rule] 12, H \[\Rule] 1. , ay \[\Rule] 0.1, az \[\Rule] 0.1,
  by \[\Rule] 0.25, bz \[\Rule] 0.13\}, \{x, 0, 4\},
  \(\text{PlotRange} \[\Rule] \text{All};\)), "Input"],
```

```
Cell[BoxData[{
  \(\text{Clear}[ay, az, by, bz, ER, x];\)), "\[IndentingNewLine]",
  \(\text{ERestML} = 13.3; \(\text{ayoML} = 0.0; \(\text{azoML} = 0.0;\), "\[IndentingNewLine]",
  \(\text{mlnlinreg} =
  \(\text{NonlinearRegress}[\text{MLpldat},
  \(\text{Conc}[x, \ 0, 1.5] /. \{u \[\Rule] 3. , \[\Theta] \[\Rule] \[\Pi]/2,
  ay \[\Rule] \text{ayoML}, az \[\Rule] \text{azoML}, ER \[\Rule] \text{ERestML}\},
  x, \{by, bz, H\},
  \(\text{RegressionReport} \[\Rule] \{\text{BestFitParameters}, \text{ParameterCITable},
  \text{EstimatedVariance}, \text{AsymptoticCorrelationMatrix},
  \text{FitCurvatureTable}, \ \text{SinglePredictionCITable}, \
  \text{MeanPredictionCITable}\}\}), "Input"],
```

```
Cell[BoxData[{
  \(\text{mlnlin}[
  x_] = \(\text{Conc}[x, \ 0, 1.5] /. \{u \[\Rule] 3, \[\Theta] \[\Rule] \[\Pi]/2,
  ay \[\Rule] \text{ayoML}, az \[\Rule] \text{azoML},
  ER \[\Rule] \text{ERestML}\}) /. \(\text{BestFitParameters} /.
  \(\text{mlnlinreg}\)), "\[IndentingNewLine]",
  \(\text{xmax} = 20;\), "\[IndentingNewLine]",
  \(\text{DisplayTogether}[\[\IndentingNewLine]\text{MLloglogdataplot} =
  \(\text{LogLogListPlot}[\text{MLpldat}, \text{PlotStyle} \[\Rule] \{\text{PointSize}[0.02]\},
  \text{PlotRange} \[\Rule] \ \{\{0.1, 25\}, \{0.1, \text{xmax}\}\},
```

```

DisplayFunction \[Rule]
Identity], \[IndentingNewLine]MLloglogfitplot =
LogLogPlot[{0.15, mlnonlin[x]}, {x, 0.1, xmax}, \
DisplayFunction \[Rule] Identity,
AxesOrigin \[Rule] {2, 9.41722/4},
Axes \[Rule] True], \[IndentingNewLine]Frame \[Rule] True, \
FrameLabel \[Rule] \ {"\<Distance from CenterLine in m\>", \
"\<Measured Mass Conc in mg/m^3\>", "\<Mud Lake Scale Test\>", "\<Nonlinear \
Regression Fit\>"}, ImageSize \[Rule] 72*7,
TextStyle \[Rule] {FontFamily -> "\<Arial\>",
FontSize \[Rule] \ 14}\[IndentingNewLine];\)\)}, "Input"
}, Open ]],

```

```
Cell[CellGroupData[{
```

```

Cell["\<
Next, use the Regression Report to estimate the CI for the single \
prediction and the mean prediction quality of the fitted function.\
\>", \
"Subsubsection"],

```

```

Cell[BoxData[
\ (MLmCItable = \((MeanPredictionCITable /. mlnonlinreg)\)\)], "Input"
], Open ]],

```

```
Cell[CellGroupData[{
```

```

Cell["\<
Multiple values occur at each distance. There is only one \
predicted value at each distance. To find confidence intervals on the fitted \
curve, it is sufficient to retain the first three lines in the table above, \
representing predicted data at {1,2,3} m, respectively. Use the Take command \
to pick the first three lines. \
\>", "Subsubsection"],

```

```

Cell[BoxData[
\ (MLmCItab = Take[MLmCItable[\([1]\)], 3)\)], "Input"
], Open ]],

```

```
Cell[CellGroupData[{
```

```

Cell["\<
The CI is defined by the last entry in each member of the table \
above. \

```

```
\>", "Subsubsection"],
```

```
Cell[BoxData[
  \(\text{MLmCIdata} = \text{Take}[\text{MLmCItab} // \text{Transpose}, \{(-1)\}][\{1\}]\), "Input"],
```

```
Cell[BoxData[{
  \(\text{disval} = \{1, 2, 3\};\), "\[IndentingNewLine]",
  \(\text{MLmcl} = \text{Map}[\text{First}, \text{MLmCIdata};\), "\[IndentingNewLine]",
  \(\text{MLmucl} = \text{Map}[\text{Last}, \text{MLmCIdata};\), "\[IndentingNewLine]",
  \(\{\text{MLmclfit} =
    \text{Fit}[\{\text{disval}, \text{MLmcl}\} // \text{Transpose}, \{x^2, x, 1\},
      x], \[IndentingNewLine]\text{MLmuclfit} =
    \text{Fit}[\{\text{disval}, \text{MLmucl}\} // \text{Transpose}, \{x^2, x, 1\}, x]\}), "Input"],
```

```
Cell[BoxData[
  \(\text{LogLogPlot}[\{\text{MLmclfit}, \text{MLmuclfit}\}, \{x, 1.0, 3.\};\), "Input"
], Open ]],
```

```
Cell[CellGroupData[{
```

```
Cell["Do the same thing for the single prediction CI. ", "Subsubsection"],
```

```
Cell[BoxData[
  \(\text{MLspCItable} = \text{SinglePredictionCItable} /. \text{mlnonlinreg}\), "Input"],
```

```
Cell[BoxData[
  \(\text{MLspCItab} = \text{Take}[\text{MLspCItable}[\{1\}], 3]\), "Input"],
```

```
Cell[BoxData[
  \(\text{MLspCIdata} = \text{Take}[\text{MLspCItab} // \text{Transpose}, \{(-1)\}][\{1\}]\), "Input"],
```

```
Cell[BoxData[{
  \(\text{disval} = \{1, 2, 3\};\), "\[IndentingNewLine]",
  \(\text{MLsplcl} = \text{Map}[\text{First}, \text{MLspCIdata};\), "\[IndentingNewLine]",
  \(\text{MLspucl} = \text{Map}[\text{Last}, \text{MLspCIdata};\), "\[IndentingNewLine]",
  \(\{\text{MLsplclfit} =
    \text{Fit}[\{\text{disval}, \text{MLsplcl}\} // \text{Transpose}, \{x^2, x, 1\},
      x], \[IndentingNewLine]\text{MLspuclfit} =
    \text{Fit}[\{\text{disval}, \text{MLspucl}\} // \text{Transpose}, \{x^2, x, 1\}, x]\}), "Input"],
```

```
Cell[BoxData[
  \(\text{MLCIplot} =
  \text{Plot}[\{\text{mlnonlin}[x], \text{MLsplclfit}, \text{MLspuclfit}, \text{MLmclfit}, \text{MLmuclfit}\}, \{x,
```

```

1, 3. }, PlotRange \[Rule] All, Frame \[Rule] True,
PlotStyle \[Rule] \[IndentingNewLine]{Thickness[0.012],
Dashing[{0.05, 0.05}], Dashing[{0.05, 0.05}],
Dashing[{0.02, 0.02}], Dashing[{0.02, 0.02}]};\)\), "Input"
}, Open ]],

```

```
Cell[CellGroupData[{
```

```

Cell["\<
The LCL for ML single prediction is negative. It can not be \
plotted on LogLog Axes.\
\>", "Subsubsection"],

```

```
Cell[BoxData[
```

```

\(\(MLloglogCIplot =
LogLogPlot[{mlnonlin[x], MLmclfit, MLmuclfit}, {x, 1, 3. },
PlotRange \[Rule] All, Frame \[Rule] True,
PlotStyle \[Rule] \[IndentingNewLine]{Thickness[0.012],
Dashing[{0.05, 0.05}], Dashing[{0.02, 0.02}],
Dashing[{0.02, 0.02}]};\)\), "Input",

```

```
Cell[BoxData[
```

```

\(\(DisplayTogether[{MLloglogfitplot, MLloglogCIplot, MLloglogdataplot},
Frame \[Rule] True, \
FrameLabel \[Rule] \{"\<Distance from CenterLine in m\>", \
"\<Measured Mass Conc in mg.m^3\>", "\<Mud Lake Scale Test\>", "\<Nonlinear \
Regression Fit\>"}, ImageSize \[Rule] 72*7,
TextStyle \[Rule] {FontFamily -> "\<Arial\>", FontSize \[Rule] \ 14},
PlotRange \[Rule] {{Log[10, 0.5], Log[10, 20]}, {Log[10, 0.1],
Log[10, 20]}},
Axes \[Rule] False\[\IndentingNewLine];\)\), "Input"
}, Open ]],
}, Open ]],

```

```
Cell[CellGroupData[{
```

```

Cell["Next, perform nonlinear fit for the lake sand data.", "Subsection",
FontSize->12],

```

```
Cell[BoxData[{
```

```

\(\(LSpm10 = {4.933, 10.045, 4.173, 4.520, 2.530, 6.610, 3.590, 2.203,
2.697, 1.627};\)\), "\n",
\(\(LSsd10 = {1.068, 2.129, 0.829, 0.479, 0.523, 1.186, 1.022, 0.416,
0.477, 0.265};\)\), "\n",

```



```

\(\(LSdis10 = {1, 2, 3, 1, 3, 1, 3, 1, 2,
3};\)), "[IndentingNewLine]",
\(\(LSpldat = Transpose[{LSdis10, LSpm10}]\)), "[IndentingNewLine]",
\(\(ls[x_] = Fit[LSpldat, {\ x\^(-2)}, x]\)), "Input",

```

```

Cell[BoxData[
\(\(lsreg = Regress[LSpldat, {\ x\^(-2)}, x]\)), "Input",

```

```

Cell[BoxData[{
\(\(LSfitplot =
LogLogPlot[{0.15, ls[x]}, {x, 0.5, 10},
DisplayFunction \[Rule] Identity,
AxesOrigin \[Rule] {2, 5.45612/4}, Axes \[Rule] True,
PlotRange \[Rule] {0.1, 15};\)), "[IndentingNewLine]",
\(\(LSdataplot =
LogLogListPlot[LSpldat, PlotStyle \[Rule] {PointSize[0.02]},
PlotRange \[Rule] \ {{0.1, 10}, {0.1, 15}},
DisplayFunction \[Rule] Identity;\)), "[IndentingNewLine]",
\(\(Show[LSfitplot, LSdataplot, DisplayFunction \[Rule] $DisplayFunction,
Frame \[Rule] True, \
FrameLabel \[Rule] \ {"<Distance from centerline [m]>", \
\*"<Measured Mass concentration [mg/!(m^3)]>"}, \*"<Inverse \
Square Law Fit for Lake Sand, \!(R^2) = \>""
NumberForm[RSquared /. lsreg, 3], \ NumberForm[ls[x], 4]},
ImageSize \[Rule] 72*7,
TextStyle \[Rule] {FontFamily -> "<Arial>",
FontSize \[Rule] \ 14};\)), "Input",

```

```

Cell[BoxData[{
\(\(Clear[ay, az, by, bz, ER, x];\)), "[IndentingNewLine]",
\(\(ERestLS = 12.2; ayoLS = 0.00; azoLS = 0.00;\)), "[IndentingNewLine]",
\(\(lsnonlinreg =
NonlinearRegress[LSpldat,
Conc[x, \ 0, 1.5] /. {u \[Rule] 2.9, \[Theta] \[Rule] \[Pi]/2,
ay \[Rule] ayoLS, az \[Rule] azoLS, ER \[Rule] ERestLS},
x, {by, bz, H},
RegressionReport \[Rule] {BestFitParameters, ParameterCITable,
EstimatedVariance, AsymptoticCorrelationMatrix,
FitCurvatureTable, \ SinglePredictionCITable, \
MeanPredictionCITable}\)), "Input",

```

```

Cell[BoxData[{
\(\(lsonlin[
x_] = \(\(Conc[x, \ 0, 1.5] /. {u \[Rule] 3, \[Theta] \[Rule] \[Pi]/2,

```

```

ay \[Rule] ayoLS, az \[Rule] azoLS,
ER \[Rule] ERestLS}) / . \((BestFitParameters /
  lsnonlinreg))\), "\[IndentingNewLine]",
\(\(xmax = 20;)\), "\[IndentingNewLine]",
\(\(DisplayTogether[\[IndentingNewLine]LSloglogdataplot =
  LogLogListPlot[LSpldat, PlotStyle \[Rule] {PointSize[0.02]},
  PlotRange \[Rule] \ {0.1, 20}, {0.1, xmax}},
  DisplayFunction \[Rule]
  Identity], \[IndentingNewLine]LSloglogfitplot =
  LogLogPlot[{0.15, lsnonlin[x]}, {x, 0.1, xmax}, \
  DisplayFunction \[Rule] Identity,
  AxesOrigin \[Rule] {2, 5.45612/4},
  Axes \[Rule] True], \[IndentingNewLine]Frame \[Rule]
  True, \[IndentingNewLine]FrameLabel \[Rule] \ {"<Distance from \
CenterLine in m>", "<Measured Mass Conc in mg.m^3>", "<Lake Sand Scale \
Test>", "<Nonlinear Regression Fit>"}, ImageSize \[Rule] 72*7,
  TextStyle \[Rule] {FontFamily -> "<Arial>",
  FontSize \[Rule] \ 14}\[IndentingNewLine];\)\)}, "Input",

```

```
Cell[CellGroupData[{
```

```

Cell["<\
Next, use the Regression Report to estimate the CI for the single \
prediction and the mean prediction quality of the fitted function.\
>", \
"Subsubsection"],

```

```

Cell[BoxData[
  \[LSmCItable = \((MeanPredictionCITable /. lsnonlinreg)\)\), "Input"]
], Open ]],

```

```
Cell[CellGroupData[{
```

```

Cell["<\
Multiple values occur at each distance. There is only one \
predicted value at each distance. To find confidence intervals on the fitted \
curve, it is sufficient to retain the first three lines in the table above, \
representing predicted data at {1,2,3} m, respectively. Use the Take command \
to pick the first three lines. \
>", "Subsubsection"],

```

```

Cell[BoxData[
  \[LSmCItab = Take[LSmCItable[\([1]\), 3]\)], "Input"]
], Open ]],

```

```

Cell[CellGroupData[{
Cell["<
The CI is defined by the last entry in each member of the table \
above. \
>", "Subsubsection"],
Cell[BoxData[
\(\text{LSmCIdata} = \text{Take}[\text{LSmCItab} // \text{Transpose}, \{-1\}][[1]]\), "Input"],
Cell[BoxData[{
\(\text{disval} = \{1, 2, 3\};\), "\[IndentingNewLine]",
\(\text{LSmcl} = \text{Map}[\text{First}, \text{LSmCIdata}];\), "\[IndentingNewLine]",
\(\text{LSmucl} = \text{Map}[\text{Last}, \text{LSmCIdata}];\), "\[IndentingNewLine]",
\(\{\text{LSmclfit} =
\text{Fit}[\{\text{disval}, \text{LSmcl}\} // \text{Transpose}, \{x^2, x, 1\},
x], \[IndentingNewLine]\text{LSmuclfit} =
\text{Fit}[\{\text{disval}, \text{LSmucl}\} // \text{Transpose}, \{x^2, x, 1\}, x]\}\), "Input"],
Cell[BoxData[
\(\text{LogLogPlot}[\{\text{LSmclfit}, \text{LSmuclfit}\}, \{x, 0.7, 3.2\}]\), "Input"
], Open ]],
Cell[CellGroupData[{
Cell["Do the same thing for the single prediction CI. ", "Subsubsection"],
Cell[BoxData[
\(\text{LSspCItable} = \text{SinglePredictionCITable} /. \text{Isnonlinreg}\), "Input"],
Cell[BoxData[
\(\text{LSspCItab} = \text{Take}[\text{LSspCItable}[[1]], 3]\), "Input"],
Cell[BoxData[
\(\text{LSspCIdata} = \text{Take}[\text{LSspCItab} // \text{Transpose}, \{-1\}][[1]]\), "Input"],
Cell[BoxData[{
\(\text{disval} = \{1, 2, 3\};\), "\[IndentingNewLine]",
\(\text{LSsplcl} = \text{Map}[\text{First}, \text{LSspCIdata}];\), "\[IndentingNewLine]",
\(\text{LSspucl} = \text{Map}[\text{Last}, \text{LSspCIdata}];\), "\[IndentingNewLine]",
\(\{\text{LSsplclfit} =
\text{Fit}[\{\text{disval}, \text{LSsplcl}\} // \text{Transpose}, \{x^2, x, 1\},

```

```
x], \[IndentingNewLine]LSspuclfit =
Fit[{disval, LSspucl} // Transpose, {x^2, x, 1}, x]}], "Input"],
```

```
Cell[BoxData[
  \(\(\LSClplot =
    Plot[{lnonlin[x], LSmlclfit, LSmuclfit}, {x, 1, 3. },
      PlotRange \[Rule] All, Frame \[Rule] True,
      PlotStyle \[Rule] \[IndentingNewLine]{Thickness[0.012],
        Dashing[{0.05, 0.05}], Dashing[{0.05, 0.05}],
        Dashing[{0.02, 0.02}], Dashing[{0.02, 0.02}]}];\)\), "Input"
  ], Open ]],
```

```
Cell[CellGroupData[{
```

```
Cell["\<
The LCL for LS single prediction is negative. It can not be \
plotted on LogLog Axes.\
\>", "Subsubsection"],
```

```
Cell[BoxData[
  \(\(\LSloglogCIplot =
    LogLogPlot[{lnonlin[x], LSmlclfit, LSmuclfit}, {x, 1, 3. },
      PlotRange \[Rule] All, Frame \[Rule] True,
      PlotStyle \[Rule] \[IndentingNewLine]{Thickness[0.012],
        Dashing[{0.05, 0.05}], Dashing[{0.02, 0.02}],
        Dashing[{0.02, 0.02}]}];\)\), "Input"],
```

```
Cell[BoxData[
  \(\(\DisplayTogether[{LSloglogfitplot, LSloglogCIplot, LSloglogdataplot},
    Frame \[Rule] True, \
    FrameLabel \[Rule] \ {"\<Distance from CenterLine in m\>", \
"\<Measured Mass Conc in mg.m^3\>", "\<Lake Sand Scale Test\>", "\<Nonlinear \
Regression Fit\>"}, ImageSize \[Rule] 72*7,
    TextStyle \[Rule] {FontFamily -> "\<Arial\>", FontSize \[Rule] \ 14},
    PlotRange \[Rule] {{Log[10, 0.5], Log[10, 20]}, {Log[10, 0.1],
      Log[10, 20]}}},
    Axes \[Rule] False\[IndentingNewLine];\)\), "Input"],
```

```
Cell[BoxData[
  \(\(5)\), "Input"],
```

```
Cell[BoxData[{
  \(\(\LSloglogCIplot // Show;\)\), "\[IndentingNewLine]",
  \(\(\LSloglogdataplot // Show;\)\), "\[IndentingNewLine]",
```

```

\(\(LSloglogfitplot // Show;)\)), "Input"
}, Open ]]
}, Open ]],

Cell[CellGroupData[{

Cell["\<
One last item. Compare Each of these with an inverse square law \
rule to see what the concentration would be at 1 m from the centerline if the \
inverse square law applied.\
\>", "Subsection",
  FontSize->12],

Cell[BoxData[{
  \(\(xmax = 20;)\)), "[IndentingNewLine]",
  \(\(DisplayTogether[\[IndentingNewLine]LogLogListPlot[MLpldat,
    PlotStyle \[Rule] {PointSize[0.015]},
    PlotRange \[Rule] \ {0.4, 20}, {0.1, xmax}},
    DisplayFunction \[Rule]
      Identity, \[IndentingNewLine]LogLogPlot[{0.15, mlnonlin[x]}, {x,
        0.1, xmax}, DisplayFunction \[Rule] Identity,
        AxesOrigin \[Rule] {2, 9.41722/4}, Axes \[Rule] True],
        MLloglogCIplot, MLloglogfitplot,
        PlotLabel \[Rule] \ "\<Mud Lake Pipe Scale\>", \
\[IndentingNewLine]Frame \[Rule]
      True, \[IndentingNewLine]Epilog \[Rule] {{Thickness[0.012],
        Line[{{0.7, 0.8}, {0.8, 0.8}}]},
        Text["\<Fitted\>", {0.92, 0.8}], \[IndentingNewLine]{Thickness[
          0.008], Line[{{0.75, 0.6}, {0.755, 0.6}}]},
        Text["\<Measured\>", {0.98, 0.6}], \[IndentingNewLine]{Thickness[
          0.001], {Dashing[{0.01, 0.01}],
          Line[{{0.7, 0.4}, {0.8, 0.4}}]}},
        Text["\<MeanPreCI\>", {1.0,
          0.4}]\[IndentingNewLine]}, \[IndentingNewLine]Frame \[Rule]
      True, \ FrameLabel \[Rule] \ {"\<Distance from CenterLine [m]\>", \
\*" "\<Mass Concentration [mg/!(m^(-3))\>|", \*" "\<Public Exposure \
Standard (PM10) = 0.15 mg/!(m^(-3))\>|", "\<Plume Center Conc at 1 m \
(PM10) = \>"} \ NumberForm[mlnonlin[1], 2]}, ImageSize \[Rule] 72*7,
      TextStyle \[Rule] {FontFamily -> "\<Arial\>",
        FontSize \[Rule] \ 14}\[IndentingNewLine];)\)), "Input"],

Cell[BoxData[{
  \(\(xmax = 20;)\)), "[IndentingNewLine]",
  \(\(DisplayTogether[\[IndentingNewLine]LogLogListPlot[LSpldat,

```

```

PlotStyle \[Rule] {PointSize[0.015]},
PlotRange \[Rule] \ { {0.4, 20}, {0.1, xmax} },
DisplayFunction \[Rule]
  Identity, \[IndentingNewLine]LogLogPlot[{0.15, lsnonlin[x]}, {x,
  0.1, xmax}, DisplayFunction \[Rule] Identity,
  AxesOrigin \[Rule] {2, 5.45612/4}, Axes \[Rule] True],
LSloglogCIplot, LSloglogfitplot,
PlotLabel \[Rule] \ "<Lake Sand Pipe Scale>", \
\[IndentingNewLine]Epilog \[Rule] { {Thickness[0.012],
  Line[{{0.7, 0.8}, {0.8, 0.8}]}},
  Text["<Fitted>", {0.92, 0.8}], \[IndentingNewLine]{Thickness[
  0.008], Line[{{0.75, 0.6}, {0.755, 0.6}]}},
  Text["<Measured>", {0.98, 0.6}], \[IndentingNewLine]{Thickness[
  0.001], {Dashing[{0.01, 0.01}],
  Line[{{0.7, 0.4}, {0.8, 0.4}]}},
  Text["<MeanPreCI>", {1.0,
  0.4}]\[IndentingNewLine]}, \[IndentingNewLine]Frame \[Rule]
  True, \ FrameLabel \[Rule] \ {"<Distance from CenterLine [m]>", \
  \["<Mass Concentration [mg/!(m^(-3))>|", \["<Public Exposure \
  Standard (PM10) = 0.15 mg/!(m^(-3))>|", "<Plume Center Conc at 1 m \
  (PM10) = \>"\ NumberForm[lsnonlin[1], 2]}, ImageSize \[Rule] 72*7,
  TextStyle \[Rule] {FontFamily -> "<Arial>",
  FontSize \[Rule] \ 14}\[IndentingNewLine];\)}}, "Input"]
}, Open ]]
}, Open ]]
},
FrontEndVersion->"5.0 for Microsoft Windows",
ScreenRectangle->{{0, 1024}, {0, 693}},
WindowSize->{1016, 666},
WindowMargins->{{0, Automatic}, {Automatic, 0}}
]

```

```

(*****
Cached data follows. If you edit this Notebook file directly, not
using Mathematica, you must remove the line containing Cacheld at
the top of the file. The cache data will then be recreated when
you save this file from within Mathematica.
*****)

```

```

(*CellTagsOutline
CellTagsIndex->{
  "S6.6.1"->{
    Cell[2933, 86, 270, 9, 138, "Input",
    CellTags->"S6.6.1"]}

```

```
}
*)
```

```
(*CellTagsIndex
CellTagsIndex->{
  {"S6.6.1", 23249, 580}
}
*)
```

```
(*NotebookFileOutline
Notebook[{

Cell[CellGroupData[{
Cell[1776, 53, 65, 1, 64, "Section"],

Cell[CellGroupData[{
Cell[1866, 58, 311, 6, 54, "Subsection"],

Cell[CellGroupData[{
Cell[2202, 68, 728, 16, 199, "Subsubsection"],
Cell[2933, 86, 270, 9, 138, "Input",
  CellTags->"S6.6.1"],
Cell[3206, 97, 458, 7, 111, "Input"],
Cell[3667, 106, 75, 1, 31, "Input"],
Cell[3745, 109, 1000, 18, 174, "Input"]
}], Open ]],

Cell[CellGroupData[{
Cell[4782, 132, 595, 10, 80, "Subsubsection"],
Cell[5380, 144, 564, 11, 90, "Input"],
Cell[5947, 157, 278, 5, 30, "Input"],
Cell[6228, 164, 623, 11, 130, "Input"],
Cell[6854, 177, 1164, 20, 210, "Input"]
}], Open ]],

Cell[CellGroupData[{
Cell[8055, 202, 169, 4, 29, "Subsubsection"],
Cell[8227, 208, 88, 1, 30, "Input"]
}], Open ]],

Cell[CellGroupData[{
Cell[8352, 214, 364, 6, 46, "Subsubsection"],
Cell[8719, 222, 72, 1, 30, "Input"]
}], Open ]],
```

```
Cell[CellGroupData[{
Cell[8828, 228, 106, 3, 29, "Subsubsection"],
Cell[8937, 233, 93, 1, 30, "Input"],
Cell[9033, 236, 407, 7, 112, "Input"],
Cell[9443, 245, 87, 1, 30, "Input"]
}, Open ]],
```

```
Cell[CellGroupData[{
Cell[9567, 251, 74, 0, 29, "Subsubsection"],
Cell[9644, 253, 91, 1, 30, "Input"],
Cell[9738, 256, 74, 1, 30, "Input"],
Cell[9815, 259, 106, 2, 30, "Input"],
Cell[9924, 263, 405, 7, 112, "Input"],
Cell[10332, 272, 382, 6, 70, "Input"]
}, Open ]],
```

```
Cell[CellGroupData[{
Cell[10751, 283, 119, 3, 29, "Subsubsection"],
Cell[10873, 288, 345, 6, 70, "Input"],
Cell[11221, 296, 558, 9, 110, "Input"]
}, Open ]],
}, Open ]],
```

```
Cell[CellGroupData[{
Cell[11828, 311, 89, 1, 37, "Subsection"],
Cell[11920, 314, 461, 8, 111, "Input"],
Cell[12384, 324, 75, 1, 31, "Input"],
Cell[12462, 327, 1001, 18, 174, "Input"],
Cell[13466, 347, 623, 11, 130, "Input"],
Cell[14092, 360, 1184, 20, 230, "Input"],

```

```
Cell[CellGroupData[{
Cell[15301, 384, 169, 4, 29, "Subsubsection"],
Cell[15473, 390, 88, 1, 30, "Input"]
}, Open ]],
```

```
Cell[CellGroupData[{
Cell[15598, 396, 364, 6, 46, "Subsubsection"],
Cell[15965, 404, 72, 1, 30, "Input"]
}, Open ]],
```

```
Cell[CellGroupData[{
Cell[16074, 410, 106, 3, 29, "Subsubsection"],
```



```
Cell[16183, 415, 93, 1, 30, "Input"],
Cell[16279, 418, 407, 7, 112, "Input"],
Cell[16689, 427, 82, 1, 30, "Input"]
}, Open ]],
```

```
Cell[CellGroupData[{
Cell[16808, 433, 74, 0, 29, "Subsubsection"],
Cell[16885, 435, 91, 1, 30, "Input"],
Cell[16979, 438, 74, 1, 30, "Input"],
Cell[17056, 441, 106, 2, 30, "Input"],
Cell[17165, 445, 405, 7, 112, "Input"],
Cell[17573, 454, 356, 6, 50, "Input"]
}, Open ]],
```

```
Cell[CellGroupData[{
Cell[17966, 465, 119, 3, 29, "Subsubsection"],
Cell[18088, 470, 345, 6, 70, "Input"],
Cell[18436, 478, 559, 9, 110, "Input"],
Cell[18998, 489, 34, 1, 30, "Input"],
Cell[19035, 492, 187, 3, 70, "Input"]
}, Open ]],
}, Open ]],
```

```
Cell[CellGroupData[{
Cell[19271, 501, 220, 5, 54, "Subsection"],
Cell[19494, 508, 1592, 26, 314, "Input"],
Cell[21089, 536, 1541, 25, 294, "Input"]
}, Open ]],
}, Open ]],
}
]
*)
```

```
(*****
End of Mathematica Notebook file.
*****)
```

## APPENDIX I REFERENCE

1. **Wolfram Research, Inc.:** Mathematica 5.0 Champaign, IL.

## VITA

Ju-Myon Park  
 Permanent Address:  
 776-27 Won-Dong  
 Osan, Kyungki-Do, Korea (ROK)  
 447-060

### ***Education***

1. Texas A&M University, College Station, TX; August, 2005.  
 Ph.D. in Interdisciplinary Engineering
2. Texas A&M University, College Station, TX; December, 2002.  
 M.S. Industrial Hygiene
3. Hoseo University, Asan, Korea; February, 1995.  
 B.E. Industrial Safety Engineering

### ***Work Experience***

1. DONGAH Kongyung Construction Co., Ltd, Seoul, KOREA.  
 Safety Engineer; January 1996 ~ September 1998.

### ***Qualification***

1. Korea Construction Engineers Association, Seoul, KOREA; October, 1998.  
 Registered construction safety engineer; Certificate of Construction Engineer Career
2. Korea Manpower Agency, Seoul, KOREA; July, 1995.  
 Certified Safety Professional; National Technical Qualification

### ***Training***

1. Instrument Certification (Transmission Electron Microscopy)  
 Microscopy Imaging Center, Texas A&M University; December, 2003.
2. Instrument Certification (Environmental Scanning Electron Microscopy)  
 Microscopy Imaging Center, Texas A&M University; June, 2003.
3. The professional education course of manpower conveyance safety instructor  
 Korea Occupational Safety & Health Agency (Korean industrial Safety and Health Act: Article 32) April, 1998.
4. The special course of safety and health engineer  
 Korea Occupational Safety & Health Agency (The enforcement regulation of Korean Industrial Safety and Health Act: Article 39) April, 1996.

Military Service in army, Porchun, Korea; March 1990 ~ July 1992.